Lentiviral vector purification using genetically encoded biotin mimic in packaging cell

UCL Cancer Institute

University College London

A thesis Presented for the Degree of Doctorate in Philosophy

Leila Mekkaoui

September 2017

Declaration

I, Leila Mekkaoui, confirm that the work presented in this thesis is my own. Where information has been derived from other sources, I confirm that this has been indicated in the thesis.

Abstract

Lentiviral vectors (LVs) are powerful tools in gene therapy that have recently witnessed an increasing demand in both research and clinical applications. Current LVs purification represents the main bottle neck in their application as several methods are employed which are time consuming, cumbersome and yield low recoveries. The aim of this project was to develop a one-step method to specifically and efficiently purify LVs, with high vector yields and reduced levels of impurities, using the biotin-streptavidin system.

Herein, packaging 293T cells were genetically engineered with biotin mimicking synthetic peptides and different cell membrane anchoring strategies for optimal streptavidin binding were tested. We have identified a flanked disulphide-constrained peptide, termed Ctag (ECHPQGPPCIEGRK), displayed on a CD8α stalk to be the most promising. LVs were modified with Ctag by its random incorporation onto viral surfaces during budding, without viral protein engineering or hindrance on infectivity. The expression of Ctag on LVs allowed complete capture of infectious particles by streptavidin magnetic beads. As Ctag binds streptavidin in the nanomolar range, we hypothesised that gentle elution from streptavidin matrix should occur by biotin's competitive binding. Accordingly, addition of micromolar concentrations of biotin to captured LVs resulted in an overall yield of ≥60%. Analysis of eluted LVs revealed high purity levels, with a ≤3-log and 2-log reduction of DNA contamination and host cell proteins, respectively. This one-step purification was also tested for scalable vector processing using streptavidin monolith affinity chromatography and preliminary results were encouraging with 20% overall yield.

In conclusion, we developed a single-step affinity chromatography which allows specific purification and concentration of infectious vectors modified with a biotin mimic. Based on intended usage, efficient LV purification can be achieved using both magnetic beads and column chromatography. This method will be of valuable use for both research and clinical applications of LVs.

Acknowledgments

I am truly grateful to my supervisors, Dr. Martin Pule, Dr. Yasu Takeuchi and Dr. Ekaterini (Nina) Kotsopoulou. Martin's unwavering support since I first joined the lab, along with his direction and insight have been vital for the success of this project and my focus throughout this PhD. Yasu's continuous guidance, rigorousness and thoroughness over the years were invaluable for the completion of this project. And finally, Nina's constant support, insight and encouragement throughout this work were crucial for the direction of this project, as well as my sanity.

I was lucky to be part of the Pule Lab with all its past and present members who have made this experience a truly unforgettable one: Gordon Weng-Kit Cheung, Eva Kokalaki, Farhan Parekh, Brian Philip, Shimobi Onuoha, Patrycja Wawryzyniecka, Cassandra Stowe, Paul Maciocia, Claire Roddie, Guilia Agliardi, Lydia Lee, Francesco Nannini, Ana Margerida Pinto De Campos, Alastair Hotblack, Annalisa Maggio, Vedika Mehra, Farhana Hussain, Simon Thomas and Shaun Cordoba**.** I am sincerely thankful for all their help, advice and mostly for filling the last 6 years with stimulating, though-provoking, laughable, wonderful and weird, with the occasional down-right unreal times. Also for humoring my never-ending questions and topics of conversation which went on against their wills I'm aware, and to Gordon goes the biggest.

I was fortunate enough to work within the hematology department of the Cancer Institute that is filled with kindest researchers that have never failed to offer a helping hand both scientifically and personally; with a very special thanks to Eva, Sara Caxaria, Solange Paredes and Micaela Harrasser; your friendship and support over the years have made this process infinitely lighter.

I am grateful for Prof Farzin Farzaneh and his team including Dr. David Darling and Dr. Glenda Dickson whose experience, advice, input and friendship were fundamental for the completion of this project.

I am also very thankful for the Takeuchi Lab's collaboration at NIBSC for their expertise and kind help with various equipment. Thanks to Dr. Giada Mattiuzzo and James Ashall for their advice and for the Nanosight experiments; and Dr. MacLellan-Gibson for the introduction and the use of electron microscopy.

My thanks are also owed to my friends outside of science who have navigated the volatile journey of my PhD with me. Their unfailing support and constant encouragement, even in the face of true pessimism, was indispensable for me throughout this period.

Last but not least, I would like to thank my family. I know I don't show it as much as I should but I am beyond grateful for everything they have done for me to allow me to get here. My biggest and warmest thanks to my parents' unwavering support and encouragement; and to my brothers' abilities to lighten up any challenge.

And finally, to my partner Hamoudi, who has trekked this journey with me from the very start; thanks for providing me endless inspiration and resilience that have eased this process and for constantly motivating me when I needed it the most.

Table of contents

List of figures

List of tables

Abbreviations

7DAPA	7,8-diaminopelargonic acid
AA	Amino Acids
AAV	Adeno-Associated Virus
AdV	Adenovirus
APC	Allophycocyanin
ASLV	Avian Sarcoma and Leukosis Virus
BSA	Bovine Serum Albumin
CAR	Chimeric Antigen Receptor
CCR5	C-C chemokine receptor type 5
CD	Cluster of Differentiation
CD8α-stalk	CD8-alpha Stalk Spacer Domain
CXCR4	C-X-C Chemokine Receptor type 4
ddH_20	Double Distilled Water
DMEM	Dulbecco's Modified Eagle's medium
eBFP	Enhanced Blue Fluorescent Protein
EGF	Epidermal growth factor
eGFP	Enhanced Green Fluorescent Protein
ER	Endoplasmic Reticulum
ELISA	Enzyme-linked Immunosorbent Assay
EtOH	Ethanol
FACS	Fluorescence-Activated Cell Sorting
FCS	Foetal Calf Serum
HEK	Human Embryonic Kidney
HIS	Histidine
HIV-1	Human Immunodeficiency Virus type 1
HRG	Heregulin
HRP	Horse Radish Peroxidase
hSCF	Human Stem Cell Factor
HSV-1	Herpes simplex virus
Ig	Immunoglobulin
IL	Interleukin
IMDM	Iscove's Modified Dulbecco's Medium
IRES	Internal Ribosomal Entry Site
Kb	Kilobase
K_D	Dissociation constant
LB	Luria Bertani
LTR	Long Terminal Repeat
LNGFR	Low-affinity Nerve Growth Factor Receptor
LV	Lentiviral Vector
M	Molar
mAb	Monoclonal Antibody
MACS	Magnetic Activated Cell sorting
MFI	Median Fluorescence Intensity
MHC	Major Histocompatibility Complex
MoMLV	Moloney Murine Leukaemia Virus
MLV-A	Murine Leukaemia Virus-Amphotropic envelope glycoprotein
mPEG	Monomethoxypoly(ethylene) glycol
NT	Non-transduced
ORF	Open Reading Frame
PBS	Phosphate-Buffered Saline
pCCL	Lentiviral 3rd generation vector backbone

PFA	Paraformaldehyde
PGK	Phosphoglycerate kinase
RD114	Feline Endogenous Virus Envelope Glycoprotein
RPM	Revolutions Per Minute
RPMI	Roswell Park Memorial Institute Medium
RT	Room Temperature
RV	Retroviral Vector
ScFv	Single Chain Variable Fragment
SFG	Retroviral vector backbone
ssDNA	Single-stranded DNA
Sulfo-NHS	N-hydroxysulfosuccinimide
TB	Terrific Broth
TBE	Tris/Borate/EDTA
VEGF	Vascular Endothelial Growth Factor
VEGFR	Vascular Endothelial Growth Factor Receptor
VSV-g	Vesicular Stomatitis Indiana Virus envelope glycoprotein

Thesis structure

This thesis developed a novel affinity chromatographic purification based the on biotin-streptavidin system for the manufacturing for gene therapy application. This thesis has the following structure:

Chapter 1 presents a review of the scientific literature for gene therapy, with an emphasis on LVs and their manufacturing. Chapter-specific literature is reviewed in each result chapter with discussion remarks.

Chapter 2 defines the experimental methods and materials used in this thesis.

Chapter 3 describes the construction of a membrane bound affinity tag biotin-mimic that reversibly binds to streptavidin.

Chapter 4 covers LV modification with the affinity tag for complete vector capture from viral supernatant using streptavidin magnetic beads.

Chapter 5 studies the desorption of captured vectors on magnetic beads by competitive elution using biotin and optimisation of elution buffer formulation for high overall yields.

Chapter 6 presents purified vector characteristics for product quality and purity in terms of both product- and process-related impurities.

Chapter 7 provides a study of scalability for the developed affinity chromatographic purification of LVs.

Chapter 8 offers a general discussion of the project with concluding remarks and ideas for future work.

Chapter 1 Introduction

1.1 Gene therapy

Gene therapy has seen dramatic changes in the last 28 years since the first human gene transfer experiment in 1989. This section offers a brief introduction to gene therapy with an emphasis on adoptive T cell transfer by (i) outlining major milestones that have defined the field, (ii) providing an overview of current ongoing gene therapy clinical trials and (iii) discussing some of the remaining challenges and limitations for the field's advancement.

1.1.1 An overview of gene therapy

Gene therapy is an emerging branch of medicine and regarded as a potential revolution in both health and pharmaceutical fields. It can be generally defined as the introduction of foreign recombinant gene into target cells for therapeutic application to treat diseases (Escors and Breckpot, 2010). In Europe, gene therapies are classified as Advanced Therapy Medicinal Products (ATMPs), which is an innovative class of therapeutics that include cell therapies and tissue engineered products in addition to gene therapies. The regulatory and legal context for ATMPs in the European Union (EU) was established by the EU commission in 2007 (Regulation EC No. 1397/2007) and applied in 2008. The European Medicine Agency (EMA) defines a gene therapy medicinal product (GTMP) as a biological medicinal product that:

- contains an active substance which contains or consists of a recombinant nucleic acid used in or administered to humans to regulate, repair, replace, add or delete genetic sequence
- its therapeutic, prophylactic or diagnostic effect relates directly to the recombinant nucleic acid sequence it contains, or to the product of genetic expression of this sequence.
- shall not include vaccines against infectious diseases.

The Food and Drug Administration (FDA) defines gene therapy as products:

- that mediate their effects by transcription and/or translation of transferred genetic material and/or by integrating into the host genome and that are administered as nucleic acids, viruses, or genetically engineered micro-organisms. The products may be used to modify cells in vivo or transferred to cells ex vivo prior to administration to the recipient.

Gene therapies' aim is to treat known causes of diseases instead of only treating the symptoms. Consequently, they may be effective on a range of currently untreated diseases such as neurodegenerative and haematological diseases and several cancers, which will be discussed in further details in later sections. The progression of gene therapy from concept to clinical application evolved from the 1960s to the 1990s due to the development of virus-based gene delivery vectors and recombinant DNA technologies (Friedmann, 1992). The first gene transfer study for human application was Federally approved in 1989 (Rosenberg et al., 1990), in which autologous tumour-infiltrating lymphocytes (TILs) were modified by retroviral vectors (RVs) and reintroduced into patients for the treatment of advanced melanoma. Although this study was not intended for a therapeutic aim, its results established both feasibility and potential of RVs for lymphocytes gene transfer (Edelstein et al., 2004). In 1990, the second federally approved study took place in which two pediatric patients with severe combined immunodeficiency (SCID) cause by adenosine deaminase (ADA)-deficiency (ADA^- SCID) were treated with autologous T cells transduced *in vitro* by retroviral (RV) vector expressing wild type ADA gene (Anderson et al., 1990; Blaese et al., 1995). Although this study did not result in the correction of the ADA^- immunodeficiency, the efficacy and safety of long term therapeutic treatment was demonstrated with transduced T lymphocytes cells found to persist up to 15 years later (Fischer et al., 2010). Due to these pioneering studies, the successive decade (1989-1999) witnessed the approval of close to 500 gene therapy trials worldwide, with its highest peak of 117 trials in 1999 (Ginn et al., 2013). Unfortunately, therapy advancements achieved during this period were overshadowed in 1999 when the first patient,

Jesse Gelsinger, was reported to have died as a direct consequence of gene transfer of adenoviral vector due to underreporting of serious adverse events to therapy (Hollon, 2000; Check, 2005; Couzin and Kaiser, 2005; Sheridan, 2011). In an effort to reinstate public trust in gene therapy research, the FDA and NIH instated new initiatives to provide greater protection for patients in gene therapy trials (McCarthy, 2000). However, in the years succeeding Gelsinger's case, the field suffered a further blow as several cases of insertional mutagenesis following γ-RV transduction were reported. A quarter of patients with X-linked SCID that were treated with autologous retrovirally transduced hematopoietic stem cells (HSCs) went on to develop T cell leukaemia. This was due to activation of proto-oncogenes as a result of RV integration (Fischer et al., 2010; Hacein-Bey-Abina et al., 2008). Insertional mutagenesis leading to the development of leukaemia were also reported in trials for the treatment of Wiskott-Aldrich Syndrome (WAS) (Galy and Thrasher, 2011) and for X-linked chronic granulomatous disease (X-CGD) (Grez et al., 2011). It is however interesting to note that insertional mutagenesis leading to oncogenesis has only been reported for genetically engineered HSCs as in marked contrast no adverse effects related to insertional mutagenesis have been reported yet in any patients infused with retrovirally modified T cells (Bonini et al., 2003; Brenner and Heslop, 2003). This observation was mirrored in animal models that have shown the lack of malignant transformation of retrovirally transduced T cells, unlike HSCs (Montini et al., 2006). Nonetheless, oncogenic formation associated with the use of early generations of RVs highlighted major safety concerns. This led to the improvement and development of analytical tools such as animal models to investigate insertional mutagenesis (Montini et al., 2009) and high-throughput analysis of insertional sites (Schmidt et al., 2007).

1.1.2 Current status of gene therapy trials

As of April 2017, a total of 2463 clinical trials related to gene therapy have been completed, on-going or approved worldwide since 1989, using the searchable database that is periodically updated on *The Journal of Gene Medicine* Gene therapy Clinical Trials Worldwide website

(http://www.wiley.com/legacy/wileychi/genmed/clinical/). The majority of clinical trials have been conducted in the USA (62.9%), followed by the UK (8.9%), Germany (3.7%), China (2.8%), France (2.3%) and Switzerland (2%). These trials are targeting several diseases and are presented in Table 1.1. Since cancer is the second leading cause of death in the West (Ortiz et al., 2012), around 65% of worldwide gene therapy trials are targeting cancer diseases with several strategies being used, most notably anti-tumour immunotherapy (Hinrichs and Rosenberg, 2014), which will be briefly discussed later.

Disease category	Gene therapy clinical trials	
	%	Number
Cancer diseases	64.5	1590
Monogenic diseases	10.5	259
Infectious diseases	7.4	182
Cardiovascular diseases	7.2	178
Healthy volunteers	2.2	54
Gene marking	2.0	50
Neurological diseases	1.8	45
Ocular diseases	1.4	34
Inflammatory disease	0.7	15
Others diseases	2.3	56
Total		**2463**

Table 1.1: Indications of gene therapy clinical trials from 1989 to April 2017. Data derived from Gene therapy Clinical Trials Worldwide website, (http://www.wiley.com/legacy/wileychi/genmed/clinical/).

The most common gene types transferred in these trials are antigens (19.2%), cytokines (15.2%), receptors (10.5%) and gene deficiency replacement (8.4%). Different types of vector types are employed to deliver the genetic material to target cells (Table 1.2) with modified viruses, termed viral vectors, used in 67.7% of gene therapy trials. Although non-viral method were first used due to their low cost and lack of insertional mutagenesis risk, the inherent ability of viruses to infect cells provided a more potent and stable gene transfer

delivery (Warnock et al., 2006). Adenovirus vectors (AVs) and RVs have been most commonly utilised, however due to the Gelsinger case and the occurrences of insertional mutagenesis, the field has drifted away from these vectors and moved towards the use of lentivirus-based vectors and adeno-associated viruses-based vectors (AAVs) (Sheridan, 2011). In January 2004, AVs and RVs were the dominant gene transfer delivery methods with 26% and 28% used in all trials, respectively; while 2.1% of trials used AAVs and the use LVs was minimal resulting in lack of reporting (Edelstein et al., 2004). By June 2012, the values of the formers had decreased to 23.3% and 19.7%, respectively, while the use of AAVs and LVs increased to 4.9% and 2.9%, respectively, in trials worldwide (Ginn et al., 2013). Following suit, as of April 2017, AVs and RVs have further decreased to 21.2% and 18.3%, respectively, while AAVs and LVs usage continues to increase to 7.3% and 6.3%, respectively, due to the advantages offered by these delivery vehicles, which will be discussed later for LVs.

Gene delivery vector	Gene therapy clinical trials	
	%	Number
Adenovirus	21.2	535
Retrovirus	18.3	462
Naked/plasmid DNA	17.1	431
Adeno-associated viruses	7.3	183
Vaccina virus	6.8	172
Lentivirus	6.3	158
Lipofection	4.6	116
Poxvirus	4.2	106
Herpes simplex virus	3.6	90
Others vectors	5.5	134
Unknown	3	76
Total		**2463**

Table 1.2: Types of viral vectors used in gene therapy clinical trials from 1989 to April 2017. Data derived from Gene therapy Clinical Trials Worldwide website, (http://www.wiley.com/legacy/wileychi/genmed/clinical/).

From April 2017, the majority of approved gene therapy trials (77.5%) are in Phase I or I/II, with a lesser portion in Phase II (17.4%) and very few studies in Phase II/III (1%) and Phase III (3.8%). This pattern is not unexpected due to the high attrition rate of 90% for clinical trials, with around 10% of new therapies within the pharmaceutical sector reach registration (Kola and Landis, 2004; Hartung, 2013). For cancer treatment, the success rates are even lower with just 5% of new therapies reaching registration (Kola and Landis, 2004). Seeing that gene therapy is an emerging field coupled with the adverse events witnessed in earlier studies, these percentages to reach registration are not unexpected; and as haematologist and president of Spark Therapeutics Katherine High mentioned "there were serious questions about whether gene therapy would ever make it" (Bender, 2016). Nonetheless, several gene therapy trials prevailed, mostly from small-scale academic studies, that "have the ability to powerfully reorient the field" says High. These small steps in studies proving efficacy of gene therapy have witness the boom of dozens of gene therapy start-ups (Bender, 2016). To date, four gene therapy products have been granted marketing authorisation. The first was Gendicine, from Shenzen SiBiono GenTech (China), which received market licensing from the State Food and Drug Administration of China in 2003 as an adenoviral vector carrying the p53 tumour suppressor gene for the treatment of head and neck squamous cell carcinoma (Pearson et al., 2004). In 2012, the EMA granted market approval to Glybera, from UniQure (Netherlands), an adeno-associated viral vectors containing functional human lipoprotein lipase (LPL) gene for the treatment of LPL deficiency (LPLD), a rare disease that inflames the pancreas (Bryant et al., 2013; Kastelein et al., 2013). In 2015, both EMA and FDA approved the oncolytic virus Imlygic (BioVex) a modified form of herpes simplex virus 1 to treat melanoma lesions (Rehman et al., 2016). And finally, in 2016, the EMA approved Strimvelis (GlaxoSmithKline) as the first RV *ex vivo* stem cell gene therapy for the treatment of paediatric ADA^{-}SCID (Schimmer and Breazzano, 2016). As gene therapies are approaching regulatory approval for marketing authorisation, several challenges to translate these therapies into commercial products are emerging as "it is only in the last couple of years that industry-sponsored programmes have achieved the

quality, robustness, safety and risk benefit at the levels necessary to gain regulatory approval" said Christian Meyer, chief medical officer at UniQure.

1.1.3 Future challenges

Gene transfer treatment using viral vectors represents a complex biological development of genetically engineered therapeutic products. Safety of these vehicles have proven to be of prime importance and improvements as well as refining exciting vector delivery systems are ongoing from both academia and industry. For examples, to reduce the risk of insertional mutagenesis, self-inactivating (SIN) viral vectors have been developed in which all promoter elements and enhancers have been deleted from the U3 region of the long terminal repeat (LTR) (Modlich et al., 2006). The first approval by the EMA granted to a gene therapy product, Glybera, has opened the door to other products seeking to gene therapy registration. With the advancement of gene therapies and their promising early results, for example of adoptive T cell therapy against B cell malignancies (Rosenberg and Restifo, 2015), an immediate concern is whether the current manufacturing practices are suitable for industrial large-scale applications. This is a concern that experts in the field agree to have received inadequate investment and attention to date and the field is witnessing the current maturation of viral vector manufacturing for scalable application (Sheridan, 2011; Dolgin, 2012; Segura et al., 2013; Merten et al., 2016).

For the commercialization of gene therapy vector products, two major obstacles are recognized (i) in the upstream process which is the lack of scalable bioprocessing that is compliant with Good Manufacturing Practice (GMP) standards and (ii) in the downstream process of vector purification and final formulation of the product (Denèfle, 2011). Fulvio Mavilio the scientific director of Généthon (nonprofit, France) described the vector processing as "primitive" and added "we're not talking about robust processes that can be scaled up for manufacturing. Not at all" (Dolgin, 2012). The fundamental problem for the upstream process is that vector production systems are usually based on adherent human-derived cell lines grown in monolayer for most viral

vectors such as adeno-associated viral (Chen, 2011), RV (Cruz et al., 2011) and LVs (Schweizer and Merten, 2010). Adherent cell based systems are difficult to scale up according to many experts in the field, as it requires the addition of extra cell culturing vessel (for scale-up) which is not feasible as it results in disproportionately large quantity of final vector product to be processed and quality tested (Sheridan, 2011). It is well recognized that this problem can be mitigated by the use of suspension-grown cells (Dolgin, 2012) or the use of adherent cell culture bioreactors allowing high cell density such as iCELLis® (Merten et al., 2016). A major hurdle in the downstream process of products are residual impurities from the upstream process, such as animal serum, nucleic acid contaminants and host cell protein (Segura et al., 2006), which will be thoroughly discussed in later section 1.3.4. These present a significant concern as they can cause unwanted immune responses in product recipient patients and thus the refinement of final vector product is a prerequisite in terms of gene therapy safety. Therefore, the development of commercially-viable, robust and scalable manufacturing routes is an area requiring significant attention for gene therapy products.

1.2 Lentiviral vector for gene therapy

In the previous section, a broad introduction to gene therapy has been provided and the specific application of lentiviral vectors as gene transfer vehicles for therapeutic application is examined in this section. As stated, the use of lentiviral vectors in gene therapy trials has increased from an unreported percentage of trials in 2004 (Edelstein et al., 2004) to 6.3% as of April 2017. The shift towards these vectors was mainly driven by several key characteristics and factors allowing them to become of increasing interest, such as their ability to transduce non-dividing cells as well as appear to have a safer insertion profile (Naldini et al., 1996; Sheridan, 2011). The general biology of lentivirus, followed by their development as viral vectors for gene therapy and their current therapeutic applications are outlined in this section.

1.2.1 General characteristics and biology of lentiviruses

Lentiviruses (LVs) are classified as disease causing pathogens that are characterized by a long incubation period, persistent and affecting multiple organs proving invariably fatality (Haase, 1986; Clements and Zink, 1996). LVs belong to a subfamily within the *Retroviridae* family of viruses, called *Orthoretrovirinae* which also includes α-, β-, γ-, δ- and ε-retroviruses (Durand and Cimarelli, 2011). However, unlike simple γ-RVs which encode a smaller genome composed of *gag-pol* and *env*, LV are complex viruses capable of encoding and expressing additional proteins by the use of the multiple splicing sites in their genome (Coffin et al., 1997). Due to the extensive body of work on the causative agent for AIDS, HIV-1 has become the most commonly engineered and used member of the lentivirus family as gene therapy vector (Lever et al., 2004). However, other family members such as HIV-2, equine infectious anamenia virus (EIAV), feline immunodeficiency virus (FIV), simian immunodeficiency virus (SIV) and bovine immunodeficiency virus (BIV) are being explored for safer and efficient gene transfer vectors (Binder and Dropulic, 2008). LVs consist of single-stranded (ssRNA) genome of 7-11 kilobases, of which two copies homodimerise and are packaged in enveloped viral particles surrounded by host lipid bilayer. Particles are slightly pleomorphic and spherical measuring ~80-120 nm in diameter (Vogt and Simon, 1999). A typical LV particle is depicted in Figure 1.1a with its main viral components. In LV native form, the two copies of RNA genome are bound to nucleocapsid (NC) proteins. This complex is enclosed within a capsid (CA) along with viral proteins required for LV life cycle (PR, protease; RT, reverse transcriptase; and IN, integrase). A layer consisting of the host cell lipid membrane encapsulates the viral core with matrix (MA) proteins interacting with transmembrane unit (TM) of viral envelope glycoprotein. The surface unit (SU) of the glycoprotein form its ectodomain and is responsible for cell receptor interaction that leads to viral infection (Wagner, 2008).

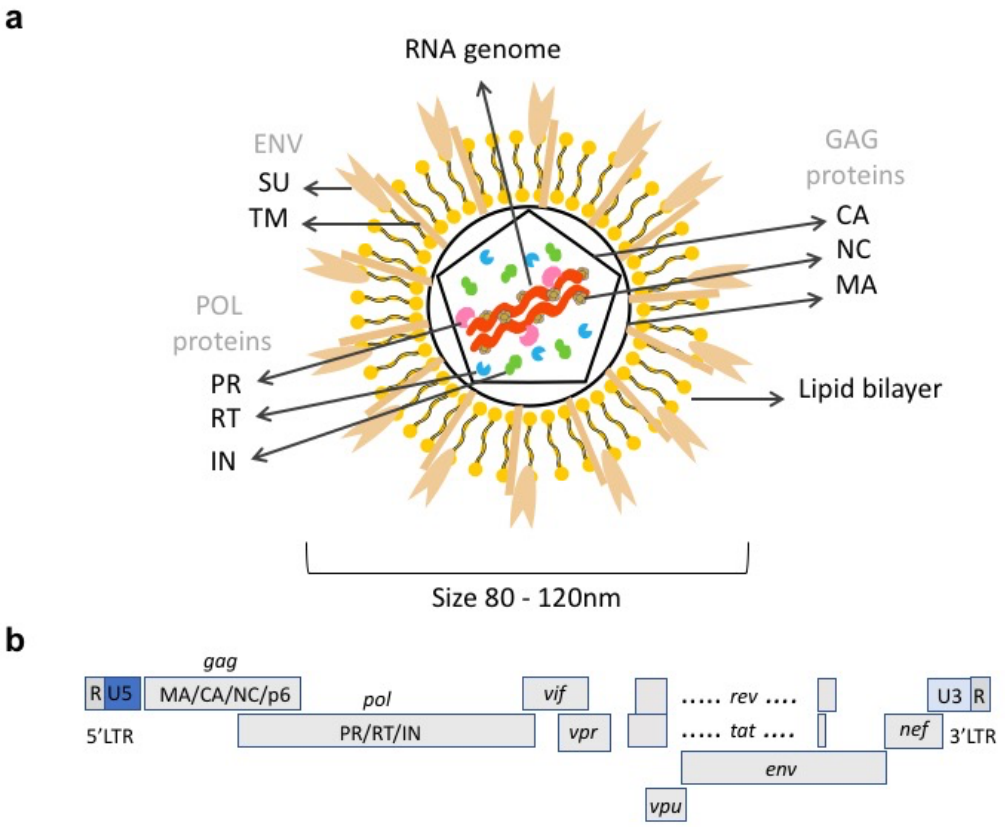

Figure 1.1: Architecture of HIV-1 virus and genome. (a) In viral particles, double stranded positive RNA strands encapsulated by viral proteins encoded by *pol* (PR, RT, IN) and *gag* (CA, NC, MA) genes. Virus is enveloped by ENV protein with host lipid bilayer. **(b)** Schemiatic diagram of HIV-1 RNA genome which is flanked by long terminal repeats (LTRs) containing R and U5 or U3 on genomes' 5'- and 3'- ends, respectively.

1.2.1.1 HIV-1 architecture: One RNA and fourteen proteins

The genetic organisation of lentiviruses is depicted in Figure 1.1b and is largely similar to the simple γ-RVs. The RNA genome is flanked on both sides by R (repeated) regions which contains transcriptions signals used in integrated proviral DNA. Following the R sequence at the 5' end of the genome is (i) a U5 non-coding cis-acting regulatory sequence (ii) a primer binding site (PBS) for cellular tRNA binding initiating reverse transcription, and (iii) a leader sequence that encompasses the genome packaging signal (ψ) as well as splice donor signals that are crucial for the generation of spliced mRNAs. The 3' end of the genome contains a polypurine tract that is fundamental for the generation of DNA from the RNA genome, followed by a U3 non-coding sequence and a second copy of the R sequence (Wagner, 2008). Similar to

simple γ-RVs, LVs genome encodes the structural and essential gene *gag, pol* and *env*; however as complex viruses, LVs also express additional accessory proteins allowing control of their gene expression and their unique life cycle enabling host cell manipulation for viral production, provirus entry and integration into host cell genome (Lever et al., 2004). Two regulatory genes *tat* and *rev* are involved on transcriptional and posttranscriptional levels, respectively (Farson et al., 2001). Tat protein promotes the transcriptional elongation by binding to the transactivation response (TAR) element in the U3 promoter of the 5'LTR; whereas Rev protein enables the nuclear export of unspliced viral RNA transcripts expressing the late viral proteins by binding to the rev-response element (RRE) (Kingsman and Kingsman, 1996). HIV-1 also carry the accessory genes *nef, vif* and *vpr,* which are common with the other members of primate immunodeficiency viruses and *vpu* that is exclusive for HIV-1 (Frankel and Young, 1998). Three distinct roles have been attributed to the Nef protein in infected cells. It has been shown to downregulate the surface expression of both CD4 molecule, one of HIV-1's host receptor, and the major histocompatibility complex I (MHC I), and enhance virion infectivity (Stumptner-Cuvelette et al., 2001; Neri et al., 2011). Vpr has been shown to be involved in nuclear import of the preintegration complex and the induction of a cell cycle arrest at the G2 phase which has been linked to an enhanced activity of HIV-1 LTR promoter (Fletcher et al., 1996). Vif protein has been shown to play an essential role in viral replication both *in vivo* and *in vitro* (Zhang et al., 2000). And finally, the HIV-1 specific protein Vpu has been demonstrated to both sequester and degrade CD4 molecules in the endoplasmic reticulum and to enhance virion budding from infected cells (Tanaka et al., 2003).

1.2.1.2 HIV-1 life cycle

A schematic representation of LV life cycle is shown in Figure 1.2.

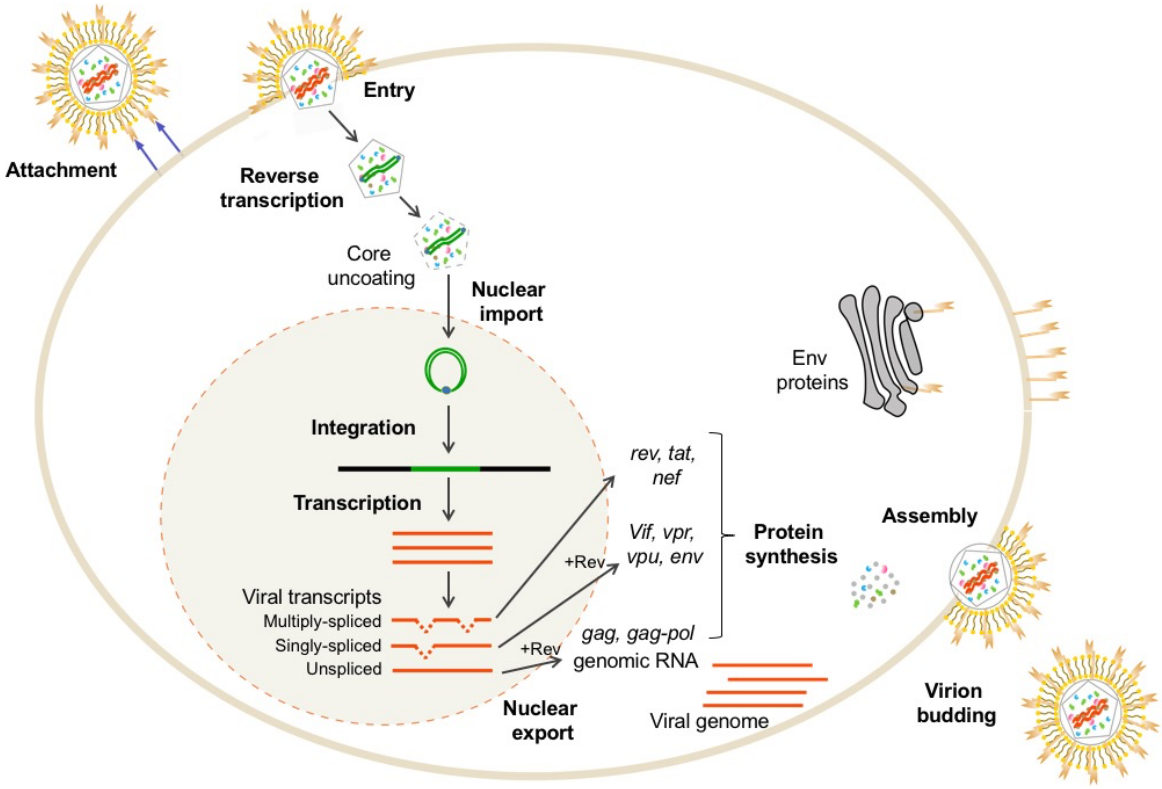

Figure 1.2: HIV-1 life cycle.

Attachment and entry

The LV lifecycle begins with viral entry which is initiated upon binding of the surface unit (SU) of envelope protein to its receptors on host cell surface. For HIV-1, its glycosylated proteins gp120 and gp41 represent SU and transmembrane (TMU) domain, respectively. Upon viral attachment to target cells, gp120 binds CD4 (Dalgleish et al., 1984), and this interaction induces a conformational change in the SU resulting in the exposure of conserved high affinity binding domains for subsequent interaction with co-receptors, CXCR4 (Feng et al., 1996) and/or CCR5 (Choe et al., 1996). Upon this binding, the TM gp41's fusion peptide, corresponding to a hydrophobic region, is exposed and interacts with host cell membrane leading to viral fusion and subsequent cell entry (Chan et al., 1997; Weissenhorn et al., 1997) . The fusion of HIV-1 virions with host cell membrane had been reported to occur in a pH-independent manner (McClure et al., 1990). A later study however demonstrated that virus

fusion can also occur after virion endocytosis in an endosomal compartment (Miyauchi et al., 2009).

Reverse transcription

Subsequent to fusion, the core is released into the host cytoplasm and reverse transcription commences by core rearrangement for the formation of the reverse transcription complex (RTC). Due to the complex nature of LVs, HIV-1 RTC has been shown to contain more protein than that of Molony MLV (MoMLV) RTC, with not only viral RNA, RT, IN, CA, but also with a phosphorylated MA and Vpr (Hu and Hughes, 2012). The reverse transcription of the *Retroviridae* family is one of its defining features. The viral protease catalyses the Gag-Pol precursor to generate an active form the heterodimer RT which is comprised of p66 and p51 subunits (Goel et al., 1993). Prior to nuclear entry, reverse transcription is performed and initiated by the binding of a specific cellular transfer RNA (tRNA), Lys3 to the PBS located downstream of U5. The synthesis of (-)ssDNA proceeds until the 5' end of the viral genome, including U5 and R, (Ratner et al., 1985; Marquet et al., 1995). Due to the instability of RNA:DNA duplex, RNA template is then degraded by the RNase H activity of RT, allowing the transfer of the newly synthesised (-)ssDNA to the 3' end of the RNA genome and hybridising to its R sequence. This priming 'hop' allows the synthesis of (-)ssDNA to the 5' end of the viral genome. Simultaneously, RNase H degrades the template RNA with the exception of RNase digestion resistant regions, namely the 3' polypurine tract (PPT) and the central PPT (cPPT), which in turn act as primers for the positive strand synthesis. This process proceeds from the 3' PPT to the end of the tRNA, whereby the synthesis is terminated upon RT encountering a methylated nucleotide in the primer. This complex process generates an area of homology at the PBS between the (+) and (-) ssDNA, allowing subsequent second strand transfer. Upon PBS alignment, a circular DNA intermediate is generated in which DNA synthesis of the positive strand is processed at both of the cPPT and transfer PPT. The synthesis of the former terminates at 100 nucleotides downstream of the cPPT at the central termination sequence (CTS), which due to its conformation, reduces the binding ability of RT leading to its termination.

This series of events leads to the generation of a 'DNA flap' between the cPPT and the CTS, theorized to aid nuclear entry (Charneau et al., 1994). Following another strand transfer, DNA synthesis continues in both direction to the end of the LTRs for the generation of blunt-ended DNA (Fuentes et al., 1996). As a result, the provirus contains a longer RNA genome with U3-R-U5 LTR found at the both ends.

Nuclear entry

The next crucial step for infectivity is viral uncoating, which is characterised by capsid loss before entry of the viral genome into the nucleus (Campbell and Hope, 2015). Precise sequences of events are not yet fully elucidated, however uncoating is known to be accompanied with the transition between RTC into the pre-integration complex (PIC); as successful reverse transcription has been shown to take place in the protected milieu provided by the capsid cone (Arhel et al., 2007; Jacques et al., 2016). Interestingly, inhibition of RT has been shown to delay uncoating suggesting that the former occurs later than the initiation of reverse transcription (Hulme et al., 2011). Although the extent of uncoating before the nuclear translocation of the RTC is not yet clear, the PIC composed of proviral DNA, MA, IN and Vpr enable nuclear import without the requirement of nuclear membrane breakage for chromatin access in non-dividing cells (Ambrose and Aiken, 2014). The molecular mechanism governing nuclear entry of PIC is not yet fully understood, however the presence of nuclear localisation signals in all PIC components may represent one possible hypothesis, with that of the IN appearing to be critical (Bukrinsky et al., 1993; Freed et al., 1995; Gallay et al., 1997; Zennou et al., 2000).

Integration

The integration of proviral DNA represents the second defining feature of LVs. This is catalysed by the IN which is also processed by the protease from Pol polyprotein. Although the organization of the integration complex between IN, proviral DNA and target DNA has yet to be determined, this process is

comprised of two catalytic steps: 3'-end processing and strand transfer. The first step occurs within the PIC in the cytoplasm and involves the cleavage of two conserved residues (CA) at both 3'-ends of the viral DNA, in a reaction exposing the terminal 3'-hydroxyl groups which in turn serve as attachment sites to host DNA (Miller et al., 1997). In the second nuclear step of integration, IN catalyses the insertion of processed proviral DNA strand transfer into target (Engelman et al., 1991). For HIV-1, the sites of target integration on two DNA strands are separated by 5 base pairs and after nucleophilic attack of target phosphodiester bonds via the 3'hydroxyle groups, proviral DNA is joined to target DNA. Due to the integration site separation of 5 base pairs for both target DNA strands, repair of this integration results in a direct duplication of the five base pairs which then flank the integrated proviral DNA. Accordingly, in the final strep of integration, the unpaired dinucleotide of the 5'ends of the proviral DNA are cleaved and the five base pair residues on both ends of the viral genome are repaired and ligated to target DNA, resulting in repeated residues flanking the provirus (Craigie, 2001). HIV integration does not appear to have specificity for host DNA site integrations, all the while favouring integration sites near active transcription units for HIV integration (Craigie and Bushman, 2012).

Transcription

Once the provirus has integrated into host genome, its transcription and translation is required for the production of infectious virions. Transcription is initiated at the 5' LTR, with the promoter in U3 and transcription start site in R, by the binding of cellular transcription factor such as TFIID and NFAT (Rittner et al., 1995; Raha et al., 2005; Bates et al., 2008). The transcription of proviral DNA results in different spliced (multiply or singly) and unspliced transcripts, all of which serve distinct functions. Non-structural proteins such as Tat, Rev and Nef are produced from multiply spliced transcripts, with Tat being the one of the first proteins to be translated. Tat proteins, owing to its name, then stimulates transcription initiations and elongation of RNA genome in a positive feedback loop by binding to the trans-activating response region (TAR) and recruiting different cellular proteins to the transcriptional complex, such as

Cdk9 and Cyclin T, thus increasing transcriptional efficiency by 100-fold (Romano et al., 1999; Kim et al., 2002; Schulze-Gahmen et al., 2014). The binding of Rev to Rev response element (RRE) in both singly and unspliced transcripts significantly enhances their nuclear export as well as increases their stabilisation (Pollard and Malim, 1998).

Translation

Singly spliced transcripts serve for the production of the remaining non-structural proteins along with the envelope glycoprotein; while the unspliced transcript serving as either template for structural proteins translation (Gag and Gag-Pol) or remaining unspliced transcript for virion packaging. The main structural proteins Gag is translated as precursor polyprotein containing MA, CA, NC, p6 and two spacer peptides, SP1 and SP2. Gag-Pol precursor polyprotein is translated by -1 ribosomal frameshit with 20:1 expression ratio of Gag:Gag-Pol (Shehu-Xhilaga et al., 2001). Post-translation, the recruitment of Gag to the plasma membrane leads to polyprotein multimerisation with the encapsidation of the viral genome by NC binding to the packaging signal, present only on the unspliced mRNA. Simulationsly, the translation of the envelope precursor glycoprotein, gp120 and gp41 for HIV-1, leads to its trafficking through the secretory pathway from the rough endoplasmic reticulum through the Golgi apparatus routing to the plasma membrane for virion recruitment (Checkley et al., 2011).

Assembly and Budding

The assembly of viral components leading to a membrane fission for the release of virions is mediated by the cellular endosomal sorting complexes required for the transport (ESCRT) pathway (reviewed in (Votteler and Sundquist, 2013)). Upon Gag multimerisation, factors in the ESCRT pathway are recruited, with ESCRT-III driving membrane scission at the virus budding site resulting in virion release from host cell surface as immature particles (Baumgärtel et al., 2011). Virions undergo maturation along with or immediately after budding by the cleavage of Gag and Gag-Pol polypeptides.

This proteolytic processing of particles results in dramatic protein rearrangement of immature spherical Gag into mature cone-shaped cores, giving rise to mature HIV-1 virions (John A.G. Briggs et al., 2003; Schur et al., 2015).

1.2.2 Lentiviral vector development and current applications

As mentioned earlier, several properties of LVs have allowed them to become a popular viral vector for genetic transfer. Similar to γ-RVs, LVs have the ability to stably integrate into target cell genome, allowing long term expression of transferred genes. However, unlike γ-RVs, LVs can also transduce non-dividing cells, such as neurons and haematopoietic stem cells, and enable the transfer of larger transgenes (Lewis et al., 1992; Naldini et al., 1996; Mátrai et al., 2010). The ability of LVs to integrate into quiescent cells has made these vectors very useful for many gene therapy applications. Although LVs transduction does not require cell division and subsequent nuclear membrane breakdown for genomic integration, cells must be stimulated to progress into the late G1 phase for efficient transduction (Sutton et al., 1999). In addition, LVs seem to have a reduced genotoxicity compared to γ-RVs, potentially due to their different pattern of integration (Qian et al., 2017), since MLV based γ-RV exhibit a preferential integration near transcription start sites (Mátrai et al., 2010; Craigie and Bushman, 2012). Moreover, LVs intrinsically low immunogenicity provides another safety advantage due to reduced capacity of innate immune responses (Abordo-Adesida et al., 2005).

LV development started in 1996 by Naldini et al., (1996) with successful *in vivo* transduction of rat neurons using an HIV-1 derived vector system that contained all HIV-1 genome proteins. This landmark study represented the 1st generation LV packaging system consisting of three plasmids, whereby all HIV-1 *trans*-acting sequences (i.e. viral encoding genes) were on one plasmid (the “packaging” plasmid), while regulatory cis-acting elements were supplied to a separate “transfer vector” plasmid, also encoding the transgene; and a third “envelop” plasmid encoding viral envelop glycoprotein such as murine leukaemia virus (MLV) amphotropic glycoprotein or the vesicular stomatitis

virus (VSV-g) envelope protein for a wider tropism (Naldini et al., 1996) (Figure 1.3).

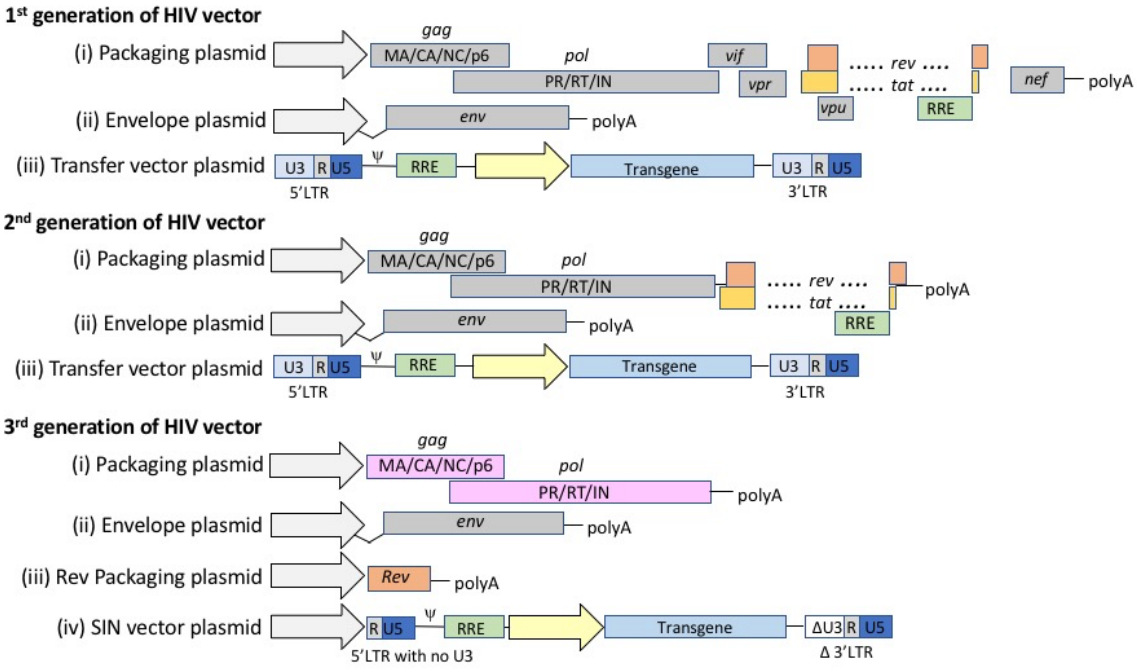

Figure 1.3: LV packaging generation systems based on HIV-1 genome. Three generations of packaging system are presented, where each plasmid is driven by a promoter (light grey arrow) and the transfer vector by an internal promoter (yellow arrow). Plasmids other than transfer vector terminate with a synthetic polyadenylation signal (polyA). 3rd generation system employs a self-inactivating (SIN) vector with a promoter fused to 5'LTR and mutated 3'LTR; also, a human codon-optimized *gag-pol* (light pink). ψ, HIV-1 packaging signal; RRE, rev response element.

The separation of HIV-1 genome into three plasmids minimized the chance of recombination events leading to replication competent lentivirus (RCL). However further improvements were required and since then several LV generations have been developed (mostly based on HIV-1) (Binder and Dropulic, 2008). Biosafety was increased with the 2nd generation system in which the accessory proteins vif, vpr, vpu and nef were removed (Zufferey et al., 1997). To further increase biosafety, 3rd generation packaging system was developed in which *tat* gene was removed and a constitutive promoter replaced U3 in the 5' LTR instead on the transfer vector, allowing for Tat-independent transcription of viral genome (Kim et al., 1998). Also to reduce

recombination events further, *rev* was supplied on a different plasmid (Dull et al., 1998). Moreover, although LV integration was reported to vary compared to γ-retroviral integration specifically in HSCs, the risk of insertional mutagenesis had to be mitigated (Biffi et al., 2011). This was achieved by the development of self-inactivating (SIN) transfer vectors in which all enhancers and promoters have been deleted from the U3 region of the 3'LTR, preventing the generation of full-length RNA vector in infected cells (Zufferey et al., 1998; Modlich et al., 2006). Finally, the inclusion of the woodchuck hepatitis virus posttranscriptional regulatory element (WPRE) in the transfer vector was shown to significantly enhance transgene expression (Zufferey et al., 1999), which was a critical progress that aided the advance of LVs to clinical application. In addition, further safety improvements were accomplished by the removal of residual sequence homology between transfer vector and packaging plasmid due to the presence of the packaging signal (Ψ) which is also present in the first base pairs of the *gag* gene (Swanstrom and Wills, 1997). This achieved by the codon optimization of the *gag-pol* constructs which rendered the translated gag-pol proteins rev-independent (Kotsopoulou et al., 2000), allowed the removal of the RRE from the packaging plasmid. Therefore, using the 3rd generation packaging system with codon optimized *gag-pol* further reduces the frequency of potential recombination events and thus improves the safety profile of LVs (Tareen et al., 2013).

The first LV-based clinical trial was initiated in 2003 for the treatment of chronic HIV infection using autologous CD4+ T cells transduced with an antisense gene against HIV envelope (VRX496^{TM}) (Levine et al., 2006). A decade after the start of this trial, a follow-up study of the 65 HIV-patient treated, reported no severe adverse events such as insertional mutagenesis, demonstrating the safety and efficacy of LVs for gene therapy applications (McGarrity et al., 2013). Up until April 2017, 158 lentiviral vector-based clinical trials have been conducted and a summary of these studies and their indications are presented in Table 1. It is interesting to note that up until 2012, LV-based trials had largely targeted monogenic diseases (n=22), although cancer diseases (n=15) was the leading cause of death in the West (Ginn et al., 2013). This observation may be explained by the fact that LVs, unlike adeno-associated viruses and

adenoviruses, can permanently and stably integrate therapeutic genes into target genome and therefore offer the potential of life-long cure of monogenic diseases (Qian et al., 2017).

Indications	Phases					
	I	I/II	II	II/III	III	Total
Cancer diseases						**83**
B cell malignancies*	23	11	10			
Melanoma	4					
Multiple Myeloma	3		1			
Neural cancers* adult/pediatric	7					
Sarcomas	1		2			
Lung squamous cell carcinoma	1	1				
Hepatocellular carcinoma	2	2				
Ovarian cancer	2					
Metastatic Expressing NY-ESO-1	4					
Mesothelin Expressing Cancer	1					
Metastatic Pancreatic	1					
Monogenic diseases						**45**
Sickle Cell anemia and beta-thalassemia	6	4			3	
X-linked chronic granulomatous disease		6	1			
Wiskott Aldrich syndrome	2	4				
Fanconi Anemia	2	1	2			
Childhood cerebral adrenoleukodystrophy				2	1	
X-Linked Severe Combined Immune Deficiency	2					
ADA deficiency		2				
Fabry disease	1					
Hemophilia A	1					
Hungtinton's disease	1					
Mucopolysaccharidosis Type VII	1					
Netherton syndrome	1					
Recessive Dystrophic Epidermolysis Bullosa		1				
X-linked ALD		1				
Hungtinton's disease	1					
Neurological disorders						**5**
Metachromatic Leukodystrophy and adrenoleukodystrophy		2				
Parkinson's Disease		2				
Amyotrophic Lateral Sclerosis		1				
Ocular diseases						**4**
Age-related Macular Degeneration	1					
Retinitis Pigmentosa Associated with Usher Syndrome Type 1B		2				
Stargardt's Macular Degeneration		2				
Infectious disease						**20**
HIV infection	10	8	1			
Cadriovascular disease						**1**
Peripheral Artery Disease	1					

Table 1.3: Indications of LV-based clinical trials from all phases performed up to April 2017. Data derived from Gene therapy Clinical Trials Worldwide website, (http://www.wiley.com/legacy/wileychi/genmed/clinical/).

However, by April 2017, not only has the total number of LV-based clinical trials almost tripled from June 2012 (n=55), there has been a dramatic increase in trials for the treatment of cancer disease (n=83) compared to monogenic disorders (n=45) (Table 1.3). This can be explained by the increase in the development in gene therapies such as hematopoietic stem cell gene therapy and anti-tumour immunotherapy. Moreover, immunotherapy is currently recognized as a fourth pillar of cancer treatments alongside, surgery, chemotherapy and radiotherapy; by harnessing the intrinsic mechanisms of the immune system to actively recognize and destroy tumours. As this is our laboratory's field of study, a brief overview of one of its main modalities, adoptive T cell therapy (ACT) will be discussed, in which tumour-specific cytotoxic T cells are infused back into a patient with the aim to hunt and eradicate tumour cells. There are numerous benefits of ACT compared to conventional treatments, as T cell responses: (i) are specific, so can distinguish between cancerous and healthy cells; (ii) can traffic to antigen expressing site thus tackling the challenge of metastasis; and finally (iii) maintain therapeutic activity against specific antigen years after initial treatment due to their response memory. As this is the scope of our laboratory's research, we shall briefly discuss the history and current status of immunotherapy using modified T cells. The first reported anti-tumour efficacy of ACT was demonstrated using Tumour Infiltrating Lymphocytes (TILs) grown from resected metastatic melanoma lesions and infused back into patients (Rosenberg et al., 1994). Even though results were encouraging, with a recent analysis indicating overall and complete response rates were almost 50% and 20% respectively (Rosenberg et al., 2011); TIL therapy has been limited to metastatic melanoma. The broad application of T cell anti-tumour efficacy can then be achieved by administration of T cells that have been genetically engineered *in vitro* to express tumour-specific-antigen receptor. These can either be α-β T cell receptors (TCRs) or chimeric antigen receptors (CARs). Desired antigen specificity could be achieved by the use of autologous gene modified T lymphocytes that express antigen-specific TCR or CAR. The use of TCR limits this strategy to intracellular antigens presented on major histocompatibility (MHC) molecules (Hinrichs and Rosenberg, 2014). Conversely, T cells engineered with antibody-based CARs provide an MHC-

independent approach to target extracellular antigens expressed on tumours cells. Now in their third generation, CARs are hybrid receptors that engage with their antigen typically through an extracellular single chain variable fragment (scFv). This is fused to an intracellular CD3-derived ITAM signaling chain and co-stimulatory signaling modules of CD28 and 41BB or OX40 (Cartellieri et al., 2010; Eshhar et al., 2014). The architecture of CARs currently used in clinical trials varies as no optimal structure has been proven. Most studies however use the hinge and transmembrane domains of CD8α or domains derived from Fc regions (Maus et al., 2014). The first study to determine anti-tumour activity of retroviral modified lymphocytes with a CAR against ovarian cancer-associated-antigen anti-folate receptor (FR) exhibited no adverse effects but due to short *in vivo* persistence of transduced T cells, no clinical benefit (Kershaw et al., 2006). Nonetheless, these findings demonstrated the safety of adoptive immunotherapy using retroviral modified CAR-T cells. After several attempts to treat solid tumours with CAR-T cells, which failed with severe effects (discussed in (Lamers et al., 2013)), different treatments of B cell malignancies (non-Hodgkin lymphoma, acute and chronic lymphocytic leukaemia) with retrovirally transduced anti-CD19-CAR T cells reported very promising results with complete remission and response (Brentjens et al., 2013; Kochenderfer et al., 2012, 2010). These encouraging results led to a surge of early phases clinical trials using lentiviral vectors for the treatment of B cell malignancies (Table 1.3). Most of these studies are currently in early phases of treatment with 23 trials in Phase I, 11 in Phase I/II and 10 in Phase II. And as these trials progress, the development of a scalable, cost-effective, efficient and GMP-compliant manufacturing processes remains a major challenge for the advancement of LVs into the clinic and eventually as therapeutic commercialized products for gene therapies (Ansorge et al., 2010; Schweizer and Merten, 2010; Segura et al., 2013).

1.3 Manufacturing of lentiviral vectors

As previously discussed, a pressing challenge for LV-based gene therapies is the establishment of scalable and efficient methods for vector bioprocessing. This section discusses current and upcoming lentiviral manufacturing approaches. The current bottleneck in LV-derived therapies are: (i) lack of scalable vector production in their upstream processing, (ii) elimination of process and product-derived impurities in vector downstream processes, (iii) concentration of viral vector for intended therapeutic purposes, and all the while (iv) retaining their infectivity throughout purification. With these in mind, the section covers all relevant applications and technologies with an emphasis of downstream processing of LVs.

1.3.1 Lentiviral vector pseudotyping

This concept was first described more than 55 years ago when it was observed that cells infected with two different viruses can produce phenotypically mixed virions (Granoff and Hirst, 1954; Závada, 1982). It involves the transfer of viral envelope glycoprotein, between different viruses. It provided the field with a simple tool to alter natural viral tropism. This played an essential role in the proliferative use of HIV-1 based vectors, as it's envelope protein has a very limited natural tropism that is highly specific for CD4-expressing cells. Envelope proteins are composed of mushroom-shaped trimer of heterodimers (Blumenthal et al., 2012). Each dimer consists of an extracellular surface unit (SU) attached to a transmembrane subunit (TM) by non-covalent interactions and a labile disulphide bond. After viral particle assembly and budding, for certain viral envelopes, such as MLV-A and RD114 variants, their cytoplasmic tail of TM proteins are processed by the viral protease at a site termed the R peptide, which produced mature TM proteins thus resulting in viral particle maturation (Green et al., 1981).

Viral vectors can now be redirected with a much wider tropism by replacing wild-type glycoproteins with foreign viral glycoproteins such as VSV-g for LVs due to the ubiquitous expression of its receptor (Bischof and Cornetta, 2010;

Finkelshtein et al., 2013). However, several limitations have been attributed to the use of VSV-g envelope such as toxicity at high concentration (Burns et al., 1993), sensitivity to human complement-mediated inactivation (DePolo et al., 2000) and stimulation of an innate immune response upon systemic administration (Pichlmair et al., 2007). Moreover, due to its fusogenicity, stable VSV-g expression induces host toxicity thus preventing its use in stable and continuous LV-producing cells (Ikeda et al., 2003). Several other γ-RV envelope proteins have been used to pseudotype LVs such as the amphotropic MLV envelope or the gibbon ape leukemia virus (GALV) envelope, which both uses sodium-dependent phosphate symporter Pit2, and Pit1, respectively (Kavanaugh et al., 1994; Leverett et al., 1998). Alternatively, the feline endogenous virus RD114 envelope can be used whose receptor a neutral amino acid transporter is widely expressed on many human tissues including HSCs (Tailor et al., 1999; Rasko et al., 1999; Kelly et al., 2000; Goerner et al., 2001; Hanawa et al., 2002; Green et al., 2004). Given the limitations of VSV-g, RD114 represents an attractive alternate envelope due to its receptor expression, lack of inactivation by sera and sustained vector stability (Hanawa et al., 2002; Ward et al., 2003; Bell et al., 2010). However, wild-type RD114 glycoproteins do not pseudotype LVs efficiently possibly due to their inadequate lentiviral incorporation and inefficient R peptide cleavage by HIV protease, which was circumvented by the modifications in RD114's C-terminal residues such as replacement of its cytoplasmic tail with the corresponding MLV sequence (Sandrin et al., 2002). An alternative improvement was achieved by the mutations in the R peptide cleavage sites which generating the RDpro variant envelope with increased LV pseudotyping efficiency (Ikeda et al., 2003). The RDpro protein was the primary envelope used in this project and a schematic diagram of its protein processing is depicted in Figure 1.4.

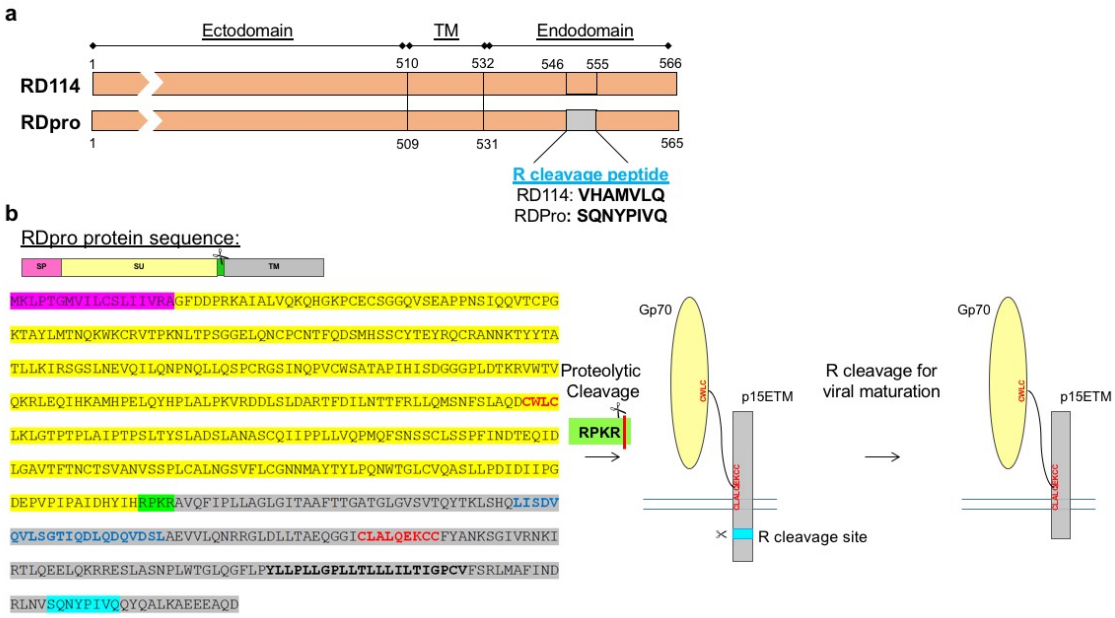

Figure 1.4: Protein processing of RD114 variant, RDpro envelope glycoprotein. (a) Schematic diagram of RD114 and its variant RDpro proteins with their difference highlighted being the R cleavage peptide site on glycoprotein's endodomian. **(b)** RDpro encodes precursor protein gp160 protein, which gets processed by furin (R-X-R/K-R) proteolytic cleavage (blue site) into a receptor binding domain surface unit gp70SU (361aa) and a transmembrane unit p15ETM (203aa) that are non-covalently linked. Post-budding, virion maturation is achieved by R cleavage site of envelop glycoprotein. SP: signal peptide, TM: transmembrane domain.

1.3.2 Lentiviral vector stability during bioprocessing

As mentioned previously, the clinical application of LVs for gene therapies requires the production of high viral titre preparations. One of the main challenges for high overall yield is the degree of complexity of this class of biology. To fully elucidate the ongoing limitations of LV manufacturing processes, viral particle stability should be emphasized as this parameter heavily influences their bioprocessing. Their inherent fragility is translated into low overall infectious recoveries which represents the main bottleneck in their processing. Therefore, to minimize their loss of infectivity, an understanding of vector stability, as well as their susceptibility to different elements would be advantageous prior to any downstream processing development.

Recombinant RVs are composed of 2% RNA, 36% lipid and 62% proteins (Andreadis et al., 1999). Thus, the lipid bilayer of viruses, the outer shell of particles, is an important factor for viral membrane fluidity and has been correlated with viral vector stability and infectivity (Beer et al., 2003). Several factors, affecting both viral membrane and components on the viral membrane such as envelope glycoproteins, have been shown to determine overall particle stability. The half-life of viral particles was reported to be affected by incubating temperature with a shorter stability at 37°C between 5 to 8 hours (McTaggart and Al-Rubeai, 2000); whereas vectors' half-life increases with a decrease in temperature with up to 8 days reported at 4°C (Higashikawa and Chang, 2001). Interestingly, the negative effect on LVs stabilisation by culturing temperature of 37°C leading to vector inactivation was reported to be caused by the loss of reverse transcription capacity (Carmo et al., 2008, 2009). Viral particle stability is in part determined by the fragility of envelope glycoproteins, as variations in the envelope proteins used to pseudotype lentiviral vector cores can determine vectors' stability, titres and target tropism (Naldini et al., 1996; Sakuma et al., 2010). As viral envelope proteins are responsible for target binding and subsequent viral fusion, the weakness of its interactions depict vector instability and in turn can cause vector inactivation. In addition, functional activity of viral vectors have been shown to be negatively impacted by the number of freeze-thaw cycles (Burns et al., 1993), which also is determined by pseudotyping envelope's rigidity to temperature alterations. Moreover, pH of both culturing conditions and viral resuspension medium has been regarded as an important factor affecting stability. Studies have demonstrated the effects of pH on particles activity with the highest stability attained at pH 7.0 at 37°C, which significantly dropped in less than 10 minutes at pH 6 or 8 (Higashikawa and Chang, 2001). However, a recent study demonstrated enhanced particle production and stability at pH 6.0 at 37°C, suggesting that a mildly acidic pH may positively impact vector stability (Holic et al., 2014). Therefore, within a narrow window of pH alterations, particle stability may be maintained or even enhanced. Thus pH-dependent particle effects seem to be correlated with effects on envelope glycoproteins, as at extreme pH (<5.5 and >8) viral envelope degradation resulted in fast and irreversible MoMLV inactivation (Ye et al., 2003). In addition, the effect of

culture medium osmolality was shown to also impact vector stability. The addition of high concentration of fructose, a slow metabolised sugar resulting in low levels of lactate production, has been described to improve vector stability (Merten, 2004). Moreover, an increase in osmotic pressure during vector production has been reported to enhance the stability of infectious particles (Coroadinha et al., 2006). Interestingly enough, this effect was attributed to a decrease in cholesterol content of viral membranes budding out from producer cells under higher osmotic pressure, and has been correlated with other studies supporting this notion for enhanced stability with more fluid vector membranes (Beer et al., 2003; Cruz et al., 2005). Conversely however, the use of high salt concentration as osmotic agent reduces vector infectivity by causing irreversible particle inactivation by morphological changes leading to broken particles (Segura et al., 2005; Coroadinha et al., 2006). Compounds such as NaCl, introduced or used in LV downstream processing, may result in vector inactivation leading to reduced overall yield. Additionally, a common desorption agent, imidazole, was used for immobilized metal affinity chromatography (IMAC), of tagged-RVs and was reported to negatively impact vectors as recovery of infectious particles increased from 35% to 56% by using half the concentration of imidazole (Ye et al., 2004). Moreover, RV sensitivity to EDTA was also described upon re-suspension of purified pellets (Pham et al., 2001). And finally, it is important to note that shear forces applied on vectors during centrifugation at high speed also majorly influences the stability of vectors and was recently reported to be a function of the type of internal viral core (Kim and Lim, 2017), as well as the established notion of mechanical stability of envelope protein (Burns et al., 1993). Therefore, both physical and chemical properties of viral particles, from their external membrane composition to internal shell formation, for each type of vector can affect their sensitivity to different stress causing agents. To attain high overall LV yield, all discussed parameters are important factors to consider for the isolation of such nanometre particles from viral supernatants. Consequently, their inherent fragility has led to a high cost of goods for their manufacturing and this elevated cost for vector production is recognised as one of the main challenges for the clinical application of gene therapy (Waehler et al., 2007; Nasri et al., 2014; Merten et al., 2016).

1.3.3 Upstream processing strategies

Scalable bioprocesses for LV production are still in their early stages of development. Several advances have been made in many aspects of the upstream processing of LVs for industrial manufacturing and are still ongoing. In this section, current methods for LV production will be discussed with an emphasis of large scale manufacturing of clinical vector material.

1.3.3.1 Transient transfection

1.3.3.1.1 Adherent cell lines

The most commonly used method for the generation of LVs has been by transient transfection of multiple plasmids into adherent HEK293-derived cells (Cockrell and Kafri, 2007; Gama-Norton et al., 2011; Schweizer and Merten, 2010). HEK293T express the SV40 large T antigen which has been shown to produce viral titre 4 to 10 fold higher than that produced with HEK293 cells (Ausubel et al., 2012; Merten et al., 2011). Although only slight changes have been made since its first application in 1990s, transient transfection production of LVs is a simple, fast and flexible method that produces high clinically relevant viral titres. In addition, this approach allows the use of cytotoxic vector components and transgenes. Accordingly, current GMP-compliant vector productions are based on transient transfection of HEK293-derived cells. As mentioned earlier, LVs are currently predominantly used by early phase clinical trials. These studies require a relatively small number of LVs and thus far, vector production by transient transfection has proved adequate. Current large-scale productions can be regarded as direct scale-up of small-scale research-grade vector production i.e. scale-out; whereby the culturing surface area is increased. This can be achieved by the use of vessels with increased culturing surface area such as Corning's HYPERflasks® which has been evaluated for LV production generating clinically relevant titres of 10^7 – 10^8 IU/mL (Kutner et al., 2009; Cooper et al., 2011). To date, the only culturing system reported to have been used in all clinical trials employing LVs is the Nunc™ Cell Factory™ (Thermo Fisher Scientific, USA) due to its ability to generate sufficient vector material for these studies. This culturing system is composed of multi-layered tissue culture trays with a culture surface area of

632 cm^2 and are usually used as 10-layer stacks (CF-10). Larger vessels can be used such as the CF-40 stacks devices, however their diminished presence in published reports is likely due to the requirement of specific handling system suitable to their increased height and weight. A summary of published GMP-compliant large scale transient vector productions from adherent cell lines are presented in Table 1.4. According to the number of CF-10 devices (12-24 devices) and the number of harvests from each, which is performed by a simple media exchange, final harvest volumes range between 20 and 52 liters from a single production run (Slepushkin et al., 2003; Negré, 2008; Merten et al., 2011). Larger volumes of more than 100 L of viral supernatant can be produced by employment of multi-production protocols over several weeks (Ausubel et al., 2012). However, although such processes can result in sufficient vector material, the requirement of a linear scale-out represents a major bottleneck for LV production from adherent cell lines. To overcome this issue, adherent cells can be seeded in a hollow fiber bioreactor, in which LV production occurs in a closed fully automated culturing system, unlike the CF-10 stacks. The potential of such a platform has recently been demonstrated by using the computer controlled Quantum bioreactor (Terumo BCT, Lakewood, CO) for transient LV production resulting in an increased vector yield equivalent to three CF-10 layer stacks (Sheu et al., 2015). To date, alternative culturing vessels that can produce large-scale vector volumes from adherent monolayers have been evaluated and hold promising potential for LV production.

Institution	Cell line - LV type	Culture system	No. of plasmids	Maximum production scale (L)	Bulk titre (IU/mL)	Reference
Virxsys	293 – HIV-1	N/A	2	36 – 52	$2.20x10^7$	(Slepushkin et al., 2003)
MolMed /Généthon	293T – HIV-1	CF-10	4	24 – 50	$1\text{-}5x10^7$	(Bellintani, 2009; Merten et al., 2011)
Oxford Biomedica	293T– EIAV	CF-10	3	72	$0.2\text{-}2x10^6$	(Stewart et al., 2010)
Beckman Research Institute	293T – HIV-1	CF-10	4	120	$0.5\text{-}1x10^6$	(Ausubel et al., 2012)
University of California Davis School of Medicine	293T – HIV-1	Hollow fiber system	4	N/A	$1\text{-}2.8x10^8$ vg/mL	(Sheu et al., 2015)

Table 1.4: Large-scale cell culturing for GMP-grade LV production. N/A, not available; vg/mL, vector genome per mL. Adapted from Merten et al., 2016.

1.3.3.1.2 Suspension cells

For the industrial manufacture of LVs, the use of bioreactors with a large surface area would be more suitable rather than culturing vessels relying on adherent monolayers. Adherent cell line compatible bioreactors can only be increased by a linear scale-out i.e. increase the number of vessels; and as a result leads to intensive labour and large equipment handling (Andreadis et al., 1999; Warnock et al., 2006; Schweizer and Merten, 2010; Merten et al., 2016). The use of suspension cell lines is thus more appropriate allowing the ease of scaling up for industrial vector production using compact bioreactors. Several cell lines that are used for vector production, such as 293T and 293FT, have been reported for suspension culture adaptation, with up to 50L scale has been demonstrated using single-use bioreactors (Ansorge et al., 2009; Witting et al., 2012; Marceau and Gasmi, 2013). Interestingly, reported viral titres for suspension culture which range from 10^7 to 10^8 IU/mL, are similar to the values published for adherent cell system ranging from 10^6 to 10^8 IU/mL (Sena-Esteves et al., 2004). It should be noted however that due to inherent differences in these reported studies, such as type of vector and analytical procedures conducted for infectious titre quantification, their relative

comparison is difficult. A limitation however in the use of suspension cells is the difficulty of multiple viral supernatant harvests which effectively increases cost. Unlike adherent cells, viral supernatant cannot be collected independently from suspension cell cultures. This can be overcome by the use of a perfusion system which would enable the continuous harvest of labile LVs (Shirgaonkar et al., 2004). The feasibility of such a complex system has been demonstrated by Ansorge et al., (2009) enabling successive medium harvests and replacement throughout 7 days. Although perfusion harvesting methods would increase manufacturing cost of goods, their potential for efficient transient transfection production is very promising. The half-life of LVs rapidly decreases at 37°C, the temperature of their production (Carmo et al., 2008, 2009). Their continuous harvest into a lower temperature would preserve thus vector infectivity until final collection. In addition, larger volume of viral supernatant can be harvested with a constant amount of plasmid DNA, thus lower the high cost of goods related to transfected plasmids, which represents a major bottleneck in the economics of transient vector production (Merten et al., 2016). Therefore, large-scale vector production by transient transfection of suspension cells holds promising productivity with adequate economics. Though further developments are necessary for its industrial translation in vector manufacturing.

1.3.3.2 Packaging and producer cell lines

With the current progression of LVs as a therapeutic product, the lack of stable and scalable manufacturing processes based on transient transfection is a rising concern (Ansorge et al., 2010; Segura et al., 2013). The current transient transfection scheme of both adherent and suspension cells, are impractical for the generation of licensed vector products as: (i) it is cost-ineffective resulting in high costs of goods for manufacturing, (ii) technically difficult to scale up, all the while (iii) retaining reproducibility thus suffering from batch-to-batch variability due to variation in transfection efficiency and plasmid expression, and (iv) results in significant quantities of naked DNA contaminations in the viral supernatant (Ansorge et al., 2010; Cockrell and Kafri, 2007; Schweizer and Merten, 2010; Segura et al., 2013; Stewart et al., 2009). To overcome these limitations, the development of stable packaging (containing all viral

components without transfer vector) and producing (containing all viral components as well as transfer vector) cell lines would provide the required production characteristics for large scale manufacturing and commercialization of LVs. However, unlike RV, the establishment of a stable LV producer cell line has proved challenging for the field as several proteins have been reported to be cytotoxic/cytostatic; thus preventing their constitutive expression, such as the protease (Kaplan and Swanstrom, 1991; Nie et al., 2002) and the most commonly used envelope VSV-g, causing syncytium formation in expressing cells (Ory et al., 1996; Yee et al., 1994). Nonetheless, several groups have published the generation of LV stable packaging and producing cell lines and detailed information are presented in Table 1.5. To overcome VSV-g's cytotoxicity, different expression regulatory methods were used, with tetracycline induction being the most common, with induction by addition (Tet-ON) or removal (Tet-OFF) of doxycycline (Farson et al., 2001; Kafri et al., 1999; Klages et al., 2000; Nie et al., 2002; Throm et al., 2009; Xu et al., 2001). Non-inducible vector producing cell lines have also been developed using alternative envelopes such RDpro and another RD114 chimera, RD114-TR (Di Nunzio et al., 2007) that was also developed to pseudotype LVs with higher efficiencies, have been used in packaging cell lines (Ikeda et al., 2003; Stornaiuolo et al., 2013; Sanber et al., 2015; Marin et al., 2016). More recently, another alternative envelope protein, that is closely related to VSV-g but differs in its lack of cytotoxicity, the cocal vesiculovirus envelope glycoprotein (Cocal) was used for the generation of LV producing cell line (Humbert et al., 2016). Another important factor to consider for optimal vector production is the method of LV plasmids integration into packaging/producing cell lines. The most common integration method used is transient transfection of LV packaging plasmids with antibiotics selection. One of its major drawback however is attenuation of expression as it has been shown to eventually result in gene silencing and expression loss (Bestor, 2000). Moreover, the use of antibiotics in LV production for human clinical trials is highly undesirable as they need to be removed from final product and require filtration through 0.2-0.22μm as a final step, which has been shown to decrease viral titre (Ausubel et al., 2012). Alternative strategies have been used for *gag-pol* and *rev* genes integrations, such as retroviral transduction

(Ikeda et al., 2003; Throm et al., 2009); recombinant hybrid baculo-AAV vector (Stornaiuolo et al., 2013) and cre-recombinase mediated cassette exchange (RMCE) technology for plasmids integration into a highly transcriptional active part of the genome (Sanber et al., 2015).

Parental cell line	Method of packaging plasmids integration	Regulatory system for expression	Pseudotyping envelope	Vector	Titre (IU/mL)	Reference
HeLa	Plasmid transfections. Clonal selection using antibiotics.	Tet-OFF	HIV-1 Env	HIV-1	7.0E+03 PACK	(Yu et al., 1996)
HeLa		Tet-OFF	HIV-1 Env	HIV-1	3.5E+04 PACK	(Kaul et al., 1998)
HEK293		Tet-OFF	VSV-g	HIV-1	3.0E+06 PROD	(Kafri et al., 1999; Xu et al., 2001)
HEK293		Tet-OFF	VSV-g	HIV-1	5.0E+06 PROD	(Klages et al., 2000)
HEK293		Tet-OFF	VSV-g	HIV-1	5.1E+05 PACK 6.6E+06 PROD	(Farson et al., 2001)
HEK293T		Ecdysone-ON	VSV-g	HIV-1	1.2E+05 PROD	(Pacchia et al., 2001)
HEK293		Ecdysone-ON	VSV-g	HIV-1	3.0E+05 PACK	(Sparacio et al., 2001)
HEK293T	MLV transduction of HIV Gagpol followed by plasmids transfection. Antibiotics selection used.	N/A	RDpro	HIV-1	1.4E+07 PACK	(Ikeda et al., 2003)
HEK293	Transfection. Clonal selection using antibiotics.	Ecdysone-ON	VSV-g	SIV	2.6E+05 PACK 2.4E+05 PROD	(Kuate et al., 2002)
HEK293	Concatemer array technique (co-transfection of linearized plasmids).	Tet-OFF	VSV-g	HIV-1	3.5E+07 PACK	(Ni et al., 2005)
HEK293	Transfection. Clonal selection using antibiotics.	Tet-OFF	VSV-g	HIV-1	2.4E+06 PACK 1.0E+07 PROD	(Cockrell et al., 2006)
HEK293T		Tet-OFF	VSV-g	HIV-1	5.0E+07 PACK	(Throm et al., 2009)
HEK293		Tet-ON	VSV-g	EIAV	1.6E+06 PACK	(Stewart et al., 2009)
					4.4E+05 PROD	(Stewart et al., 2011)
HEK293T	Concatemer array technique (co-transfection of linearized plasmids).	Tet-OFF	VSV-g	HIV-1	3.0E+07 PROD	(Lee et al., 2012)
HEK293T	RD-MolPack system: Recombinant hybrid baculo-AAV vector for gagpol-rev with *hygro* resistance. VSV-g SIN-LVs transduction of env and transfer vector.	N/A	RD114-TR	HIV-1	3.0E+05 PACK 1.2E+06 PROD	(Stornaiuolo et al., 2013)
HEK293T	Concatemer transfection. Clonal selection using antibiotics.	Tet-OFF	VSV-g	HIV-1	1.0E+07 PROD	(Wielgosz et al., 2015)
HEK293FT	HIV-1 Gagpol integrated via Cre recombinase-mediated cassette exchange (RMCE). Plasmids transfection. Clonal selection using antibiotics.	N/A	RDpro	HIV-1	1.0E+06 PROD	(Sanber et al., 2015)
HEK293T	Transfection. Clonal selection using antibiotics.	N/A	Cocal	HIV-1	1.9E+06 PACK 1.0E+06 PROD	(Humbert et al., 2016)
HEK293T	RD-MolPack system: Recombinant hybrid baculo-AAV vector for gagpol-rev with *hygro* resistance. VSV-g SIN-LV transduction for *tat* and env with *puro* selection. Transfection for SIN-transfer vector with *zeo* selection.	N/A	RD114-TR	HIV-1	1.8E+06PROD	(Marin et al., 2016)

Table 1.5: Published LV packaging and/or producing cell lines. N/A, not available.

The use of stable producing cell line for clinical-grade vector production would effectively reduce the cost of manufacturing, all the while enhancing the development and implementation of these vectors for their applications in late phase clinical trials. To the best of our knowledge, one report to date has been published for GMP-grade large scale vector production for the treatment of SCID-X1, using Throm et al., (2009) VSV-g stable inducible cell line. The production strategy utilizes a 50L WAVE bioreactor (GE Healthcare, UK), which consist of a disposable bag chamber that can be rocked mechanically to facilitate oxygen transfer and fluid mixing. The culturing of producing cells onto Fibra-Cel discs which were suspended in the bioreactor allowed the production of 138 L of 0.5-1 $x10^7$ IU/mL of viral supernatant by continuous vector harvesting for 3 to 8 days post induction (Greene et al., 2012). Based on these encouraging results, more recently, the same producing cell line was further engineered for the generation of clinical grade LVs for Wiskott-Aldrich syndrome treatment (Wielgosz et al., 2015). In this report, further improvements in the producing cells were achieved by the addition of the chicken hypersensitive site 4 (HS4) chromatin insulator in the deleted U3 region of the hWASp transfer vector to avoid transgene silencing by chromatin condensation (Gaszner and Felsenfeld, 2006). Accordingly, isolated producer clone was reported to produce a stable viral titre of 1.0 $x10^7$ IU/mL for up to 8 weeks in culture and are planned to be utilized in the near future in clinical trials at the St. Jude Children's Research Hospital (Bonner et al., 2015).

1.3.4 Downstream processing strategies

With the current advancement made in upstream LV processing for increased harvest volumes and vector yields, their downstream processing is recognised as an important factor in LV manufacturing for higher overall productivity of viral vectors with decreased costs of goods. In biopharmaceutical manufacturing, downstream processing is estimated to account for 75-80% of operational costs (Kramberger et al., 2015). Following viral supernatant harvest, downstream processing is vital for the (i) purification of viral vector from surrounding contaminants and impurities that may impact safety and efficacy, (ii) concentration of harvested low-titre viral supernatants for gene therapy applications and (iii) final vector formulation in appropriate buffer for subsequent use and stability (Segura et al., 2006; Merten et al., 2014). Over the past several years, considerable advancements have been made for vector design and large scale production, however less effort has been invested in the development of purification processes to handle large vector volumes. As gene therapy can be currently regarded as an emerging field, regulatory agencies have not yet defined strict guidelines on vector manufacturing in regards to critical product quality for safety and potency. Thus, as treatments approach commercialisation, these guidelines are likely to be reassessed with emerging clinical data. It is worth noting that many of the current applied processes have been largely adapted from technologies originally developed for recombinant protein purification by exploiting size and surface characteristics of viral particles. However, given the inherent fragility of LVs (discussed in section 1.3.2), maintaining viral infectivity throughout the sequential steps of purification is vital for any purification schemes. This section will provide a detailed understanding of both (i) the composition of viral vectors in terms of contaminants and (ii) general downstream processing steps with the current technologies employed for LV purification. This section covers both clinical and research-grade vector productions, with an emphasis on the former.

1.3.4.1 Compositions of vector products

Post-production, harvested viral supernatants undergo a series of processing steps that are aimed at removing impurities while retaining functionality of vectors. Two broad types of contaminants can be found in viral supernatants due to the nature of their production, which are depicted in Figure 1.5. Product-related impurities represent molecular contaminants derived from viral vectors which can impact intact vectors' functionality. These include non-infectious physical particles which may be (i) intact defective/empty virions, (ii) particles lacking the glycoprotein envelopes or (iii) damaged particles (Yang et al., 2012). Interestingly, the majority of virions produced from host cells are non-infectious physical particles (Thomas et al., 2007). The ratio of transducing unit (or infectious particle) over physical particles (TU:PP) is well recognized parameter of vector product purity (Zimmermann et al., 2011) and the reported ratio for HIV-1 have a very wide range of 1:100 (Bourinbaiar, 1994), 1:10,000 (Klasse and McKeating, 1993), to 1:100,000 (Klasse, 2015). The reported discrepancies of the TU:PP ratio is likely caused in part by experimental differences between published reports. Nonetheless, it should be kept in mind that infectious particles represent a small portion of total physical particles and downstream processing methods should aim for the concentration of infectious particles with a TU:PP ratio closer to 1 demonstrating vector efficacy. Viral aggregates and soluble envelope proteins can also be found in viral supernatants, which have been shown to act as transduction inhibitors by competitive binding to cellular receptor thus competing with envelope proteins on infectious particles (Kwon et al., 2003). The elimination of these impurities represents a challenge for most methods applied for LV downstream processing, as they share common physical and chemical characteristics to functional particles (Segura et al., 2013). The second type of contaminants are process-related impurities which are derived from different elements used in vector production such as (i) animal serum from culture medium, (ii) residual DNA plasmids and transfection agent from transient transfection production process, (iii) host-cell derived elements such as proteins and nucleic acids, and finally (iv) contaminants from the purification process itself such as nucleases and buffers compositions. The quantification of these impurities in

the final vector product is a regulatory prerequisite analysis to determine purity and quality levels. The methods employed for the detection and quantification of the main vector impurities (both process- and product-related) will be thoroughly discussed in Section 6.2.

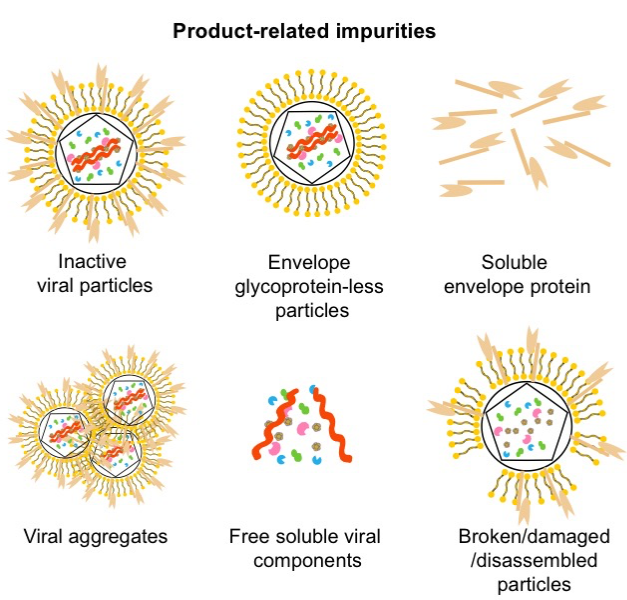

Process-related impurities	
Culturing medium derived	• Serum • Proteins, peptides, aminoacids • Lipids, phospholipids • Salts, sugars and buffer trace elements like vitamins
Production derived	• Plasmids DNA • Transfection agent • Endotoxins
Host cell derived	• Host proteins • Host nucleic acid • Membrane vesicles and cell debris • Protoeglycans
Purification derived	• Nucleases • Buffers components such as salt • Detergents

Figure 1.5: Commonly found product and process-derived impurities in LV viral supernatants.

1.3.4.2 Overview on clinical grade downstream processes

Due to the infancy of gene therapy trials, regulatory authorities are currently satisfied with only provided information of vector impurities characterisations by final product release testing. In the UK, BioReliance is commonly used for GMP testing of final vector product demonstrating compliance with regulatory guidelines. Of interest, these guidelines according to the FDA Title 21 of Code of Federal Regulations Part 211.165 and Part 610 of the General Biological Products Standards, do not specify quantitatively acceptable levels of contaminants such as nucleic acid or host cell proteins, with only the following stated; “If serum is used at any stage, its calculated concentration in the final medium shall not exceed 1:1,000,000”, Subpart 610.15. Removal of product-

and process-related contaminants is an essential prerequisite for any downstream processing schemes of viral vectors; as removal of serum and derivatives from producer cell line have been shown to prevent immune responses and local inflammatory and immune responses *in vivo* (Scherr, 2002; Baekelandt et al., 2003) as well as decrease transduction efficiencies *ex vivo* (Yamada et al., 2003). Therefore, for clinical applications, several purification steps must be undertaken for viral supernatants to ensure safety, quality and potency. A general flow outline of the typical steps involved in published downstream processing schemes is shown in Figure 1.6. Given the lability and biological complexity of LVs, a downstream processing scheme with few steps and change in vector medium composition is highly desirable to both minimize vector inactivation and to retain maximum levels of infectivity (Segura et al., 2011).

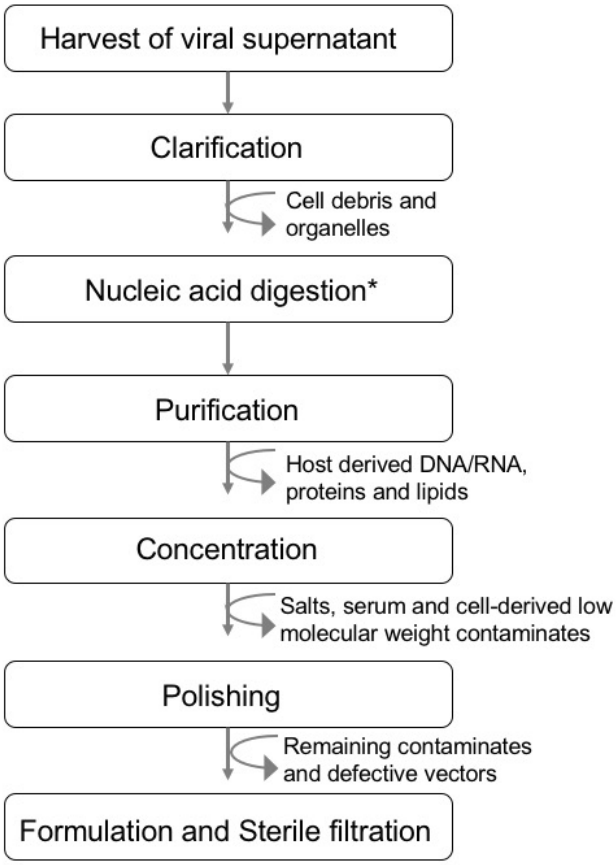

Figure 1.6: General steps in LV downstream processing. Adapted from Segura et al., 2006. (*) Nuclease treatment only applicable for vector production using plasmid transfection and can be found at different stages on downstream processing.

Current large scale processing of clinical-grade LVs employs several methods in the multi-process of viral downstream processing. By combining individual technologies, these schemes ultimately aim at capturing viral particles, eliminating contaminants and polishing vectors products, depending on type of virus and intended application requirements in terms of production size (Schweizer and Merten, 2010; Wolf and Reichl, 2011). Few complete schemes are described in the literature in details from supernatant harvest to final product, with overall recoveries in the literature. A summary of clinical-grade purification 'trains' from different institutions are depicted in Figure 1.7 with overall yields ranging between 20-40%. Currently, overall yields higher than 30% are considered acceptable for human pharmaceutical vector products (Wolf and Reichl, 2011; Segura et al., 2013).

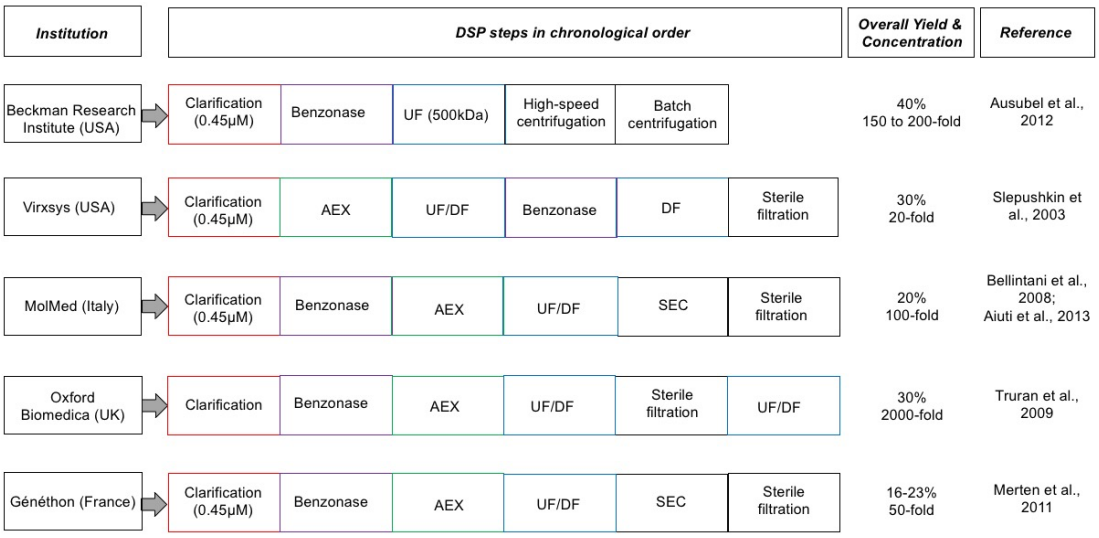

Figure 1.7: Summary of downstream processing for the manufacturing of clinical grade LVs. AEX, anion exchange chromatography; UF, ultrafiltration; DF, diafiltration; SEC, size exclusion chromatography. Adapted from Merten et al., 2014.

1.3.4.3 Clarification

Clarification of harvested viral supernatant is the first step in the downstream step required for the elimination of producer cells and cell debris to provide a 'cleaner' viral particle-feed for the subsequent purification steps. For research scale production, this is accomplished by centrifugation followed by microfiltration through 0.45µm low protein binding membranes (e.g. PVDF) (Segura et al., 2006). For large scale purification, a single-step clarification is preferred and is usually achieved by dead-end membrane filtration, in which the feed moves directly towards the membrane filter. Although practical, this may cause membrane clogging which in turn may lead to vector loss resulting in reduced recoveries. Moreover, with the use of bioreactors, the amount of cell debris may pose a challenge for single-step filtration methods. Alternatively, a depth filtration can be employed which consists of a fibrous structure which removes impurities either by mechanical entrapment or adsorption by electrostatic interactions, usually employing capsule of 0.8±0.45 µm pore sizes (Venkiteshwaran et al., 2015). The use of depth-filtration for large vector volume processing is scalable with good economics and thus has been demonstrated for large scale clarification of LV supernatant with >90% recoveries (Kutner et al., 2009; Bandeira et al., 2012). In addition, clarification of large vector volumes, which are representative of clinical material, have been demonstrated with efficient debris clearance using step filtration with decreasing pore sizes thus minimizing membrane clogging (Reeves and Cornetta, 2000; Segura et al., 2005; Slepushkin et al., 2003; Merten et al., 2011). This method is attractive due to the lack of prior centrifugation step thus resulting in efficient clarification with minimal loss of functional vectors.

1.3.4.4 Concentration

One of the main current limitations of LVs for gene therapy applications is the low concentration yield, in terms of TU per mL, attained which is insufficient for therapeutic applications *in vivo* and *ex vivo*. Therefore, following clarification, viral supernatants are concentrated early in the multi-step purification schemes which is a timely advantage as it reduces the feed volume

for subsequent steps and thus in turn decreases the size of required equipment (columns, vessels and pumps, etc.).

1.3.4.4.1 Centrifugation

The most widely used method for research-grade LV isolation is ultracentrifugation (UC). Concentration factors up to 100 have been reported using this method and both high-speed (20,000 – 90,000xg for 2 hours) and low-speed (6,000 – 7,000xg for 16 – 24hours) centrifugation can be used to purify and concentrate viral particles (Segura et al., 2006). Although very efficient in small particle sedimentation, UC suffers from several disadvantageous for large scale applications. Its long processing times and harsh hydrodynamic shear forces required for viral pelleting have been shown to result in partial loss of vectors, hence the proliferative use of VSV-g envelope to confer increased particle stability during UC (Burns et al., 1993). Although UC has been used for the purification of clinical-grade LVs (Ausubel et al., 2012), its limited volume capacity and in turn difficulties in reproducible viral pellet resuspension (Zhang et al., 2001), represent UC's main disadvantageous for scaled-up purifications. And finally, the use of this method results in the sedimentation of both process and product derived-impurities along with viral vectors thus resulting in a reduced potency of LVs and requirement of further purification schemes for their removal (Transfiguracion et al., 2003; Slepushkin et al., 2003). Alternatively, density gradient UC (DG-UC) can be employed for the concentration and isolation of particles, with sucrose and cesium chloride being the most widely used gradient media for LV purification (Segura et al., 2005). Although this powerful method enables the separation of LVs from different impurities such as defective vectors, it suffers from several disadvantageous such as loss of infectivity due to high viscosity of gradient medium, difficulty to scale-up, with long processing times and requiring technical expertise (Segura et al., 2006). Therefore, the implementation of adsorption chromatographic methods were strongly encouraged to replace purification methods relying on centrifugation due to their numerous disadvantageous (Andreadis et al., 1999).

1.3.4.4.2 Ultrafiltration

Ultrafiltration (UF) represents the method of choice for current viral particles concentration due to its gentle conditions, ease of scalability, efficiency in volume reduction and adaption to GMP manufacturing (Segura et al., 2006). Conveniently, in addition to vector concentration UF provides a level of purification for viral supernatant by the washing off impurities, through the enrichment of viral particles in the retentate and the removal of solution and small molecular weight molecules with the permeate. Typically, pore sizes ranging from 100 to 500kDa are used for UF of LVs, with greater pore sizes resulting in greater purity with shorter processing time (Rodrigues et al., 2007). Additionally, diafiltration (DF) can be combined to the same UF unit providing a convenient and efficient method for buffer exchange either into a specified buffer for subsequent purification steps or into a final formulation buffer (Merten et al., 2011). Due to its advantageous properties, UF/DF are the preferred methods employed in all published clinical grade LV purification schemes (Figure 1.7) (Slepushkin et al., 2003; Truran et al., 2009; Merten et al., 2011; Ausubel et al., 2012; Aiuti et al., 2013). Different filtration modes, such as dead-end or tangential-flow filtrations (TFF), and devices, such as hollow fibres or cassettes, can be employed. Off these, TFF is the most widely used for LV purification resulting in efficient particle concentrations with minimal membrane fouling, which is the main drawback of UF (Geraerts et al., 2005; Cooper et al., 2011; Merten et al., 2011; Segura et al., 2011).

1.3.4.5 Purification

The purification of concentrated viral supernatant is required to obtain high vector purities which is advantageous for clinical applications. This purification step can either be preceding, proceeding or even coupled to the concentration step, for example by using UF with DF which allows for buffer exchange. Generally, viral vector isolation from surrounding contaminants can be divided into two separate operations: purification and polishing, with the former aimed at debulking the viral supernatants from large impurities, while the latter is used to remove remaining low trace impurities.

1.3.4.5.1 Chromatography

Chromatography-based purification has increasingly become the pillar for the downstream processing of biological products at an industrial large scale setting due to its efficiency in high purity yields. An increasing number of chromatographic purification of viral vectors have been reported over the past years (thoroughly reviewed in (Kramberger et al., 2015)). Different types of chromatographic resins have been evaluated for the purification of LVs (Scherr, 2002; Slepushkin et al., 2003; Kutner et al., 2009; Cheeks et al., 2009; Lesch et al., 2011; Zimmermann et al., 2011); and their recent development and mechanical characteristics will be thoroughly covered in Section 7.2.2. Due to its scalability, reproducibility, fast processing times and potential for automation, chromatographic-based technologies for viral purification have been employed in all large-scale clinical-grade processes (Figure 1.7).

1.3.4.5.1.1 Anion exchange chromatography

Ion exchange chromatographic techniques exploit the charge interactions between viral particles and ion exchange ligands immobilised on a matrix. Lentiviral particles have an overall negative charge at neutral pH, thus allowing their capture by positively charged groups, making anion exchange chromatography (AEX) an appropriate method of viral purification. The simultaneous selectivity of this method, while allowing for concentration of the feed, has rendered AEX as the most widely used technique for current research and clinical-grade LV purification (Figure 1.7) (Scherr, 2002; Slepushkin et al., 2003; Yamada et al., 2003; Kutner et al., 2009; Lesch et al., 2011; Merten et al., 2011; Zimmermann et al., 2011; Bandeira et al., 2012; Marino et al., 2015). In these reports, two varying anion exchange ligands in binding strength were used quaternary ammonium (Q) and diethylaminoethyl (DEAE), with varying yields ranging between 30 to 80% of infectious particle recoveries, with no apparent superiority in the choice of ligand used. Although efficient in isolation, one of the main disadvantages of this method is the requirement of high salt concentration (0.5 -1 M NaCl) for the desorption of captured viral particles. As discussed in section 1.3.2, LVs functionality is susceptible to high salt concentration resulting in partial loss of infectivity

(Segura et al., 2005). To circumvent this negative effect on vectors, two studies demonstrated that either stepwise gradient elution (Marino et al., 2015), or stepwise elution coupled with immediate virus dilution post-chromatographic run (Bandeira et al., 2012), improved overall eluted yield, resulting in the highest reported LV recovery of 80% for both studies.

1.3.4.5.1.2 Affinity chromatography

Affinity chromatography allows the separation of biological compounds in a highly specific manner by selective interaction between a target bait protein and its respective ligand bound to the matrix. It relies on specific and preferentially reversible adsorption followed by elution of captured vectors from the immobilized ligand. Unlike AEX, the high specificity of affinity-based purification enables the selective capture of target vectors from surrounding supernatant, rather than the debulking of surrounding supernatant. This in turn provides an increased product yield, while reducing the number of steps currently required for vector purification, thus decreasing the cost of manufacturing. To date, several ligands have been used for affinity-based chromatographic purification of γ-RV particles and an excellent review can be found in Wolf and Reichl (2011) for further details. A recent study developed an affinity chromatography for the recovery of viral-like particle based on RVs containing vector-binding peptides isolated by phage display screening (Fernandes et al., 2016). However, even though the latter is a powerful technology for the isolation of RV specific peptides, its limitations lies in the desorption of subsequent captured vectors from resin. As for the affinity chromatography of LVs, few reports have been published in the scientific literature and are summarized in Table 1.6. As there are no specific LV ligands, published reports have utilized vectors' natural abilities to bind generic ligands such as heparin. After the capture of vectors from clarified supernatants, elution using 350mM NaCl resulted in 53% recovery of infectious virus (Segura et al., 2007). Alternatively, LVs have been engineered to express affinity tags on their surface such as hexahistidine for immobilized metal affinity chromatography (IMAC) and avidin-biotin affinity chromatography, both of which resulting in partial purification of LVs (Yu and Schaffer, 2006; Cheeks et

al., 2009; R. Chen et al., 2010). However as previously discussed, elution from IMAC columns requires the use of imidazole, which has been shown to cause LV inactivation (Ye et al., 2004; Cheeks et al., 2009). Otherwise, the avidin and biotin system has been used by labeling viral particles with a biotin analogue, desthiobiotin, allowing purification from monomeric avidin columns. Seeing that this analogue binds avidin at a lower affinity than biotin (Hirsch et al., 2002), the loading of 2mM biotin onto the column of captured vectors resulted in the recovery of 68% of infectious virus (R. Chen et al., 2010). Therefore, although superior in terms of specificity, the lack of vector-specific ligand could be argued to have hindered the widespread application of affinity-based chromatography for LV purification.

Affinity chromatography	Vector	Resin	Desorption reagent	Recovery (%)	Reference
IMAC	His_6-engineered VSV-g LV	Ni-NTA resin	250mM imidazole	50	(Yu and Schaffer, 2006)
Heparin	VSV-g LV	Fractogel® Heparin column	350mM NaCl	53	(Segura et al., 2007)
IMAC	His_6-tagged VSV-g LV	CIM monolith	150mM imidazole	69	(Cheeks et al., 2009)
Biotin-streptavidin	Desthiobiotin -tagged VSV-g LV	Monomeric avidin	2mM biotin	68	(R. Chen et al., 2010)

Table 1.6: Affinity chromatographic purification of VSV-g pseudotyped LVs. IMAC, Immobilized metal affinity chromatography; His_6, hexahistinde; CIM, convective interaction media.

1.3.4.5.1.3 Size exclusion chromatography

Size exclusion chromatography (SEC), or gel permeation, exploits the large size of LV particles for their separation in a non-adsorptive manner. LV particles are generally recovered in the void volume of the column, while proteins and small molecular contaminants are retained within the internal

pores of the column (Segura et al., 2013). Although gentle operating conditions are employed in this method thus maintaining viral infectivity, its drawbacks include low loading capacity resulting in slow flow rates, and product dilution due to its linear operation (Segura et al., 2006; Merten et al., 2016). Due to these practical disadvantages, SEC is utilized as a polishing step to remove remaining impurities in current clinical grade vector production for final buffer exchange into vector formulation solution (Figure 1.7). In one study, this method was reported as the main purification step for VSV-g pseudotyped retroviral particle but was however preceded with UC and proceeded with a second concentration step by UF (Transfiguracion et al., 2003). The use of this method therefore is dependent on the levels of impurities clearance of any purification process or scheme.

1.3.4.6 Nucleic acid digestion

Due to the nature of their current transient production, LV supernatants are contaminated with several process- and product-related impurities, with nucleic acids representing the major contaminant (Sastry et al., 2004). This occurs as a result of both plasmid DNAs used for viral production and/or released cellular DNA, which has been reported to increase in concentration with harvest time (Segura et al., 2005). The presence of nucleic acid impurities is however highly undesirable from a safety regulatory point of view, as it can potentially induce an immune response (Pichlmair et al., 2007). Moreover, DNA impurities may cause difficulties in the different steps of vector purification by increasing sample viscosity (Segura et al., 2013). Importantly, the physical separation of viral vectors from DNA has proved challenging as they both share common characteristics that are exploited for viral isolation such as a strong negative charge, resulting the co-purification of DNA impurities by AEX. Therefore, nuclease treatment of vector product is performed to reduce DNA contamination, with Benzonase® treatment as the most commonly used. The importance of DNA elimination is highlighted by the fact that Benzonase® treatment is used in all clinical-grade downstream processing schemes, albeit at different stages in each purification 'train' (Figure 1.7) (Slepushkin et al., 2003; Truran et al., 2009; Merten et al., 2011; Ausubel et al., 2012; Aiuti et al.,

2013). However, the subsequent removal of both digested contaminants and nuclease is necessary and represents a another limitation for all vector downstream processes (Merten et al., 2016). The introduction of the nucleic acid digestion step early in the schemes may maximize the removal of its impurities by subsequent steps such as TFF or SEC (Merten et al., 2011). The nuclease treatment of unconcentrated large vector volumes requires an increased amount of enzyme required. which represents another limitation as it inevitable increase in vector manufacturing cost (Schweizer and Merten, 2010)

1.3.4.7 Sterile filtration and formulation

The last operating step in most clinical-grade schemes is typically sterile membrane filtration through 0.2µm of purified vector products (Figure 1.7). However, significant viral losses have been reported as a consequence of the filtration of ~120nm particles into 200nm pores (Segura et al., 2013). Consequently, this step is omitted in certain vector manufacturing protocols by ensuring sterilisation through their downstream processing (Ausubel et al., 2012). More importantly, post-processing, LVs are typically stored at -80°C for protection from thermal inactivation. As such, viral vectors require to be formulated in a buffer that can ensure functional stability during storage by reducing viral loss and retaining infectivity. However, possibly due to their infancy as therapeutic vectors, very few reports investigating these critical aspects of product formulation have been published in the scientific literature. To date, vector have been formulated in cell culture media used for *ex vivo* cell culture, such as CellGenix's CellGro® and Lonza's X-vivo™ (Merten et al., 2011; Aiuti et al., 2013;), which contain a mixture of both sugars and proteins, potentially offering some degree of cryoprotection for viral particles. Interestingly, formulation using a histidine hydrochloride based buffers were recently shown to maintain up to 74% of starting vector titres after 8 days at 25°C (Fan et al., 2015). Given their complex biology and their inherent instability, optimisation of viral vector formulation would inevitably aid the spread of their application for different gene therapies by enhancing their stabilization for storage.

1.4 Thesis aim and objective

With the advancement of LVs in clinical applications, the development of an affinity-based viral purification method that simultaneously yields high recovery with reduced product-related impurities, is highly desirable. Current purification schemes employ several, at least 4, technologies in clinical-grade LV downstream processes, which are cumbersome, time consuming, require both technical expertise and equipment and generate ~ 30% overall yield (Rodrigues et al., 2007; Segura et al., 2013). Thus, the currently employed purification schemes for LVs downstream processing represent the main bottleneck for the clinical and commercial progression of these vectors (Merten et al., 2014, 2016).

The lack of a simple and selective LV purification method, with efficient adsorption and mild desorption, was the basis behind this project. The selective capture of labile LV particles by a vector-specific affinity peptide would provide increased vector purity due to its specificity. And in turn, the reversible binding of the affinity peptide by affinity competition would effectively determine the efficiency in functional vector recovery. Such an affinity-based strategy of purification is highly attractive as it would specifically isolate viral particles from starting supernatants, thus relieving both product- and process-related impurities i.e. potentially reducing the number of steps required in LV downstream processing. The aim of this project was to develop such a one-step affinity purification of viral purification based on the biotin-(strept)avidin system with high overall yield. This would be achieved by the expression of a biotin mimicking peptide on the surface of viral particles which enables their selective capture by streptavidin. With orders of magnitude difference in binding affinities between the mimic and biotin, the addition of the latter should allow the release of captured virus by competitive elution. The objectives of this study are:

- To develop and validate a cyclical-synthetic peptide for efficient and reversible streptavidin binding enabling suspension cell isolation (Chapter 3).

- To modify functional LV viral particles with the synthetic biotin mimicking peptide for their selective capture from viral supernatant by streptavidin binding (Chapter 4).
- To demonstrate elution of captured modified LVs by biotin-mediated competitive elution (Chapter 5).
- To characterize quality of affinity-purified vectors (Chapter 6).
- To establish the feasibility of our method for large-scale LV downstream processing based on affinity chromatography (Chapter 7).

Chapter 2 Materials and Methods

2.1 Molecular Biology

2.1.1 Molecular cloning

2.1.1.1 DNA synthesis by overlap extension PCR

Overlap extension PCR allows the fusion of several pieces of DNA at certain junctions that are complementary. This occurs in two PCR reactions as depicted in the below schematic Figure 2.1, whereby in a primary PCR reaction (*Table 3*) sequences of DNA are amplified with overlapping base pairs at their extremities. Subsequently, in a secondary PCR reaction complementary sequences overlap and by amplification result in fusion of the two DNA sequences. Due to its 3' to 5' proof reading activity, Phusion polymerase (NEB M0530L) was used for all PCR runs, with its 5X High Fidelity buffer (NEB, B0518S), in the following conditions: initial denaturing and polymerase activation at 98°C for 120s; followed by a 3-step cycle repeated for 35 time: denaturing at 98°C for 40s, primer annealing at 65°C for 40s and polymerase extension step at 72°C for 1min / kb with a final polishing step at 72°C for 10min. PCR products were separated by gel electrophoresis and extracted using QIAquick Gel Extraction kit (Qiagen 28704). Primary overlapping PCR products were then combined together is a secondary PCR reaction using the same condition as above. After screening products by gel electrophoresis, PCR runs were cleaned up using QIAquick PCR Purification kit for subsequent restriction digest and subcloning into appropriately digested based expression plasmids (see section 73)

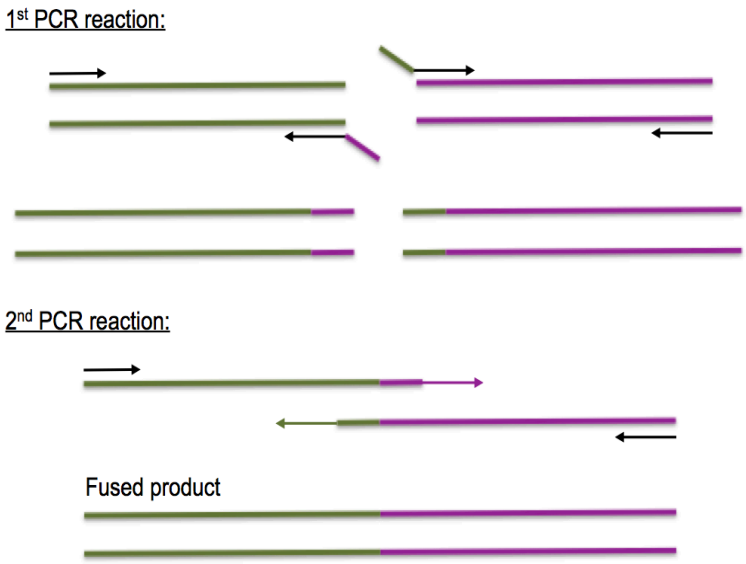

Figure 2.1: Schematic diagram of Phusion PCR reactions.

2.1.1.2 DNA extraction for bacterial colonies screening

2.1.1.2.1 Small scale DNA preparation

To assess and screen transformed clones, DNA was prepared as follows: single colonies from bacterial transformation were picked from agar plates and grown in 4mL LB supplemented with 100µg/mL carbenicillin or another corresponding antibiotic. Following overnight culture at 37°C with 220 RPM, QIAprep Spin Miniprep kit (Qiagen, 27104) was used to isolate plasmid DNA according to manufacturer's instructions. Ligated constructs were verified by restriction digest and/or DNA sequencing.

2.1.1.2.2 Large scale DNA preparation

For the generation of DNA for *in vitro* use, 100mL of TB were inoculated with 250- 500µL of correct small scale bacterial culture and incubated for 16-18 hours in a bacterial shaking incubator at 37°C with 220 RPM. DNA was extracted according to Nucleobond ® Xtra Midi protocol (Macherey-Nagel, 740410.10).

2.1.1.3 Measurement of DNA concentration

DNA concentration reflects the property of DNA absorbance of light at 260nm wavelength. The ratio of absorbance at 260:280nm can be used to establish purity with 1.8 ratio indicating a high degree of DNA with little RNA or protein contamination. Concentrating and purity of plasmid DNA was determined using a nanodrop ND-1000 spectrophotometer.

2.1.1.4 Restriction endonuclease digestion

Restriction digests were performed according to manufacturer's protocol (NEB) in order to generate cloning DNA fragments with 'sticky' compatible ends to allow DNA ligation. For inserts generated by PCR, the entire sample was used after PCR clean up, whereas for its corresponding vector backbone, 5ug of plasmid DNA was used. In both instances, reaction volumes were adjusted with molecular grade water such that the final reaction volume was 100µL. For double digests, buffer selection was defined by manufacturer with a final enzyme concentration of 5% v/v of the final reaction volume. In the occasion of incompatibility of enzyme buffers, digestions were preformed serially with digestion sample prepared between the reactions using Qiagen QIAquick clean-up kit.

2.1.1.5 Gel electrophoresis

Size verification of PCR products, restriction digested DNA plasmids and fragments was accomplished by DNA separation using agarose gel electrophoresis. 1% agarose gels were prepared in 1x TBE buffer with agarose solubilisation achieved by microwave heating of the solution. Subsequently, the melted agarose was cooled and 0.5-1µg/mL of ethidium bromide or SYBR® Green I nucleic acid gel stain (Thermofisher scientific, S7585) to enable UV/blue light transilluminator visualization of the DNA. Samples were mixed with loading buffer diluted 5X prior to loading into wells molded into the gel upon solidification along with appropriate DNA ladder. Agarose gels were electrophoresed at 110V in 1X TBE buffer until adequate separation was achieved for clear visualization.

2.1.1.6 Gel extraction

To prevent UV-mediated mutagenesis, following separation of DNA fragments by agarose gel electrophoresis bands were visualized using a dark reader blue light transilluminator and excised from the gel using a clean scalpel. Gel extraction was then carried out using Qiagen QIAquick or Macherey Nagel gel extraction kits, according to manufacturer's instructions.

2.1.1.7 PCR clean up

Following fusion PCR reactions, QIAquick PCR Purification kit (Qiagen 28104) was used according to manufacturer's instructions to remove contaminants from samples before downstream usage.

2.1.1.8 DNA ligation

After gel extraction of digested vector plasmid and insert fragments DNA ligation was preformed using Quick Ligase Quick Ligation Kit (NEB, M2200L) with a vector:insert molar ratio between 1:3-1:6,, according to manufacturer's instructions. Following incubation for 5 mins at RT followed by inactivation of ligase for 2 mins at 4°C, 2µL of ligation reactions were used for bacterial transformation of high efficiency C2987 (NEB) chemically competent *E. coli* bacteria.

2.1.1.9 Plasmids

γ-RV SFG, LV pCCL and expression plasmid pMono (Invitrogen) were used for all constructs used or constructed during this course of research as stated. SFG is based on the Moloney MLV, with the start codon of the transgene located at the start site of the deleted viral envelope gene (Büeler and Mulligan, 1996). Bicistronic transgene expression was attained by one of two strategies; either the inclusion of the encephalomuocarditis internal ribosomal entry site (IRES) downstream of the stop codon of the transgene, allowing expression of downstream reporter gene eGFP. In an alternative strategy, two genes were transcribed and translated as one frame due to the use of the self-cleaving activity mediated by the TaV (*Thosea asigna* virus) 2A sequence. Unlike IRES, this self-cleaving peptide allowed equimolar expression of both transgenes.

2.1.2 Bacterial manipulation

2.1.2.1 *Growth and maintenance of E. coli*

DH5α *E. coli* bacteria were grown in liquid Luria-Bertani (LB) or terrific broth (TB) medium (for small and large scale cultures, respectively) supplemented with 100µg/mL antibiotics and cultured ay 37°C with agitation at 220RPM or spread on LB-agar infused with 100µg/mL antibiotics in a static 37°C incubator.

2.1.2.2 Bacterial Transformation

Chemically competent DH5α *E. coli* bacteria (NEB, C2987H) were transformed by a heat shock protocol as follows: after thawing 25µL of bacteria on wet ice, 2µL of ligation mix or 1µL of large-scale DNA preps for retransformation to replenish DNA stock, was added to the bacteria and incubated for 20mins at 4°C. Bacteria were transiently heat-shocked by incubation at 42°C for 35 secs then incubating at 4°C for 2 mins, followed by a recovery step by incubating mixtures with SOC medium (NEB, B9020S) at 37°C, 220rpm for 30mins. Subsequently, transformed bacteria were spread on LB-agar plates infused with 100µg/mL antibiotics and incubated in an inverted orientation at 37°C overnight.

2.2 Cell culture

2.2.1 Propagation of adherent cell lines

The adherent cell line HEK293T was cultured in sIMDM (Lonza 12-726F) supplemented with 10% FCS (Biosera, FB1001/500) and 1% Glutamax (Gibco, 35050-061) in 175cm^2 tissue culture coated flasks at 37°C with 5% CO_2. Cellular passage was preformed once 80-90% confluency was reached as follows: cells were washed with 1x PBS, incubated with 5mL trypsin-EDTA (Sigma, T4049) for 5 minutes at RT for cellular dissociation. Cells were then harvested and trypsin was inactivated by washing the flask with 10mL of sIMDM. After a centrifugation step at 400G for 5 minutes, pellets were resuspended and plated in a new flask at 1:4 – 1:10 dilution.

2.2.2 Propagation of non-adherent cell lines

The non-adherent, suspension cell line K562 was cultured in sIMDM in 80cm^2 tissue culture coated flasks placed in vertical orientation at 37°C with 5% CO_2. Cell densities were maintained approximately between 0.2-1 x 10^6 cells/mL, by 1:10-1:20 dilution with fresh sIMDM of confluent cultures as indicated by discolouration of phenol red indicator dye in the medium.

2.2.3 Cryopreservation and recovery of cell lines

Engineered cell lines were cryopreserved for long term storage as follows: during optimal growth conditions, cells were harvested and after centrifugation pellets were resuspended at 5x10^6 cell/mL in chilled cryopreservation medium (Lonza) and aliquoted into 1mL aliquots in cryovials (Corning). Tubes were placed in a Mr. Frosty™ freezing container which was stored in at -80°C. The isopropanol bath in the container maintains a controlled cooling rate at 1°C/minute. The following day, frozen vials were then transferred to into liquid nitrogen tank for long term storage. The cryopreservation medium contains a toxic concentration of DMSO, therefore it is imperative to minimize its exposure to actively metabolizing cells during recovery. Cryovials were thawed by suspension in a 37°C water bath and immediately washed in 25mL of pre-warmed complete media and resuspended in a T175 flask which was then transferred to a 37°C incubator with 5% CO_2.

2.2.4 Transient transfection of HEK293T cells for protein expression analysis

Transient transfections were performed in multiwall TC-treated dishes or plates. Genejuice® reagent (Merck Millipore, 70967) was used as transfection reagent and reactions for different uses were prepared as indicated in Table 2.1. Genejuice is a lipid-based reagent that complexes with DNA to mediate DNA transport into cells during transfection.

Table 2.1: Transfection reactions for HEK293T cells

Plate	GeneJuice (µL)	Media (µL)	DNA (µg)
10cm	30	470	12.5
6-well	5	95	2

Cells were seeded at a density of 2.1 x 10^5 cell/cm^2 and 2.7 x 10^4 cell/cm^2 for 6-well (2mL/well) and 10cm plates (10mL), respectively. Cellular confluence was assessed by microscopic examination for optimal density prior of transient transfection of protein and viral vectors.

Taking 10cm plate conditions as reference, transfection mixtures were prepared as follows: 30µL of Genejuice was added to 470µL of plain media for each transfection condition. After 5 minute incubation to allow formation of Genejuice micelles, 12.5µg of plasmid DNA was added to the mixture, mixed well and incubated for 15 minutes. Transfection was performed by dropwise addition of DNA incubated mixture over HEK293T culture.

2.2.5 In vitro magnetic suspension cell using streptavidin Dynabeads

Dynabeads® MyOne™ Streptavidin T1 (Thermo Fisher, 65601) were used to isolate cells as required. It should be noted that these beads are developed for nucleic acids and antibodies/proteins isolation, therefore manufacturer's protocol was adapted as indicated. Cells were resuspended after washing with chilled PBS and incubated with 100µL of washed beads, as manufacturer's protocol. Following 30-minute incubation on ice, cells were washed with chilled PBS and beads were immobilized by placing tubes in appropriate magnetic racks. Subsequent steps for bead washing were followed as manufacturer's protocol. Finally, magnetic beads were resuspended in sIMDM and cultured in flask for subsequent analysis.

2.2.6 Lentiviral transduction of primary T cells

For T cell transduction whole blood was collected from healthy donors and using Ficoll (GE Healthcare, 17-1440-02) Peripheral Blood Mononuclear Cells (PBMC) were isolated by gradient centrifugation. Subsequently PBMCs were resuspended at $1x10^6$ cells/mL and seeded in a 24-well plate with complete RPMI supplemented with 10% FCS and 1% Glutamax. Cells were stimulated overnight with both monoclonal antibodies MACS GMP CD3 (OKT3 clone, Miltenyi Biotech, 170-076-116) and CD28 (15E8, clone, 170-076-117) at 0.5 μg/mL for each. Subsequently, 24 hrs later IL2 (Genscript, Z00368-1) was added to both conditions at a concentration of 100U/mL and incubated at 37C with 5% CO2 for 6 hours. Subsequently, non-tissue culture treated wells, which were previously coated with the recombinant human fibronectin fragment CH-296 (Retronectin, Takara), were pre-loaded with 250μL of lentiviral supernatants for 30mins at 4°C. Then PBMCs were harvested and $3x10^5$ cells were seeded in each well with 100U/mL of IL2 topped with 1.5mL of lentiviral supernatant. Plates were then spun at 1000G for 40mins and placed at 37°C with 5% CO2. PBMCs were then recovered and resuspended in fresh complete RPMI with 100IU/mL of IL2. Transduction efficiency and activation of transduced cells were assessed 48hrs later by Flow Cytometry.

2.3 Viral vector production, processing and characterization

2.3.1 γ-RV work

2.3.1.1 γ-RV transient production

$2.25 x10^6$ HEK293T cells were plated in 10cm plates and 24 hours later cellular confluency was assessed by microscopic examination to ensure optimal density for transfection of 50-60% confluence. Transfection mixture containing 470μL plain media and 30μL GeneJuice were prepared for each plate to be transfected. Following 5 minute incubation, a total amount of 12.5μg of packaging plasmids were added in the following ratio: 3/8 Gagpol, 2/8 RDF

envelope, 3/8 retroviral SFG-based vector. Mixtures were incubated for 15 minutes prior to dropwise addition to HEK293T cultures. Virus containing mediums (VCM) were harvested 48 and 72 hours post-transfection and frozen down at -80°C for storage.

2.3.1.2 γ-RV transduction of adherent cell lines

Stable protein expression in HEK293Ts was achieved by γ-retroviral transduction. Briefly, $1x10^6$ cells were seeded in 6-well plate and 24 hours later 1mL of VCM was gently added onto cells with 5μg/mL of Polybrene (Merck Millipore, TR-1003-G). Once cells had recovered, cultures were passages twice before functional usage.

2.3.1.3 γ-RV transduction of suspension cell lines

Prior to transduction, non-tissue culture plates were pre-coated with Rectronectin (Lonza, T100B) diluted 1:125 in PBS with 500uL/well of 24-well plates stored at 4C. 24 hours later, cells were harvested and resuspended at a density of 6 x 10^5 cells/mL. 0.5mL of this culture were seeded in each well after rectronectin removal from wells and 1.5mL of RV-VCM was overlaid onto cells for a final volume of 2mL/well. Plates were centrifuged at 1000g for 40 minutes to enhance infectivity by spinoculation and then incubated at 37°C with 5% CO2 for 48 hours. Cells were then harvested and resuspended in fresh sIMDM for a further 72 hours for recovery.

2.3.2 LV work

2.3.2.1 LV transient production

A second-generation packaging system was used for the purpose of this project. Accordingly, three-plasmids were co-transfected into HEK293T cells for the production of LVs. 1.5 $x10^6$ cells were seeded in 10cm plates and 48 hours later, cells were transfected with Genejuice with the following plasmids: 4.17 μg of pCCL.PGK.eGFP (transfer vector), 5.42 μg of pCMVR8.74 and 2.92 μg of envelope plasmid. Three envelopes were used in this project: 1- pRDpro, RD114-derived envelope expression plasmid, kindly given by Prof. Mary Collins laboratory, whereby the R cleavage site of envelope's endodomian was

replaced with the protease cleavage site between matrix and capsid proteins of gagpol polyprotein (Ikeda et al., 2003); 2- pMD2.G, VSV-g envelope expression plasmid (Naldini et al., 1996) and 3- pALF, MLV-A expression cassette, both of which were kindly provided by Prof. Wassem Qasim laboratory. Depending on which pseudotyping glycoprotein was used, VCM were harvested either 48 hours or 48 and 72 hours post-transfection for RDpro and VSV-g/MLV-A pseudotyped LVs, respectively. Collected VCM were subjected to a centrifugation at 1000g for 10min at 4°C for the removal of cellular debris. VCM were then purified by microfiltration using 0.45µm filters. Processed VCM were either kept at wet ice for immediate use or frozen down at -80°C for storage.

2.3.2.2 LV purification and concentration using 20% sucrose cushion

LVs were purified by ultra-centrifugation on a 20% sucrose cushion. 24 hours before viral purification, 20% sucrose was prepared in 50mM sodium phosphate and sterile filtered through 0.22um and placed at 4°C. Ultra-centrifugation polyallomer tubes (Beckman ultra-clear 326823) were sterilized then washed with 70% EtOh and 1X PBS, and left to dry in tissue culture hood for 2-5 min. After thawing on wet ice, ¾ of VCM was gently overlaid on ¼ 20% sucrose solution in a final volume depending on centrifugation tubes maximum capacity. Using a SW32 Ti rotor, tubes were placed in corresponding buckets, balanced to 0.1g and carefully inserted with the rotor into pre-chilled ultracentrifugation machine. Tubes were spun at 23,000 rpm for 2 hours at 4°C with acceleration of 9 and deaccelerating of 4. Tubes were then carefully removed from buckets and inverted onto sterile plastic dishes after discarding supernatant, to remove all remaining liquid. 50X – 100X volume reduction of reduced serum OptiMEM medium (Gibco, 31985-062) was very gently added onto viral pellets and tubes were incubated on ice to allow dissociation with gentle vortexing every 15 minutes. Pellets were then pooled together and further resuspended by pipetting very gently for more than 40 times, avoiding bubbles, and aliquoted into tubes for -80°C storage.

2.3.2.3 LV titration methods

2.3.2.3.1 Infectivity assay

The infectious titre of each vector preparation was determined by flow cytometric analysis of eGFP expression following transduction of HEK293T cells. 1 x 10^5 and 5 x10^4 cells were seeded in wells of 6-well and 24-well plates, respectively, in 1mL with 5μg/mL of Polybrene. To determine the count of infectious units, only transduction efficiencies between 1 – 25% of eGFP positive cells can be taken into account. RDpro/MLV-A LV and VSV-g LV viral supernatants were serially diluted into 3 and 6 fractions at 1:5 and 1:10, respectively, in cell culture medium supplemented with Polybrene. 250μL of each dilution was added into each well for transduction. 72 hours post-transduction, cells were trypsinized using cell dissociation solution (Sigma, C5914) and resuspended in PBS. eGFP expression was analyzed then by flow cytometry using BD LSR Fortessa™ X-20 cell analyzer and Flowjo software. Viral titres were calculated from virus dilution with transduction efficiencies between 1 – 20% eGFP expression using the following formula:

$$Titers\left(\frac{IU}{mL}\right) = \frac{\left(no.of\ cells\ at\ transduction\ \times \frac{\%\ eGFP\ positive\ cells}{100}\right)}{(VCM\ volume\ (mL)\ \times\ dilution\ factor)}$$

2.3.2.3.2 p24 ELISA

Physical particles of LV samples were determined by measuring p24 levels using enzyme linked immunosorbent assay (ELISA). The QuickTitre™ Lentivirus Titre was used to specifically determine lentivirus-associated HIV rather than free p24 proteins (Cell Biolabs, VPK-107-T). The manufacturer's protocol was followed and samples were assayed in duplicates. After the incubation with kit's ViraBind™ reagents and virus inactivation, the principle of the assay is based on the binding of p24 to anti-p24 antibodies coated on a microwell plate. This is followed by incubation with a secondary FITC-conjugated anti-HIV1 p24 monoclonal antibody (1:1000). Subsequently, wells are exposed to a horse radish peroxidase (HRP)-conjugated anti-FITC monoclonal antibody (1:1000). The, the soluble colorimetric substrate solution 3.3'5.5'-tetramethylbenzidine (TMB) is added which then reacts with HRP to

form a blue-by product whose intensity id directly proportional to the amount of HRP, which itself is proportional to the amount of bound p24 in the wells. Next the reaction of the by-product is terminated by the addition of sulfuric or phosphoric acid stop solution (not specified) as indicated by the sample color change to yellow. The absorbance was read immediately at 450nm using an absorbance microplate reader (Varioskan™ LUX multimode, Thermofisher) and the SkanIt® software. Along with vectors samples, standard curve dilutions of the recombinant p24 standard supplied with the kit were prepared in sample diluent for a range from 100 to 1.5625 ng/mL.

2.3.2.4 LV impurities quantification

2.3.2.4.1 dsDNA quantification

Viral vectors were assessed for double stranded (ds) DNA contamination after purification using Invitrogen's Quant-iT™ PicoGreen® dsDNA Assay kit (P7589). Using an ultrasensitive fluorescent nucleic acid stain, Quant-iT™ PicoGreen®, DNA concertation as little as 25pg/mL can be quantitated. DNA concentration of viral samples were determined according to manufacturer's protocol. Briefly, high-range (1ng/mL - 1µg/mL) lambda DNA standards which was set up by dilution in 1X TE and purified LV samples were added to 1mL of TE-diluted 20X Quant-iT™ PicoGreen® dsDNA reagent and incubated for 2 to 5 minutes at room temperature in the dark. Subsequently, samples were loaded in triplicates manner on Thermo Scientific™ Nunc™ F96 MicroWell™ black polystyrene plate and samples fluorescence at 520nm were detected. Then, after having subtracted the fluorescent value of the reagent blank from all wells (standards and samples), dsDNA concentrations of viral samples were determined using standard curve generated by the standard controls.

2.3.2.4.2 Silver staining

Purity of viral samples, both crude or purified, were analyzed by silver staining using SilverXpress kit (Invitrogen, LC6100). First denatured samples were resolved by protein electrophoresis on pre-casted 1.0mm NuPAGE™ Novex 4-12% Bis-Tris Gels (Invitrogen, NP0322BOX). For denaturation of samples, briefly, NuPAGE® Sample Reducing Agent (10X) was added to maintain

proteins in a reduced state, and NuPAGE® LDS Sample Buffer (4X), which contains lithium dodecyl sulfate allowing maximum efficiency of reducing agent. Final sample volume of 20µL was achieved by adding ddH_20. Samples were then incubated at 90°C for 10 minutes followed by ice incubation for 2-3 minutes. Denatured samples were then loaded onto pre-casted gels and resolved by applying 200V for 25 minutes. Subsequently, protein gels were subjected to SilverXpress® silver staining by several incubation steps as per manufacturer's protocol. Stained gels were visualized using Syngene G:BOX Gel and Blot imaging system.

2.3.2.4.3 HEK293 host cell protein quantification

Total host cell protein (HCP) were measured by ELISA with HEK-293 HCP kit which has a threshold of 300 pg/mL (Cygnus Technologies, F650). The manufacturers' protocol was followed and samples were assayed in duplicates. The principle of this assay is similar to that of p24 ELISA (Section 2.3.2.3.2) but using a microplate coated with a capture goat anti-HCP antibody by manufacturer, onto which 100µL of enzyme-conjugated anti-HEK 293-HRP was added in each well. 50µL of standards and diluted samples with diluent buffer (Cygnus, I028-500) were then added to the enzyme-conjugated antibody and the plate was incubated on a rotator at 400rpm for 2 hours at room temperature. Subsequently, wells were washed four times with diluted wash buffer and then 100µL of TMB substrate was added and plates incubated for 30 minutes at room temperature without shacking. Absorbance was measured at 450nm after the addition of 100µL stop solution, using the Varioskan™ LUX multimode microplate reader and analyzed using the SkanIt® software.

2.4 Flow Cytometry

Flow cytometry was preformed using Becton Dickinson (BD) LSR Fortessa™ X-20 instrument (BD Biosciences).

2.4.1 General staining protocol

Typically, 2 x 10^5 cells were washed with PBS, and if required stained with antibodies or appropriate ligands then washed again and resuspended in FACS buffer and placed on ice pending analysis. When multiple staining steps were required, samples were washed with PBS in between individual staining steps to remove unbound antibodies. Non-transduced/non-transfected controls were included as controls to establish appropriate benchmark for comparison. All staining steps were performed at room temperature in the dark with 30 minutes staining incubations unless indicated otherwise.

2.4.2 Compensation

When using several fluorophores in a FACS experiment, spillover of certain fluorophores into adjacent channels can occur leading to false positive. To avoid this problem, compensation was required whereby single-stained samples which were both beads (OneComp eBeads, eBioscience) and cells were used to record positive and negative populations of each fluorophore, allowing the calculation of compensation matrices using FACS Diva (BD) or FlowJo software.

2.4.3 Flow-based sorting of adherent cells

Engineered cell lines expressing exogenous proteins were expanded in 75cm^2 flasks. When sufficient cell numbers were reached (usually referring to 80-90% confluency) cells were harvested and washed with sterile PBS supplemented with 1% FCS. Cells were to be sorted by fluorescent protein expression and so were resuspended in 0.5 – 1mL of PBS supplemented with 1% FCS and 100μg/mL normocin. Sterile FACS tubes were prepared containing sterile-filtered FCS supplemented with 100μg/mL normocin for collection of sorted cells. Cell sorting was performed on BD FACS Aria, typically after live cell gating by FSc/SSc and doublet exclusion the sorted populations were selected depending on required expression. Sorted cells were collected directly into the pre-prepared FACS tubes containing FCS/normocin. Following sorting, cells were gently washed in PBS supplemented with 1% FCS and then transferred

directly to tissue culture plates/flasks, depending on the number of sorted cells collected, containing 1:1 ratio of sIMDM and FCS with 100ug.mL normocin. Cells were allowed to recover for 1 – 2 passages before further experimental use.

2.5 Immunofluorescence

For immunostaining of adherent cells, HEK293T cells were cultured in 24-well plates in sIMDM and staining was preformed when confluency was 80 - 90%. All incubation steps were performed at room temperature unless stated otherwise. Medium was removed and cells were gently washed with PBS. Cells were then fixed with 4% PFA for 20 minutes at room temperature. Cells were then washed with PBS 3 times and blocked with PBS supplemented with 0.1% BSA for 30 minutes. Strepravidin conjugated to a fluorophore was then added at 1:100 dilution in blocking solution incubated for 1 hours. Stained cells were then washed 3 times with BPS to remove unbound streptavidin and a nuclear stain was preformed using propidium iodide (PI) 1:3000 diluted in PBS for 5 minutes. Cells were washed again with PBS 3 times and 0.5mL PBS was added to each well for imaging. Fluorescent imaging was done using ZEISS fluorescence microscopy with Colibri illumination system.

2.6 Electron Microscopy

Viral samples in OptiMEM, purified by 20% sucrose cushion, were thawed on ice for electron microscopy analysis. Aliquots of 20µL were mixed with 5µl of streptavidin-colloidal gold conjugate, with a mean particle size of 8-12nm (Sigma, S9059) and were incubated at 37°C for 30 minutes. Samples were washed with blocking buffer (1% cold water fish skin gelatine, 1% tween 20 in PBS) for 1 hour prior to negative staining. Negative staining was performed by the sequential drop method; briefly each grid was placed sample side down on top of a 50 µl droplet of deionised H_2O for 30 seconds, followed by a 2 minute staining on top of a 50 µl droplet of 2% aqueous ammonium molydbate (pH 7.5) (Agar Scientific). Excess stain was wicked off using a Whatman type 1 filter paper and the grid was allowed to air-dry. Grids were examined at 200

kV in a JEM2100 TEM (JEOL U.K. Ltd., Welwyn Garden City, U.K.) at 10-60,000 times magnification, areas with the most even stain levels were selected for imaging.

2.7 Statistical Analyses

Data presented in this thesis were analyzed using the GraphPad Prism v7.0 statistical software package. Unpaired two-tailed Student's t test was used for comparison of matched values with only two sets of data present. Two-way ANOVA was used for comparison of groups with two variables presents across more than two sets of data.

Chapter 3 Development of a cyclical biotin mimic as an affinity purification tag

3.1 Overview

As the aim of this project was to develop an affinity-based method for LV purification based on the biotin and streptavidin system; in this chapter, different surface expressing streptavidin binding peptides, i.e. biotin mimics, were explored for efficient and reversible ligand binding. Then, with a candidate chosen, to validate its potential for viral particle capture, the isolation of suspension cells expressing it on their surface was also demonstrated.

3.2 Introduction

An important aspect of affinity-based purification is the use of a simple and efficient method that would allow high-throughput approaches for the purification of target proteins- or viral vectors for the purpose of this project. Numerous genetic affinity-based methods have been developed for the purposes of protein purification. These are primarily based on the use of specific antibodies or affinity tags that are fused to target proteins (Jarvik and Telmer, 1998; Rigaut et al., 1999). Among the different affinity-based purification prominent is the biotin-(strept)avidin system. The interaction between streptavidin and biotin is one of the strongest non-covalent biological binding known, with a dissociation constant (K_D) of ~ 10^{-15} M (Green, 1975; Holmberg et al., 2005a). The specificity of this system has led it to be the most widely used affinity binder in biological assays (Holmberg et al., 2005a). However, the strength of this interaction hinders the recycling of streptavidin matrices. This has led to an abundance of research to develop peptides that can bind streptavidin with a lower affinity, termed biotin mimics. An important requirement for using these peptides is their displacement by biotin for streptavidin binding to allow the release of purified targets. In this section, we will discuss the specifics of this system, as well as biotin mimicking peptides development and its application for the purpose of this project.

3.2.1 Biotin/streptavidin system

Since their discovery in the middle of the 20th century, biotin and (strept)avidin have been at the centre of a very large array of techniques used in science, medicine, molecular engineering and nanotechnology (Wilchek and Bayer, 1990; Savage, 1996). Avidin, isolated originally from chicken eggs (Seshagiri and Adiga, 1987) and its bacterial counterpart streptavidin (SA), isolated from *Streptomyces avidinii* (Chaiet and Wolf, 1964), have an extraordinarily high affinity for biotin – in the femtomolar range (10^{-15}) (Green, 1990). This represents the strongest non-covalent interaction known in nature which is several orders of magnitude higher than the affinity of commonly used affinity tags or antibodies. This system offers several advantages for protein purification; its femtomolar affinity reduces background binding which is often observed with other affinity tags such as histidine-based tags (Kimple et al., 2013). Moreover, unlike antibody-mediated cross reactivity, there are very few naturally biotinylated molecules thus reducing the chance of cross reactivity (Boer et al., 2003). Due to these unique features, this versatile system has been extensively exploited in many different kinds of biotechnological and universal applications.

3.2.1.1 Molecular characteristics

Biotin (244Da, also known as vitamin H or B_7) is an essential vitamin involved in carboxylation reactions (Figure 3.1a). In mammalian cells, active biotin is covalently bound to specific lysine residues in several carboxylases, which catalyse pathways involved in fatty acid biosynthesis, gluconeogenesis and tricarboxylic acid cycle (Zempleni et al., 2008). In mammalian cells. biotin conjugation is catalysed by biotin protein ligase (also known as a holocarboxylase synthetase), which has a bacterial counterpart- biotin ligase BirA for biotinylation reactions (Beckett et al., 1999; Sueda et al., 2011).

Avidin (63KDa) and Streptavidin (66KDa) are two interesting sides to the same coin. They share only 30% of their amino acid sequences but form similar quaternary structures consisting of four identical subunits arranged as homodimers and most of the biotin binding residues are conserved between

the two proteins (DeLange, 1970; Argaraña et al., 1986). Each subunit is made up of 8 anti-parallel ß-strands which fold into an up-down barrel with four identical ß-barrels in their quaternary structures, each with a biotin-binding pocket. Both proteins exhibit high stability against heat, pH changes, denaturing compounds and proteolytic enzymes (Wilchek et al., 2006). Moreover, to date streptavidin homologues have been found in several species such as fungus, bacteria and frogs (Jain and Cheng, 2017) but none have been found to be endogenously expressed in mammalian tissues. However, despite these similarities there are distinct structural differences between avidin and streptavidin that depict their differential suitability for specific applications. Unlike streptavidin, avidin is heavily glycosylated with N-linked asparagine-glycolsyl groups and is positively charged with an isoelectric point of ~10 (DeLange, 1970; Bruch and White, 1982). The attached sugars and charge results in significant non-specific binding of avidin which weakens its performance for specific high affinity interactions (Gitlin et al., 1990; Dundas et al., 2013). Streptavidin on the other hand is not glycosylated with a lower isoelectric point of ~6 resulting in negligible non-specific binding, making streptavidin the preferred biotin-binding-protein for capture or detection methods (Liu et al., 2016).

3.2.1.2 Binding interactions

A diverse set of experimental and computational methods have been used to study the biotin-streptavidin system as a model for high affinity protein-ligand interactions and in turn have elucidated the molecular mechanism of binding. The remarkable thermodynamic and kinetic properties of this affinity is due to several key supramolecular features of the complex (Jain and Cheng, 2017). Streptavidin subunits are not actually independent, with functional interplay occurring between adjacent subunits for ligand binding (subunit 1 and 3 interact with 2 and 4, respectively in an identically manner), owing to the highly conserved Trp120 (Sano and Cantor, 1995). Upon ligand binding in one subunit pocket, Trp120 from its adjacent subunit helps to stabilise biotin binding. Therefore, even if streptavidin folds into a tetramer, it can be regarded as a dimer comprising two homodimers. Nonetheless, each subunit of the

tetramer contains a binding pocket thus resulting in an overall tetravalency for biotin binding. Quaternary structures of biotin binding pockets have complementary shapes to biotin and are lined with a mixture of hydrophobic and polar residues that are key in stabilising ligand binding. Residues Val47, Trp79, Thr90, Trp92, Trp108 and Leu110 form a hydrophobic pocket and interact with ligand through Van der Waals' forces. Upon ligand binding, biotin's urea domain forms hydrogen bonds with Asn23, Ser27, Ser45, Tyr43, Asp128 and its carboxylate moiety is recognized by Ser88 and Asn49 on streptavidin (Chilkoti et al., 1995; Chilkoti and Stayton, 1995; Stayton et al., 1999; Qureshi et al., 2001). These interactions stabilize the biotin-streptavidin complex along with a flexible loop (residues 45-62) which is proximally situated to the binding site of streptavidin. This lid-like loop is a key element for ligand binding stability and affinity. In the absence of biotin, the binding site adopts an open, flexible, semi disordered confirmation (Figure 3.1b-c, blue chain). Upon ligand binding, the loop closes on the binding pocket, adopting a more stable conformation due to electrostatic and hydrophobic interactions with biotin (Figure 3.1c, red chain) (Freitag et al., 1997; Perbandt et al., 2007; Song et al., 2015). The importance of this loop in ligand binding affinity is highlighted by the fact that it is conformationally the most variable motif in all different structures of streptavidin and its mutants deposited in the Protein Data Base (PDB) (Korndörfer and Skerra, 2002; Perbandt et al., 2007). In line with this, site-specific mutagenesis experiments of loop residues have created a range of streptavidin mutants with varying properties, such as traptavidin (S52G, R53D) that exhibits a 10-fold lower dissociation constant (Chivers et al., 2010, 2011). Intriguingly, deletion and mutagenesis experiments on binding loop residues have shown that the loop is not required for association, but accounts for the high affinity binding of biotin, through the modulation of dissociation kinetics (Freitag et al., 1999). It is interesting to note that since streptavidin seems to handle extensive mutations, several mutants have been developed as engineering tools and for specific binding applications, These range from single residue substitution or rational design to large scale protein engineering studies, altering both tertiary topology and quaternary structures (Sano et al., 1998; Howarth et al., 2006; Laitinen et al., 2006; Lim et al., 2013; Wu and

Wong, 2013; Yumura et al., 2013; Baumann et al., 2016; Baugh et al., 2016); which are also extensively reviewed in the literature (Laitinen et al., 2007; Dundas et al., 2013; Lim et al., 2013; Jain and Cheng, 2017).

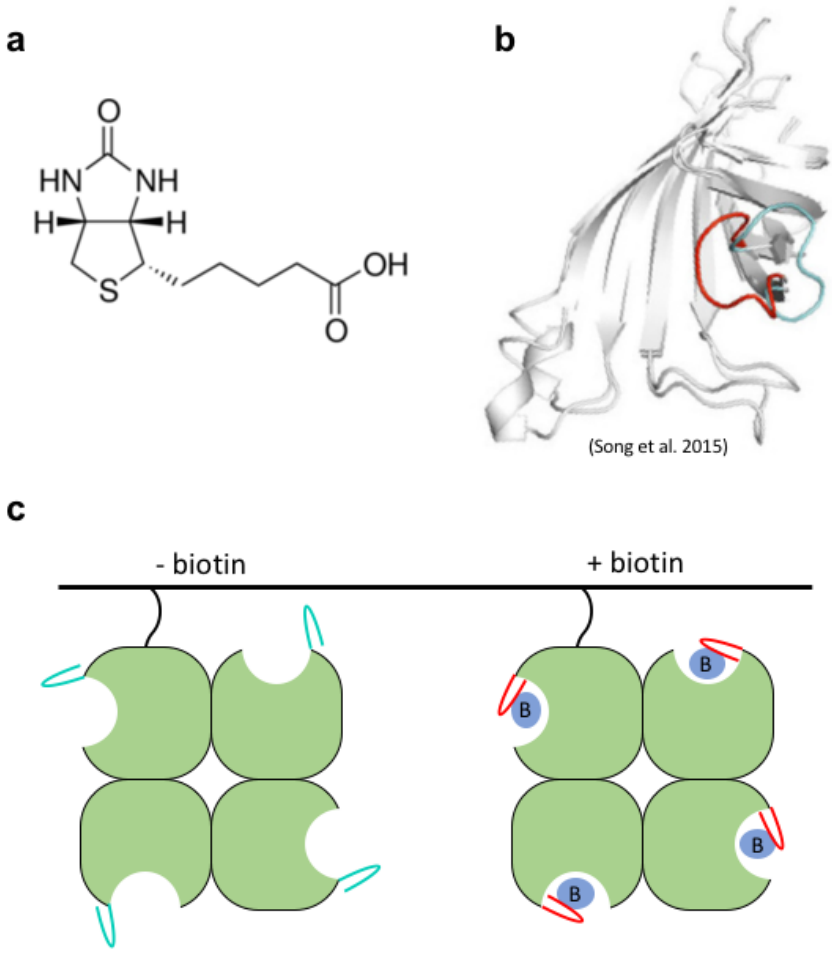

Figure 3.1: Biotin and streptavidin binding characteristics. (a) chemical structure of biotin. **(b)** monomeric subunit of streptavidin, highlighting the flexible loop in an open (blue) and closed (red) conformation. **(c)** Schematic diagram of immobilised tetrameric streptavidin, in the absence of its natural ligand with flexible loops of binding pockets adopting an open (blue) or closed (red) conformations in the presence of biotin (B) binding.

3.2.2 Artificial applications of biotin/streptavidin system

There is a plethora of reports and technologies using the biotin-(strept)avidin system for various protein and cellular applications, such as detection, bridging, isolation, targeting, immobilization, and imaging (reviewed in Laitinen et al., 2007; Dundas et al., 2013; Jain and Cheng, 2017). In all of these systems, one component is labelled with either 1- biotin or one of its analogues, by a process known as biotinylation, or 2- a biotin mimicking peptide, allowing for natural receptor binding, which can be used for various downstream applications.

3.2.2.1 Biotinylation

Besides its carboxylic acid moiety (Figure 3.1a), the relative inertness of biotin allows its conjugation to target proteins without loss of receptor binding activity. The first use of this conjugation system was through chemical biotinylation of recombinant proteins and antibodies; where biotin is covalently attached to amino acid side chains of target proteins in a non-specific manner. This method required further purification steps and has been shown to cause inactivation of labelled proteins (Stolz et al., 1998). As a result enzymatic biotinylation was developed and its use was first described in bacterial and yeast expression systems (Cronan, 1990) and then adapted in mammalian cells, requiring the genetic engineering of a biotin acceptor peptide (BAP) to target proteins (Parrott and Barry, 2001). Once translated, BAP fused to target protein is then covalently biotinylated by cellular or exogenously-expressed biotin protein ligase (BPL), with bacterial ligase BriA most commonly used in living cells (Beckett et al., 1999; Fairhead and Howarth, 2015). Unlike chemical biotinylation, enzymatic modification allows the production of site-specific lysine-biotinylated proteins, vectors and vaccines for subsequent purification or targeting (Parrott et al., 2000; Parrott and Barry, 2001; Barry et al., 2003; Campos et al., 2004). BAPs have since been developed and optimized into smaller peptides that can be either fused to target proteins, such as commercially available Avitag (Fairhead and Howarth, 2015), or expressed as a cell surface protein such as Lodavin (Murugan et al., 2012) for strept(avidin) binding. However, a well-recognized caveat of these technologies is the

requirement of harsh conditions to break biotin-strept(avidin) bonds; such as high concentrations of urea and thiourea, which causes protein denaturation with 90% recovery of biotinylated BSA from streptavidin sepharose (Rybak et al., 2004). Therefore, for purification application, biotinylation is not ideal for the isolation of labile macromolecules. To benefit from nature's strongest binding affinity, using synthetic peptides that bind streptavidin with a lower binding affinity than biotin, would allow elution of captured target molecules by the addition of biotin, through simple affinity out-competition.

3.2.2.2 Streptavidin binding synthetic peptides

Synthetic peptides have proved to be a very powerful tool for numerous biotechnology applications. Small peptides, usually discovered by phage display, that are able to interact with a protein's natural receptor are called peptide mimics or mimetopes. There are obvious advantages of fusing target proteins to small artificial mimetopes compared to larger sequences such as BAP for streptavidin binding. Firstly, small peptides do not require the co-expression of exogenous proteins or are not dependent on endogenous biotin ligases for receptor binding. Secondly, they are less likely to affect conformational structure or functionality of resulting fusion proteins. Thirdly, these peptides are not likely to be biotinylated by endogenous biotin ligase. Lastly, small peptides are very easy to synthesise or produce by molecular biology and amenable to many applications requiring bioconjugation strategies. In this section, we will focus on synthetic biotin mimics and their applications.

3.2.2.2.1 Biotin mimics

This class of mimics represent the most successful and widely used type of synthetic peptides. The fusion of small peptide ligands that functionally mimic biotin to proteins of interest, enabled the expansion of streptavidin application for affinity purification and immobilisation technologies. Since the affinity of biotin is too strong, affinity of peptide mimics could be fine-tuned through screening or rational design to bind streptavidin with lower affinities. This in

turn allows the displacement of mimics by biotin for natural receptor binding, therefore allowing gentle elution of purified/immobilised mimic-fused target.

3.2.2.2.1.1 Identification of HPQ motif

Mimics that can bind streptavidin were first identified through phage display-based strategies. In the first screenings, a streptavidin binding consensus domain His-Pro-Glu (HPQ) was identified in almost all selected binders (Devlin et al., 1990; Lam et al., 1991). Competitive binding studies then demonstrated that this sequence recognises the same streptavidin binding site as its natural ligand, supporting the notion that this motif is required for a functional biotin mimic (Patricia C. Weber et al., 1992; Katz, 1995). Therefore, given that HPQ-containing peptides occupy the same binding site as biotin, with dissociation constants determined in the millimolar range, whereas biotin binds with femtomolar affinity, these peptides are ideal for affinity purification applications as they can be easily displaced from streptavidin binding pocket by biotin. Thus, the fusion of HPQ containing peptide to target of interest, which can range from a protein to a viral particle, should first allow their binding to streptavidin matrix resulting in their capture. Subsequently, with orders of magnitude difference in affinities, the addition of biotin should displace the mimic from streptavidin binding pocket, resulting in elution of purified complex through competitive binding ligand (Figure 3.2).

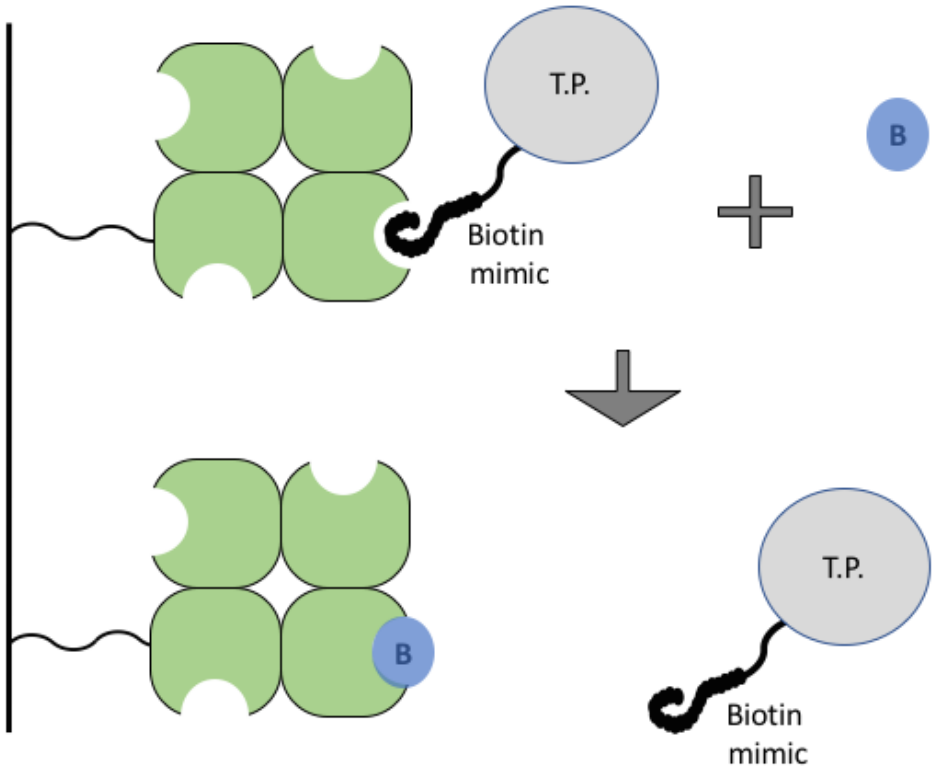

Figure 3.2: Schematic diagram for biotin mimic fused target protein purification. Genetic engineering of target protein (T.P.) with a biotin mimic allows streptavidin receptor binding. In the presence of biotin (B), the biotin mimic is displaced from biotin pocket due to higher biotin affinity leading to T.P. elution from streptavidin.

3.2.2.2.1.2 Binding kinetics of HPQ motif and biotin

Intriguingly, both molecular similarities and differences have been reported between receptor binding of HPQ motif-containing peptides and biotin. In the former case, residue H forms hydrogen bond with Ser88, as does the carboxylate domain of biotin. Streptavidin Ser45, which is involved in biotin's urea domain binding, interacts with residue P on its carboxyl terminus. Moreover, residue Thr90 in streptavidin forms hydrogen bonds with Q residue. However, this residue interacts through hydrophobic contact with biotin. (Perbandt et al., 2007; Dudak et al., 2011). Although HPQ motif and biotin have some binding differences, similarities in their receptor binding pocket contacts makes these motifs ideal for biotin-based displacement of receptor binding.

3.2.2.2.2 Development of linear mimics

Many advancements in peptide development have been made since the identification of HPQ-motif bearing peptides mimics. Several streptavidin binding peptides now exist with affinities ranging from μM, such as Streptag and its derivatives, to nM such as SBP-tag and Nanotag. These biotin mimics are widely used in various application for research and commercial purposes. These peptides adopt a linear conformation and along with their engineered derivatives are listed in Table 3.1.

Streptag was the first HPQ-containing mimic reported as an affinity tag (Ala-Trp-Arg-**His-Pro-Gln**-Phe-Gly-Gly) (Schmidt et al., 1996). Its first derivative was shown to only be functional when placed on the carboxyl terminus of fused proteins. Molecular analysis of streptavidin interaction indicated that the peptide did not penetrate as deep into the binding pocket as biotin does. Moreover, the carboxyl terminal glycine adopted a conformation forming a salt bridge with Arg84 in streptavidin explaining the reason behind its restrictive location to the carboxyl-terminus. In an effort to develop a peptide with no locational restrictions, Streptag-II was generated with a carboxyl lysine preceded by a glutamic acid, which it's side chain interacts with streptavidin in a similar fashion to C-terminal glycine in original Streptag. However, Streptag had a slightly lower binding affinity for streptavidin than Streptag-II. Thus, authors randomly mutated residues 44 - 47 in streptavidin's flexible loop. A streptavidin mutant, termed streptactin, in which amino acids ESAV of the binding loop were changed to VTAR, was isolated with a higher binding affinity to Streptag-II. (Schmidt et al., 1996; Skerra and Schmidt, 1999). These substitution mutations were shown to lower the conformational entropy of the loop by freezing it in an open state, causing a 10-fold decrease in the K_D for Streptag-II binding from 13 μM to 1.3 μM i.e. 10-fold increase in affinity (Korndörfer and Skerra, 2002). Furthermore, authors have generated Streptag-III which consists of two peptide sequence of Streptag-II flanked by a long serine-glycine linker as the final peptide derivative for this system (Junttila et al., 2005a). Streptag peptides have been used for various

applications from protein purification to protein tethering for biophysics experiments (Baumann et al., 2016).

Biotin mimics	Derivatives	Length (aa)	Sequence	Terminus conjugation restriction	Streptavidin affinity (K_D)
Streptag	I	8	WR**HPQ**FGG	Carboxy-	37 μM
	II	8	WS**HPQ**FEK	None	13 μM
	III	28	WS**HPQ**FEKGGGSGG GSGGGSWSHPQFEK	None	N/A
SBP	-tag	38	MDEKTTGWRGGHVVEGLAG ELEQLRARLEH**HPQ**GQREP	None	2.5-4.9 nM
	-tag2	25	GHVVEGLAG ELEQLRARLEH**HPQ**GQREP	None	2.5 nM
Nanotag	Nanotag15	15	fMDVEAWLGARVPLVET	Amino-	4 nM
	Nanotag9	9	fMDVEAWLGAR	Amino-	17 nM
	Nanotag7	7	fMDVEAWL	Amino-	N/A

Table 3.1: Common streptavidin binding peptides and their derivatives. Certain peptides were constrained to either terminus of target protein. N/A; not available.

The second class of biotin mimics is the SBP-tag peptides. The first derivative of SBP-tag mimics was an 88-mer peptide that was derived from mRNA display in vitro selection procedure (Wilson et al., 2001). This large peptide was further optimized to generate a smaller 38-mer mutant with a K_D of 2.5 – 4.9 nM to streptavidin (A. D. Keefe et al., 2001). Binding studies have determined two separate points of SBP interactions with streptavidin; HVV sequence from its N-terminus and the HPQ motif on its C-terminus; with the former failing to fill the binding pocket as the latter does. A drawback in using this peptide is that its binding affinity to streptavidin was shown to decrease once fused to target proteins (Barrette-Ng et al., 2013). Similarly to Streptag-II, a 25-mer mutant was then developed- SBP-tag2 along with its own

streptavidin mutant, SAVSBPM18 in an effort to retain SBP affinity while decreasing that of biotin by substitution of two residues important for biotin binding, G48T and S27A (Wu and Wong, 2013). More recently, authors have developed a stronger, covalent-based interaction between SBP-tag and mutant receptor by the strategic addition of cysteine residues in both components generating SBP(A18C) and SAVSBPM32 (Fogen et al., 2015).

Nanotag peptides are another class of biotin mimics however they do not harbor the HPQ motif. Three derivatives were developed with lengths ranging between 15 and 7 residues, with the former exhibiting the tightest binding with high affinity to streptavidin (Lamla and Erdmann, 2004). Although Nanotag peptides have the highest binding affinities, with K_D in nanomolar range, compared to other streptavidin binding peptides; Nanotag peptides can only be fused to the N-terminus of target proteins. Their high binding capacity is attributed to the formylation of initiating methionine (fMet) residue in peptides, thus restricting the use of Nanotag to bacterial production. Protein interaction studies revealed a remarkable resemblance in fMet's molecular interaction with streptavidin to that of biotin binding. Only when expressed on the N-terminus of target proteins can fMet bind deep into the binding pocket without steric restraints (Perbandt et al., 2007).

3.2.2.2.3 Cyclical biotin mimics

All currently used biotin mimics have a linear topology and although the field has primarily focused on this property for their applications, there is reason to suggest other structural conformations such as cyclical biotin mimics might be superior to linear tags as synthetic peptides. Soon after the discovery of HPQ-motif as a bona fide biotin mimic, studies aiming to optimize binding and further understand the design rules of biotin mimics, discovered the superiority of cyclical flanked HPQ-motifs as streptavidin binder. Early phage display library screenings demonstrated that flanking the HPQ motif with 2-18 random amino acids, making longer peptides, allowed for a more stable binding conformation (Kay et al., 1993). Furthermore, an increase in peptide ligand affinity was achieved by constraining peptides with disulfide bonds producing cyclical

biotin mimics (McLafferty et al., 1993). The importance of these bonds in enhanced binding conformation was shown by the significant decrease in affinity once treated with DTT, which breaks disulphide bonds, compared to linear peptides (Weber et al., 1995). Although phage display studies have demonstrated increased stability and higher binding of cyclical flanked peptides, current streptavidin binders like Streptag-II and SBP-tag are linear peptides. To date, the use of cyclical mimic as streptavidin binding peptides has not been tested yet, to the best of our knowledge. Thus, given their increased binding kinetics, the potential of these cyclical mimic as affinity purification peptides should be of interest to the field, but has yet to be explored.

3.3 Aims

In this study, we aimed to develop a novel method for LV purification based on the expression of a streptavidin affinity tag on the surface of vector particles. In this first chapter, a flanked cyclical HPQ-peptide (C**HPQ**GPPC) was tested as an affinity purification tag for biotin mimicry with reversible binding. This peptide was derived from a phage display screen of 6, 7 or 8 aa ($CX_{4/5/6}C$) cyclical peptide library screen against streptavidin (Giebel et al., 1995). Using Surface Plasmon Resonance biosensor, the peptide's affinity was determined at a 230nM, which was found to be 3 orders of magnitude higher than the corresponding linear peptide. In order to validate this peptide as a biotin mimic that could be applied for viral vector purification, the aims of this Chapter are the following:

- To evaluate streptavidin binding of the cyclical peptide and compare binding affinities of two variants in which the peptide's cysteine residues are flanked (ECHPQGPPCIEGRK) or un-flanked (CHPQGPPC).
- To compare cyclical mimics' streptavidin binding to the most commonly used linear mimic, Streptag-II.
- To determine cyclical peptides' optimal ectodomain/transmembrane structure for lipid bilayer expression, between CD8α stalk and GPI anchors, for highest streptavidin binding.
- To assess biotin-mediated reversible binding of peptides to streptavidin.
- To establish the proof of principle of affinity purification by testing purification of peptide-expressing cells as a model for viral vector application.

3.4 Comparison of three biotin-mimics for streptavidin binding on different structural formats

An HPQ-containing biotin mimic peptide isolated by Giebel et al., (1995), with significantly lower binding affinities than biotin (K_D 230nM), was chosen to be tested for the purpose of this project. Two variants of this peptide were used:

1- Original sequence isolated by the phage display study, termed Ctag (ECHPQGPPCIEGRK) consisting of CX_6C peptide flanked with a glutamic acid (E) in its amino-terminus and factor Xa cleavage site on its carboxy-terminus (IEGRK),
2- An un-flanked version of CX_6C peptide mimic termed short Ctag (sCtag) (CHPQGPPC).

These two formats were tested as the benefit of the extra flanking residues of CX_6C for epitope binding had not yet been determined. Moreover, we tested these variant peptides against the most commonly used linear biotin mimic, Streptag-II. With three synthetic peptides chosen to be examined, ultimately for viral purification application, we decided to first test them for streptavidin binding and subsequent biotin displacement on the plasma membrane of cells rather than fused to purified proteins. This is due to the fact that cells and their lipid bilayer resemble viral vectors but at a much larger size. Therefore, an optimal cell surface expression structure had to be tested. To that end, the three peptides were cloned in 4 different structural formats. All constructs cloned for this project are depicted in Figure 3.3. All open reading frames (ORF) were expressed on the commonly used retroviral SFG backbone (see section 2.1.1.9), co-expressed with eGFP as a marker gene separated by an IRES. Two distinct cell surface expression structures: GPI anchor sequence and CD8α stalk (consisting of CD8α's endo- and transmembrane-domains)- were tested for expression and binding. Since CD8α stalk is longer than that of GPI's length, mimics containing 2x epitopes' ORF linked by CD8α-derived linker, expressed on GPI anchor sequences were also constructed (x2-GPI), to allow longer cell surface display using GPI modifications. Also, peptides were fused to CD8α transmembrane domains without an ecto-domain (Flush)

to assess steric hindrance for streptavidin binding. Schematic diagrams of plasmids maps and protein sequences are shown in Figure 3.3 and a diagram of peptides and constructs' protein structures are depicted in Figure 3.4.

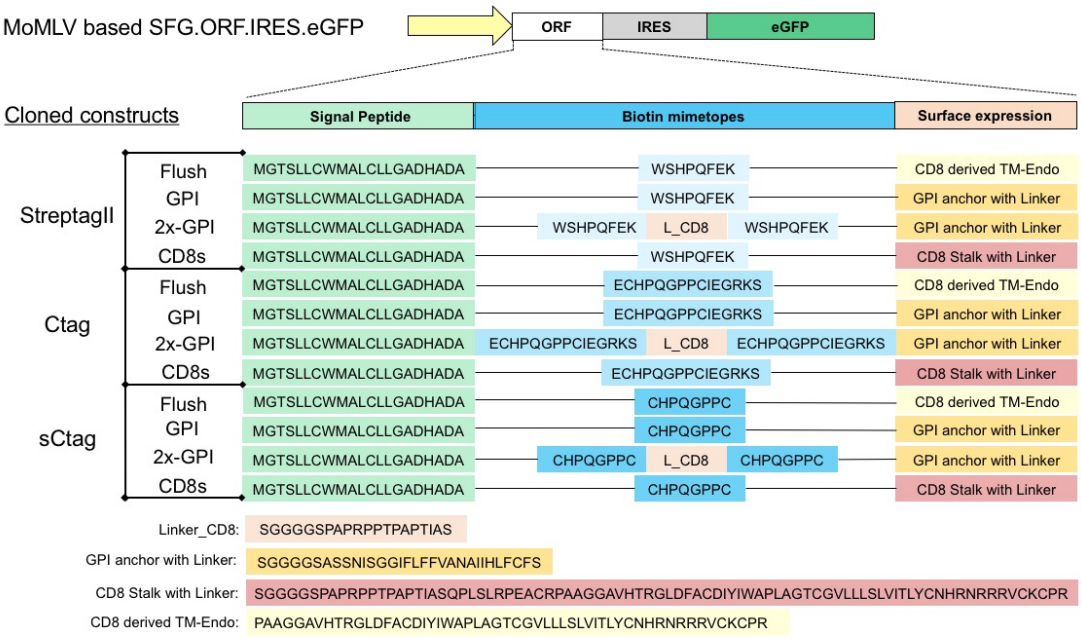

Figure 3.3: Schematic diagram of cloned SFG γ-retroviral plasmid constructs and protein sequences. All constructs were cloned into a retroviral plasmid termed SFG derived from Moloney murine leukemia virus (MoMLV). Open reading frames were clones upstream of marker gene eGFP expressed using an IRES. Four open reading frames were generated for each binder: (1) Flush: consisting of a CD8-derived transmembrane (TM) and endodomain (Endo); (2) GPI: consisting of GPI anchor sequence (25aa), is modified by cellular machinery leading to the addition of GPI at the anchor sequence, with a serine-glycine linker (6aa); (3) x2-GPI: consisting of 2 copies of epitopes' ORF separated by serine-glycine linker with the first 14aa of CD8α stalk ectodomain (Linker_CD8), on a GPI anchor sequence; (4)CD8s: consisting of CD8α stalk comprising of the ecto-, transmembrane and endo-domains of human CD8 molecule, with a serine-glycine linker.

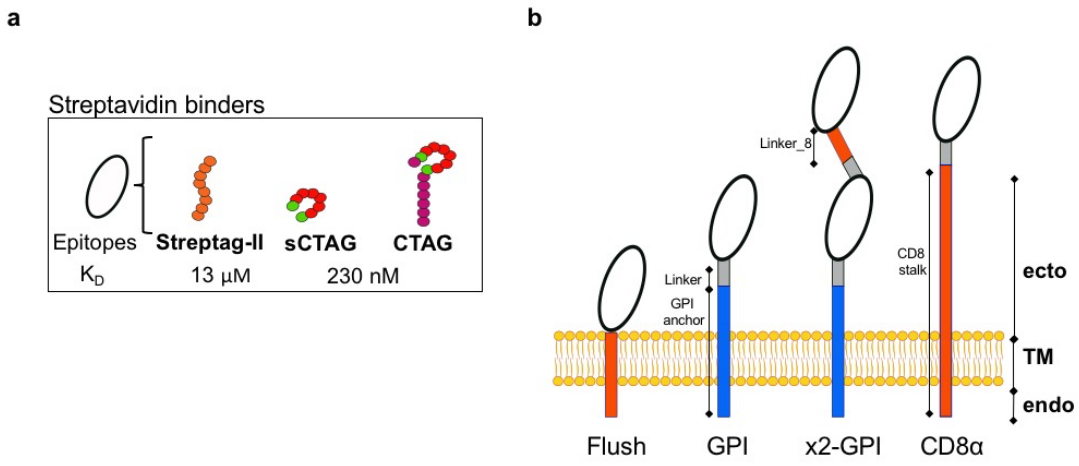

Figure 3.4: Diagram of streptavidin binders and their different surface expression structures. (a) Schematic representation of the chosen streptavidin binders with their reported dissociation constants (K_D). **(b)** Four surface expression structures were tested for each peptide.

To test binding efficiencies of constructs and levels of expression, plasmids were transiently transfected into HEK293T cells and after 48 hours cells were labelled with APC conjugated streptavidin. For comparison, streptavidin binding of eGFP positive cells was analysed and expression profile and median fluorescence intensities are shown in Figure 3.5a-b. Expression of epitopes on GPI anchors did not result in significant streptavidin binding as seen in Figure 3.5c. Interestingly, peptides expressed in a flush format i.e. without ectodomain, seemed to result in streptavidin binding that was significantly higher than that on GPI anchors for all peptide mimics. Streptag-II expression on 2x-GPI format resulted in a similar binding intensity than its flush version with MFI of 3440 ±255. However, both sCtag and Ctag expressed on 2x-GPI format resulted in higher binding intensities than their flush version with MFI of 5228 ±249 and 10804 ±1204, respectively. This pattern of epitope binding efficiency was also observed when epitopes were expressed on CD8α stalks which resulted in significantly higher binding intensities to streptavidin than the other structural formats with the lowest MFI for Streptag-II of 8049 ±1064, followed by 10043 ±186 for sCtag and the highest intensity of 14957 ±1668 for Ctag.

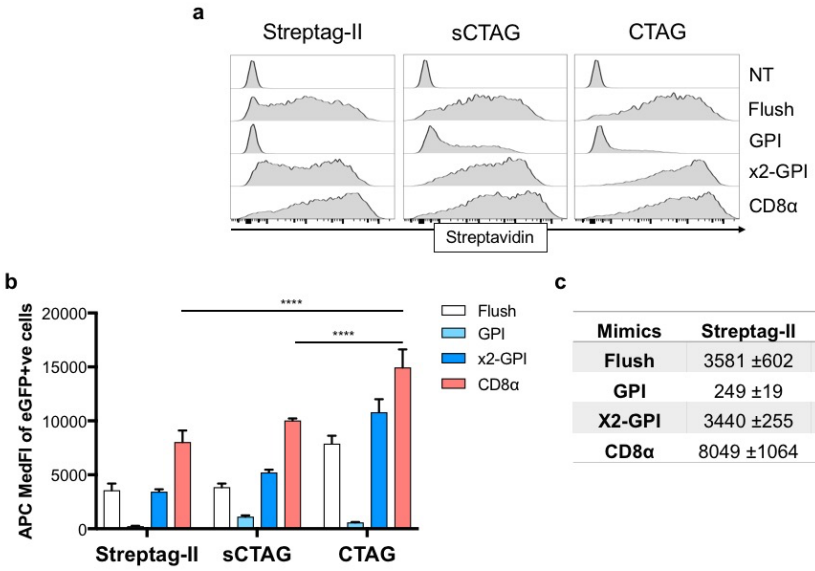

Mimics	Streptag-II	sCTAG	Ctag
Flush	3581 ±602	3864 ±330	7899 ±723
GPI	249 ±19	1124 ±120	595 ±33
X2-GPI	3440 ±255	5228 ±249	10804 ±1204
CD8α	8049 ±1064	10043 ±186	14957 ±1668

Figure 3.5: Testing the synthetic surface expressing peptides for streptavidin binding. (a) HEK293T cells were transiently transfected with all cloned constructs and stained with APC conjugated streptavidin 48 hours later and histograms of eGFP-positive cells along with NT are presented as staggered plots for each peptide. **(b)** The median fluorescence intensity (MFI) of streptavidin binding of eGFP-positive cells are presented in a graph **(b)** and in a table **(c)** ± standard deviation (SD) of three independent transient expression experiments (n=3) with **** $p<0.0001$ and ns as non-significant.

Therefore, epitopes expression on CD8α stalk seemed to result in the highest streptavidin binding compared to GPI anchors, with the highest binding attributed to Ctag. The superiority of CD8α stalk for streptavidin binding may be due to difference in binding efficiencies as well as peptide expression density on GPI anchors. However, as we required the highest streptavidin binding, Ctag expressed on a CD8α stalk was chosen to be taken forward.

3.5 Demonstration of peptide displacement by biotin for streptavidin binding

Since the CD8α stalk resulted in optimal properties for affinity peptide in surface expression and Ctag resulted in highest streptavidin binding, we tested the efficiency of streptavidin bound Ctag-CD8 displacement by biotin. To that end, HEK293T cells were transiently transfected either Ctag expressed on CD8α stalk (from Figure 3.3) or an irrelevant protein; the beta chain of T cell receptor co-expressed with eGFP by an IRES on an SFG plasmid, as a negative control. Cells were then stained with streptavidin-APC 48 hours later and streptavidin expression of eGFP-positive cells are presented as overlaid histograms (Figure 3.6a, grey and red population). Subsequently, Ctag-CD8 transfected cells stained with streptavidin were incubated overnight with an excess of biotin at 1mM in PBS. Afterwards, cells were washed with PBS to remove unbound streptavidin-APC and the expression profile was determined (Figure 3.6a, blue population). The addition of 1mM biotin decreased Ctag-expressing cells bound to streptavidin by 60%. The MFI of streptavidin binding of eGFP-positive cells before and after biotin incubation are plotted in Figure 3.6b and indicate a 90% drop in streptavidin binding intensity in the presence of 1mM biotin. However, using 1mM biotin does not seem to be sufficient to displace all Ctag bound to streptavidin and higher concentration of biotin may have resulted in a larger population displacement of more than 60%. Nonetheless, the addition of biotin seems to successfully outcompete a major fraction of streptavidin bound Ctag-cells, thus in turn allowing the release of Ctag-expressing cells.

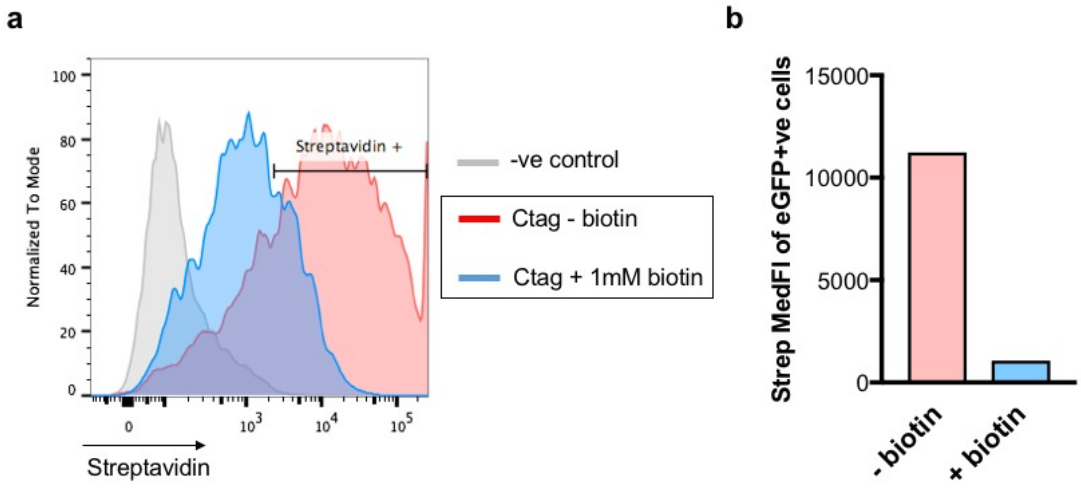

Figure 3.6: Reversible streptavidin binding of Ctag by biotin displacement. HEK293T cells were transiently transfected with SFG plasmid expressing Ctag on CD8α stalk (Ctag-CD8s) or a control SFG plasmid expressing the beta chain of T cell receptor protein (-ve, negative control), both of which co-express eGFP. 48 hours post-transfection, cells were stained with streptavidin-APC. Cells were then incubated with 1mM biotin in PBS overnight at room temperature. **(a)** Overlaid histograms of eGFP-positive cells' streptavidin binding of –ve control (grey population), Ctag-CD8 expressing cells (- Biotin, red population) and Ctag-CD8 cells incubated with biotin (+ 1mM Biotin, blue population). **(b)** MFI of streptavidin binding of eGFP-positive cells are plotted in the absence (- biotin) and presence (+ biotin) of 1mM biotin.

3.6 Characterization of Ctag as a streptavidin specific binding peptide

To determine whether Ctag peptide is a universal biotin mimic, its binding to avidin was also tested. Cells expressing the biotin mimic were generated by transient transfection of Ctag construct (from Figure 3.3). These cells were stained, alongside non-transfected cells, with either streptavidin-APC or avidin-APC ,48 hours after transfection (Figure 3.7). As expected, Ctag exhibited high intensity binding to streptavidin with around 86% ±0.3 cells positive for streptavidin. Ctag however did not to bind avidin, with 1.5% ±0.4 cells positive for avidin staining (Figure 3.7a). Moreover, streptavidin positive cells had a relatively high MFI of 28768 ±1289, whereas avidin staining resulted in a below zero intensity, once background staining of negative control was subtracted from both individual staining (Figure 3.7b). Therefore, Ctag is not a universal mimic as it does not seem to bind avidin.

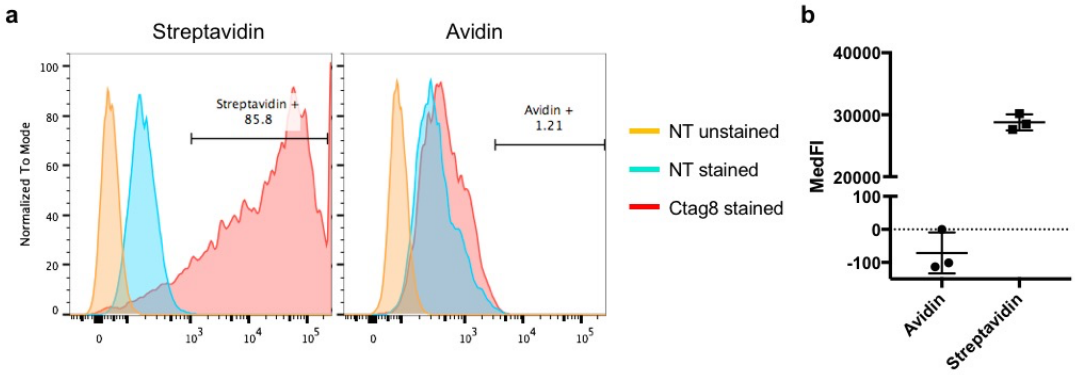

Figure 3.7: Ctag biotin mimic does not bind avidin. HEK293T cells were transiently transfected with an SFG γ-RV plasmid expressing Ctag on a CD8α stalk without a fluorescence marker. 48 hours post-transfection, cells were harvested and stained with streptavidin and avidin, both conjugated to FITC. **(a)** Overlaid histograms are presented with stained and unstained negative control, non-transfected (NT) cells. **(b)** Median fluorescence intensities (MFI) of streptavidin/avidin positive populations, after background staining subtraction of control staining, are presented ± standard deviation (SD) of triplicate determinations.

3.7 Establishment of proof of principle by cell sorting epitope-expressing suspension cells using streptavidin magnetic beads

To obtain proof of principle that the epitope Ctag can allow the purification of LV particles expressing it on their surface, suspension K562 cells expressing Ctag on their surface were tested for cell sorting using streptavidin magnetic beads. If cells with much larger mass were successfully purified, then purification of viral particles should be possible in a similar manner. K562 cells were chosen to model for viral purification due to their ease of handling, generation and detection of surface protein expression. To that end, K562 cells were γ-retrovirally transduced with retroviral vector encoding Ctag on CD8α stalk as well as eGFP as a marker gene. A transduction efficiency of 10.5% (pre-sorting) was achieved based on eGFP expression (Figure 3.8). Transduced cells were then incubated with superparamagnetic streptavidin beads that are commonly used for various applications, MyOne streptavidin Dynabeads (1µm diameter). It should be noted that these beads are not designed for cell or virus isolation. They were nevertheless chosen as they offer several advantages compared other magnetic beads designed for cell

isolation, such as Miltenyi's streptavidin microbeads. Dynabeads do not require customized columns for isolation of bound macromolecules and are large enough to be manipulated in magnetic racks that can hold 1.5/15mL tubes. A cellular pellet containing $1x10^6$ Ctag-transduced K562 cells was incubated with an excess number of magnetic beads (~3.5×10^7) and incubated for 1 hour. Subsequently, using a magnetic rack, magnetic beads were isolated from flow-through fraction into sorted fraction, both of which were cultured separately before isolation analysis. Subsequently 12 days post-sorting, during which cells were passaged to remove the majority of magnetic beads as not to interfere with flow cytometry analysis, the sorted fraction contained 93.6% of eGFP-positive cells, whereas the flow-through fraction was depleted from eGFP-positive cells and contained 97.4% eGFP-negative cells. This result indicated the successful capture and sorting of Ctag-expressing K562 cells using MyOne streptavidin Dynabeads.

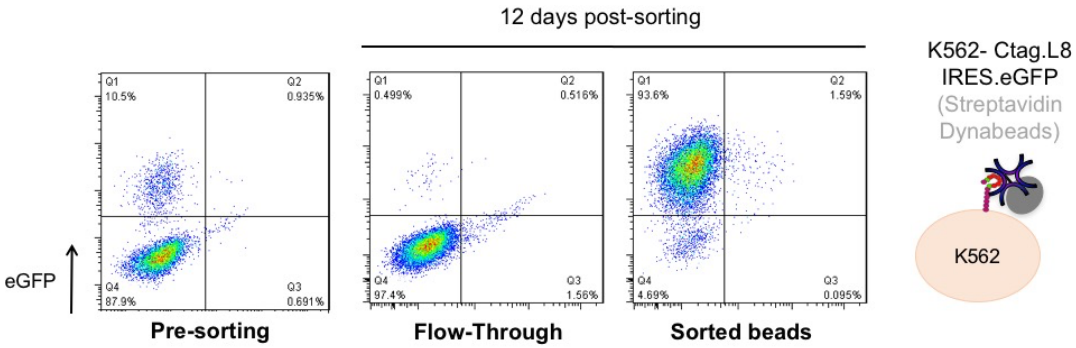

Figure 3.8: Proof of concept for cellular sorting using Ctag with streptavidin coated magnetic beads. K562 cells were γ-retrovirally transduced once to express SFG.Ctag.IRES.eGFP. Transduction efficiency was determined by flow cytometry and 10.5% of the cells were eGFP (y-axis)-positive (x-axis of plots is blank to account for auto-fluorescence of dead cells). Cells were then sorted with Dynabeads® MyOne™ Streptavidin T1 magnetic beads (10mg/mL) by incubating beads with cells for 1 hour at room temperature. Beads-sorted and flow-through fractions were then collected and assessed 12 days post-sorting to allow enough cellular division to dilute magnetic beads for better flow-cytometry detection. A schematic diagram depicts K562 cell (beige oval) expressing Ctag on a CD8α stalk bound to tetrameric streptavidin bound to magnetic bead (grey circle).

3.8 Discussion

In this Chapter, we have constructed and validated a surface expressing flanked cyclical biotin mimic (Ctag, 16aa) as an affinity purification tag from Giebel et al., (1995).

Ctag contains two aspects of peptide designs that were shown to enhance binding and stabilize structural conformation; flanking HPQ motifs and constraining it in a cyclical manner (Kay et al., 1993; McLafferty et al., 1993). The effect of further residues flanking the cyclical sequence was unknown, therefore both un-flanked (sCtag) and flanked cyclical peptides (Ctag) were tested alongside the commercially used Streptag-II. In all cases, serine-glycine based linker sequences were added on C-terminus of peptides to project biotin mimics away from cell surface leading to increased conformational flexibility. Expression of peptides on CD8α stalks (250aa) resulted in higher streptavidin binding when compared to GPI anchors (75aa). GPI anchors have been shown to localize in lipid rafts (Legler et al., 2005) and therefore expression of peptide on these anchors may have resulted in limited cell surface presentation for receptor binding compared to the distal CD8α stalk. Moreover, with the difference in length between these two surface structures, it could be suggested that expression on CD8 increases peptide accessibility to streptavidin, thus resulting in higher binding. However, since an indirect measurement was performed based on eGFP expression; this could be further investigated by determining the density of epitopes expressed on both CD8α stalks and GPI anchors on the surface of expressing cells. As previously mentioned, constraining biotin mimics with into a cyclical structure resulted in an increase in ligand affinity (McLafferty et al., 1993). Both cyclical peptides tested in this chapter sCtag and Ctag resulted in higher streptavidin binding on CD8α stalk compared to linear Streptag-II. This could be investigated further by determining epitopes' binding affinities to streptavidin to evaluate the effect of peptide architecture on binding kinetics. Additionally, flanking HPQ motif has been demonstrated to result in increased stable binding confirmation (Kay et al., 1993). Interestingly, our results seemed to indicate further flanking of

cyclical-flanked-HPQ motifs may enhance binding stability, as shown by the higher binding intensity of Ctag compared to sCtag. However, further experiment determining binding kinetics of these variants would elucidate the impact of Ctag's further flanking residues. Nonetheless, in this chapter we have demonstrated bound Ctag's displacement by the presence of biotin owing to its extraordinary affinity to streptavidin, thus demonstrating reversible Ctag binding to streptavidin.

A true biotin mimic should bind all biotin's natural receptors. However, few studies have subjected their isolated peptides to determine their universal mimicry and most have failed (Dudak et al., 2011). In line with these results, Ctag did not exhibit avidin binding, making it a streptavidin only binder, semi-mimicking biotin. This could be explained by further zooming into the molecular interplay between biotin and its receptors' binding. Binding pockets of avidin and streptavidin have certain structural differences. Upon ligand binding, aromatic residue Phe72 in avidin plays an important role in stabilizing ligand binding. This residue or rather its interactions, does not exist in streptavidin (Livnah et al., 1993). Therefore, HPQ motif may not be able to form the required contact, such as Phe72, for avidin binding. Furthermore, avidin does not contain a residue corresponding to Ser45, which plays an essential role in both biotin and HPQ-motif binding. These reasons could account for the preference of HPQ-containing mimics to streptavidin rather than avidin. Further investigation into the molecular interactions of HPQ to streptavidin could elucidate its full interplay, which in turn would highlight key features that are responsible for streptavidin or avidin specific binding of mimics

In this Chapter, Ctag's binding affinity has proven to be sufficient for the capture of suspension cells using streptavidin labeled magnetic beads, thus making it an effective affinity tag for the purification of large molecular structures. We reasoned that since Ctag binding to streptavidin allowed cell isolation, this interaction should be sufficient to purify particles that are 16,000x smaller in surface area than suspension cells, such as LVs.

Chapter 4 Streptavidin-mediated complete capture of Ctag- modified LVs by passive incorporation

4.1 Overview

In the previous Chapter, a cyclical peptide was validated as a reversible biotin mimic, which allowed the isolation of suspension cells expressing it on their surface, by its interaction with streptavidin. In this Chapter, we investigate different methods for LV particle modification to allow viral surface expression of Ctag peptide, while retaining vector infectivity, for efficient vector capture from viral supernatant.

4.2 Introduction

An overview of the different methods of viral vector surface modifications is presented in this section. And then more specifically, examples of LVs modification for biotin/(strept)avidin applications are also discussed.

4.2.1 Viral vector surface engineering concept

Modification of viral particle surfaces has a wide range of applications both in basic and applied molecular biotechnology. It is an attractive concept as it opens up several possibilities such as precise high efficiency targeted infection or even impose new functions on these particles. This can be accomplished either by modulation using regulatory elements in the transfer vector, such as tissue specific promoters, or by altering the protein composition of the vectors' physical shell i.e. the viral surface. Manipulation of these surfaces can be broadly classed into either pre- or post-virion budding. The former involves the genetic manipulation of vector producing cells by transfection or transduction of engineered viral or viral-associated proteins thus, relying on packaging cells' cellular machinery for vector modification. Conversely, post-budding strategies can modify vectors either after or just before cell exit by modifying vector

packaging cells' membrane, allowing modification incorporation in budding virions. Post-budding strategies are generally independent of the genetic material so can be established once and applied to a wide range of vectors. Moreover, unlike a strategy that manipulates vectors after production, a host cell membrane-dependent incorporation eliminates the need to remove non-viral associated modification proteins and the time required for manipulation which may impact infectivity (Metzner et al., 2013a). Therefore, a strategy in which vectors are manipulated upon virion budding from vector producing cells' membrane is preferred.

4.2.2 Methods for enveloped virus surface modification

4.2.2.1 Vector incorporation of virus/cell-derived proteins

Upon budding from infected cells, virions are surrounded by a lipid bilayer, termed envelope. This layer is derived from the packaging cells and contains both virus and cell-derived proteins. The only viral proteins on this surface are envelope glycoproteins which are responsible for target cell receptor recognition and cell entry (Liang et al., 2009). Prior to budding, the precise location and mechanisms of viral particle assembly are not fully understood yet. Nonetheless, apart from viral proteins, particles also contain host cell-derived proteins. Three types of general particle incorporations have been theoretically proposed:

1. Interaction with viral proteins, such as cyclophilin A with HIV-1 viral gag proteins (Hammarstedt and Garoff, 2004).
2. Directed co-localization, such as CD55 and CD59 proteins which are anchored by GPI motifs that tend to localize in lipid rafts; a proposed LV viral assembly site (Pickl et al., 2001; Popik et al., 2002).
3. Random/passive incorporation.

It is rather difficult to discriminate between type 2 and 3, as it is difficult to demonstrate the former. It has however been proposed that most inclusions occur passively through random incorporation (Hammarstedt and Garoff, 2004).

As for vector surface engineering, the field has widely developed and advanced for non-enveloped, naked viruses such as AAV and AdV due to their inherent increased particle stability (reviewed in Waehler et al., 2007; Buchholz et al., 2015). These applications were extended to assess viral surface engineering of enveloped virus engineering testing, which is the scope of this section. Surface manipulation of envelope vectors can be generally separated into five sections, which are schematically depicted in Figure 4.1.

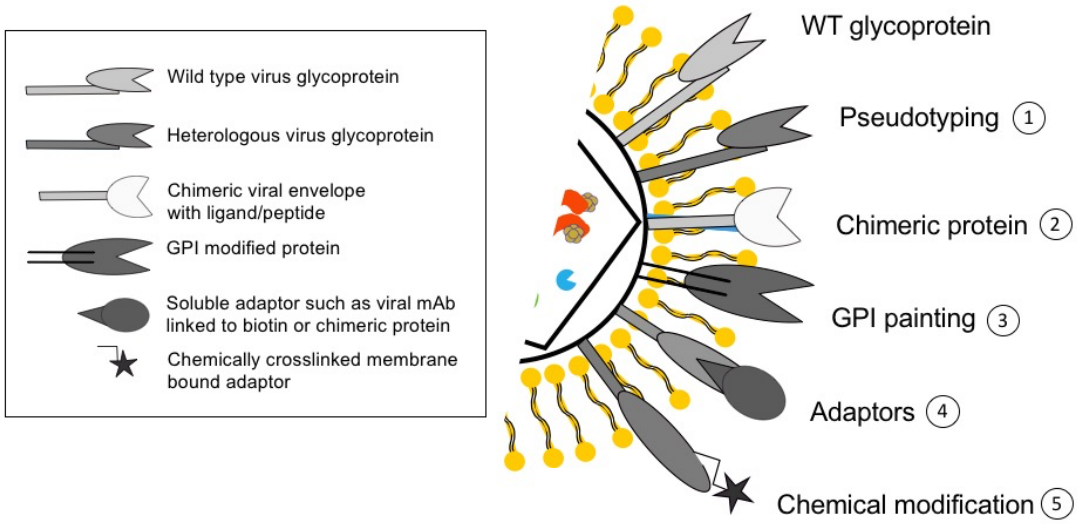

Figure 4.1: Overview of different viral surface modifications.

4.2.2.2 Pseudotyping

This concept was covered in Section 1.3.1 and involves the transfer of envelope glycoprotein between different viruses. It is regarded as a viral surface modification and accordingly several studies attempted to understand the incorporation of heterologous envelopes. It is generally believed to involve specific membrane domains such as lipid rafts used for viral assembly, which in of themselves are rather controversial (Pickl et al., 2001; John A. G. Briggs et al., 2003). Nevertheless, applying the methods of incorporation of cell-derived proteins to heterologous glycoproteins, pseudotyping can be considered a type 2 incorporation i.e. a direct co-localization with viral proteins

during virion assembly. A later study then proposed an indirect model for incorporation involving interaction with viral protein, thus making it a type 1 incorporation (Jorgenson et al., 2009). Unfortunately, pseudotyping is limited due to the restricted number of viral glycoproteins available and their respective receptors.

4.2.2.3 Genetically engineered chimeric envelopes

To overcome the limitation of heterologous glycoproteins, the field has moved on to the genetic modification of chimeric envelopes. Envelope glycoproteins can tolerate a degree of genetic manipulation and several attempts have been made for targeted transduction. Many polypeptides such as growth factors, cytokines and synthetic peptides have been displayed on RV/LV envelope proteins as either; N-terminal fusions, inserted into proline-rich hinge region or even as N-terminal substitution (Larochelle et al., 2002). In these studies, insertion sites had either been determined by structural information of the receptor's binding domain or by screening a large pool of chimeric mutants; or in most cases it was determined heuristically (Rothenberg et al., 2001). However these attempts were met with several difficulties due to the nature and role of envelope glycoproteins.

Murine leukaemia virus (MLV) glycoprotein is the most commonly altered envelope for targeted transduction with modifications including peptide insertion in pre-folded domains (Valsesia-Wittmann et al., 1994; Wu et al., 1998; Gollan and Green, 2002), expression of peptides as additional domains (Chadwick et al., 1999; Cosset et al., 1995; Fielding et al., 1998; Martín et al., 2002; Maurice et al., 1999, 2002) and peptides fused directly to the transmembrane part of the envelope (Chu et al., 1994; Chu and Dornburg, 1995; Matano et al., 1995; Jiang et al., 1998). Most N-terminally substituted chimeric envelopes studied to date had either had very low viral incorporation or absence of transduction of target cells. For example, RVs with glycoproteins modified with chemokines (Katane et al., 2002) or an integrin binding peptide (Wu et al., 2010) were shown to have poor transduction efficiencies. Additionally, a chimeric MLV glycoprotein containing aCD33 single chain

variable fragment (scFv) on its amino-terminus could not induce fusion activation and subsequent viral entry on target cells (Zhao et al., 1999). This was also observed when EGF-MLV greatly impaired infection of EGFR-positive cells only but not EGFR-negative cells (Cosset et al., 1995). These observations were suggested to be caused by receptor sequestration on plasma membrane followed by receptor-mediated-endocytosis, which routed viral entry down to a lysosomal path, thereby inhibiting transduction. This finding led to the idea that ligand expressing virus can selectively target cells that do not express its receptor i.e. indirect targeting (Lavillette et al., 2001b; Verhoeyen and Cosset, 2004; Metzner and Dangerfiel, 2011). And in line with Cosset et al., (1995), a modified vector was generated to express the stem cell factor (SCF) ligand and was shown to selectively inhibited transduction of c-Kit expressing cells (Fielding et al., 1998). Moreover, when measles virus glycoprotein was engineered to express either a scFv against CD3 (Maurice et al., 2002) or IL7 (Verhoeyen et al., 2003) on its N-terminus and even though modified viral particles specifically targeted T cells, infectivity was very poor due to deficient fusion activity. Inefficient infection was also observed when MLV glycoprotein was engineered with scFv against MHC class II to specifically transduce dendritic cells (Gennari et al., 2009). This was reasoned to either be due to fusion deficiency of bound viral particles or their sequestration by cell surface molecules. Several studies investigating the molecular mechanisms between receptor binding and fusion activation domains of envelop proteins indicated that these two features are very closely coupled with highly coordinated functions that begin with viral receptor binding, which leads to alteration of protein configuration to induce fusion (Barnett and Cunningham, 2001; Lavillette et al., 2001a). To overcome this major limitation of genetically engineered viral envelopes and rescue infectivity, chimeric glycoproteins were co-expressed with wild-type glycoproteins which also seemed to enhance viral incorporation; indicating a possible type 1 incorporation (Maurice et al., 2002; Tai et al., 2003; Verhoeyen et al., 2003). However, infection rescue for genetically engineered glycoprotein comes at the price of its specificity for target transduction and thus required the expression of different envelopes in

which a modified protein account for targeted binding and another wild-type glycoprotein allows particle infectivity (Frecha et al., 2012).

It is generally accepted that loss of infectivity of pH-independent engineered glycoproteins, such as VSV-g and MLV, is caused by failure of inducing conformational change required for fusion upon cell receptor binding for infectivity by fusion (Larochelle et al., 2002; Metzner and Dangerfield, 2011). This is highlighted by the fact that envelope glycoproteins that use a pH-dependent fusion activation pathway, that does not rely on receptor binding, can be engineered and used to pseudotype LVs without loss of infectivity; such as sindbis virus (Pariente et al., 2007), influenza (Lin et al., 2001; Yang et al., 2006) and measles virus (Funke et al., 2008; Anliker et al., 2010; Ageichik et al., 2011). The binding and fusion domain of these envelopes have been shown to function independently, thus being amenable for genetic modification. The fusion molecule of sindbis is very flexible for genetic engineering and several studies have successfully targeted immune cells (Froelich et al., 2010), B cell compartment specifically (Lei et al., 2009) and even tumor vasculature using a VEGFR2 specific single domain antibody (Ahani et al., 2016). Nonetheless, a major limitation using genetically engineered envelopes is that their accuracy in targeting comes at the price of low gene transfer efficiency.

4.2.2.4 GPI modification

In eukaryotic cells, around 0.5% of proteins are post-translationally modified with a GPI moiety (Eisenhaber et al., 2001) which, as discussed in Chapter 3, functions as a cell surface anchor for proteins. Any protein expressing GPI-signal sequence (GSS) at its carboxyl end is recognized by transaminase enzyme in the ER which processes it by GSS cleavage and replacement with GPI-anchor. A wide range of functions can be attributed to GPI anchored proteins from signal transduction (Haeryfar and Hoskin, 2004), human complement regulatory activity; and viral infectivity restriction (Swiecki et al., 2013). These proteins have been shown to frequently associate with lipid rafts (Legler et al., 2005). Most strikingly, GPI proteins have a mechanism of spontaneous membrane release with intact anchors which is reversible and

has been demonstrated in a wide range of systems for lipid bilayer reinsertion both *in vitro* and *in vivo* (Väkevä et al., 1994; Kooyman et al.,1995; Rooney et al., 1996; Dunn et al., 1996). This cell painting phenomenon was first described in the 1980s with the incorporation of CD59-his onto cells (Medof et al., 1984). It was recently demonstrated that the lipophilic parts of these anchors are responsible for this hypermobility mechanism (Metzner et al., 2013b). This mechanism was extended to viruses with protein attachment to MLV and HIV-1 based vectors, herpes virus and influenza virus (Shaw et al., 2008; Metzner et al., 2008a; Fitzpatrick et al., 2010; Gregory et al., 2014). This process is dynamic allowing simultaneous viral painting of two different GPI proteins (Metzner et al., 2013b); as well providing modified viruses with new functions, such as immune protection by CD95 painting (Heider et al., 2016). Two strategies have been developed for lentiviral modification using GPI proteins:

1. Membrane co-localization at possible viral budding site such as lipid rafts (Nguyen and Hildreth, 2000; John A. G. Briggs et al., 2003), therefore requiring co-transfection with vector packaging plasmids;
2. Viral painting of vectors after packaging cell budding, which requires purified GPI proteins.

Although this type of modification is highly versatile, GPI's inherent hypermobility can be seen as its own Achilles' heel, as its reversible attachment is not stable and can dissociate spontaneously. Such a modification is not ideal for viral vector downstream processing applications.

4.2.2.5 Adaptors

As discussed previously, engineering viral proteins on the surface of particle is difficult without any collateral damage to their functions. Using adaptor molecules, either soluble or membrane bound proteins, can circumvent this issue by bridging viral particles and target cells.

4.2.2.5.1 Soluble adaptors

Soluble adaptors are diverse in function and structure with a primary aim of bridging infection and targeted transduction. The most commonly used forms

are bispecific molecules that can contact viral vectors from one side and target cells from the other. These proteins have many different forms, for example two antibodies binding both entities can be bridged using (strept)avidin. The feasibility of such a highly versatile and flexible bridging adaptor was demonstrated in 1989 with biotinylated antibodies against viral envelope protein and target cells' MHC II molecules (Roux et al., 1989). However, viral entry was shown to occur via MHC molecule, which resulted in low gene transfer as RV were routed via another endosomal pathway. Moreover, the (strept)avidin/biotinylated antibody complex is quite large and bulky, which may interfere with viral fusion entry. Another 'smaller' bridging strategy is the use of soluble chimeric proteins, in which one side can bind viral proteins and the other is a ligand to a receptor on target cells. This strategy was tested using a chimeric protein consisting of ASLV's cell receptor, which binds its glycoprotein; fused to different growth factors such as EGF, VEGF and HRG, for targeted transduction of RV to cells expressing their respective receptors, such as tumor cells (Snitkovsky et al., 2000, 2001; Snitkovsky and Young, 2002). Moreover, nanobody can be used instead in chimeric proteins for target receptor binding, and their use was demonstrated with the retargeting of enveloped HSV-1 vectors to tumor cells bearing CEA antigen (Baek et al., 2011). Although soluble adaptors offer a wide range of versatility for virus-cell bridging, their use is impracticable, inefficient and costly. Additionally, suboptimal stability of viral vector-adaptor complex could hinder target cells gene transfer. Moreover, their coupling efficiencies have been reported to vary between batches. Also, their use in a large-scale setting would require scaling up their production which has its own technical difficulties (Waehler et al., 2007). And finally upon design of these adaptors, competition from serum antibodies for binding *in vivo* should be taken into considerations, as they may lead to increased viral dissociation (Yang et al., 2006).

4.2.2.5.2 Membrane-bound adaptors

The most common conformation of membrane bound adaptors is the genetic fusion of viral glycoprotein's ecto- and transmembrane domains to either a ligand of a receptor on target cells, or in most cases to (strept)avidin due to

their extraordinary affinity, as discussed in Section 3.2. For example, monomeric avidin was genetically fused to membrane anchoring domain of VSV-g, which upon viral incorporation allowed dual imaging and targeting usage (Kaikkonen et al., 2009a). This method is attractive as using envelop protein's membrane stalk would allow co-localization of chimeric protein leading to viral incorporation. Other approaches have utilized biotin acceptor peptides (BAPs) thus requiring biotinylation by co-expression of BirA for metabolic modification. To that end, BAPs have been fused to either ecto- and transmembrane domains of VSV-g glycoprotein (Etemadzadeh et al., 2015) or sindbis glycoprotein (Morizono et al., 2009); or to that of non-viral proteins such as LNGFR (Nesbeth et al., 2006). Using such a system actually involves the use of several viral modification methods. For example, particle modification in the latter study involved the membrane incorporation of a chimeric protein that upon chemical modification resulted in engineered viral vectors. This type of modification also represents a random incorporation of non-viral chimeric protein.

4.2.2.6 Chemical modification

Direct chemical conjugation is used to link adaptors to viral vectors by targeting specific sites or compounds on viral surfaces. This method involves rather harsh conditions and therefore has been often used on naked non-enveloped viruses such as AAV/AdV, (Croyle et al., 2000, 2002; Schaffer et al., 2008; Bartel et al., 2011). Conversely, chemical modification of enveloped viruses hasn't been easy due to their relative instability. Nonetheless, several attempts have been made to chemically manipulate enveloped viruses for various applications. For example, galactose moieties were chemically added onto ecotropic MLVs which led to targeted transduction of human hepatoma but with reduced infectivity (Neda et al., 1991). Moreover, chemical modification can impose a new function of particle such as host' immune system manipulation. This was demonstrated by the PEGylation of VSV-g pseudotyped LVs, by covalent attachment of mPEG to lysine residues, which resulted in protection from inactivation by human/murine complement system (Croyle et al., 2004). Additionally, direct chemical modification of viruses can

also result in biotinylation of viral particles (see Section 3.2.2.1). Using sulfo-NHS-biotin, RVs were successfully chemically modified and bound to a neutral avidin analogue, neutravidin (Yang et al., 2005). Another approach would be the introduction of BAP as an envelope fusion protein as a membrane adapter requiring metabolic biotinylation for vector modification. In many cases, direct modification is rather difficult in practice as chemical procedures may interfere with particle stability or function leading to defective infectivity. Moreover, unbound chemical molecules would require removal by another step which may prolong downstream processing of viral vectors. Therefore, milder modification methods are preferred for labile viral particles such as LVs.

4.2.3 Application of surface engineered LVs for purification using biotin

As discussed in section 4.1.2, modification of viral vectors can be used for several applications such as; (i) targeted infection of specific cell types; (ii) monitoring vector administration *in vivo* and biodistribution; (iii) modulating host's immune responses; and (iv) purification and concentration of vectors from crude viral supernatant for both research and clinical use. For the purpose of this project, this section will focus on the last application of published reports that have specifically utilized streptavidin magnetic beads to purify biotin-modified lentiviral vectors.

4.2.3.1 Purification of biotin modified LVs using streptavidin magnetic beads

Purification of viral vectors is a key issue in gene therapy in terms of achieving high yield, high purity and short processing time coupled with good economics. Generally, all current methods used rely on either de-bulking the surrounding environment of viral particles or non-specifically capturing vectors based on its charge. Modification of vector particles with a synthetic peptide opens up the possibility of developing vector-specific purification methods. In this case, the development of such processes would rely on viral vectors with a diameter ranging between 100-120nm, thus making them bionanotechnological devices. It has been proposed that such modifications thus become functionalisation of viral particles (Metzner and Dangerfield, 2011). To that

end, several methods have been developed based on the modification of LV particles using the biotin-(strept)avidin system leading to particle functionalisation, for either targeted transduction or purification of vectors and owing to the versatility of this system, many variations have been applied (Chan et al., 2005; R. Chen et al., 2010; Etemadzadeh et al., 2015; Kaikkonen et al., 2009b; Lesch et al., 2009; Morizono et al., 2009; Nesbeth et al., 2006). In the interest of this project, studies that have utilized streptavidin paramagnetic beads to capture biotin-modified RV/LV particles and along with their respective efficiencies, are summarized in Table 4.1. The use of magnetic beads as adsorbent particles to bind biotin-modified viruses was first demonstrated by Hughes et al., (2001), resulting in selective capture of 90% of infectious modified RV particles. Williams et al., (2005) compared different adsorbent solid phases, including magnetic beads, to capture chemically biotinylated RVs. The highest fold increase in vector capture efficiency was reported using non-porous the adsorbent structure of streptavidin MagneSpheres compared to porous configurations of Fractogel, Sepharose and STREAMLINE streptavidin adsorbents. Accordingly, a subsequent study reported >90% capture of biotinylated-LVs, modified by random incorporation of non-viral BAP-fusion protein, using MyOne streptavidin magnetic Dynabeads (Nesbeth et al., 2006). Furthermore, another study biotinylated LVs by genetic engineering of Sindbis glycoprotein with BAP, which also allowed selective capture of modified particles to streptavidin magnetic beads (Morizono et al., 2009). However, even though 91.5% of viral particles were captured, 3-6% of modified vectors bound beads pre-treated with biotin. This highlights a major limitation using biotin since biotinylated particles cannot be blocked or easily displaced by free biotin due to its strong affinity. This limits the efficiency of capture in culturing medium containing endogenous concentrations of biotin; as well as efficiency of release of modified vectors by free biotin. Chen et al., (2010), addressed this issue by modifying LVs with a biotin analogue, desthiobiotin which is easily displaced by biotin due to its lower affinity to streptavidin. This modification was introduced into viral particles in the same manner as Nesbeth et al., (2006). This was achieved by the addition of desthiobiotin ligase BioD in vector packaging cells, which upon

culture supplementation of 7-DAPA, catalysed the production of desthiobiotin that was subsequently bound to membrane anchored BAP by BirA, which got randomly incorporated into LVs. Although this method resulted in efficient LV modification, capture efficiency was higher using monomeric avidin (89%) than streptavidin beads (52%) due to desthiobiotin's higher affinity for the former than the latter. A more attractive approach would be to use streptavidin binding biotin mimics as modifying vector proteins, as they can easily be displaced by free biotin due to their significantly lower affinities to streptavidin. All of these studies nonetheless, cumulatively indicate the feasibility and potential of simple and effective capture methods for biotin-modified LVs using streptavidin magnetic particles.

Viral vector	Type of LV modification	Type of non-viral protein incorporation	Type of Beads	Capture efficiency	References
RV	Chemical biotinylation of vector packaging cells with biotin-NHS ester.	Random	Streptavidin magnesphere, Promega	90%	(Hughes et al., 2001)
LV	Exogenous expression of non-viral proteins in vector packaging cell. Then, incubation of harvested viral supernatant with respective antibodies congated to biotin.	Random	Streptavidin magnesphere, Promega	70%	(Chan et al., 2005)
RV	Chemical biotinylation of MoMLV envelope protein from VPC	-	Streptavidin magnesphere, Promega	65%	(Williams et al., 2005)
LV	Metabolic biotinylation of membrane bound fusion protein, BAP-LNGFR	Random	MyOne streptavidin Dynabeads	95%	(Nesbeth et al., 2006)
LV	Genetically engineered Sindbis E2 envelope with BAP	-	Streptavidin beads, Pierce	91.5% *	(Morizono et al., 2009)
LV	Metabolic desthiobiotinylation of membrane bound fusion protein, BAP-LNGFR	Random	Streptavidin magnesphere, Promega	52%	(R. Chen et al., 2010)

Table 4.1: Studies of biotin modified vector capture using streptavidin magnetic beads. RV/LVs were modified in different ways to express biotin on viral surfaces by modification of viral proteins or incorporation of non-viral proteins. Modified vectors were captured using different streptavidin magnetic beads and efficiencies were assessed by infectivity assays, or by p24 ELISA quantification (*). BAP, biotin acceptor peptide.

In conclusion, there are many different strategies, individually or several combined, that have been used to tag/label viral vectors. Depending on the type of virus and its intended application, the choice of modification should be determined. As LVs are labile and fragile vectors, methods that require harsh reagents or conditions and extended time for modification are not ideal for their bioprocessing. Accordingly, strategies that have been applied for LVs modification with biotin for example, relied on 'gentler' methods that do not alter viral proteins, such as random incorporation of biotinylated proteins. This in turn allowed the efficient and selective capture of biotinylated-LVs from vector containing media.

4.3 Aims

In this Chapter, the cyclical biotin mimic of Chapter 3, Ctag, was used to modify LVs pseudotyped with the RDpro variant of the RD114 envelope. This in turn was hypothesized to allow efficient adsorption of Ctag-modified vectors to streptavidin magnetic beads for vector capture. Given the different methods of viral surface modifications discussed and their respective limitations, the aims of this Chapter are:

- To test different methods of LV surface modification with Ctag by:

1. Co-localization of Ctag-RDpro membrane-bound fusion protein.
    - The advantage of this method would be its potential simplicity and specificity for viral incorporation; since fusion protein would express RDpro's transmembrane domain. However, it may result in unstable surface expression due to its chimeric amino acid sequence, as residues on both sides of the membrane stabilizes protein surface expression.
2. Genetic engineering of RDpro with Ctag peptide.
    - This method should allow for the incorporation of Ctag-expressing envelope glycoprotein. However, as

discussed, genetically engineering Ctag into RDpro may affect receptor binding or infectivity of chimeric glycoproteins.

3. Random/passive incorporation of Ctag onto viral surface of budding virions.
    - This method represents the easiest technical modification. However, it may not result in sufficient Ctag expression per virion to allow efficient capture by streptavidin beads.

- To test successfully modified Ctag-LVs' binding to streptavidin magnetic beads.
- To develop a methodology allowing complete capture of modified Ctag-LV by streptavidin from viral supernatant.
- To demonstrate that capture of modified vectors is dependent on Ctag binding to streptavidin.

4.4 Testing cell surface co-localization of biotin mimic with viral envelope

In an attempt to express the chosen biotin mimic, Ctag, on the surface of viral particles, we reasoned that the surface expression of the peptide on the transmembrane and endodomain of viral envelope RDpro could allow the co-localization of Ctag and envelope, enabling its passive incorporation into virions upon budding. To that end, Ctag with a CD8α ectodomain was genetically fused with RDpro transmembrane and the Ctag-∆p15ETM fusion protein was cloned. (Figure 4.2a). Along with control plasmid encoding epitope expressed on a CD8α stalk, constructs co-expressing eGFP were transiently transfected into HEK293T cells and 48hrs post-transfection, transfected and non-transfected cells were harvested and stained with streptavidin (Figure 4.2b). As expected, cells transfected with Ctag on CD8α stalk resulted in streptavidin binding of eGFP positive cells. However, cells transfected with Ctag expressed on RDpro transmembrane and cytoplasmic domain did not exhibit any streptavidin binding. The lack of streptavidin binding indicated absence of surface expression of fusion protein highlighting the difficulties in engineering chimeric surface expression structures. Therefore, the strategy for co-localization of biotin mimic with viral envelope for lentivirus surface incorporation would not be successful.

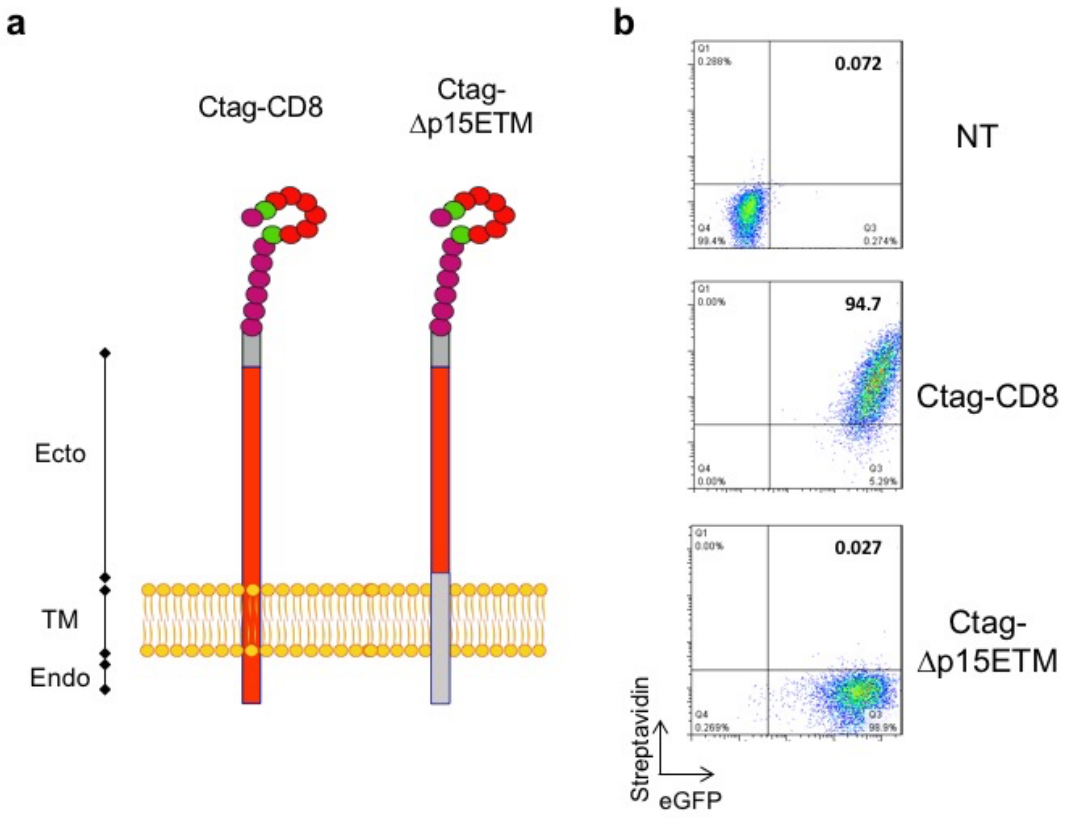

Figure 4.2: Generation of Ctag-Δp15ETM fusion protein. (a) Schematic diagram depicting wild-type Ctag on CD8α stalk and fusion protein of Ctag with CD8α ectodomain fused to RDpro's p15ETM transmembrane domain, termed Ctag-Δp15ETM. **(b)** Dot plots of streptavidin stained transiently transfected 293T cells with plasmids along with non-transduced (NT) cells.

4.5 Genetic engineering attempts of viral envelope glycoprotein with Ctag

As a second attempt for Ctag expression on viral surfaces, we decided to test the genetic engineering of viral glycoprotein RDpro with the peptide sequence and its serine-glycine linker. Unlike, VSV-g and MLV-amphotropic, the genetic manipulation of RD114-derived envelope has never been tested. Known insertion sites of synthetic sequences for the former glycoproteins were chosen to be tested on RDpro. To that end, Ctag was cloned in two locations, as depicted in Figure 4.3a:

- After its signal peptide sequence on the N-terminus of its SU domain, and was termed Ctag-RDpro
- After the furin cleavage site leading to its expression on the N-terminus of TM domain of RDpro, and was termed RDpro-SU.Ctag.TM.

Ctag was cloned into an RDpro plasmid co-expressed with an epitope surface marker expressed on a CD8α stalk, MYC8, by self-cleaving peptide FMD2A. These constructs were first tested for Ctag-engineered envelopes surface expression by transient transfection of plasmids in 293T cells along with Ctag-CD8α plasmid as a control. 48 hours post-transfection, Ctag-CD8α and the two engineered MYC8-2A-RDpro transfected cells were stained with streptavidin alone and streptavidin with anti-MYC antibody, respectively (Figure 4.3b). Ctag-RDpro and RDpro-SU.Ctag.TM MYC8-positive cells resulted in 55% and 63% of cells positive for streptavidin binding, respectively; with 75% streptavidin-positive for control cells. These results indicated surface expression of engineered RDpro glycoproteins with functional biotin mimics that can bind streptavidin. Subsequently, engineered proteins were tested for functional lentiviral vector production. Third-generation packaging plasmids, with pCCL.PGK.eGFP as transgene, were transiently transfected into HEK293T cells and viral supernatants were harvested 48 hours later and the presence of infectious vectors was detected by one-point transduction of target cells (Figure 4.3c). Unlike positive control vectors pseudotyped with wild type RDpro, neither engineered envelope produced any functional viral particles, as seen by the absence of eGFP positive target cells. These results could have been caused by either (i) inhibition of RDpro receptor binding on target cells due to Ctag engineering on its surface unit, or (ii) failure of inducing either precursor cleavage or fusion due to peptide insertion into RDpro's transmembrane domain leading to a defective viral envelope. Therefore, although addition of Ctag onto the two engineered proteins resulted in plasma membrane mimic expressions, these engineered glycoproteins on their own failed to produce detectable infectious particles. The co-expression of wild-type envelopes along with these variants can be tested for functional particle

production. However, since we aimed to develop a single simple strategy, this was not further investigated.

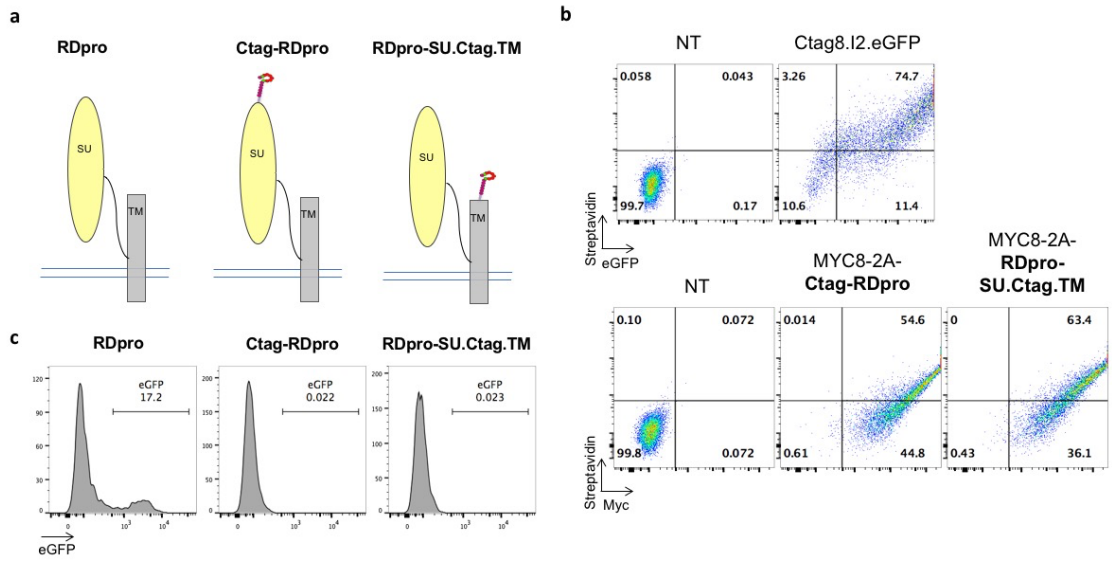

Figure 4.3: Genetic engineering of RDpro glycoprotein with biotin mimic Ctag. **(a)** Schematic diagram of 1-wild-type RDpro protein and two genetic engineered variants; 2-Ctag-RDpro with peptide inserted on its N-terminus after protein's signal peptide with a serine glycine linker; and 3-RDpro-SU.Ctag.TM with peptide inserted after furin cleavage site also on a serine glycine linker to get expressed on the N-terminus of p15ETM. **(b)** Constructs were transfected into 293T cells with 1-Ctag on CD8α stalk (Ctag8) co-expressed with eGFP as control for streptavidin staining; and 2-engineered RDpro for both variants were co-expressed with surface marker MYC on CD8α stalk separated (MYC8) by FMD2A self-cleaving peptide. This plasmid was used in order to have a stainable marker for transfection efficiency that is independent of Ctag and so cells were stained with streptavidin-APC and anti-cmyc-DyLight549 48 hours after transfection. **(c)** Wild-type RDpro and both engineered variants were used as envelope glycoproteins to test for LV production by transient transfection of 3rd generation LV packaging system with pCCL.PGK.eGFP as transfer vector. 500µL of viral supernatants were harvested from packaging cells and presence of infectious particles was tested by inoculation onto 293T cells in which cells were assessed for transgene expression 72 hours post-transduction.

4.6 Passive incorporation of Ctag onto viral particle surface for peptide tagging of LVs

As mentioned in section 4.2.2.1, incorporation of non-viral host proteins onto the surface of lentiviral vectors have been demonstrated. So far in this Chapter, several strategies were taken to modify LVs with Ctag expressed on CD8α stalk with failed attempts. As a third option, we reasoned that high surface expression of Ctag on virion producing cells should allow its passive incorporation in the viral envelope in the same manner as the random particle inclusion of host cell derived membrane bound proteins. High stable biotin mimic expression in virus producing cells would be achieved through γ-retroviral transduction. Subsequent transfection with lentiviral packaging plasmids, independently of these components, should then produce virions that acquire Ctag on their surface while they are budding out of Ctag-expressing producer cells. (Figure 4.4).

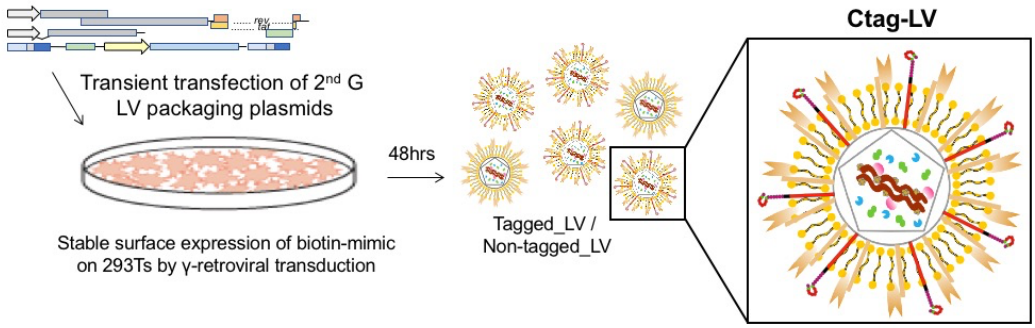

Figure 4.4: Random incorporation of Ctag peptide on LV model. Proposed hypothesis on the production of Ctag-modified LVs by random/passive incorporation of peptide onto viral surfaces once stably expressed by in packaging cells. Upon transient transfection of Ctag-expressing cells with 2nd generation (G) LV packaging plasmids, virions produced would incorporate Ctag on their viral surfaces.

To test this theory, HEK293T cells were transduced with γ-RV encoding Ctag co-expressed with eGFP. Transgene expression of Ctag-293T cells was determined by streptavidin binding, by which 97% of transduced cells were double positive for streptavidin and eGFP marker gene (Figure 4.5a). Given

that the membrane location of LV virion budding from host cells is not well understood, it was important to assure abundant plasma membrane expression of Ctag on the CD8α stalk. Its membrane expression was shown by immunofluorescence to be ubiquitous on Ctag-293T cells, with high expression in cells' protrusion-like structures (Figure 4.5b).

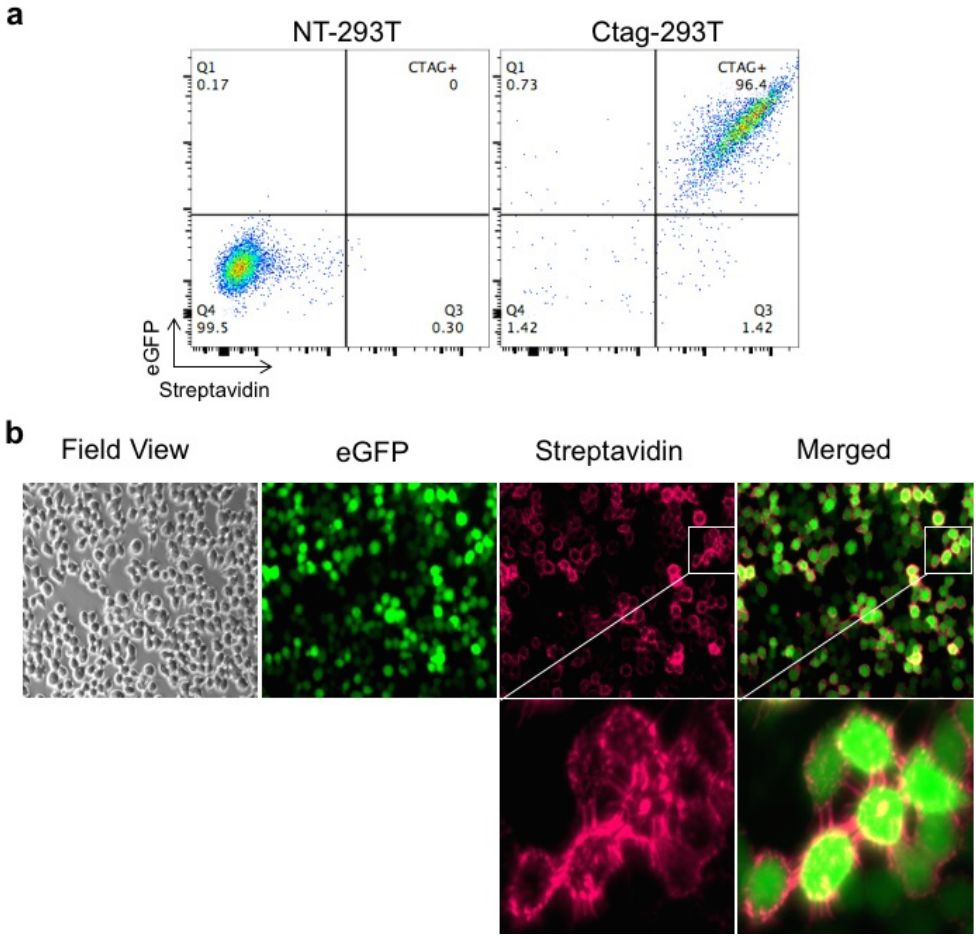

Figure 4.5: Generation of Ctag expressing 293T cells by γ-retroviral transduction. Cells were transduced with Ctag co-expressed with eGFP separated by IRES. Transduced cells were analyzed for Ctag expression by **(a)** flow cytometry and **(b)** immunofluorescence staining with streptavidin-APC.

To test our hypothesis, we developed a streptavidin magnetic bead-based purification protocol, shown in Methodology 1. If virions acquire Ctag peptide on their surfaces then these modified vectors should be selectively captured by streptavidin magnetics beads, resulting in detectable viral particles in the bead fraction. Control non-modified LVs should not be captured by streptavidin

beads thus indicating that capture of modified vectors was due to Ctag expression on their surfaces. To demonstrate this, non-transduced (NT) and Ctag-293T cells were transiently transfected with second generation LV packaging plasmids pseudotyped with either VSV-g or RDpro and viral supernatants were subjected to proposed streptavidin purification (Methodology 1). Cells were transfected with two different pseudotyping envelopes to determine the broad applicability of such a method in an envelope-independent manner.

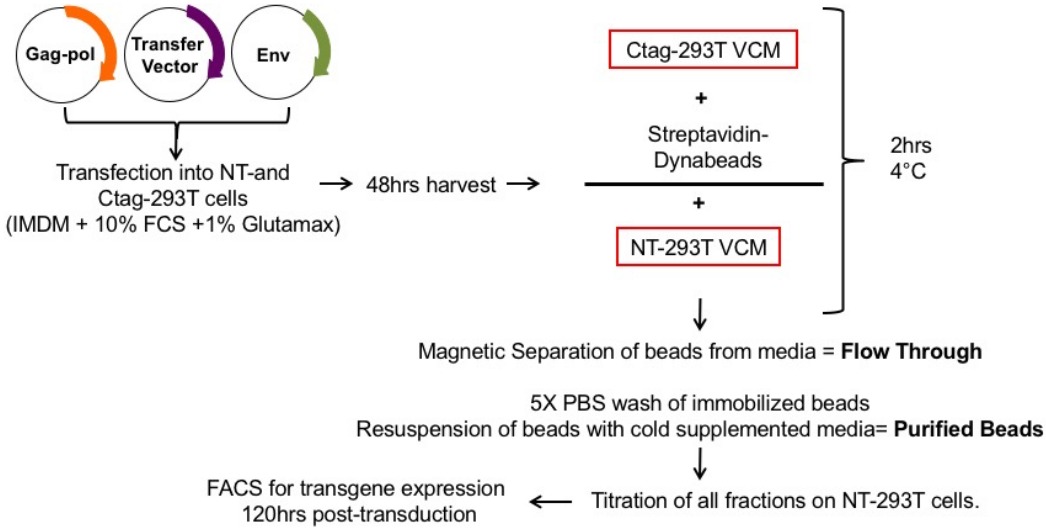

Methodology 1: Preliminary protocol for streptavidin-mediated magnetic capture of LV produced from Ctag-293T cells. Second generation packaging plasmids were transfected into both NT- and Ctag-293T cells cultured in supplemented IMDM (10% FCS + 1% Glutamax). Vector contaiing media (VCM) i.e. viral supernatants, were harvested 48hours later and processed to remove cellular debris by centrifugation and ultrafiltration using 0.45um filters (Neat fraction, 1X volume). Then LV supernatants were incubated with Dynabeads® MyOne™ Streptavidin T1 magnetic beads (0.5 mg beads per mL of LV supernatants), that were previously washed with PBS 5X as per manufacturer's protocol and resuspended in 1X cold IMDM, for 2 hours at 4°C with gentle rotation in falcon tubes. Afterwards, falcons were placed in magnetic rack and left to stand for 1 min followed by the separation of the supernatant from immobilized magnetic beads (Flow Through fraction, 1X volume). Then, falcons were removed from magnetic rack and beads were gently resuspended with cold PBS and placed again on magnetic rack for 1 min to allow beads immobilization. This washing step was repeated 3X and beads were then resuspended in cold supplemented IMDM (Purified Beads fraction, 1X volume). All fractions (Neat supernatant, Purified Beads, Flow-Through) were serially diluted and added onto NT-293T cells in the presence of 5µg/mL of Polybrene to determine viral titre. 72 hours post-transductions, all transduced conditions were split 1:2 – 1:3 to dilute out magnetic beads. 48 hours later, cells were harvested and stained for transgene expression to determine transduction efficiencies by Flow Cytometry (FACS).

LVs pseudotyped with VSV-g produced from both NT-and Ctag-293T cells contained functionally infectious viral particles as indicated by the high transduction efficiencies of neat (i.e. crude harvested supernatant) columns of 80.2% and 76.8%, respectively (Figure 4.6a.1). As postulated, target cells transduced with purified streptavidin beads (i.e. beads incubated with modified vectors then subjected to PBS washes by magnetic selection and release) of NM-LV and Ctag-LV resulted transduction efficiencies of 1.9% and 77.2%, respectively (Figure 4.6a.2). This result indicated that viral particles produced by Ctag-293T cells were successfully tagged with biotin mimic through passive incorporation. It also demonstrated the selective capture of Ctag-tagged-LV by streptavidin magnetic beads. However, there remained non-tagged and/or non-purified LV particles produced by Ctag-293T cells as indicated by high transduction efficiency of flow through fraction (77.2%) (Figure 4.6a.3).

This purification process was also tested on RDpro pseudotyped LVs. NT- and Ctag-293T cells produced infectious particles as indicated with transduction efficiencies of 75.8% and 84%, respectively (Figure 4.6b.1). Upon subjection of Methodology 1 on both viral supernatants, Ctag-LV purified beads fraction resulted in a transduction efficiency of 44.1%, while no detectable transduction was observed with beads fraction of NM-LV, indicating selective capture of Ctag-LV pseudotyped with RDpro (Figure 4.6b.2). However, similarly to VSV-g, streptavidin magnetic beads did not seem to capture all infectious titre produced as indicated by the high transduction efficiency of the flow-through fraction of 84.6% (Figure 4.6b.3). Therefore, although Methodology 1 did not seem to capture all virions produced from Ctag-293T cells, the biotin mimic Ctag was successfully incorporated into LVs by random viral surface incorporation irrespective of the envelope glycoprotein used. This modification in turn allowed subsequent capture of virions produced from Ctag-293T cells by streptavidin magnetic beads.

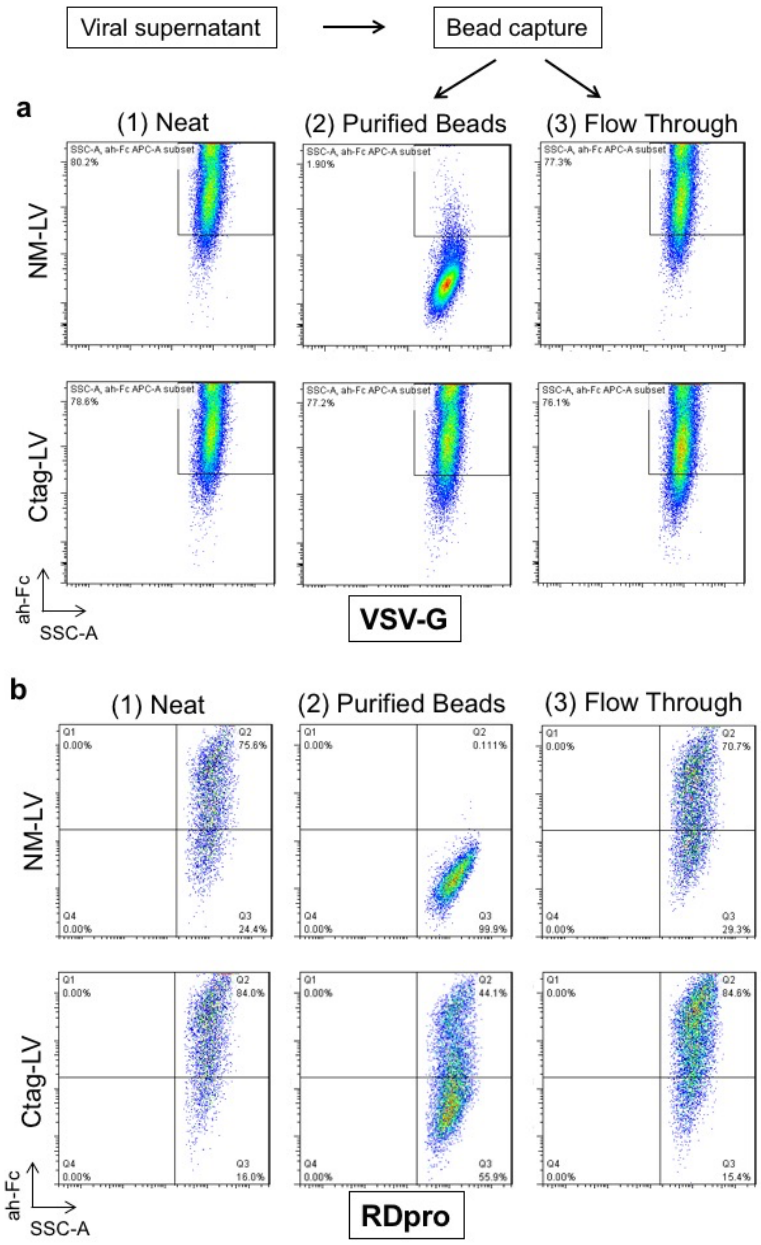

Figure 4.6: Purification of Ctag-LV from cellular supernatant using Methodology 1. VSV-G **(a)** and RDpro **(b)** pseudotyped LV particles encoding a chimeric antigen receptor (CAR) with a human-Fc spacer were produced from both NM- and Ctag-293T cells. Both virus supernatants (NM-LV and Ctag-LV) were then subjected to streptavidin beads purification as depicted in Methodology 1, with column fractions representing the following: (1) Neat: crude virus supernatant; (2) Purified beads: streptavidin beads incubated with supernatants and captured; and (3) Flow-through: supernatant collected after beads immobilization by magnetization. Target cells that were transduced with these fractions were harvested and stained with an anti-human-Fc (ah-Fc-649) antibody to determine transduction efficiencies by Flow Cytometry (FACS). Dot plots of ah-Fc vs SSC-A represent cells transduced with either 20µL of VSV-G and 50µL of RDpro of all fractions for both NM-LV and Ctag-LV. Positive cells were gated based on staining of NT-293T cells with the antibody accounting for background signal.

Moreover, given that the scope of our laboratory involves the genetic engineering of T cells, the infectivity of modified Ctag-LV was assessed compared to non-modified vectors for T cell transduction. To that end, T cells from a healthy donor were isolated and transduced with both NM-LV and Ctag-LV using retronectin-coated plates (Appendix 3). Both supernatant resulted in similar transduction efficiencies of 89.3% and 91.7% for NM-LV and Ctag-LV respectively. Thus, this result indicated that Ctag-modified LV particles are able to transduce T cells with the same efficiency as non-modified vectors.

4.7 Successful streptavidin-mediated capture of all Ctag-tagged RDpro LVs from serum free medium

The presence of viral particles in Ctag-LV flow through fractions was reasoned to either be due to non-tagged-LV, streptavidin bead saturation or the presence of biotin in both IMDM (53.2nM biotin, provided by supplier) and the supplemented FCS (unknown biotin concentration). Therefore, an optimized protocol was developed to address all of the above and is depicted in Methodology 2. This differed from Methodology 1 in that, 24-hours post LV transient transfection, both NM and Ctag-293T cells, which were cultured in serum supplemented IMDM, were gently washed and cultured in plain DMEM. The latter does not contain biotin, based on manufacturer's information, and was used plain i.e. without FCS supplementation, in order to assess its effect on capture efficiency. Additionally, to determine whether remaining viral particles in flow through fraction of Ctag-LV purification was due to bead saturation or non-tagged LV, flow through of the 1st purification was subjected to a second round of incubation with streptavidin magnetic beads (Methodology 2).

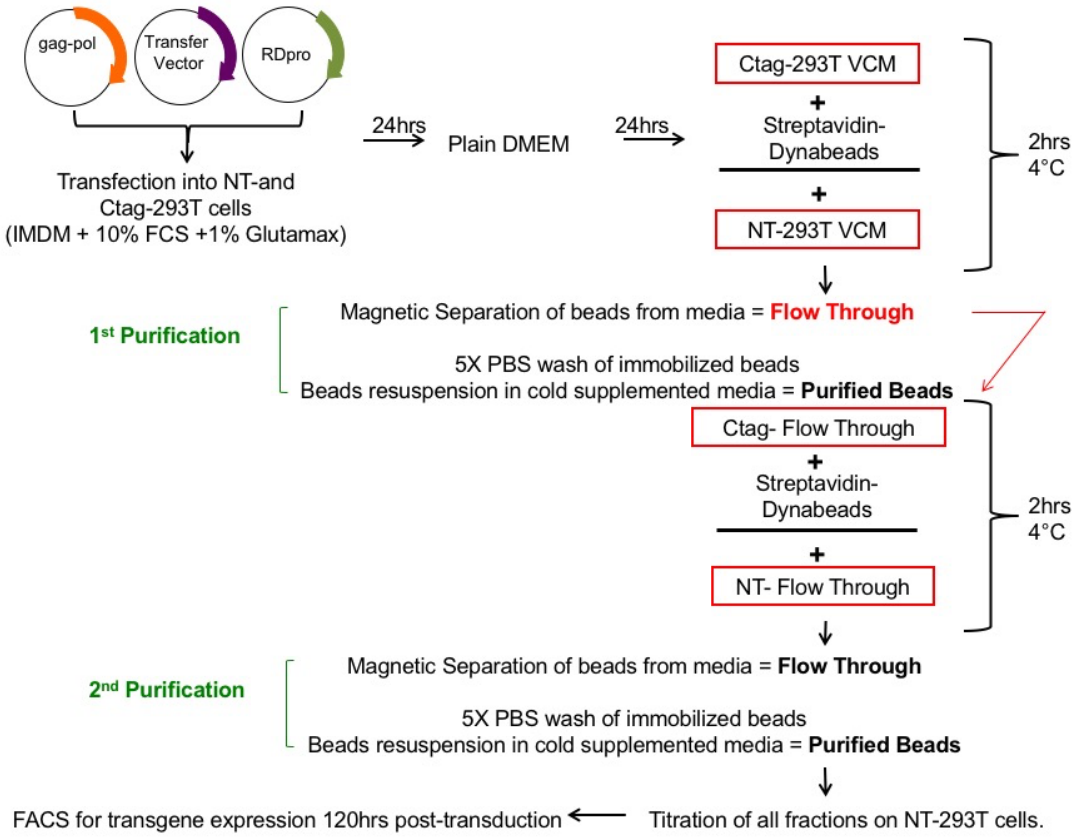

Methodology 2: Biotin-free protocol for Ctag-LV capture using streptavidin magnetic beads. LV plasmids transfected NT- and Flankedccstreptag-293T cells cultured in supplemented IMDM (10% FCS + 1% Glutamax) were gently washed with PBS 24 hrs post-transfection and cultured in plain DMEM. LV supernatants were harvested 24hour later and processed (Neat, 1X volume). LV supernatants were then incubated with Dynabeads® MyOne™ Streptavidin T1 magnetic beads (0.5 mg beads per mL of LV supernatants), that were previously washed with PBS 4X as per manufacturer's protocol and resuspended in 1X cold IMDM, for 2 hours at 4°C with gentle rotation in falcon tubes. Afterwards, falcons were placed in magnetic rack and left to stand for 1 min followed by the separation of the supernatant from the immobilized magnetic beads (Flow Through fraction, 1X volume). Then, falcons were removed from magnetic rack and beads were gently resuspended with cold PBS and placed again on magnetic rack for 1 min for bead immobilization. This washing step was repeated 3X and beads were then resuspended in cold supplemented IMDM (Purified Beads fraction, 1X volume). This process was repeated in the exact steps but with the Flow Through fractions of the first purification for a second round of purification with streptavidin beads. All fractions (Neat, Purified Beads and Flow-Through) were serially diluted and added onto NT-293T cells in the presence of 5µg/mL of Polybrene to determine viral titre. 72 hours post-transductions, all transduced conditions were split 1:2 – 1:3 to dilute out magnetic beads; and 48 hours later cells were harvested transduction efficiencies determined by eGFP expression using flow cytometry.

LV supernatants produced from NT- and Ctag-293T cells cultured in plain DMEM and subjected Methodology 2, produced functional infectious particles as indicated by the neat columns with transduction efficiencies of 34.1% and 23.3%, respectively (Figure 4.7a). Moreover, Ctag-LVs seemed to have been successfully completely captured by streptavidin beads with one round of purification as indicated by a transduction efficiency of 27.5% in the 1st purified fraction, with negligible transduction efficiencies in both its flow through and subsequent fractions of 2nd round of purification (Figure 4.7a). This purification method was Ctag-specific, as both the neat and 1st flow through fractions of NM-LV were not captured by streptavidin beads, giving void transduction efficiencies in both the 1st and 2nd purified beads fractions. These results were successfully reproduced in three independent experiments (n=3) as indicated by the viral titres plotted in Figure 4.7b, in which neat Ctag-LV (1.7 ±1 x10^5 IU/mL) are recovered in the 1st purified bead fractions (1.66 ±1.1 x10^5 IU/mL), with no statistical significance observed between these fractions. Neat NM-LV (1.5 ±0.4 x10^5 IU/mL) followed through into flow through fractions of the 2nd purification (1.1 ±0.2 x10^5 IU/mL), with no significant difference detected between the viral titres of these fractions. Consequently, Methodology 2 proved that the remaining viral particles observed in the flow through fractions of Figure 4.6 was due to the presence of biotin in both IMDM and FCS, rather than bead saturation or untagged viral particles. The presence of biotin would effectively competitively bind streptavidin beads, thus not allowing complete Ctag-LV purification. Therefore, in its absence, passive incorporation of Ctag onto LV viral surfaces allowed complete capture of modified vectors from virus supernatant using streptavidin magnetic beads. Moreover, it could then be concluded that 90 streptavidin Dynabeads per 1 infectious particle (calculation based on Dynabeads density of 3.16x10^5 beads/µL) was sufficient to capture all modified vectors from a total viral supernatant volume of 10mL in 2 hours.

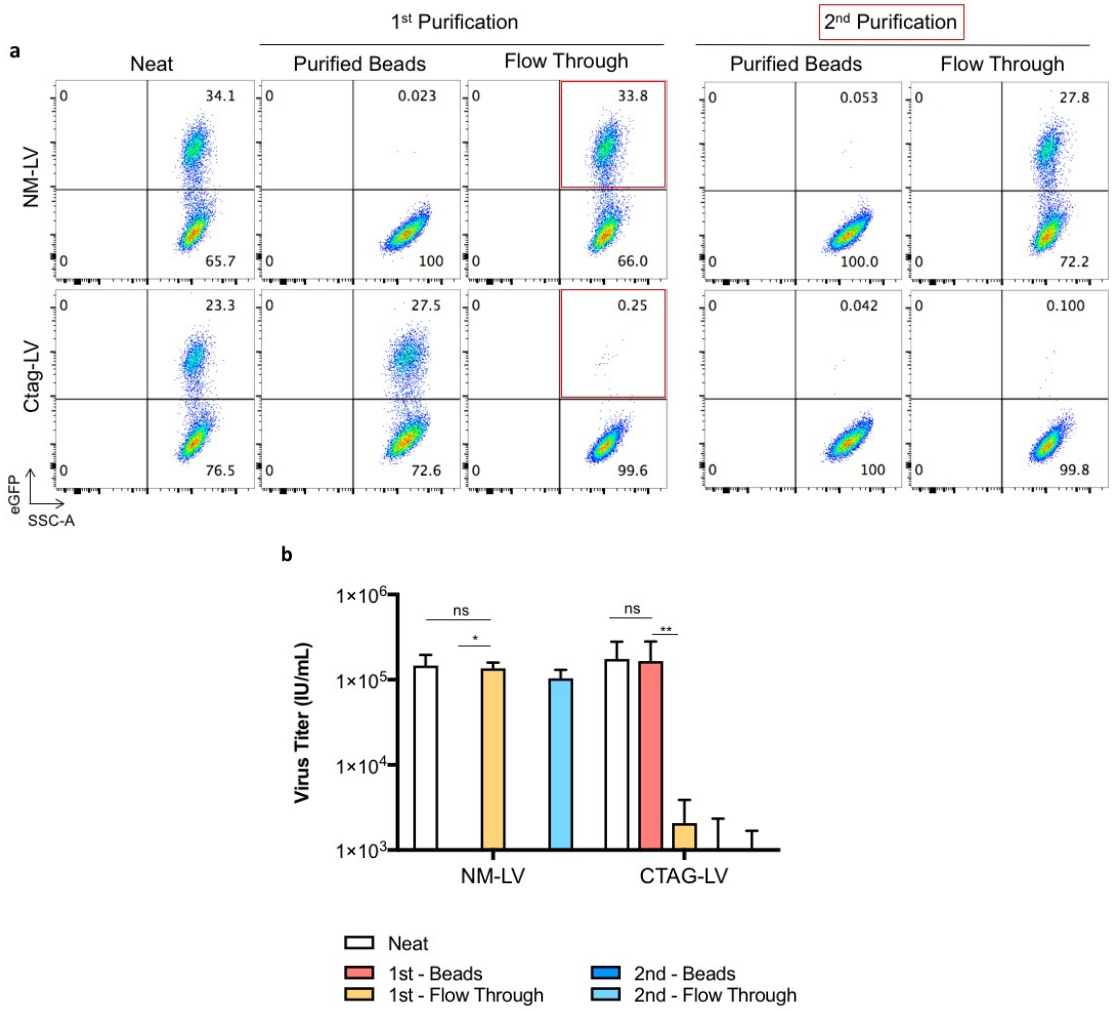

Figure 4.7: Capture of Ctag-LV from cellular supernatant using Methodology 2. RDpro pseudotyped LV particles encoding a eGFP (pCCL.PGK.eGFP) were produced from both NM- (Non-Modified-LV) and Ctag (Ctag-LV) 293T cells. Both negative control and experimental supernatants were then subjected to streptavidin beads purification as depicted in Methodology 2. At each stage, aliquots of all fractions were collected for viral titration determination by infectious assay on NT-293T cells. Target cells, transduced with all relevant fractions, were harvested and eGFP expressions were determined by Flow Cytometry (FACS). (a) Dot plots of eGFP vs SSC-A represent cells transduced with 250µL of all fractions for both NM-LV and Ctag-LV and (b) viral titres of all fractions are plotted with values representing infectious titres ± standard deviation (SD) of three independent experiments (n=3) with * $p < 0.05$, ** $p < 0.01$ and non-significant (ns) $p > 0.05$.

4.8 Optimization of Ctag-dependent streptavidin capture conditions resulting in increased infectious titre

In the previous experiment, we demonstrated complete capture of LVs by streptavidin magnetic beads. Since the number of beads and incubation of capture were chosen in excess, capture parameters were therefore optimised. Firstly, we optimized the surface area (SA) (i.e. total number of streptavidin binding capacity) of streptavidin beads per infectious unit of virus by incubating Ctag-LV with decreasing amount of Dynabeads (i.e. decreasing surface area of streptavidin molecules) and assessing capture efficiency (Figure 4.8a). An amount of 25µL (equivalent to SA $2.48x10^7$ μm^2) of streptavidin beads/mL of Ctag-LV was sufficient for viral capture on purified beads, with an increased viral titre of 2.4 ±0.23 $x10^5$ IU/mL compared to the starting neat at of 7.6 ±0.4 x 10^4 IU/mL, resulting in 3-fold increase in infectious titre without any volume reduction, with less than 8 ±0.1 $x10^3$ IU/mL left in the flow-through. This increase in infectious titre was also observed when capture time and temperature parameters were further optimised. Using 25µL of beads/mL of Ctag-LV, capture incubation was optimized by testing its efficiency during 15 to 120 minutes, at room temperature (RT) and 4°C. Purified bead fractions of 60 and 120 minutes' capture incubation at both temperatures resulted in the highest yield, with 2 to 3-fold increase compared to neat (Figure 4.8b). Statistical difference was observed in viral titre captured on streptavidin beads between 30 and 120 minute incubations at both temperatures. Additionally, although no difference was observed between capture incubation of 60 and 120 minutes at both temperatures, the latter did appear to result in higher captured viral titre. However due to practical reasons as well as lack of statistical significance, incubation of 60 minutes was chosen as standard incubation for any following capture. Therefore, for all subsequent experiments, 25µL of streptavidin magnetic beads/mL of supernatant were incubated for 60 minutes at room temperature.

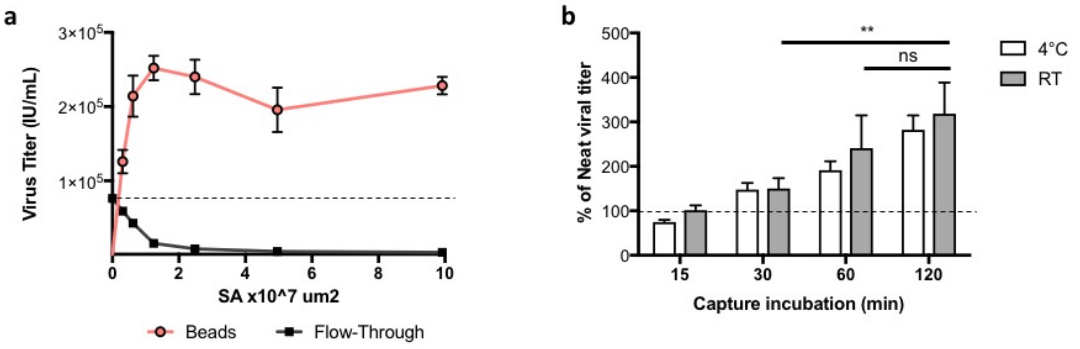

Figure 4.8: Optimization of Ctag-LV capture conditions. (a) Number of magnetic beads, in terms of surface area (SA) (with 3.14 μm^2/bead and $3.16x10^5$ beads/µL) per mL of LV supernatant, was optimized by incubating decreasing number of beads (starting with 100µL ($9.92x10^7$ SA) of beads/mL of LV, 1:2 serial dilutions for 6 points, ending with 3.125µL ($3.1x10^6$ SA) of beads/mL of LV) with the same volume of Ctag-LV supernatant with a viral titre of 7.6 ±0.4 x 10^4 IU/mL for 2 hours at 4°C. The volume of both starting-capture and resuspensed-post beads removal were kept the same for proper analysis of viral titre in IU/mL. Resuspended beads and respective flow-through fractions were then assessed for infectivity. **(b)** Both time and temperature of Ctag-LV capture with 25µL of beads/mL of LV were optimized by incubation reactions for 15 to 120 minutes, at room temperature (RT) and 4C. Results are plotted as viral titre for (a), and percentage of neat viral titres for (b) ± standard deviation (SD) of three independent experiments (n=3) with ** $p < 0.01$ and non-significant (ns) $p > 0.05$. Dashed lines for comparison to 100% of neat fraction value.

4.9 Ctag-mediated capture is independent of pseudotyping envelope

Our developed purification was so far successful in complete viral capture of RDpro pseudotyped Ctag-LVs (Figure 4.7). We aimed to demonstrate that our process can completely capture infectious particles independently of pseudotyping glycoprotein envelope. Since Ctag modification of LVs occurs through random incorporation of the peptide, pseudotyping viral particles with any envelope should allow the complete capture of modified particles. To demonstrate this, LV stocks were produced from both NT- and Ctag-293T cells pseudotyped with RDpro, MLV-A and VSV-g in serum-free media. NM and Ctag-LV stocks of each glycoproteins were then titred on NT-293T cells (Figure 4.9a-b). There was no significant difference in viral titres between NM and Ctag-LVs produced for each of the three glycoproteins, with the highest titres of 10^7 IU/mL for VSV-g pseudotyped vectors. Next, tagged and non-tagged MLV-A and VSV-g viral supernatant from stocks, along with RDpro

pseudotyped vectors as control, were then subjected to our optimized capture methodology by incubation with streptavidin magnetic beads for 1 hour at room temperature. Then, after flow-through fractions separation, infectious titres were determined for all fractions and plotted as a percentage of neat viral titres (Figure 4.9c). As expected, Ctag-LV pseudotyped with RDpro, MLV-A and VSV-g were successfully captured by streptavidin beads as indicated by increased viral titres of all bead fractions, with 2.8, 3.5 and 2.2-fold higher viral titres compared to neat fractions for RDpro, MLV-A and VSV-g LVs, respectively (Figure 4.9c). These results validated the independency of our purification methodology from viral pseudotyping glycoproteins.

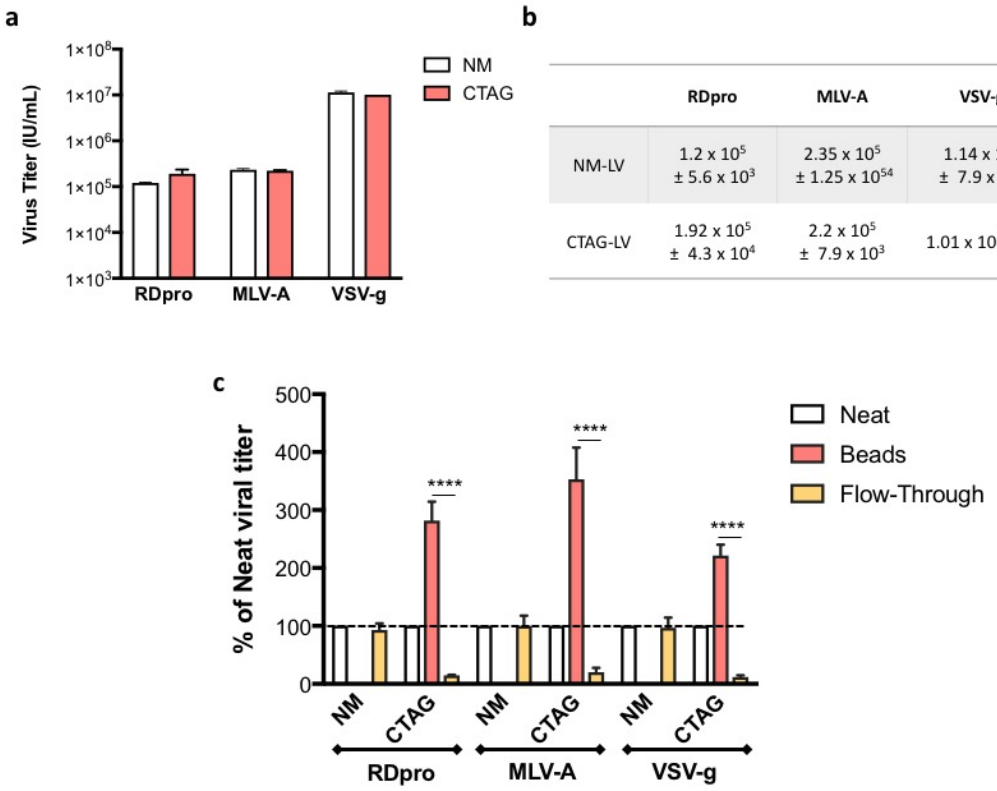

Figure 4.9: Application of developed streptavidin-mediated capture protocol using three different pseudotyping envelopes for Ctag-LV. (a-b) LVs were produced from both NT- and Ctag-293T cells in plain DMEM, pseudotyped with either RDpro, MLV-A or VSV-g glycoproteins. Viral supernatants were frozen and viral titres of stocks were determined by infectivity assay. Results of viral titres are presented as grouped columns in (a) and corresponding values in table (b) with ± standard deviations (SD) of triplicate determinations. **(c)** RDpro, MLV-A and VSV-g NM- and Ctag-LVs were subjected to capture protocol using optimized conditions. Neat, beads and flow-through fractions were collected and viral titres were determined by infectivity assay. Results are plotted as percentages of respective neat fractions with standard deviations (SD) of three independent experiments (n=3) carried out on the same vector stocks, with **** $p < 0.0001$.

4.10 Streptavidin capture of Ctag-LV is blocked by biotin.

As intended, Ctag-LVs' streptavidin-mediated capture was shown to be specific on viral surface incorporation of the biotin mimic Ctag, by the absence of NM-LV capture. To further validate that this purification method exclusively depends on Ctag binding to streptavidin, capture was tested using streptavidin beads pre-incubated with biotin. Since the displacement of Ctag by biotin has already been demonstrated on cells (Chapter 3), pre-incubation of Dynabeads with biotin should block Ctag binding and thus result in the lack of Ctag-LV capture. To demonstrate this, streptavidin Dynabeads were as usually washed and then incubated with either plain PBS as control, or with PBS supplemented with an excess of 15mM biotin. To mirror capture conditions, these incubations were performed for 1 hour at room temperature. Then, after PBS washing, RDpro pseudotyped NM- and Ctag-LVs were incubated with both pre-treated beads for 1 hour at room temperature. After flow-through separations, infectious titres were determined for all fractions by infectivity assay (Figure 4.10a-b). Consistently, Dynabeads pre-incubated with PBS only, resulted in significant 5-fold increase in viral titre of captured Ctag-LV compared to starting material, and only 17 ±2% of titre remaining in flow-through. As anticipated, pre-incubation of streptavidin Dynabeads with 15mM biotin blocked Ctag-LV binding resulted in lack of capture, with 100% of Ctag-LV found in the flow-through fraction. Accordingly, an increased statistical difference was observed between viral titres of PBS- and biotin pre-incubated Dynabeads fractions with $p < 0.0001$. Therefore, this result established the dependency of this developed purification methodology on streptavidin's ability to bind the biotin mimic Ctag.

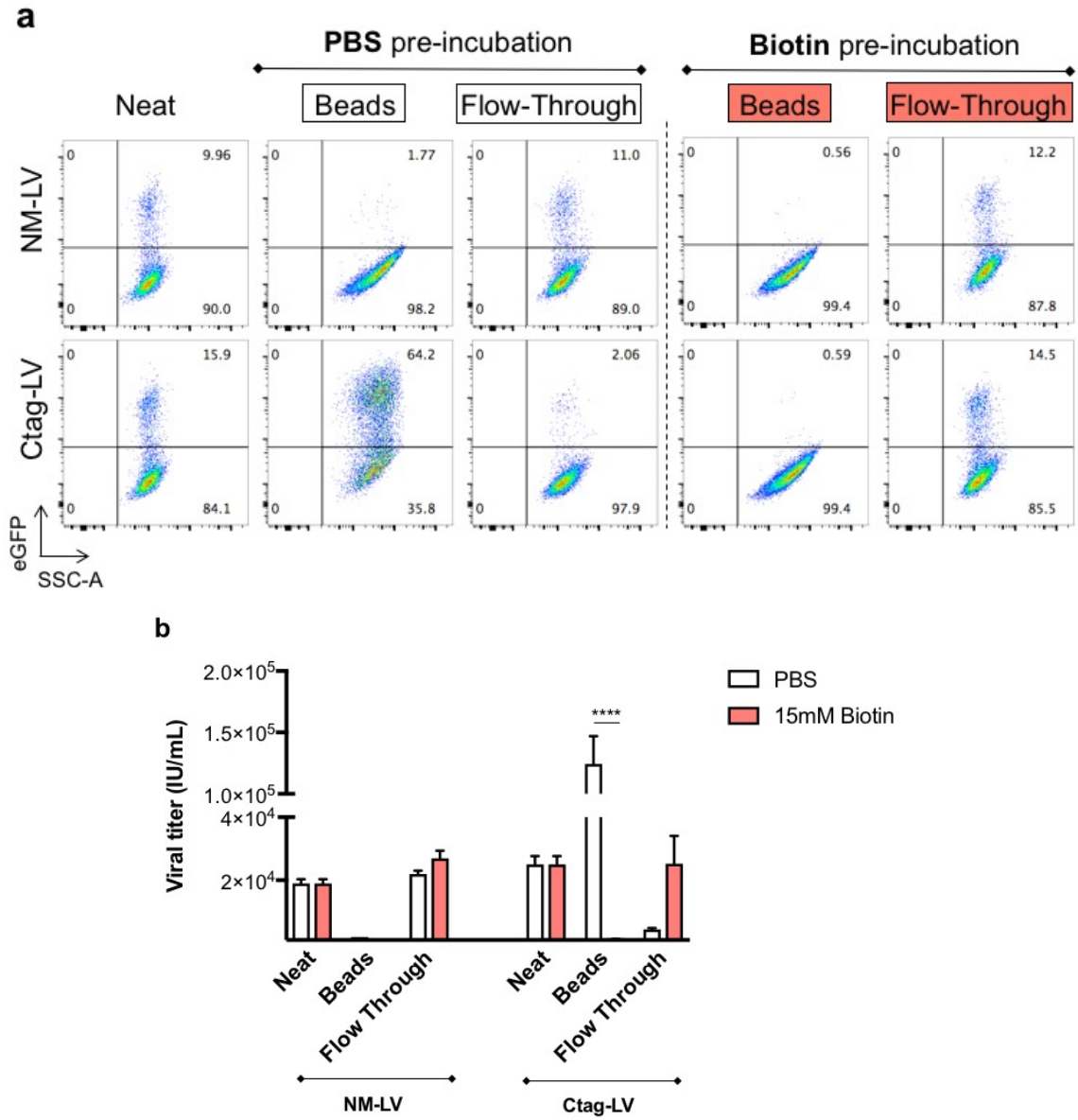

Figure 4.10: Pre-treatment of streptavidin magnetic beads with biotin for Ctag-LV capture. Streptavidin magnetic beads were pre-treated either with plain or 15mM biotin PBS for 1 hour at room temperature. After several washes with 1X PBS, pre-treated beads were incubated with NM-LV and Ctag-LV using optimized conditions. Neat, and both pre-treatments'' beads and flow-throughs fractions were collected and viral titres were determined by infectivity assay. **(a)** Dot plots of eGFP vs SSC-A represent cells transduced with 250µL of all fractions for both NM-LV and Ctag-LV without any volume reduction. **(b)** Viral titres of all fractions are plotted with values representing infectious titres ± standard deviation (SD) of three independent experiments (n=3) with **** $p < 0.0001$.

4.11 Discussion

In this Chapter, we have modified LVs with Ctag, a surface expressing biotin mimic, by its random incorporation during virion budding from vector packaging cells expressing the mimic on their surfaces. This modification permitted subsequent streptavidin magnetic beads capture of all infectious RDpro, VSV-g and MLV pseudotyped Ctag-LVs in an epitope-dependent manner.

Initially different methods of viral surface incorporation were tested in this Chapter. First, we constructed a chimeric protein consisting of Ctag-CD8α ectodomain fused to RDpro transmembrane and cytoplasmic domain, for potential co-localization of hybrid protein with envelope glycoprotein. However, its expression was not detected on cells' surface, suggesting potential protein instability. The engineering of a hybrid surface expressing structure by fusing ecto- and transmembrane domains from different proteins is not as straight forward as anticipated.

As second strategy, we attempted to genetically engineer RDpro at two sites that were hypothesized to potentially allow peptide insertion without significant hindrance on envelop glycoprotein folding and function. Accordingly, Ctag was fused to either the N-terminus of RDpro's SU or TM domains. And although these engineered RDpro were successfully expressed on the cell membrane, as determined by streptavidin detection of Ctag on transfected cells; they failed to produce detectable infectious viral particles. Peptide engineering on RDpro's SU may have inhibited its receptor binding domain on target cells. On the other hand, peptide incorporation on its TM domain may hindered its required conformational change for fusion activity. Both of these possibilities would be in line with the generally accepted limitations of envelope glycoprotein engineering (Buchholz et al., 2015; Friedel et al., 2015; Lévy et al., 2015). Failure to detect infectious particles may also have been caused by insufficient surface expression of engineered glycoproteins required for efficient pseudotyping of LVs. This could have been assessed by staining for RDpro alongside biotin mimic. However, this was not possible due to the lack of commercial or in-house RDpro antibody at the time of the experiment.

Assessing physical vector particles compared to infectious particles by p24 ELISA may have also helped to determine whether the lack of infectious particles was caused by hindrance of envelope functionality for infection (both its receptor binding and fusogenic function) or insufficient membrane expression, had caused the lack of infection observed with both engineered variants of RDpro. Nonetheless, these results indicate the difficulty faced when attempting to genetically engineer envelope glycoproteins with intertwined receptor binding and fusion domains.

Finally, as a third strategy for viral modification, we tested the random incorporation of Ctag by genetically engineered packaging cells. There is sufficient evidence to suggest that proteins expressed on vector producing cells could get incorporated on budding virions' surfaces. LVs have been reported to assemble at lipid rafts, and as a consequence GPI proteins residing in these microdomains are reported to incorporate into budding particles (Nguyen and Hildreth, 2000; Popik et al., 2002; Saad et al., 2006; Metzner et al., 2008b). Interestingly, Ctag CD8α stalk's ubiquitous membrane expression seemed sufficient for LV incorporation, which in turn allowed subsequent viral particle capture by streptavidin magnetic beads. This highlights the ease of cell-derived membrane protein incorporation onto viral vectors. Furthermore, this result strengthens the proposed model of passive inclusion of both virus and cell-derived proteins, on viral surfaces as suggested by Hammarstedt and Garoff (2004). Ctag's passive inclusion is, as expected, independent of pseudotyping glycoproteins, as indicated with complete streptavidin bead capture of both VSV-g and MLV-A pseudotyped vectors. Moreover, vector infectivity does not seem to be affected by Ctag's modification, as no significant difference was observed between modified and non-modified LVs. Therefore, given its inertness on viral function, the genetic engineering of vector producing cells with a surface protein, such as Ctag, is an attractive method to impose new functions onto viral particles. In this case, a cell line expressing an affinity tag would be established once and applied to a wide range of enveloped vectors currently used.

The indirect expression of Ctag molecules on each viral particle, which was acquired upon budding from vector producing cells, was sufficient to bind streptavidin magnetic beads and allow their purification and subsequent separation from viral supernatant. In addition, this interaction was shown to be dependent on Ctag's binding to streptavidin as indicated by the lack of capture with biotin-pretreated streptavidin beads. Interestingly enough, after process optimization, an increase in infectivity, and thus in turn of viral titres, of modified vectors bound to streptavidin Dynabeads was observed, without volume reduction. This observation of increased viral titres from modified vectors bound to magnetic particles has been previously documented (Hughes et al., 2001; Scherer et al., 2002; Nesbeth et al., 2006), with significantly higher fold increases in viral titres, indicating an enhancement in infection rates with vectors bound to larger particles. This phenomenon could be explained by the difference in the number of vectors exposed to target cells between those bound to large particles compared to those in harvested viral supernatants. Due to the higher gravitational pull of 1μm magnetic particles compared to diffusion rates of free-floating vectors, a higher number of infectious viral particles would come into close proximity to target cells, thus resulting in increased transduction efficiencies, without any volume reduction.

In this Chapter, LVs surfaces were modified to express the synthetic biotin mimic, Ctag by its random incorporation during virion budding. The density of Ctag on viral particles was sufficient to allow their complete capture from viral supernatant by streptavidin magnetic beads in a one-step protocol, also resulting in increased infectivity. This interaction was demonstrated to be specific on the biotin mimic's binding to streptavidin binding pockets. These sites of interaction have been validated to occupy the same binding pocket as biotin, as demonstrated by the lack of Ctag-LV capture by biotin pre-incubated streptavidin beads. We therefore reasoned that, with orders of magnitude higher binding affinity to streptavidin, the introduction of biotin should outcompete Ctag-LV's binding, allowing gentle elution of capture LVs from streptavidin.

Chapter 5 Purification of Ctag-LV by biotin-mediated competitive elution

5.1 Overview

In the previous Chapters, LVs were modified with Ctag biotin mimic which allowed their successful capture by streptavidin from surrounding clarified viral supernatant. As the affinity of this peptide to streptavidin (K_D 230nM) is orders of magnitude lower than its natural ligand biotin (K_D 10^{-15} M), this Chapter investigates the efficiency of Ctag displacement by biotin for LV competitive elution.

5.2 Introduction

The extraordinary strength of the biotin - streptavidin bond comes at the expense of its fundamentally irreversible binding for biotinylated target protein elution. However, recovery of captured targets is essential for any purification method. In response to this major challenge, several different approaches have been developed and employed to induce reversible binding of targets. To begin with, incubation of biotin-streptavidin interactions at temperature >70°C has been shown to result in bond breakage (Holmberg et al., 2005b). In addition, >90% recoveries of biotinylated proteins have been reported using denaturing conditions with SDS and common harsh desorption agents such as urea and thiourea and involving an incubation step at 96°C (Rybak et al., 2004). Alternatively, biotin derivatives with reduced affinities such as iminobiotin can be used, which binds in a pH-dependent manner binding at pH11 and dissociating at pH4 (Hofmann et al., 1980). Also, chemically modified molecules can be utilised such as photocleavable biotin which results in streptavidin bond cleavage by light (Olejnik et al., 1995). Otherwise, streptavidin binding site can be engineered to reduce binding affinity to biotin by conjugation of temperature or light sensitive polymers to the active site (Ding et al., 1999; Shimoboji et al., 2002). And Finally, an external protease cleavage sites can be introduced such as TEV (tobacco etch virus) protease

site between biotin tag and target protein (Rigaut et al., 1999). Therefore, various different approaches can be used for the purification of biotinylated proteins. However, to circumvent the strength of biotin-streptavidin interaction, harsh conditions are required, which may be sufficient for protein purification but may not be applied for the purification of labile complexes such as viral vectors all the while retaining their infectivity.

5.2.1 Elution of biotinylated viral vectors

Due to the remarkable specificity of biotin-streptavidin interaction and its potential, a handful of studies have reported the capture and purification of biotinylated viral vectors from (strept)avidin matrices. As a benchmark, the field attempted to apply elution conditions optimized for biotinylated protein recoveries, on viral vector purification. However, as mentioned, almost all elution methods for the recovery of biotinylated proteins relied on harsh conditions. Accordingly, Williams et al. (2005) tested different desorption agents such as urea and guanidine-HCL for elution of streptavidin-bound biotinylated viral vectors and resulted in vector inactivation. Conversely, the use of 0.6mM biotin as specific desorption agent for vectors bound to streptavidin Fractogel® polymeric beads, resulted in a low yield of 5%. This highlight the inefficiency of biotin displacement by free biotin in excess owing its low dissociation constant (K_D 10^{-15} M). Low recoveries were also reported for elution of biotinylated AAV purified using 5mM biotin from monomeric avidin, which has a lower binding affinity to biotin than tetrameric (strept)avidin, resulting in 17% elution (Parrott et al., 2000). As an alternative strategy, Chen et al., (2010) modified lentiviral particles with desthiobiotin, which as a biotin analogue, has a lower binding affinity (K_D 10^{-11} M) than biotin to biotin-binding proteins. Although only 52% of desthiobiotinylated-LVs captured by streptavidin Magnesphere®, elution with 2mM biotin resulted in 68% of bound vector recovery, making an overall yield of 35% of purified LVs. Therefore, even though biotin-mediated elution of desthiobiotinylated vectors was efficient, its viral vector metabolic modification required (i) exogenous expression of two enzymes and (ii) the supplementation of synthesize

compound that may be contaminated with biotin. This in turn could account for the relatively low capture yield.

5.2.2 Recovery of biotin mimic modified targets from matrices

5.2.2.1 Concept of competitive elution

The development of biotin mimicking peptides has allowed for specific purification by competitive elution resulting in target elution from resin. This process is very attractive for labile complexes, such as LV particles, it is a passive process that only requires first the dissociation of complex to allow a competitor, with a higher on-rate, to bind and result in displacement of bound targets. Moreover, currently used active elution of different affinity chromatography may be regarded as inferior compared to competitive elution, as they consist on changing overall buffer composition. This in turn alters the nature of interacting molecules causing the release of purified target for example by pH shifting. Therefore, as an elution strategy, competition binding provides key advantages over other currently used active elution processes, in that it is milder and confers a second specificity step, as only selectively captured targets are displaced from binding pockets.

5.2.2.2 Elution of recombinant proteins engineered with biotin mimics

Biotin mimics discussed in Chapter 3, whose application is not restricted to bacterial cells, have been widely used for the purification of target proteins. These mimics are genetically fused to targets; either individually or with other affinity tags for tandem affinity purifications. This enables specific purification of target bait proteins and their subsequent recovery by competitive elution with biotin or its analogue desthiobiotin. This section will cover to date applications of these mimics for modified target purifications.

5.2.2.2.1 SBP-tag

The large SBP-tag (38 amino acids) has been utilized for either purification of recombinant proteins by capture on streptavidin beaded polyacrylamide resin (Anthony D. Keefe et al., 2001) or immobilisation of cells expressing surface recombinant protein SBP-ΔLNGFR on magnetic beads (Matheson et al.,

2014). In both studies, engineered proteins and cells were recovered from resin with 2mM biotin. Although eluted samples conferred high purity, overall yields however were not mentioned. Conversely, when SBP-tag was used with in tandem affinity purification with either protein-G (Bürckstümmer et al., 2006), hemagglutinin (Glatter et al., 2009), or with hexa-histidine (Li et al., 2011), around 50% recoveries were achieved with denaturing SDS-containing elution buffer with 1-2mM biotin. The use of SDS was shown to be required for higher yield but came at the expense of specificity. Nonetheless, since these studies aimed at analysing interacting partners of engineered targets by mass spectrometry (MS), the addition of denaturing agent in elution buffer was possible. This would not be the case for the elution of captured viral vectors as retaining infectivity in overall eluted yield is a prerequisite for any viral purification method.

5.2.2.2.2 Strep-tag

The Strep-tag® peptides have been widely used for various applications ranging from purification of recombinant proteins such as metalloenzyme proteins (Maier et al., 1998) and phosphatases (Junttila et al., 2005b) and multimerisation of MHC molecules (Knabel et al., 2002). Additionally, Streptag® have been used in several tandem affinity purifications with hexa-histidine (Cass et al., 2005; Locatelli-Hoops and Yeliseev, 2014). The streptavidin mutant StrepTactin immobilised on sepharose resin was used for target capture for all Strep-tag® purification. Moreover, Streptag-III (or commercially known as Twin-Strep-Tag from IBA), containing two versions of Streptag-II separated by a linker, has been shown to exhibit higher binding kinetics to StrepTactin compared to Strep-tag-II; and is currently manufacturer's recommended Streptag® for target affinity purification (Schmidt et al., 2013). The analogue desthiobiotin is the recommended desorption agent for the elution of Streptag® fused protein from StrepTactin resin. StrepTactin resin can then be regenerated by applying the azo dye HABA in excess, which binds at a lower affinity to the same pocket as Streptag® or biotin, leading to desthiobiotin displacement.

In practice, different recoveries of Streptag® fused target purifications from StrepTactin using 2.5-5mM desthiobiotin have been reported for recombinant proteins with overall yields of 70% using Streptag® alone, and of a maximum yield of 38% in tandem affinity purifications applications (Maier et al., 1998; Cass et al., 2005; Junttila et al., 2005a; Locatelli-Hoops and Yeliseev, 2014). However, desthiobiotin-mediated displacement has faced certain limitations for competitive overall yields. Purification of plant-derived Streptag-II fused kinases from StrepTactin resin using 10mM desthiobiotin was unsuccessful and required SDS-containing elution solution (Witte et al 2004). This was later resolved by using 10mM biotin as a stronger competitor for target displacement (Werner et al 2008). Furthermore, incomplete elution was also reported for the highest affinity peptide Streptag-III displacement, using 15mM biotin rather than desthiobiotin, compared to elution buffer containing 1% SDS (Ivanov et al., 2014). Moreover, the use of SDS for elution of Streptag-III was shown to cause undesirable sample contamination with StrepTactin monomers released from resin. Authors circumvented this problem by first chemically cross-linking monomers using BS3 (bis(sulfosuccinimidyl)suberate), then eluting Streptag-III fused target protein and its associated interacting proteins with denaturing elution buffer containing 1% SDS, 25mM Tris-HCL at pH 8 (Ivanov et al., 2014). This methodology however, may not be used for fragile protein complexes, such as lentiviruses, as structures may dissociate due to the use of solutions containing high salt concentrations and ionic detergents.

Almost all of the discussed purification reports that have used Streptag® or SBP-tag were developed for downstream proteomics analysis by MS, in which retaining protein functionality is not required. It should be noted that, to the best of our knowledge, the use of these mimics for viral vector purification has not been reported yet. For the development of such an application, selective capture of modified vectors should be combined with gentle and milder elution conditions for efficient purification of LVs with high overall yield and purity.

5.3 Aims

In the previous Chapter, the interaction between Ctag expressed on lentiviral vectors and streptavidin allowed the compete capture of viral titre using streptavidin conjugated magnetic beads. As mentioned above, a pre-requisite for any viral purification method is the release of purified infectious vectors from resin with high purity and yield. We have previously demonstrated that (i) Cell membrane expressed Ctag's binding to streptavidin was displaced by biotin, releasing bound cells and (ii) Ctag-LV's capture by streptavidin magnetic beads was blocked by pre-incubation of beads with biotin. Therefore, to develop our purification method for viral recovery from streptavidin matrix, the aims of this Chapter are:

- Testing and developing the elution of Ctag-LV bound to streptavidin beads resulting in competitive overall yields.
- Assessing biotin mediated toxicity on infectious Ctag-LVs.
- Attempting to quantify the density of randomly incorporated Ctag proteins onto individual viral particles.

5.4 Preliminary testing of biotin-mediated release of Ctag-LV bound to streptavidin beads

As this project aimed at developing a one-step vector purification protocol, subsequent elution of captured vectors from beads is desirable. Since the displacement of Ctag bound to streptavidin by biotin has been previously demonstrated (Chapter 3), the recovery of Ctag-LV from streptavidin magnetic beads by biotin was tested. To that end, Ctag-LVs were captured by streptavidin beads as per Methodology 2 (Section 4.8). The beads were then incubated with DMEM supplemented with a saturating concentration of biotin at 30mM, for 2 hours at 4°C (Figure 5.1). Subsequently, fractions were separated into eluate (collected after bead magnetization containing displaced Ctag-LV) and beads eluate (containing beads post-eluate collection) to assess for remaining vector. Additionally, resuspension volumes of fractions were equivalent to the starting material and thus no volume reduction occurred in this experiment. As expected incubation of neat Ctag-LV (2.6 ±1.5 $x10^5$ IU/mL) with streptavidin beads resulted in complete viral titre capture (3.0 ±1.4$x10^5$ IU/mL) (Figure 5.1a-b). The subsequent incubation of Ctag-LV bead fraction with DMEM containing excess 30mM biotin resulted in the elution of a portion of bound vector (6.2 ±1.0 $x10^4$ IU/mL), which represented 24% of starting vector particles. However, 17% of Ctag-LV neat particles were found in the bead eluate fraction (4.3 ±4.0 $x10^4$ IU/mL), indicating the incomplete displacement of Ctag-LV by biotin. Given the significantly lower affinity of Ctag compared to biotin for streptavidin (Giebel et al., 1995), the saturating concentration of 30mM biotin should allow the dissociation of all Ctag-LV bound to streptavidin magnetic beads. The inconsistency in the overall yields of beads eluate in the three experiments performed should be, as irrespective of its viral titre, only around 40% of neat Ctag-LV has been detected post elution incubation. In an effort to investigate this, different parameters that may have attributed to the loss in infectivity post-elution were troubleshooted.

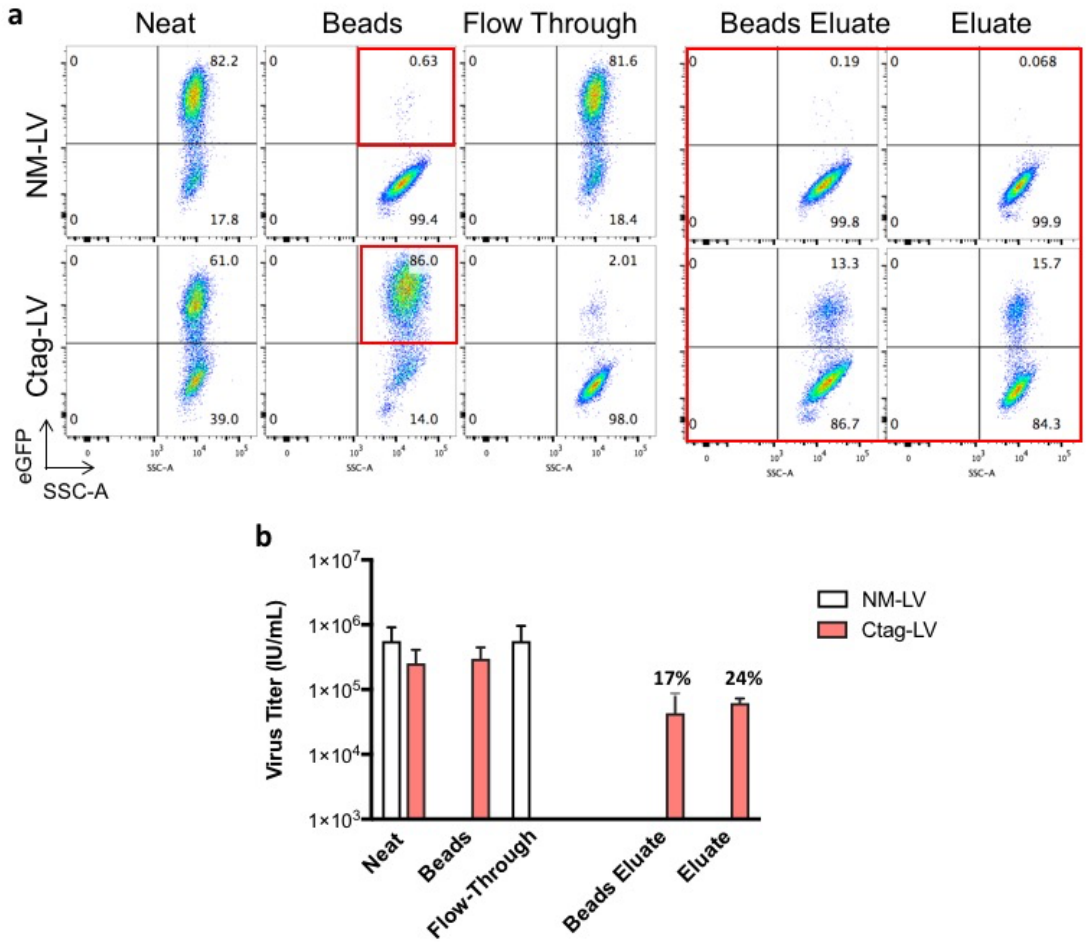

Figure 5.1: Elution of bead bound Ctag-LV by biotin in DMEM. NM- and Ctag-LV from stocks were thawed and incubated with streptavidin Dynabeads as developed methodology. PBS washed beads fractions of both LVs (red squared) were then incubated with plain DMEM supplemented with 30mM biotin for 2 hours at 4°C. Eluate was separate from beads eluate by magnetic immobilization of beads. All fractions were collected and viral titres were determined by infectivity assay on NT-293T cells. **(a)** Dot plots of eGFP vs SSC-A represent cells transduced with 250µL of all fractions. **(b)** Viral titres of all fractions are plotted with values representing infectious titres ± standard deviation (SD) of three independent experiments (n=3).

5.4.1 Troubleshooting infectious vector loss during elution

5.4.1.1 Effect of polystyrene container

First, during these experiments, all incubations were done in polypropylene standard plastic containers. And after the last incubation, magnetic particles were observed to adhere to the walls of incubation containers, regardless of the several washing steps performed. Given their size (1µm), their detection by the naked eye indicated a substantial number of beads bound to container surfaces'. This may have in turn have accounted for the detection of only 40% of infectious Ctag-LVs post-elution. In order to test this hypothesis, the experiment was repeated using both polypropylene and glass containers, and then viral recoveries of eluates and beads eluates compared to starting vector were determined (Figure 5.2). Although a small difference was observed in overall yields between glass (19%) and polypropylene containers (15%); around 60% of infectious starting viral titre was still uncounted for with only 16% and 13% of viral titre detected in both beads eluate fractions, respectively. Therefore, the loss of infectious titre could not be attributed to magnetic beads non-specifically adhering to polypropylene plastic containers.

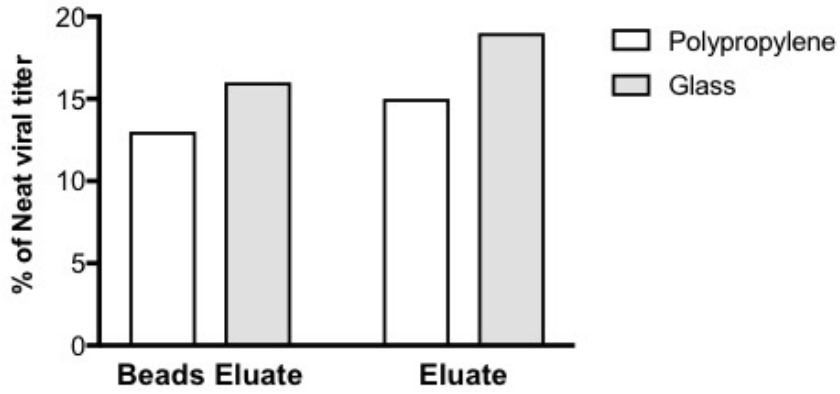

Figure 5.2: Testing different container for increased elution recovery. Elution experiment was repeated in plastic polystyrene and glass 15mL falcon tubes and viral titres of both beads eluate and eluates are plotted.

5.4.1.2 Effect of protein additives supplementation

Thus far, elution experiments, which require the out-competition of Ctag by biotin from streptavidin binding pocket, were performed in plain DMEM. This basal medium contains no growth promoting agents or proteins. Therefore, an alternative hypothesis for the loss of infectivity was postulated that DMEM's relative lack of protein supplements may have caused aggregation and/or inactivation of labile RDpro pseudotyped LVs. It should be mentioned that this phenomenon might have occurred in the bead captured fraction but was undetected due to the increased viral titre achieved with vector bound to magnetic particles. It should also be noted that since we only focused on infectivity assessment of recovered vectors, physical particles were not investigated. Nevertheless, we first decided to test elution of captured Ctag-LV in the presence of fetal calf serum (FCS), dialyzed to remove biotin (dFCS). Moreover, to determine whether the loss of titre observed in previous experiments was due to lack of protein stabilizers and/or the labile nature of RDpro pseudotyped LVs, the elution experiment was also tested on Ctag-LV pseudotyped with VSV-g, which is known to confer increased particle stability (Cronin et al., 2005). To that end, LV pseudotyped with both RDpro and VSV-g were produced from NT and Ctag-293T cells and subjected to our purification methodology in plain DMEM; followed by incubation of captured beads with plain DMEM supplemented with either 15mM biotin or 15mM biotin with 5% dFCS (Figure 5.3). Starting with RDpro pseudotyped Ctag-LV, neat fraction in this experiment has a relatively low viral titre (6.0 $x10^4$ IU/mL) and as expected Ctag-LVs were captured by streptavidin beads resulting in increased viral titre (9.2 $x10^4$ IU/mL) and transduction efficiency (52%) compare to its neat fraction (16.5%) (Figure 5.3a). Subsequently, eluate fraction collected after incubation of vector captured beads with 15mM biotin, resulted in an undetectable infectivity of target cells. Conversely, eluate collected from incubation with 15mM biotin in the presence of 5% dFCS resulted in the recovery of 61% of starting vectors with a viral titre of 3.65 $x10^4$ IU/mL.

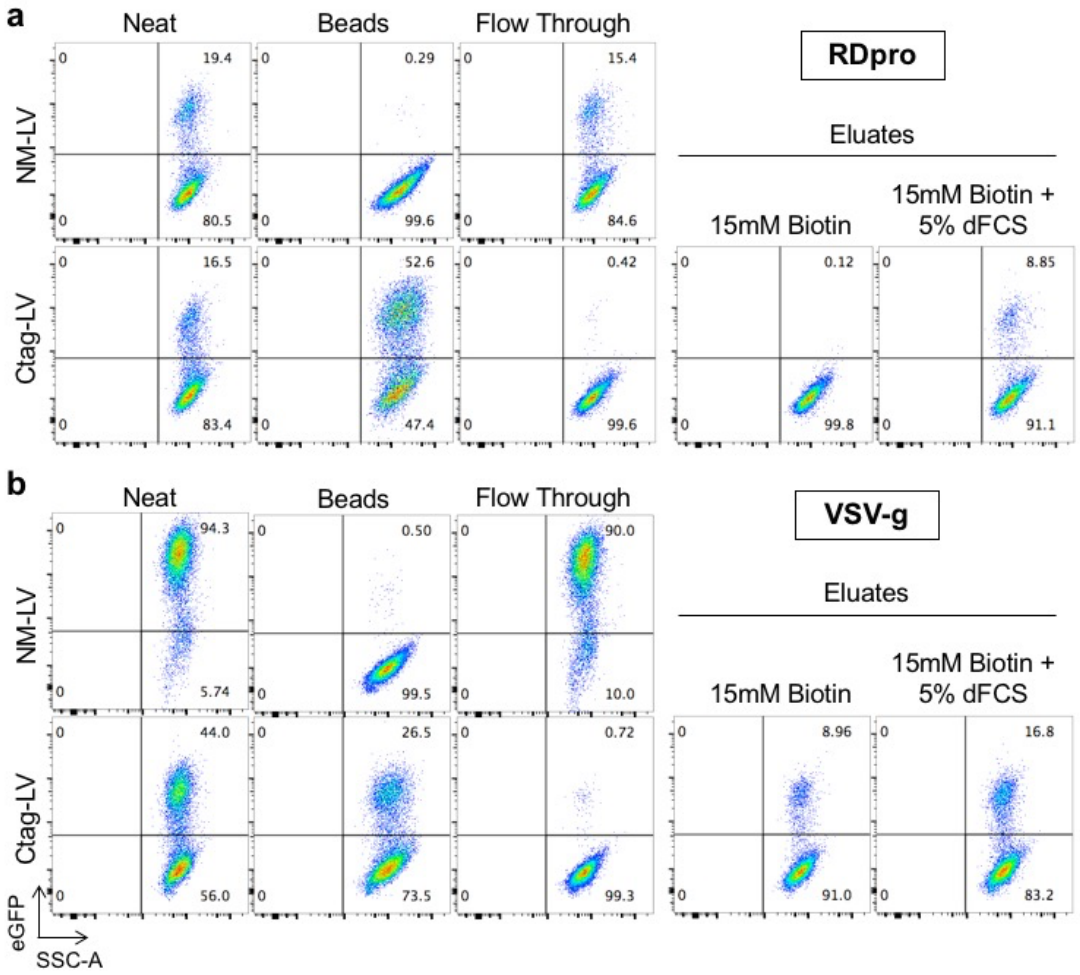

Figure 5.3: Elution efficiency comparison of infectious Ctag-LV by biotin in the presence of protein additives. Control and modified LVs pseudotyped with either RDpro or VSV-g were produced by transient transfection of NT- and Ctag-293T cells and subjected to subjected to the developed methodology and washed bead fractions were then incubated with either DMEM supplemented with 15mM biotin only or with the addition of 5% dialyzed fetal calf serum (dFCS) for biotin removal. Eluates were then collected and fractions were assayed for viral titre. Dot plots of eGFP vs SSC-A represent cells transduced with 250µL of RDpro **(a)** and VSV-g **(b)** fractions.

This result indicated that the presence of dFCS, which contains a cocktail of proteins, reduced the loss of infectivity of Ctag-LV and thus in turn increased recovery of infectious particles from streptavidin magnetic beads. Moreover, interestingly, Ctag-cells producing VSV-g pseudotyped vectors resulted in log lower viral titre (1.2 x10^5 IU/mL) than that produced from NT-293T cells (1.4 x10^6 IU/mL), an observation not seen with RDpro pseudotyped LVs (Figure 5.3b). A possible explanation for this difference was that after γ-RV

transduction of 293T cells to express Ctag on CD8α stalk, may have caused it to be less transfectable than NT-293T cells. This however was not the case when tested by eBFP transient expression (see Appendix 1). An alternative explanation may be that Ctag-293T cells were transduced to produce high levels of an exogenous protein (Ctag), which may have caused a translational burden which may have impacted their cellular machinery to produce virions at the same efficiency as non-transduced 293T cells, thus resulting in lower viral titre of VSV-g and not RDpro LVs. Nonetheless, in this experiment only 53% of VSV-g Ctag-LV titre was captured by streptavidin beads. This low percentage of capture was only observed in this experiment as almost complete capture of VSV-g pseudotyped Ctag-LV has already been demonstrated in a reproducible manner in Section 4.9. Nevertheless, incubation of beads captured Ctag-LV with 15mM biotin resulted in elution of 54% of the captured particles, whereas in the presence of 5% dFCS, 99% of capture vectors were recovered in eluate fraction. These results first highlight the inherent lability of RDpro as pseudotyping envelope relative to VSV-g. And secondly, further validated the hypothesis that the loss of vector activity post-elution observed in previous experiments was most likely due to the need of protein supplements, such as serum proteins, in the elution buffer for increased viral particle recoveries.

5.5 Optimisation of elution conditions for improved overall yield

5.5.1 Determining elution buffer composition for vector recovery

For all elution experiments presented so far in this chapter, viral supernatant was produced each time by transient transfection of both NT- and Ctag-293T cells. A large stock of NM- and Ctag-LV in plain DMEM was produced and frozen down for usage in all subsequent experiments in this chapter, unless otherwise stated. The effect on infectivity of freeze-thawing LVs in plain medium was measured between fresh and freeze-thaw samples and a 35%

decrease in infectivity was determined for both NM- and Ctag-LV batches with viral titre of 1.35 $x10^5$ and 2.27 $x10^4$ IU/mL, respectively (Figure 5.4a).

Subsequently, we evaluated the potential adverse effects of biotin in excess on infectivity of both NM- and Ctag-LVs. Accordingly, control and modified viral supernatants were incubated with plain DMEM supplemented with decreasing concentrations of biotin starting with 15mM, diluted 1:2 for 6 points, down to 468.75µM biotin, and incubated for 2 hours at 4°C. The viral titres were determined for all incubations and consistently no decrease in infectious titres with any biotin concentration in DMEM was observed compared to incubation with plain DMEM; with 2.23 $x10^5$ and 3.86 $x10^4$ IU/mL viral titres after 15mM biotin incubation and 2.05 $x10^5$ and 3.58 $x10^4$ IU/mL after plain media incubation, for NM- and Ctag-LV, respectively. (Figure 5.4b). These results indicated that the addition of free biotin in excess does not seem to negatively impact LV infectivity. Subsequently, overall yields of desorbed Ctag-LV from streptavidin beads was tested with the decreasing concentration of biotin in the presence of protein additives (Figure 5.4c). A neat viral titre of 3.5 $x10^4$ IU/mL was captured, with increased infectivity of 5.44 $x10^4$ IU/mL, and then subjected to incubation with biotin titration from 15mM to 468.75µM in DMEM supplemented with 5% dFCS, for 2 hours at 4°C. Eluate fractions were collected after beads immobilization by magnetization and viral titres were determined by infectivity. Interestingly, the elution of Ctag-LV from magnetic beads seemed saturated with an average overall yield of 69%. Therefore, high overall yield can be achieved using biotin-mediated competitive elution and requires the presence of bovine serum proteins. However, due to the latter's uncharacterized mixture, alternative defined protein additives, such as BSA and human albumin solution (HAS), were compared to 5% dFCS for overall eluted viral yield. Moreover, in an effort to further increase elution efficiency, a chemically defined, serum-free medium, X-vivo™ was tested as an elution solution alongside DMEM. Unlike the latter, X-vivo™ contains proteins and has been designed for hematopoietic cell culture and is widely used for viral formulation for subsequent *ex vivo* T cell transductions, which represents the research scope conducted in our laboratory. To that end, elution efficiencies

were compared between DMEM with 500μM biotin+5% dFCS and X-vivo™ with 500μM biotin was supplied with either 0.1% or 0.5% of BSA or HAS, separately. In this experiment, high titre fresh Ctag-LV viral supernatant was produced (2.5 x10^5 IU/mL) for elution testing and was thus subjected to streptavidin magnetic beads capture, resulting in 2.2-fold higher viral titre of 5.34 x10^5 IU/mL. Subsequently, captured Ctag-LV was incubated with the different conditions shown in Figure 5.4d for 2 hours at 4°C. Eluates fractions were then collected and viral recoveries were determined by infectivity. Consistent with previous results, the addition of 5% dFCS to DMEM+500μM biotin resulted in higher overall yield (48%, 1.2 x10^5 IU/mL) compared to biotin alone (18%, 4.35 x10^4 IU/mL). Moreover, unlike DMEM, incubation of bead-bound Ctag-LV in plain X-vivo™ recovered a small fraction of 6% (1.52 x10^4 IU/mL) of viral particles, whereas the addition of 500μM biotin to X-vivo™ increased that recovery to 39% (9.7 x10^4 IU/mL). Furthermore, a stable recovery of 48% (1.2 x10^5 IU/mL) was achieved with X-vivo™+500μM biotin supplemented with 0.1% BSA, 0.1% and 0.5% HAS; whereas a slightly higher recovery of 62% (1.54 x10^5 IU/mL) was observed with 0.5% BSA. Although this experiment was not repeated, given that X-vivo™ with 500μM biotin and 0.5% BSA resulted in the highest overall elution yield from streptavidin magnetic beads, this formulation as elution buffer was taken forward for subsequent experiments.

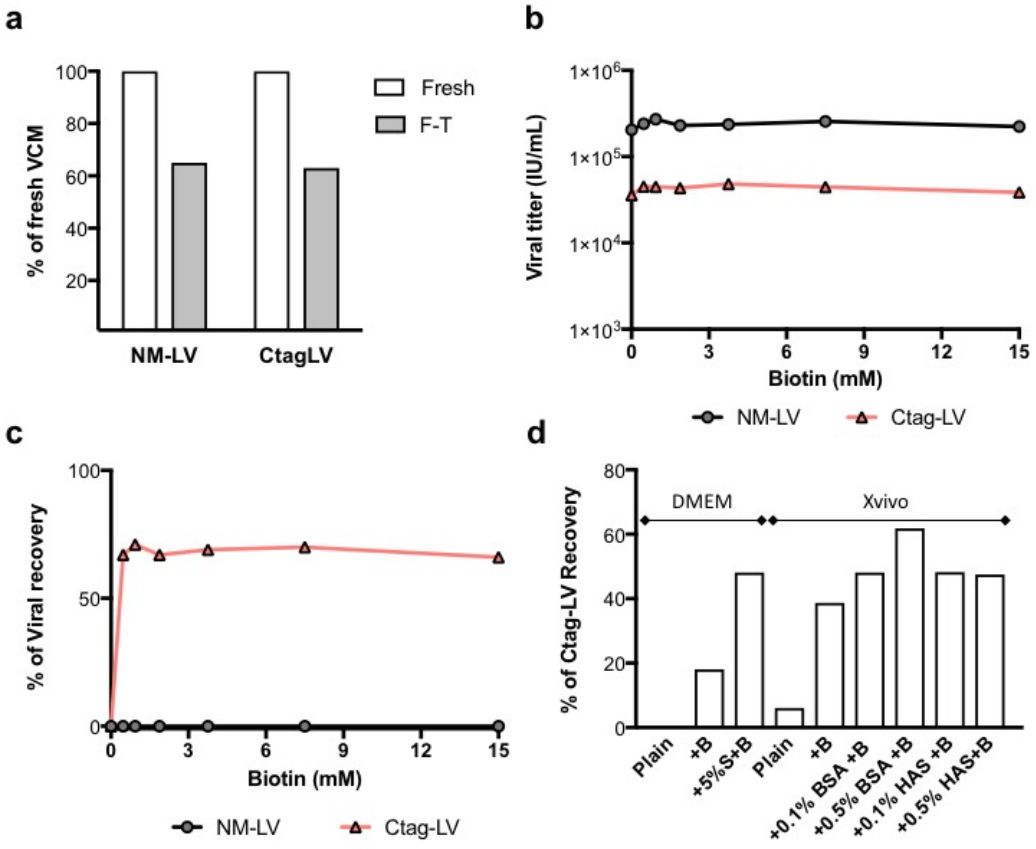

Figure 5.4: Optimization of viral recovery and elution buffer formulation. (a) Large batch of fresh NM-LV (2.05 x10^5 IU/mL) and Ctag-LV (3.58 x10^4 IU/mL) vectors were produced and viral loss due to one cycle of freeze-thawing (F-T) of the stock was determined by comparing it to fresh viral supernatant. **(b)** Viral titres of both NM- and Ctag-LVs are plotted in which thawed VCM were incubated with seven decreasing concentration of 15mM biotin in DMEM of 1:2 dilutions for 2 hours at 4°C. **(c)** Viral recoveries of bead-captured vectors fractions for both Ctag-LV and control NM-LV were tested by incubation with seven decreasing concentration of 15mM biotin in DMEM of 1:2 dilutions for 2 hours at 4°C. **(d)** Ctag-LV recovery efficiency from Dynabeads was tested in either DMEM or X-vivo™-15 in different formulations for both, either plain or supplemented with 500µM biotin (+B) and different additives: 0.5% dialyzed FCS (+0.5%S); 0.1% or 0.5% of bovine serum albumin (BSA) or human albumin solution (HAS).

5.5.2 Titration of biotin concentration in elution buffer

In the previous section, the addition of carrier proteins such as BSA to biotin containing elution buffer, was demonstrated to result in increased viral recoveries. However, elution recovery appeared to be saturated with a wide range of biotin concentration (15mM to 500µM). Therefore, to determine

biotin's half maximal effective concentration (EC50) for vector elution, Ctag-LV from stock (1.2 ±0.11 $x10^5$ IU/mL) was captured by streptavidin magnetic beads, and subsequent bead fraction (1.9 ±0.09 $x10^5$ IU/mL), was incubated with 7 different conditions of X-vivo™ supplemented with 0.5% BSA, containing decreasing biotin concentrations starting with 15mM diluted 1:100 to 15fM, for 2 hours at 4°C. Eluate fractions were then collected and their viral load were determined by infectivity assay and a dose-dependent displacement graph was generated (Figure 5.5a-b). Interestingly, there wasn't a significant difference in elution recoveries of 31% ±1, 28% ±3 and 26% ±1.5 using 15mM, 150µM and 1.5µM biotin, respectively. Crossing into the nanomolar concentration of biotin, starting from 15nM, 150pM, 1.5pM and 15fM, significantly reduced the displacement efficiency of bound vectors to 3% +/- 1, 2.3 ±0.5%, 1.3 ±0.5% and 1%, respectively. These results indicate that increasing the number of biotin molecules by 100-fold did not seem to relatively increase displacement efficiency. Moreover, although we could not have achieved a dose-dependent elution with recoveries higher than 30%, the EC50 was determined at 208nM biotin, which is the required concentration to displace 50% of maximal recovery of 30%. In addition, the sigmoidal graph generated a Hill slope of 1.089, indicating that biotin may be competing with multiple binding sites on Ctag-LV, which may explain the incomplete dissociation of captured vectors. Taking into consideration the number of biotin molecules in these concentrations, a significant amount of biotin seemed to be required for the competitive elution of a portion of bound Ctag-LVs. More specifically, a 208nM concentration of biotin in the volume used (0.5mL) contained 6.26 $x10^{13}$ number of biotin molecules. This concentration successfully out-competed 15% of neat Ctag-LV which contained 1.86 $x10^4$ IU; which can be regarded as 1.86 $x10^7$ physical particles, if we were to assume the accepted ratio of 1 infectious particle per 1000 physical particles for LVs. Therefore, it could be postulated that almost 3 $x10^6$ biotin molecules were required to displace 1 PP from streptavidin magnetic beads. It should be mentioned that the number of binding sites per magnetic beads is not provided by the manufacturer and thus unknown. Nevertheless, taking these results together, it could be suggested that there may be physical hindrance for biotin

to reach streptavidin binding pockets occupied by Ctag or alternatively, multiple Ctag molecules per viral particles may increase virions' overall avidity thus requiring longer elution incubation times.

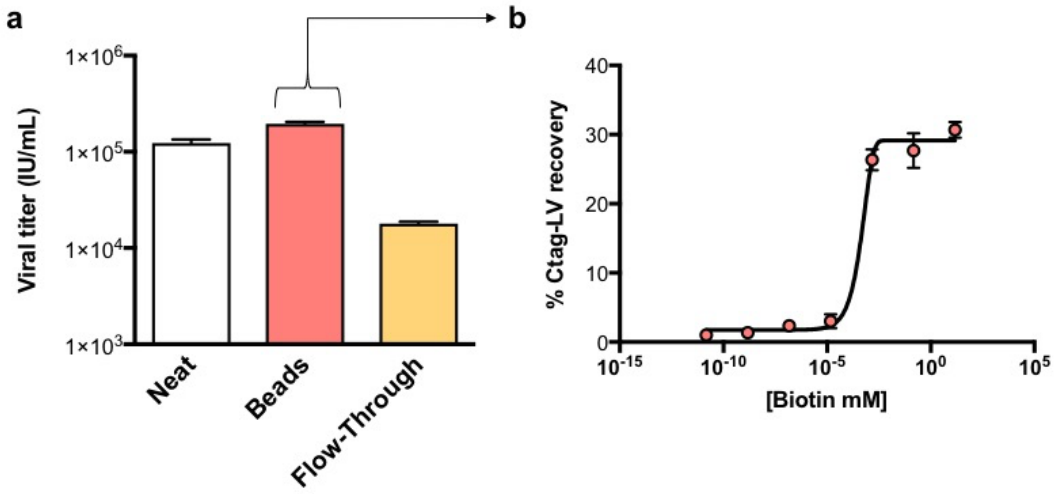

Figure 5.5: Dose-dependent biotin-mediated elution. (a) Ctag-LV from vector stock was captured by streptavidin Dynabeads as per developed methodology and bead fraction was incubated with seven decreasing concentration of 15mM biotin of 1:100, in X-vivo^{TM}-15 supplemented with 0.5% BSA, for 2 hours at 4°C. **(a)** Capture fractions were collected and assayed for viral infectivity and values ± standard deviation (SD) of triplicate determinations are presented. **(b)** Dose-dependent displacement graph of percentage of Ctag-LV recovered in the different relative to starting neat supernatant is presented. Biotin concentrations values on the X-axis were transformed for the non-linear regression analysis of the results.

5.5.3 Sequential elution of Ctag-LV and vector characterization by Nanosight

In the previous sections, we have established the partial recovery of Ctag-LV from streptavidin resin by biotin competitive elution. It was known by infectivity assay that the remaining non-desorbed Ctag-LV particles remained bound to streptavidin beads after elution incubation. We wanted to therefore assess the consecutive displacement of Ctag-LV by sequential exposure to biotin of beads eluate (containing non-displaced Ctag-LV). In addition, in this experiment we aimed to analyze eluted Ctag-LV by Malvern's Nanosight that use the nanoparticle tracking analysis (NTA) software to characterize

nanoparticles from 10-2000nm. This analysis relies on the tracking of nanoparticles and requires particles resuspension in solution with velocity coefficient of 1. Therefore, for the purpose of Nanosight analysis, Ctag-LV could not be eluted in X-vivo^{TM} medium due to its high concentration of endogenous particles. As an alternative, PBS was chosen as elution buffer by its supplementation with 500µM biotin and 0.5% BSA. However, before the sequential elution of Ctag-LV, PBS as a viable elution buffer was tested for compared to X-vivo^{TM} and no differences in overall yield of both eluate and beads eluate fractions were observed (see Appendix 2). Next, neat Ctag-LV (5.6 ±0.4 x10^4 IU/mL) was captured on streptavidin magnetic beads as per developed methodology and resuspended in the same volume as starting viral supernatant; resulting in a 3.3 ±0.1 -fold increase in viral titre (1.84 ±0.09 x10^5 IU/mL) (Figure 5.6a). Bead-bound Ctag-LV fraction was then subjected to a first round of elution using 150X PBS elution buffer in which reactions were incubated for 2 hours at 4°C. Subsequently, eluates (150X) were collected and then beads eluate were re-incubated with 150X elution buffer for two more rounds of elution incubations. Individual viral recoveries of collected eluates (150X) were determined and samples were then pooled together into a 50X eluate-all fraction (Figure 5.6a-b). After a first round of elution incubation, eluate fraction (E1) recovered 29 ±2% of Ctag-LV, with a 39 ±0.8-fold increase in viral titre of 2.34 ±0.04 x10^6 IU/mL. This result is consistent with previous elution experiment which resulted in 28% recovery using micomolar range of biotin concentration. Second incubation of beads eluate with fresh elution buffer (E2) resulted in the recovery of 6 ±0.5% of Ctag-LV, with 8 ±0.03-fold increase in infectious titre of 4.87 ±0.02 x10^5 IU/mL compared to starting material. Moreover, a third round of elution (E3) also resulted in the recovery of 2% of Ctag-LVs, with a 2.3 ±0.07-fold increase viral titre of 1.42 ±0.04 x10^5 IU/mL.

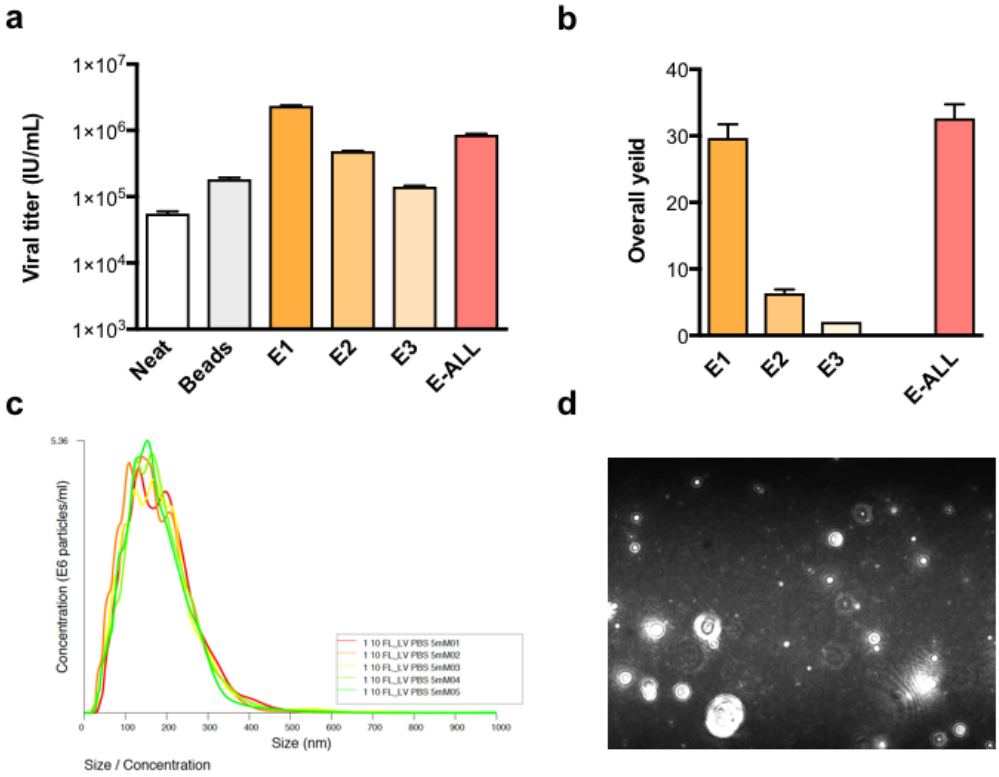

Figure 5.6: Serial elution of Ctag-LV and eluate characterization by nanoparticle tracking analysis. Captured Ctag-LVs from stock by streptavidin Dynabeads were incubated with 150X volume reduction of PBS-based elution buffer containing 500µM biotin and 0.5% BSA for 2 hours at 4°C. After eluate collection (E1), beads eluate fraction was incubated again with the elution buffer at the same conditions for a second (E2) and a subsequent third (E3) time. Each eluate was sampled for viral titration at 150X volume concentration and then pooled together (E-ALL) with a final 50X volume concentration compared to neat. **(a)** Viral titres of all collected fractions and **(b)** overall viral yield of eluates ± standard deviation (SD) of triplicate determinations are presented. **(c)** Nanoparticle tracking analysis for E-ALL product characterization by Nanosight technology which records five separate video analysis of samples to determine its overall concentration in particles/mL. (d) Image representing screenshot of one of the captured videos for visualization of E-ALL particle composition.

Intriguingly, these results indicated that initial exposure to biotin seemed to displace a certain percentage of Ctag-LV bound to beads (29%), followed by a smaller portion displaced with second elution incubation and similarly for a third elution incubation. No pattern of elution could have been detected from the sequential elution of Ctag-LV by free biotin. However, this experiment does indicate that after a second round of biotin exposure, displacement is not as

efficient as the first time. It should however be mentioned that recoveries have been observed to vary greatly between different elution experiments, as shown later within this Chapter. Nonetheless, it is difficult to investigate the process of biotin-mediated competitive elution without the knowledge of how many Ctag molecules are present on individual viral particles. Even if Ctag, as a biotin mimic, has a significantly lower binding affinity to streptavidin than biotin, several epitopes may be expressed on single viral particles thus resulting in a significantly higher avidity, thus representing a limiting factor for higher elution rates. In an attempt to both characterize and quantify the number of Ctag molecules per LV particles, all three eluate fractions where pooled together (E-ALL); resulting in a viral titre that was 14 ±0.48-fold higher than neat, with 8.61 ±0.28 $x10^5$ IU/mL, representing an overall yield 32 ±2%; and subjected to characterization using Malvern's Nanosight instrument. This was carried out on frozen-thawed eluate samples at NIBSC with the kind help of Dr. Giada Mattiuzzo. The instrument was configured with a green-yellow laser therefore allowing the possibility of staining Ctag-LVs with streptavidin conjugated to FITC, in order to attempt the quantification of biotin mimic per particle. NTA analysis of frozen-thawed eluted Ctag-LV (50X) vectors by Malvern's Nanosight resulted in the characterization of two distinct particle size populations as indicated by the two peaks of the five-separate analysis summarized in Figure 5.6c. Accordingly, both small particles and large aggregates can be visually seen in Figure 5.6d, which represents an image of one of the videos acquired by the NTA software. Consequently, size distribution analysis determined a mean size of 180 ±3.0 nm, with a mode of 151 ±6.9nm, which are larger than the accepted size of LVs of ~ 120nm. Given the lack of single size nanoparticle detection, any characterization of Ctag-LVs, such as concentration of particle/mL, would not have been accurate. Moreover, fluorescent staining of Ctag-LV had failed, not allowing the quantification of Ctag molecules/particle. Therefore, although PBS was chosen for its endogenously clean composition analysis of eluted Ctag-LV was not possible due to the presence of large aggregates. This result highlights the complex and aggregate-rich milieu of eluted modified LVs.

5.5.4 Indirect differential expression of Ctag on LVs for increased overall yield

Elution recoveries thus far indicated the presence of substantial number of Ctag-LVs that cannot get displaced even in the presence of high concentration of biotin. This in turn raised two potential issues that may be limiting for higher recoveries; 1- possible avidity issues correlated to the number of Ctag-LV per viral particle, and 2- possible difficulty for biotin accessibility to streptavidin's binding site due to aggregation or molecular crowding. The latter scenario unfortunately was not tested in the experimental scope of this project due to the difficulty in assessing both particle composition and interaction on a nanometer scale. Nonetheless the former possibility was tested by indirectly altering the expression of Ctag on viral particles and evaluating whether altered vector avidity can lead to increase viral recoveries from streptavidin magnetic beads by excess biotin. Since LVs acquire Ctag molecules by passive incorporation while budding from vector producing cells, we reasoned that altering the density of Ctag on these cells should in turn alter its density on LV particles produced from these cells. Therefore, 293T cells were γ-retrovirally transduced with Ctag on CD8α stalk, co-expressed with eGFP and once cells had recovered, they were sorted by flow cytometry into low, medium and high Ctag expressers (Figure 5.7a). It is worthwhile mentioning that Ctag's expression on low and medium sorted cells were in close range, as indicated by their streptavidin expression of eGFP-positive cells, with 3073 ±493 and 4801 ±459 MFI, respectively. Ctag-high sorted cells had a significantly higher mimic density with an MFI of 14162 ±622 for streptavidin staining of eGFP-positive cells (Figure 5.7b-c).

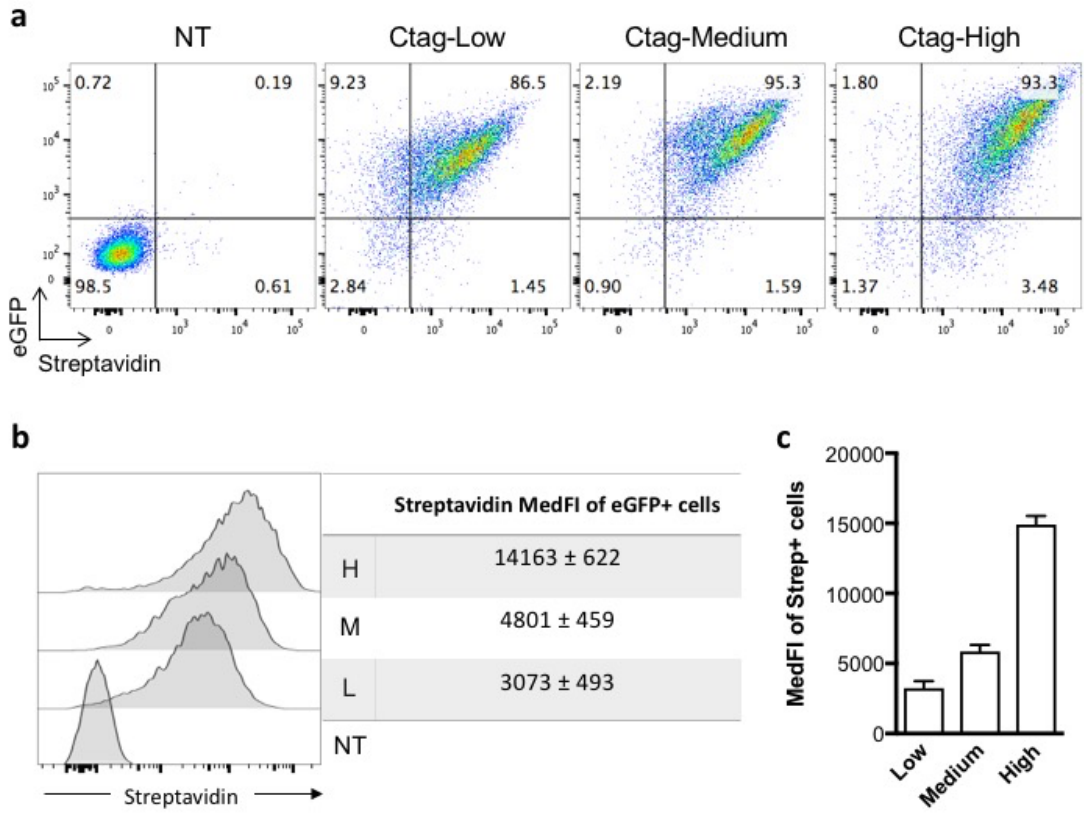

Figure 5.7: Establishing differential Ctag-293T cells expressers. (a) Dot plots of non-transduced (NT) and sorted Ctag.IRES.eGFP-293T cells into low, medium and high expressers' staining with streptavidin conjugated to APC. **(b)** Half-offset overlaid histograms of control and sorted populations with streptavidin MFI values, **(c)** which are also plotted as columns, ± standard deviation (SD) of triplicate determinations are presented.

Once sorted cells recovered, LVs were produced from all three populations (Ctag-L, Ctag-M and Ctag-H LVs) along with NT-293T cells as a control. Viral supernatants were then subjected to purification by incubation with streptavidin beads. Elution was then performed by bead fractions incubation with X-vivo^{TM} containing 500µM biotin and 0.5% BSA, without any volume reduction. As in previous experiments, all fractions were collected and their viral loads determined by infectivity assay (Figure 5.8). In this experiment, the effect of differential Ctag expression on LV particles was tested for both streptavidin capture and biotin mediated elution efficiencies. Starting with capture, a significant difference was observed between viral titres of neat (2.5 ±0.18 x10^5 IU/mL) and bead-captured (1.7 ±0.2 x10^5 IU/mL) fractions

produced only from Ctag-low 293T cells. This indicated that passive incorporation of Ctag's density from low expressing cells onto viral particles was not sufficient for complete viral particle capture (Figure 5.8a). No significant difference was observed between neat viral titres produced from both medium- (1.44 ±0.11 $x10^5$ IU/mL) and high- (1.88 ±0.26 $x10^5$ IU/mL) expressers compared to their bead-captured fractions, with viral titres of 1.8 ±0.56 $x10^5$ and 2.55 ±0.53 $x10^5$ IU/mL, respectively. Taken together these results implied that a minimum density of Ctag on LVs surfaces seemed to be required for significant vector capture by streptavidin magnetic beads. Accordingly, using Pearson product-moment correlation coefficient, a positive correlation was detected between Ctag's MFI on 293T cells and capture efficiencies. However, the correlation between these variables was not statistically significant (Figure 5.8b). Moreover, by plotting the viral titres of all fractions as percentage of respective neat viral titres, significant differences were observed for the beads fractions between Ctag-M and Ctag-H compared to Ctag-L LVs (Figure 5.8c). This further indicates that an expression of the mimic similar to that of medium-sorted cells seemed to be necessary and sufficient for optimal magnetic bead capture from viral supernatants.

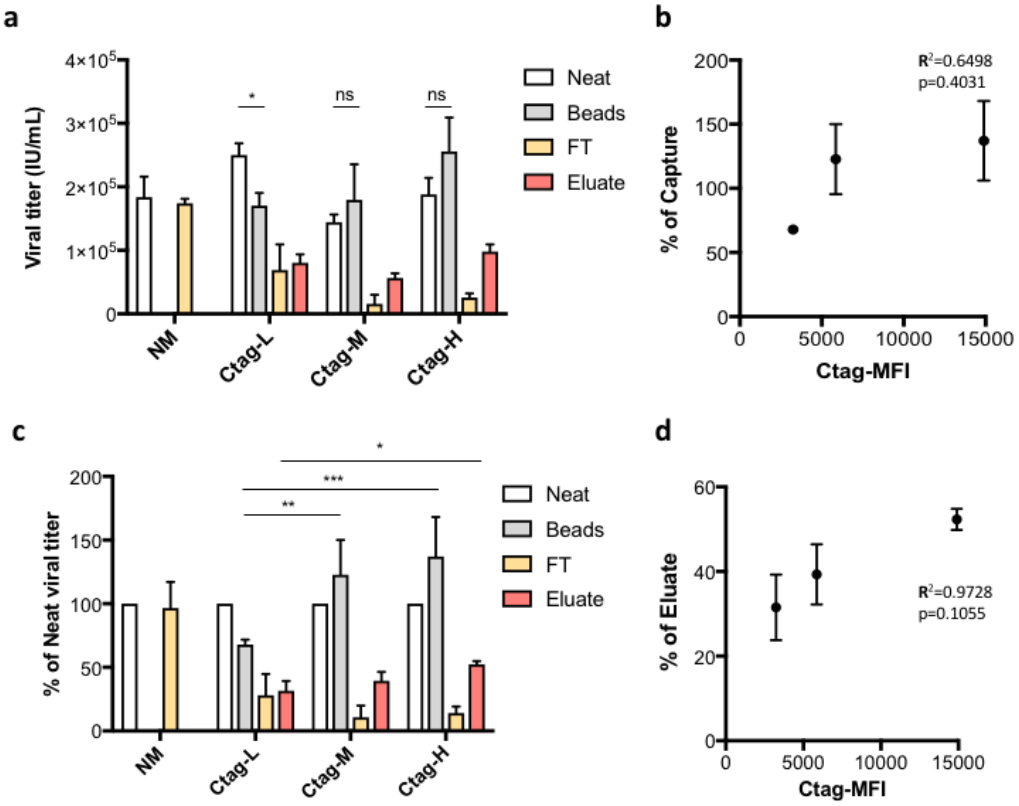

Figure 5.8: Capture and displacement efficiency with differential Ctag expression of LVs. LVs were produced from low (L), medium (M) and high (H) Ctag-expressing 293T cells by transient transfection. VCMs were then subjected to capture of developed methodology by streptavidin Dynabeads. Beads fractions were then incubated with X-vivo^{TM}-15 elution buffer containing 500µM biotin and 0.5% BSA for 2 hours at 4°C. **(a)** Viral titres of process fractions (neat, beads, flow-through and eluate) were determined by infectious assay. **(b)** Correlation between percentage of viral titre capture by streptavidin beads and the mean fluorescent intensity (MFI) of Ctag's expression on sorted L, M and H Ctag-293T cells. **(c)** Process fractions' viral titres plotted as a percentage of their relatively neat fractions. **(d)** Same correlation as (b) but between viral recoveries and Ctag's MFI on packaging cells. All values are presented with ± standard deviation (SD) of three independent experiments (n=3), with ns $p \geq 0.05$, * $p \leq 0.05$, ** $p \leq 0.01$ and *** $p \leq 0.001$. R^2 as coefficient of determination.

This experiment was also conducted to assess whether differential Ctag expression on viral particles would alter the saturated elution recovery rates observed. It was postulated that this may have occurred due to an increased overall avidity of Ctag-LVs. Accordingly, differential expression of mimic would alter virion avidity which may result in altered increased recoveries. Elution

using X-vivo™ supplemented with 500μM biotin and 0.5% BSA resulted in recoveries of 32 ±7.8%, 39 ±7.0% and 52 ±2.5%, for low, medium and high Ctag expressing LVs, respectively (Figure 5.8c). A significant difference in overall yield was only observed between that of Ctag-L and Ctag-H LVs. A positive correlation was also observed between Ctag's expression of sorted cells and their respective viral recoveries from magnetic beads (R_2=0.9728). However similarly to the correlation of capture, the results were not statistically significant (Figure 5.8d). Therefore, viral vectors produced from Ctag-H expressers seemed to result in the highest capture and elution recoveries.

5.6 Biotin-mediated elution in different solutions

The hematopoietic cell culturing medium X-vivo™ supplemented with carrier proteins BSA has been used as elution buffer in most elution experiments thus far into this Chapter. In order to assess the wide applicability of our developed purification methodology, different media commonly used for virus production and cultivation, such as OptiMEM and DMEM, were tested as elution buffers. In this experiment, X-vivo™, DMEM and OptiMEM were tested as elution buffers, either plain or supplemented with 500μM biotin and 0.5% BSA (Figure 5.9). Both NM-LV (4.48 ±0.25 x10^4 IU/mL) and Ctag-LV (4.3 ±0.5 x10^4 IU/mL) viral supernatants were subjected to streptavidin bead capturing as per optimized methodology, for 1 hour at room temperature. Consistently, magnetic bead capture of Ctag-LV resulted in a 3-fold increased viral titre of 1.6 ±0.14 x 10^5 IU/mL (Figure 5.9a). Unlike previous experiments, elution incubations were performed at room temperature for 1 hour, which lead to higher elution recoveries of 67% ±5.6, 58% ±8% and 59% ±9 using X-vivo™, DMEM and OptiMEM, respectively (Figure 5.9b). The presence of BSA in the elution buffer resulted in significant increase of recoveries for all media compared to their respective conditions with only 500μM biotin. Additionally, in line with previous results, in the presence of only biotin, X-vivo™ resulted in superior elution recovery compared to DMEM and OptiMEM, highlighting its endogenous protein composition that seemed to aid in higher yields. These

results indicated that our one-step purification methodology can be applied to various culturing media supplemented with biotin and 0.5% BSA, resulting in ≥60% elution recoveries of infectious LVs.

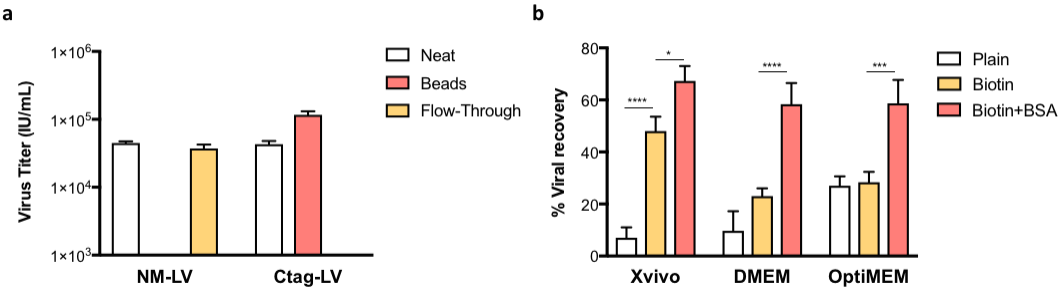

Figure 5.9: Efficient Ctag-LV recovery using different culture media as elution formulation. NM- and Ctag LVs from stock were captured by streptavidin Dynabeads and **(a)** viral titres of process fractions were determined by infectivity assay. Ctag-LV bead fraction was then subjected to elution in three different media: X-vivo^{TM}-15, DMEM and OptiMEM, each supplemented with plain, 500µM biotin and 500µM biotin with 0.5% BSA. **(b)** Viral recoveries of different conditions were determined. All values are represented with ± standard deviation (SD) of three independent experiments (n=3), with * $p \leq 0.05$ and *** $p \leq 0.001$.

5.7 Attempts for Ctag density determination on viral particle surfaces

In our developed purification, LVs are modified by the random and passive incorporation of Ctag onto their viral surfaces. It has been shown that the density of Ctag on LV particles can impact both vector capturing by streptavidin, and its subsequent elution by biotin. However, without determining the number of Ctag molecules on the surface of viral particles, overall avidity of modified vectors for streptavidin may represent a limiting factor for improved elution rates. Moreover, identifying Ctag's density per particle may help understand the underlying molecular mechanisms of capture of vector by magnetic beads, in terms of mechanical interactions of two differential size spheres. Additionally, Ctag's density may also help further advance biotin-dependent elution in a different capture milieu, such as column

based purification. And finally, determining the biotin mimic's density on viral particles may also enable the analysis of viral surfaces in terms of host cell-derived proteins. Technically, determining Ctag's density per viral particle is rather challenging as it would require the analysis of the molecular profile of individual viral vectors' surfaces. Two different strategies were investigated for this purpose; an indirect theoretical method relying on the quantification of Ctag on vector producing cells; and a direct method using electron microscopy of streptavidin gold-labeled LVs.

5.7.1 Mimic quantification on vector packaging Ctag-293T cells

It is common practice to quantify antibodies bound per cell (ABCs) to determine the density of a certain antigen. We reasoned that though streptavidin is not an antibody, this method could be applied to quantify Ctag on the surface of vector producing 293T cells. To that end, BD QuantiBRITE PE beads were used which are designed to estimate ABCs by flow cytometry using PE-labeled antibodies. The principle of this process relies on converting the PE fluorescent intensity of the beads, which have a known number of PE molecule on them, to that of the target cells stained with a PE antibody. And with known PE:antibody ratio, the fluorescent intensity can then be converted from PE molecule per cell to antibodies bound per cell. This process permits the identification of how many molecules are engaged with a given antibody. Since, Ctag-H 293T cells resulted in the highest bead capture and elution of modified LVs, the biotin mimic's surface density on these cells was investigated. Cells were therefore harvested and stained with streptavidin conjugated to PE and expression was determined by flow cytometry along with resuspended lyophilized QuantiBRITE^{TM} PE (Figure 5.10a-b). The beads contain four distinct population with known numbers of PE molecules. After having determined their respective geometric means of fluorescent intensity, a linear regression was plotted of Log10 of PE molecules per bead (information provided from manufacturer) against Log10 of their geometric means (Figure 5.10b). Subsequently, before determining the number of Ctag molecule/cell by the geometric mean of streptavidin expression of eGFP-positive cells, a ratio of 1:1 for streptavidin and PE was confirmed by supplier. However, as a

tetramer we have reasoned that a maximum of two binding sites on streptavidin can be occupied by Ctag peptides expressed on the surface of cells at a given time, thus making the ratio of 1:2 for PE:Ctag-binding sites (Ctag-BS). Accordingly, with a geometric mean of 10217, 49082 Ctag molecules were calculated to be expressed per Ctag-H cell (Figure 5.10c). It was proposed that Ctag expression on LV particles can then be theoretically estimated based on surface area of 293T cells compared to that of LVs, since these particles acquire the cells' lipid bilayer. Therefore, assuming that the diameter of a 293T cell is 15μm and that of LV is 120nm, then the surface of cells is 15639 times larger than the surface of a viral particle. Taking into account the estimated number of Ctag molecules on the surface of Ctag-H 293T cells, each modified Ctag-LV particle would by extrapolation express around 3 copies of Ctag peptides on its surface (Figure 5.10c). It should be noted that this number is based on the assumption that Ctag's density per cells' surface per μm^2 is equivalent to that on viral surface per μm^2. And thus, this result does not represent a quantitative analysis of a mimic's density on viral surfaces. Since we aimed at testing a different method for the determination of the mimic's density on LV surfaces, this result would serve as a theoretically estimated number of Ctag molecule per viral particle.

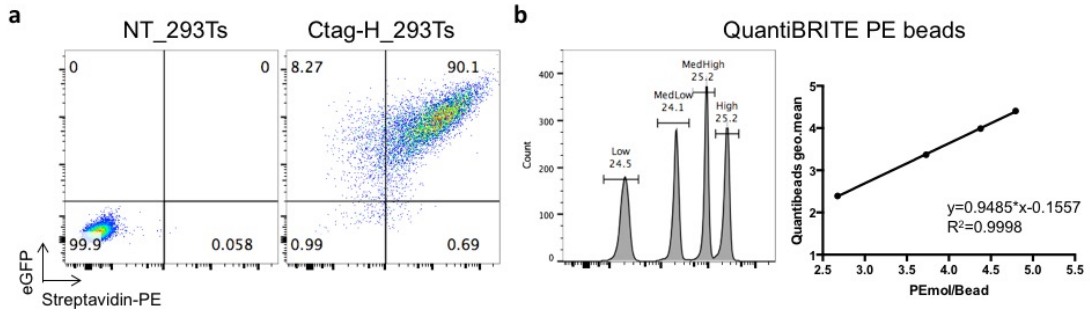

c

Ctag quantification on 293T cells	Quantibright Equation	Log10(GM) = y = 0.9487*x-0.1557
	PE geometric mean of eGFP+Streptavidin+ cells	10217
	Log(10) of eGFP+Streptavidin+ cells	4.009
	X (PE mol/cell)	24541
	Total number of Ctag molecule/cell based on 1:2 ratio of PE:Ctag-BS	**49082**
Ctag quantification on LV by extrapolation	SA of 293T cell (15µm)	706.9 µm^2
	SA of LV particle (120nm)	0.0452 µm^2
	SA ratio of 293T:LV	15639
	Theoretical number of Ctag/LV particle based on SA ratio	**~ 3**

Figure 5.10: Quantification of Ctag on packaging cells. (a) Dot plots of NT and Ctag-High 293T cells stained with streptavidin conjugated to PE. **(b)** Histogram of flow cytometry acquisition of QuantiBRITE-PE beads with defined four populations. Their respective quantitative geometric means (Log10 of their geometric means) were plotted against Log 10 of known amount PE molecules per bead for a linear regression analysis with R^2 as coefficient of determination. **(c)** Calculations conducted for the theoretical quantification of Ctag per LV particle by extrapolation of its quantification on Ctag-H-293T cells. Surface areas (SA) were calculated based on SA = $4*\pi*r^2$, with r as radius.

5.7.2 Viral detection of Ctag-LV by scanning electron microscopy

Viral vectors such as LVs are commonly visualized and characterized using electron microcopy (EM) (Goldsmith and Miller, 2009; Earl et al., 2013). Given their small size, we attempted to visualize our Ctag modified viral particles by scanning electron microscopy (SEM) which, unlike transmission EM, focuses on the surface of samples and their compositions. Moreover, streptavidin conjugated to gold particle can be used to detect Ctag molecules on modified vectors. Ideally, we wanted to visually determine Ctag-LV purified from our developed method. However, since viral particles acquire Ctag's expression on their surfaces while budding from producing cells, the aim of this experiment was to visualize the surface of modified vectors, regardless of the method of

purification. In order to increase viral titre, which is recommended for particle detection using SEM, both NM- and Ctag-LV stocks were purified by ultracentrifugation on a 20% sucrose cushion and concentrated 100X in OptiMEM. First, control and modified LVs were pseudotyped with RDpro and sucrose purified vectors resulted in a 23-fold increase in viral titres for both NM and Ctag-LVs, with 2.54 ±-.18x10^6 IU/mL and 1.26 ±0.62 x10^6 IU/mL, respectively (Figure 5.11a). However, it was then decided to use VSV-g pseudotyped LVs due to its relative stability to freeze-thaw cycles and increased viral titres compared to RDpro. Correspondingly, purification of VSV-g pseudotyped vectors resulted in 18 and 27-fold increases in viral titres for NM- and Ctag-LVs with 3.97 ±0.37 x10^7 and 6.87 ±0.36 x10^7 IU/mL, respectively. Next, the binding of thawed purified VSV-g vectors to streptavidin magnetic beads was demonstrated before staining with gold-labeled streptavidin (Figure 5.11b). Subsequently, samples were processed for negative staining and examined by SEM to determine whether intact viral particles can be visually detected also before streptavidin-gold staining. This was carried out on frozen-thawed samples at NIBSC with the very kind help of Dr. Kirsty MacLellan-Gibson. Examination of both specimens resulted in the detection of electron dense images of intact particles of around 130-150nm for both NM- and Ctag-LV, appearing as whole viruses (Figure 5.11c). Internal structures of particles resembling viral capsids can be seen in both LV images. Moreover, both cores were observed to be surrounded by a membrane with protruding surface structures that resemble trimeric envelop glycoproteins in a ‘lollipop’-shape. These results indicated that thawed purified LVs resuspended in OptiMEM resulted in the visual determination of intact viral particles. Subsequently, thawed samples were then stained with streptavidin-gold particles prior of negative staining for SEM for 1 hours at room temperature with gentle shacking to keep mixture in suspension (Figure 5.11d). As expected, whole particles were observed by SEM for both samples. Moreover, unlike NM-LV, 3 streptavidin gold particles were detected by naked eye, lying in close proximity to Ctag-LV viral particle. However, due to the significant background binding of streptavidin-gold observed, the former observation was void. Background binding may have been specific for free biotin present in

OptiMEM or non-specific binding to the copper grid. Consequently, no further analysis could have been taken for Ctag's expression on these observed particles. Nonetheless, SEM allowed the visual determination of both modified and control viruses with similar morphologies.

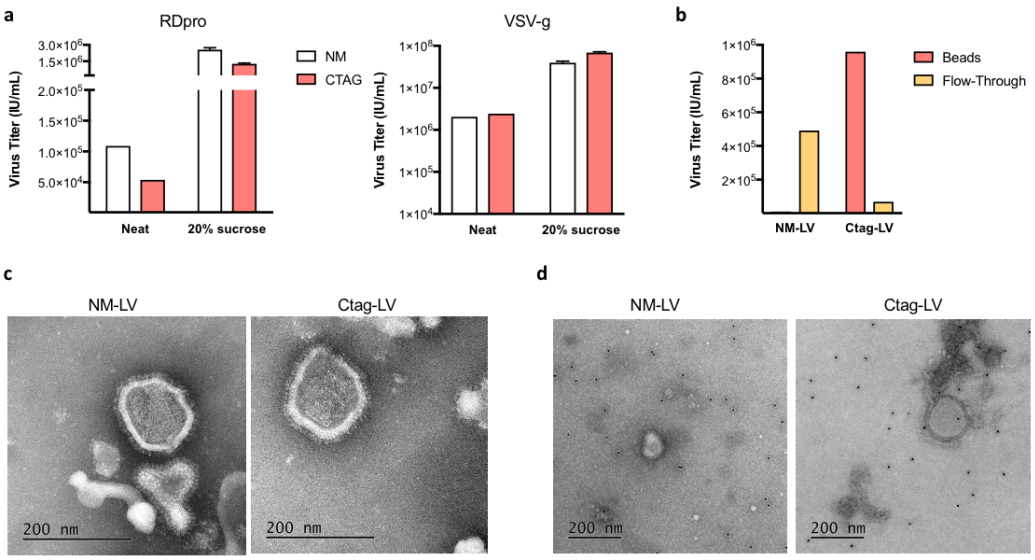

Figure 5.11: Scanning electron microscopy of sucrose-cushion purified LVs. (a) NM- and Ctag-LV pseudotyped with RDpro and VSV-g were purified by ultracentrifugation on 20% sucrose cushion and assayed for viral titres. **(b)** Purified VSV-g pseudotyped NM- and Ctag-LVs were thawed and assayed for streptavidin Dynabeads capture. Sucrose purified vectors were negative stained and **(c)** Negative stain of NM- and Ctag-LV samples and analyzed by scanning electron microscopy (SEM). **(d)** SEM analysis of vector samples stained with streptavidin-colloidal gold conjugate (~10nm).

5.8 Discussion

In this Chapter, we have demonstrated efficient displacement of bead-captured Ctag-LV by competitive elution using free biotin, resulting in recovery of ≥ 60%. This required the presence of protein additives such as BSA and can be achieved using different cell culture formulations. We have also demonstrated that passive Ctag incorporation does not alter physical morphology of vectors allowing wide applications of this developed purification. It should be mentioned that to the best of our knowledge, purification of any viral vector using a biotin mimic and its natural receptor, albeit it avidin or streptavidin, has not been reported yet. Therefore, no body of work in the literature exists to compare this chapter's results. Elution of metabolically biotinylated AAV from monomeric avidin has been reported (Parrott et al., 2000). However, given the differences in their physical properties and levels of fragility, purification methodologies between AAV and LVs cannot be readily interchanged.

A major limitation in the early elution experiments preformed in this chapter was the quantification of only infectious particles after elution and not of physical particles. The effect of bead-bound vectors resuspension in elution buffers on physical particles should have been determined by quantifying total physical particles. This in turn limited the investigation into the loss of titre observed in elution experiments performed in plain media supplemented with high concentration of biotin. Nonetheless, as the ultimate aim of our methodology was the purification of infectious LVs, assessing infectivity of overall yield was our main end point during the development of this desorption. It was postulated that excess concentrations of biotin may have caused some toxicity on viral particles, thus impairing their infectivity. On cells however, concentration as high as 50mM of biotin were reported as non-toxic for T cells with no evidence of change in cellular function or toxicity (Knabel et al., 2002). In line with these results, no toxicity in terms of decrease in infectious titre was observed with the addition of up to 15mM biotin in plain DMEM, on both modified and unmodified viral vectors. Therefore, the loss of infectivity

observed during elution in plain DMEM does not seem to be caused by high concentration of biotin.

Alternatively, this loss may have been caused by viral aggregation. The presence of viral aggregates is a common product-related impurity found in viral supernatants. Aggregates can be formed by covalent or non-covalent binding, such as disulphide bonds; or weaker forces such as Van Der Waals, hydrogen bonding or electrostatic interaction. The causes and extent of viral aggregation is not well understood but it is known that conformational changes and chemical modification may stimulate protein multimerisation (Mahler et al., 2009). Large aggregates were detected in Ctag-modified LVs eluted in the presence of 0.5% BSA and 500μM biotin by Nanosight analysis. These aggregates may have either been captured from starting viral material or were formed during the process. The former theory may be attribute to the fact that aggregates display larger number of Ctag molecules accessible for multipoint streptavidin binding. This theory has been postulated for the purification of viral aggregates using AEX, in that aggregates possess higher number of negatively charged molecules i.e. aggregates bind anion exchange resin more strongly than single viruses (Segura et al., 2013). The latter theory of aggregates forming during purification process may be attributed to the high concentration of proteins in a phenomenon called macromolecular crowding. Its influence is not well understood for viral vectors. However, crowding is a nonspecific force and has been shown to cause the formation of macromolecular complex or insoluble aggregates (Tabaka et al., 2014). Although increase in protein concentration has been shown to be directly related to the occurrence of aggregates (Treuheit et al., 2002), the addition of 0.5% BSA to biotin rescued infectivity of eluted Ctag-LVs. In line with these results, BSA has been shown to mediate a significant increase in protein catalytic activity by crowding-promoter stabilization (Kuznetsova et al., 2014). Moreover, stabilization of viral vectors for vaccine for examples has been done through formulation and addition of albumin have been commonly used for vaccine stabilization (Brandau et al., 2003). Therefore, it could be proposed that the lack of vector stabilization seemed to have caused the loss of

infectivity observed. This stabilization may be related to non-specific interactions with the surface of the containers thereby preventing vector damage; which would explain the loss of infectivity observed during elution in the absence of albumin proteins, regardless of the type of container (glass or polystyrene). The investigation for optimal formulation for LVs in the literature is an uncharted area, possibly due to the lack of commercialized treatments using LVs. Nonetheless, elution using the commonly used Lonza's X-vivo™ medium for viral manipulation (Merten et al., 2011; Aiuti et al., 2013) resulted in increased infectious vector recovery compared to plain DMEM. This in turn may highlight the importance of media formulation as X-vivo™ contains a mixture of proteins and sugars which may have impacted vector stabilization during biotin-mediated displacement of Ctag from streptavidin resin. This result is in line with Carmo et al., (2008) which demonstrated that, unlike γ-RVs, LVs increased stability required the addition of both human serum albumin and a protein solution derived from bovine serum. These results further highlight the difficulty in LV stabilization and specifically for elution reactions that may be prone to vector damaging caused by aggregation, non-specific interactions or macromolecular crowding.

In this Chapter, we have developed an efficient viral purification using gentle elution with excess biotin which competes against Ctag for streptavidin binding pockets. This competitive elution was efficient resulting in overall yields of ≥60%, using biotin supplemented with BSA. It is interesting to note that preliminary elution recoveries with decreasing concentrations of biotin from 15mM to 1.5nM were very similar, indicating a possible avidity effect resulting in small differences in elution recoveries, in the presence of 100-fold increases in biotin concentration. Although biotin has ~ 8 orders of magnitude higher kinetics than Ctag, the simultaneous binding of several Ctag to streptavidin may have led to this avidity effect; leading to a synergistic affinity of all the interacting bonds formed between mimic and streptavidin. Individually, each binding interaction can be displaced by biotin. But when many of these interactions are present at the same time, the release of one binding site does not cause the release of bound vector for elution from resin. This synergistic

avidity effect can have drastic effects of overall affinity with up to 1000-fold increase conferred with double the number of binding sites (Metzner and Dangerfield, 2011). However, it has been suggested that this situation changes entirely in the presence of a competitive binding protein (Schmidt et al., 2013). In its presence, any interaction between Ctag and streptavidin that dissociates is unlikely to re-associate as biotin should immediately block streptavidin's binding sites. With that in mind, it may be postulated that the incomplete recovery of total Ctag-LV titre captured by streptavidin may be due to insufficient incubation times of elution reaction. Therefore, longer elution incubation period may allow for the displacement of all Ctag interactions with streptavidin by biotin, leading to complete viral recovery. Accordingly, incubation of elution at higher temperature resulted in higher yield due to the higher rate of displacement reactions occurring at room temperature compared to 4°C. Alternatively, incomplete elution of Ctag-LV from streptavidin beads could be caused by non-specific binding of vectors to streptavidin magnetic beads. This in turn would not adhere to biotin-mediated competitive elution from streptavidin, resulting in incomplete recovery of viral titres. However, non-specific binding of Ctag-LV to streptavidin magnetic beads has not been detected. Control unmodified LVs did not exhibit any non-specific binding to streptavidin beads either by non-specific protein interactions or physical trapping of vectors in the porous surface of magnetic beads (Chapter 3). Moreover, pre-treatment of these beads with biotin was shown to block Ctag-LV capture, indicating that both Ctag and biotin bind to the same binding pocket on streptavidin tetramers (Chapter 4). Thus, the only possibility of non-specific binding may be mediated by the biotin mimic itself or the CD8α stalk it is expressed on. However, these two options are unlikely to have occurred given the results presented thus far. Nevertheless, if increased incubation time for biotin-mediated elution does not increase the recovery of bead-bound vectors; then non-specific binding can be tested by expressing a peptide-less CD8α stalk on the surface of LVs and assessing their non-specific capture to streptavidin magnetic beads.

During the course of these experiments, it became apparent that determining the number of Ctag interaction per viral particle would have allowed better insight into the incomplete, yet sequential, elution observed for bead-bound Ctag-LVs. However, this is rather difficult to achieve as it involved quantifying the number of given molecule on the surface of each viral particle; which with its random incorporation, does not follow a uniform distribution. Nonetheless, in an effort to characterized the required density of Ctag on viral particles, its expression was altered indirectly by manipulation of Ctag-engineered VPC. Interestingly, Ctag's density per virions seemed to impact the efficiencies of both capture and elution, with the highest expression of Ctag resulting in both significant capture and highest overall yield, compared to lower mimic expressions. Moreover, although a significant difference in recoveries between the highest and lowest Ctag expression was observed; the difference in viral recoveries were not statistically significant. This could have been further interpreted if Ctag's density on viral particles was known. First, we attempted to estimating its density by quantifying Ctag's expression on VPCs by streptavidin and then theoretically proposed a density on viral particles based on surface areas. However, streptavidin's tetrameric nature added another layer of theoretical assumptions to our quantification based on surface areas. And thus, the use of monomeric or monovalent streptavidin may have offered a superior analysis of Ctag's density on vectors packaging cells as it ensures a 1:1 binding interaction ratio between Ctag and its ligand. Nevertheless, our theoretical assumption proposed 3 Ctag molecules expressed per viral particles. Furthermore, in a second effort to quantify Ctag's density on the surface of viral particles, scanning electron transmission of streptavidin-gold labeled LVs was performed and coincidently 3 streptavidin gold particles were visually detected in close proximity of Ctag-LV viral particle. Although this fits in our theoretical model of Ctag density, this cannot be concluded due to streptavidin's high non-specific background. Nonetheless, Ctag modification of viral vectors did not seem to alter vector morphology.

In this Chapter, we have established the gentle elution of streptavidin captured Ctag-LV by biotin-mediated competition, in a one-step protocol. In this

preliminary body of work, high recoveries were achieved with different elution formulations supplemented with biotin and protein additives. Due to its highly selective mechanism in vector capturing, it could be postulated that eluted vectors may represent higher levels of purity in terms of product and process-related contaminants compared to other current non-specific downstream processing techniques.

Chapter 6 Product characterization of concentrated and purified Ctag-LVs

6.1 Overview

In previous Chapters, the reversible binding of modified LVs to streptavidin in the presence of biotin was demonstrated with recoveries ≥ 60% achieved in a one-step process. The composition of purified vectors is as equally important as the recovery for overall efficacy of downstream vector processing. Thus, in this Chapter Ctag-purified LVs are characterized in terms of impurities commonly detected during vector manufacturing.

6.2 Introduction

LV products intended for human clinical trials must be characterized in terms of both infectious titre as well as product and process-related impurities to guarantee product safety, quality and efficacy. The high degree of complexity of viral vectors, in terms of their biology, represents a major challenge for vector product characterization. Nonetheless, various methods have been employed to both quantitate LVs as well as characterize their composition in terms of purity.

6.2.1 Quantitation methods for LVs

LVs can be quantified by several methods resulting in distinct measurements. First, total viral particles present in a vector product can be quantified. This is most commonly achieved by the measurement of viral gag proteins, such as p24 capsid protein for HIV-1-based vectors or p30 for MLV-based vectors, by an enzyme-linked immunosorbent assay (ELISA). Although, this assay is simple, fast and easy to run, it cannot distinguish between intact, infectious particles and free proteins. In addition, it relies on calculating particle numbers based on a conversion equation assuming a defined number of proteins per virion. As presented in Section 5.5.3, new technologies have also been

developed now to count physical viral particles and are commercially available, such as the nanoparticle tracking analysis (NTA) using Nanosight or VirusCounter devices. (Heider and Metzner, 2014). The former method enables the determination of viral particle concentrations, as well as provides physical characteristics such as median particle size. A certain concentration of particles per mL is however required for such single particles measurement, for example between 10^7 and 10^9 particle/mL for Nanosight analysis. Moreover, presence of background particles or host cell debris have been shown to represent limiting factors for single particle analysis as these are included within the quantification for example cell derived exosomes (Mironov et al., 2011). Thus, similarly to p24 measurement, single particle tracking technologies result in an overestimation of the infectious titres as these methods cannot discriminate between physical and infectious viral particles (Gutiérrez-Granados et al., 2013).

Second, functional (i.e. infectious or transducing) particles can be quantified. The determination of the functional (or infectious) titre, which is the number of IP (or TU) per mL, can be achieved by the limiting dilution of vector followed by transduction of target cells for the measurement of marker protein expression, with eGFP being the most commonly used (Geraerts et al., 2006). The use of this method allows the quantification of viral particles that can bind their receptor on target cells and induce viral entry for vector genome integration i.e. transducing particles. However, to fully elucidate this method its biological mechanics need to be examined. In order to infect, viral vectors must first travel the distance to target adherent cells, which is governed by their diffusion rates in culturing solutions. However, the efficiency of infectivity is depicted by the half-life of each vectors. For example the half-life at physiological temperatures is between 6-18 hours for different strains of HIV-1 (Layne et al., 1992). Considering that the depth of culturing medium of adherent cells is usually several millimeters, it could be postulated that a small portion of vectors would reach target cells for infectivity during its half-life, thus underestimating the functional titre (Klasse, 2015). Another important parameter to consider while using this method is the permissiveness of target

cells for transduction by viral vectors. This is governed by (i) transducing conditions used that facilitate target cell and particle interactions such as the use of Polybrene, retronectin or spinoculation; and (ii) mainly by the envelope glycoprotein chosen to pseudotype vectors and its receptor density on target cells. Accordingly, viral glycoprotein's receptor density depicts the degree of permissinvess for each cell type towards LVs. This concept interestingly is highlighted by the observation that LVs pseudotyped with measles virus glycoproteins were able to efficiently transduce previously LV-resistant quiescent lymphocytes, due to the high surface expression of measles envelope's receptor proteins CD46 and SLAM (Frecha et al., 2011). Due to these varying factors, it is important to mention that comparison between published titration protocols is complicated due to the differences in pseudotyping envelope, target cell type, cell density and inoculation time and conditions.

And finally, vector product can be quantified by determining the amount of viral genome in the viral supernatant or integrated proviral DNA copies by quantitative polymerase chain reaction (qPCR). This method when applied to the viral supernatant however leads to the overestimation of viral titre as it includes non-infectious particles i.e. bald particles, that do not express viral envelope, as well as free-floating RNA genome in vector material. Therefore, its use has been limited to high throughput screening of vector titres during producer cell line development for example (Ansorge et al., 2010).

6.2.2 Quality analysis of purified LVs

As discussed in section 1.3.4.1, vector products are composed of both process- and product- related impurities, which are summarized in Figure 1.5. Product-related impurities mainly consists of defective particles (envelope-less i.e. bald, damaged, inactive and aggregates) and free viral proteins; whereas process-related impurities are contaminants derived from vector production such as host cell proteins (HCP) and host cell nucleic acids. It should be noted as the viral envelope of virions is composed of the host cell membrane, host cell protein is also part of the product. Due to the infancy of LVs as gene

therapies as well as the confidentiality of manufacturer data, insufficient information on vector product purity is available in the public domain. Nonetheless, different methods are used to evaluate vector quality and measure both product- and process-related impurities present in viral stocks.

A useful indicator of product quality is a derivative calculation based on the ratio of transducing unit to total physical particles (TU:PP), termed infectivity. Moreover, determining the levels of cell-culture process impurities are important parameters for vector purity. Residual levels of host cell protein and DNA (process-related) or plasmid derived DNA (product-related) are routinely measured in final vector product intended for clinical use. Nucleic acid impurities such as residual packaging plasmid DNA can quantified by quantitative PCR using designed primers against relevant sequences in helper plasmids (Sastry et al., 2004; Yang et al., 2012). Host cell-derived DNA impurities can be detected and quantified in viral product by using a fluorescent nucleic acid stain such as PicoGreen® (Bandeira et al., 2012). As for proteins, different method have been used for total protein analysis of LVs such as polyacrylamide gel electrophoresis and protein staining (Baekelandt et al., 2003). Moreover, specific host cell-derived proteins can be detected and quantified using an ELISA, in which specific detection antibodies were generated by animal vaccination using host-cell lysates (Merten et al., 2016).

As discussed in Section 1.3.4.1, the removal of these contaminants is essential to vector product efficacy as several studies have reported adverse effects and reduced transduction efficiencies when poorly purified vectors have been used *in vivo* (Scherr, 2002; Baekelandt et al., 2003). Moreover, although LVs possess significant adjuvant activities compared to other vectors (Breckpot et al., 2010; Rossetti et al., 2011), contaminants present in vector products have also been reported to cause an anti-viral immune response (Pichlmair et al., 2007). Accordingly, due to the potential immunogenicity of HCP, regulatory agencies require their specific quantification in final gene therapy products (FDA Guidance for Industry, 1998). Taking these factors into consideration along with the added risk of immunogenic nature of residual DNA, these

parameters further emphasize the need for impurity removal by downstream processing steps for any vector product intended for human applications. Therefore, the strength of a downstream processing technique lies in its ability to eliminate vector contaminants while maintaining infectivity, without the need of additional processing steps such as nucleic acid digestions or polishing steps.

6.3 Aims

In this chapter, we assessed the potential of our purification method to efficiently clear contaminants present in final vector product. We sought out to characterize the composition of eluted Ctag-LV from our developed one-step purification in terms of both product and process-related impurities. Therefore, the aims of this chapter are:

- Demonstrate concentration of eluted Ctag-LV by simple volume reduction during desorption from streptavidin beads
- Determine the TU:PP ratio for quality assessment of eluted vectors
- Measure both nucleic acid and HCP concentration in final eluted vector product.

6.4 Concentration of eluted vectors from streptavidin resin

The development of any downstream processing strategy for viral vectors should allow for vector concentration. To demonstrate this with our methodology, Ctag-LV from stock was subjected to capture by streptavidin Dynabeads, followed by elution in 50X volume reduction of the starting material, using 500μM biotin with 0.5% BSA in OptiMEM. Concentration of eluted Ctag-LV was theoretically possible throughout this Chapter due to the ease in manipulation of elution volume post-capture by magnetic beads. Consistently, almost all Ctag-LV viral particles were captured on streptavidin Dynabeads with increased transduction efficiencies on target cells resulting in 1.35-fold higher viral titre (4.89 ±0.55 $x10^4$ IU/mL) compared to starting supernatant (4.17 ±0.04 $x10^4$ IU/mL) (Figure 6.1a-b). As anticipated, elution of Ctag-LV from beads by resuspension in biotin-containing elution buffer at 50X volume reduction, resulted in 26-fold increase in viral titre of eluate (1.09 ±0.04 $x10^6$ IU/mL), which represented 60% of starting viral particles (Figure 6.1c).

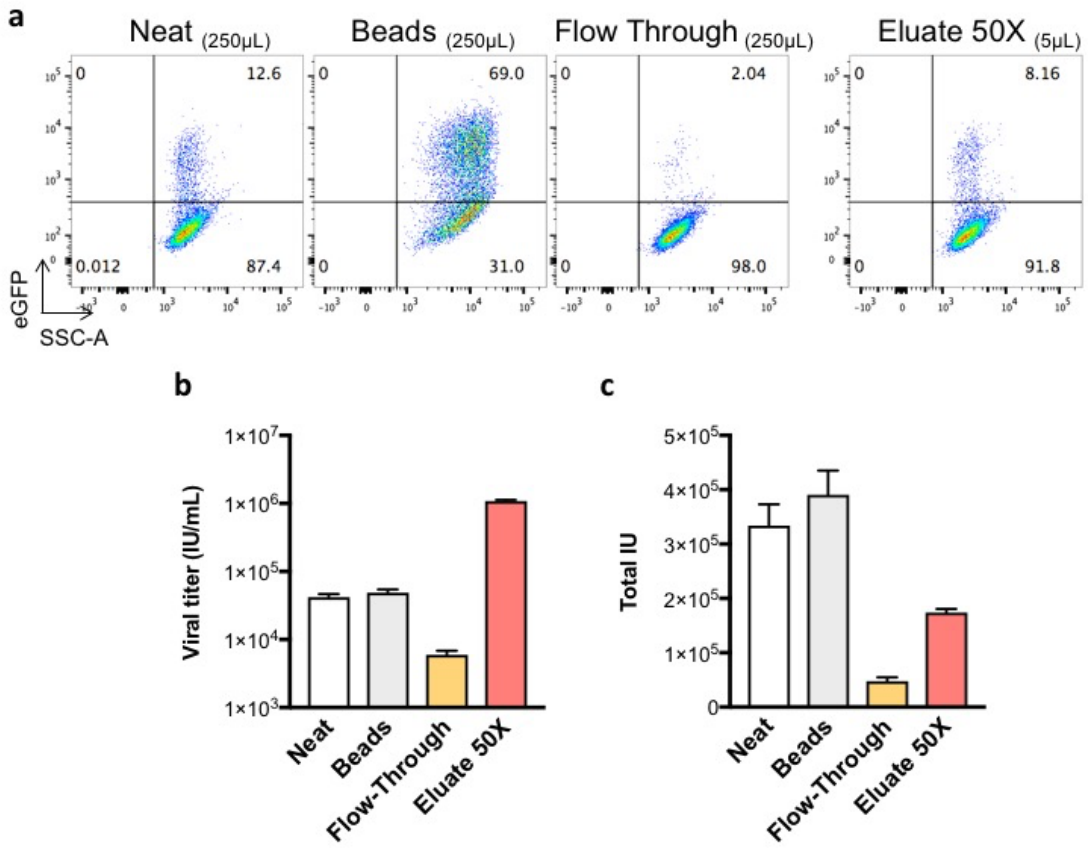

Figure 6.1: Concentration and purification of Ctag-LVs. Ctag-LV viral supernatant from stock was subjected to streptavidin Dynabeads capture followed by biotin-mediated elution using OptiMEM with 500µM biotin and 0.5% BSA in a 50 times volume reduction (50X) of eluted vectors. **(a)** Dot plots of eGFP vs SSC-A represent cells transduced with the different collected fractions of the purification. **(b)** Viral titres **(c)** total infectious unit (IU) are presented for all fractions. All values are represented with ± standard deviation (SD) of three independent experiments (n=3).

6.5 Purity characterization of eluted vectors

In any viral purification method, the purity of final vector product is an important parameter to consider. High purity in terms of removal of both process and product-related impurities is a prerequisite for overall efficacy of purified vectors. Since our developed purification selectively captures Ctag-LV from surrounding supernatant and recovery from matrix is selective by biotin binding competition, it could be postulated that eluted modified vectors should not contain the different impurities usually detected in vectors purified by current methods.

6.5.1 Product-related impurities analysis of infectious particles to physical particles ratio

The ratio of TU/PP is generally accepted to determine the quality of any vector product. The quantification of LV physical particles is largely performed by p24 ELISA. This type of measurement however not only accounts for free capsid proteins and infectious particles, but also for nonfunctional/empty particles and immature particles, which are not capable of integrating into target cells. In order to quantify viral particles only (functional or not) and exclude free p24, the lentivirus-associated p24 ELISA kit from Cell Biolabs was used to determine the ratio of TU/PP. This kit enables the separation and quantification of virus-associated p24 rather than p24 by a proprietary technology. As free p24 is discarded with this kit, and since our purification selectively captures all Ctag-expressing viral particles, it could be assumed that there shouldn't be a significant difference in the ratios of TU:PP between starting supernatant and eluted vectors. To test this, neat and 50X eluate from the experiment performed in Figure 6.1, were thawed and subjected to both infectivity assay for IU/mL and p24 ELISA kit for PP/mL (Figure 6.2a-b). Unlike freshly determined infectious titre of 50X eluate sample, one round of freeze-thaw decreased the transducing titre by almost 2 folds with 4.29 ±1.0 $x10^5$ IU/mL, which was still higher than that of the neat sample (6.59 ±0.6 $x10^4$ IU/mL). These results suggested titre loss by freeze-thawing cycle for RDpro to be significant. Nonetheless, the physical particle titre was quantified by determining the amount of p24 (ng/mL) in both samples based on p24 standard curves and after subtraction of corresponding background of virus containing media (i.e. DMEM for neat and OptiMEM for eluate). Unfortunately, the neat sample was assayed once whereas the purified sample was assayed three times, resulting in 10 ng/mL and 31 ±4 ng/mL of p24, respectively. There are approximately 2000 molecules of p24 per lentiviral particle (Scarlata and Carter, 2003), therefore based on the following equation:

$$1\ LV\ physical\ particle = \frac{2000\ x\ 24\ x\ 10^3}{6\ x10^{23}}\ of\ p24 = 8\ x10^{-5}\ pg\ of\ p24$$

$$1\ ng\ p24 = 1.5\ x10^7\ LV\ pysical\ particles$$

Accordingly, the quantification of physical particles by p24 ELISA resulted in a 3-fold increase between physical titre of purified eluate (3.89 ±0.6 x10^8 PP/mL) compared to neat sample (1.25 x10^8 PP/mL). Therefore, there was a 2-fold increase in the TU:PP ratio between starting vector material and purified eluate with 1:1896 and 1:907, respectively. And although this difference was not statistically significant, due to the lack of triplicate determination for the neat fraction, it demonstrates the purified vector is of equal if not higher quality with regards to infectivity.

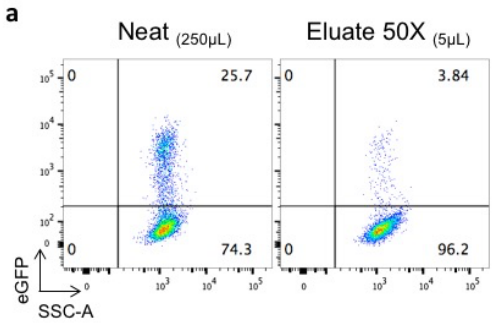

b

Fraction	IU/mL	p24 ng/mL	TU:PP ratio
Neat	6.59 ±0.6 x 10^4	1.25 x 10^8	1 : 1896
E50X	4.29 ±1.0 x 10^5	3.89 ±0.6 x 10^8	1: 907
Concentration factor (E50X/Neat)	6.5	3.11	

Figure 6.2: Quantification of physical and infectious particle of purified concentrated Ctag-LV. (a) Dot plots of eGFP vs SSC-A represent cells transduced with thawed viral supernatants of starting material (neat) and eluted vectors (Eluate 50X) to determine infectious viral titres (IU/mL). Given the 50X volume reduction of eluate, an appropriate volume of vector of 5µL was chosen for titration and the experimental standard for of 250µL of neat was tested. **(b)** Comparative analysis of IU/mL and physical viral titre by quantifying p24 ng/mL in both neat and concentrated eluate (E50X). Transducing unit:physical particle (TU:PP) ratio are presented for each fraction. Concentration factor between the fractions are presented for both infectious and physical titres. All values, except for neat p24 ng/mL, are presented ± standard deviation (SD) of three independently purified eluate samples for E50X (n=3).

6.5.2 Process-related impurities: analysis of host cell DNA and proteins

6.5.2.1 Undetectable host cell-derived nucleic acid in eluted vectors

Another important purity parameter to determine was the level of host-cell derived DNA contamination. Given the specificity of our vector purification, it could be anticipated that host-cell derived nucleic acid would not be present in our eluate vector, as DNA does not exhibit any binding to streptavidin. Accordingly, dsDNA concentrations were determined for the eluted LV samples from Figure 6.2 immediately after elution by PicoGreen® assay kit, that can detect down to 1 ng/mL of nucleic acids. No traces of dsDNA were detected in the concentrated eluate, indicating a minimum 3-log decrease in quantified dsDNA contamination from starting material which contained 108 ng/mL of dsDNA (Figure 6.3a-b). Since dsDNA does not exhibit non-specific binding to streptavidin, unlike AEX anion ligands, the majority of dsDNA that was present in the starting viral supernatant was found in the flow-through fractions. Thus, this result demonstrated the high degree of specificity of our purification method to selectively capture modified viral particles resulting in the absence of detectable host-derived DNA contamination.

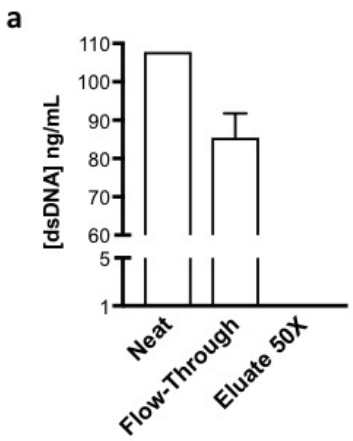

b

Fraction	% [dsDNA] Reduction
Neat	0
Eluate	>99.1 ±0

Figure 6.3: Quantification of DNA contamination in purified vectors. (a) Collected fractions from our purification (neat, starting viral supernatant; flow-through fraction (FT) and concentrated eluate 50X) were assayed for dsDNA presence by PicoGreen®. **(b)** Percentage of dsDNA concentration reduction compared to starting material (neat) are presented. Values for flow-through and purified eluate are presented ± standard deviation (SD) of three independent experiments (n=3).

6.5.2.2 Minimal host cell-derived protein (HCP) contamination in eluted vectors

HCP contamination represents another major process-derived impurity during the production of LVs. Their removal is prerequisite for any viral purification process for vectors intended for human therapeutic application. It should be kept in mind however, viral particles themselves contain host cell-derived proteins on their viral surfaces. Due to the specificity of our affinity purification of Ctag-LVs, and similarly to the reduction of nucleic acids, it could be suggested that the enrichment of Ctag-expressing particles would be greater, which in turn leads to lower amounts of HCP. To test this, purified Ctag-LV samples from Figure 6.2 were compared to starting vector supernatant by first evaluating their protein content by silver stain analysis (Figure 6.4). Culturing medium (plain DMEM) and elution buffer OptiMEM, with elution excipients biotin and BSA, were included as controls to account for their respective endogenous proteins. Protein profiles of neat and flow-through fractions were identical, indicating major protein clearance during streptavidin capture. The elution buffer resulted in dense protein profile with a heavy band representing likely BSA at 66.5 kDa. Purified eluate samples were assayed at different dilutions in ddH_20 (1:10, 1:50 and 1:100) with a protein profile similar to that of the elution buffer with detectable BSA band at 1:100. This staining should have included elution buffer diluted at 1:100 for appropriate protein comparison to purified eluates. Nevertheless, the most abundant detectable protein around 65kDa in the eluate sample at 1:100, seemed to represent BSA which is present in all OptiMEM samples supplemented with it, alone or with biotin. Although not quantitative, this method of protein content staining suggested efficient protein clearance from starting vector material compared to purified vectors.

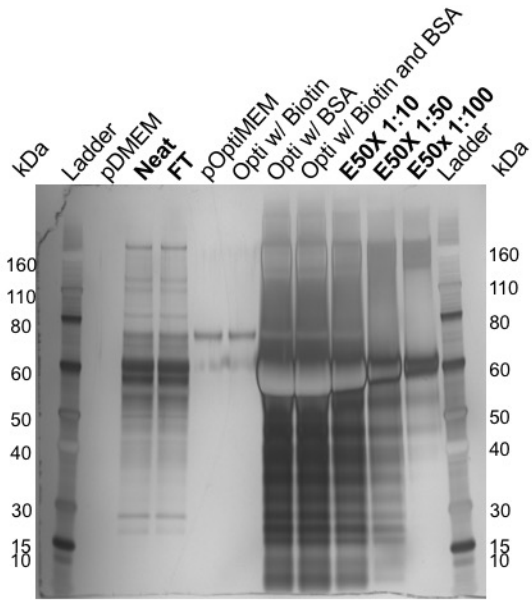

Figure 6.4: Analysis of protein content in purified Ctag-LVs. Silver staining of collected samples from purification of neat, flow-through and eluted vectors in three dilutions (in bold). All culture media and buffer generated were included as controls with plain DMEM (pDMEM), plain OptiMEM (pOptiMEM), OptiMEM with 500µM biotin (Opti w/ biotin), OptiMEM with 0.5% BSA (Opti w/ BSA) and elution buffer (Opti w/ biotin and BSA). Lanes on the edges of the gel were loaded with protein ladder (kDa).

HEK293 host cell proteins were also quantified in starting supernatants and purified viral vectors by immunoreactivity using HEK 293 HCP ELISA (Figure 6.5a). A control consisting of cellular supernatant from NT-293T cells was included along the starting and purified viral vectors of Figure 6.2. The transfection of cells to produce transient LVs resulted in an increase in host derived proteins detected in viral supernatant with 1856 ±56 ng/mL of HCP compared to 1139 ±274 ng/mL of HCP quantified in non-transfected 293T cells. This increase could have resulted from the HCP detected on viral particles but more likely, represents the cellular debris due to the transfection and viral production of HEK293T cells. In this first experiment, in order to quantify HCP, samples were diluted to fit within the standard curve. Protein quantification of purified Ctag-LV from our purification resulted in undetectable amounts of protein (<100ng/mL) at the highest dilution of 25X. Therefore, the immunoreactivity was repeated with lower dilutions (Figure 6.5b) which

resulted in 1468 ±181 ng/mL of HCP detected in starting viral supernatant compared to 12 ±4 ng/mL detected in purified Ctag-LV eluate. Therefore, our developed affinity purification resulted in a significant 122-fold reduction of host cell proteins (p=0.0005) in a one-step viral purification process.

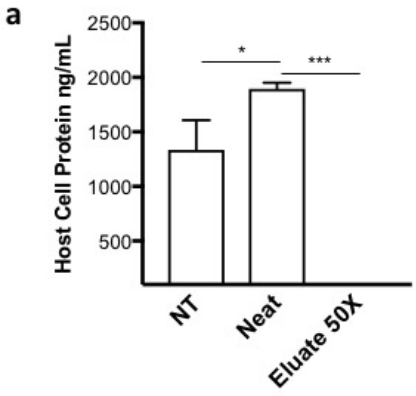

Fraction	Total immunoreactive HEK293 HCP ng/mL
NT	1334 ±273
Neat	1896 ±56
Eluate	< 100ng/mL

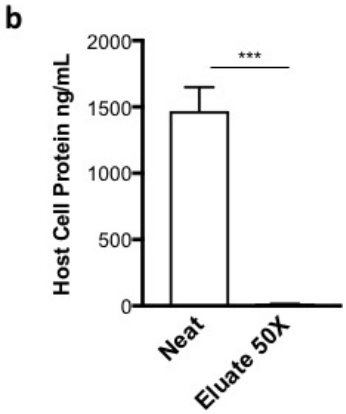

Fraction	Total immunoreactive HEK293 HCP ng/mL
Neat	1468 ±181
Eluate	12 ±4

Figure 6.5: Analysis of HCP in purified Ctag-LVs. (a) Total immunoreactive HEK 293 host cell protein (HCP) detected in cell supernatant of non-transfected 293T cells (NT), starting viral supernatant (neat) and purified Ctag-LV (eluate 50X). Samples were diluted 25X, 50X and 100X for assay using sample diluent buffer. **(b)** Immunoreactivity was repeated for neat and purified vector samples, with smaller dilution for eluted Ctag-LVs of 4X, 6X and 8X. All values are presented ± standard deviation (SD) of triplicate determinations with * $p \leq 0.05$ and *** $p \leq 0.001$.

6.6 Discussion

In this Chapter, we have demonstrated that our one-step vector purification enables (i) ease in vector concentration and (ii) results in remarkable levels of purity in purified vectors, containing no detectable trace of DNA contamination (<1ng/mL) and >2-log reduction in host cell proteins.

Our developed purification could be regarded as superior to currently employed schemes due to its efficiency in both product- and process-related impurities clearance in a one-step capture process. All current purification schemes employed in viral downstream processing have a common DNA elimination step by nuclease treatment such as benzonase (Merten et al., 2016). It is worth mentioning that even nucleic acid digestion of vector products processed for clinical use does not result in the complete removal of dsDNA with reduction ranging between 99.1% (Bellintani, 2009) and 99.84% (Merten et al., 2011). Strikingly, owing to its specificity in target capture, dsDNA contamination was reduced by at least 3-logs in eluted Ctag-LV, indicating that the use of our purification eliminates the requirement of a DNA digestion step. This in turn would decrease the cost of manufacturing at a large scale, as well as abolish the requirement of more steps needed to eliminate and/or measure the nuclease itself from processed vector sample. In addition, a 2-log reduction in host cell protein was achieved by the one-step capture and elution of Ctag-LV from streptavidin by competitive elution. Current downstream processing report levels lower than 200ng/mL (Merten et al., 2011); whereas we reported an order of magnitude lower (12 ng/mL) detected in purified Ctag-LVs; which to the best our knowledge is the lowest reported value for HCP contamination in LVs.

Our developed purification therefore offers a substantially improved purification process compared to the currently used purification schemes for both research and clinical vector applications. For its potential in both pre-clinical and clinical applications, alternative streptavidin resin should be tested that, unlike magnetic beads, allow the processing of large vector volumes with good economics.

Chapter 7 Large-scale application of Ctag-dependent LV purification by affinity chromatography

7.1 Overview

In previous Chapters, we have demonstrated successful purification by compete capture of Ctag-LV by streptavidin matrix and their subsequent competitive elution by biotin. We have also established superior levels of vector product purity from our developed method. However, for its potential as a wide-spread vector purification technique, this Chapter investigates its scalable applicability for large vector volume processing.

7.2 Introduction

7.2.1 Current processes for the manufacturing of large scale LVs

Downstream processing of viral vector purification represents a major part in gene therapy vector production. In biopharmaceutical manufacturing, downstream processing is estimated to account for 75-80% of its operational costs (Kramberger et al., 2015). Purification of viral vectors is currently achieved through a series of processing steps involving different aspects of several technologies such as filtration methods and chromatographic steps. However, with the rising demand for larger processing vector volumes as LV progress as therapeutic products, these methods suffered from several drawbacks; (i) they offered poor scalability of purification, which in turn caused (ii) poor economics and (iii) resulted in inadequate product purity that did not meet regulatory requirement. The development of advanced technologies in chromatography-based media has enabled efficient processing for larger viral vectors productions. Its potential quickly recognized due to its ease in scalability, fast processing times, consistency and automation. As a result, chromatography is presently the most implemented technology for the

purification of LVs by exploiting either LV charge (anion exchange chromatography, AEX) and/or size (size exclusion chromatography).

The large-scale processing of clinical grade LVs which was discussed in Section 1.3.4.2, combines several methods within multi-step processing schemes. A summary of these clinical-grade purification 'trains' from the different institutions are depicted in Figure 1.7**.** As expected, chromatography-based purification is a common step used in all of the summarized clinical grade manufacturing of LVs. Nonetheless, owing to the complex mechanism of these schemes along with LVs' fragile stability, overall yields range between 20-40%, with concentration factors in the range of 20 up to 200 with the use of ultracentrifugation, or up to 2000 using tangential flow filtration twice. Consequently, yields higher than 30% are currently considered acceptable for pharmaceutical vector products (Wolf and Reichl, 2011). As LVs advance in clinical trial phases, the overall acceptable yield will have to improve to supply the growing clinical demand of LVs.

7.2.2 Chromatographic purification of viral vectors

Chromatographic separation is based on the differences in interaction to the functionalised stationary phase between viral vectors and other components present in the mobile phase. Generally, two characteristics of chromatography's stationary phase must be considered for a successful viral purification: its physical structure and surface chemistry (Jungbauer and Hahn, 2008).

7.2.2.1 Physical structure of stationary phase: particles, membranes and monoliths

For the chromatographic purification of viruses, typically three different types of stationary phases have been used. The most common stationary phase of chromatographic columns are packed-resin/beads columns, which consists of porous bead-particles filled into a column. The binding sites of these adsorbent beads are located within pores located on the surface of these particles. Typically for viral purification, porous particles are used with pore sizes ranging

between 10-100nm (Jungbauer and Hahn, 2008) and up to 400nm (Morenweiser, 2005). It should be mentioned that the majority of chromatography resins currently available for viral purification have been initially optimized for protein purification, which explains the relatively small pore sizes. Consequently, viruses that can enter larger pores have been shown to diffuse into the intra-particle channels 2-100-fold slower than proteins (Ljunglöf et al., 1999). Therefore, given that the mass transfer within a particle-based column is limited to diffusion, this type of stationary phase can only accommodate for low flow rates to allow enough time for viral vectors to diffuse in and out of the pores. Additionally, it has also been demonstrated that the use of POROS® HS 50 particle packed columns, which has a pore size distribution of 100nm to 500nm, for the purification of 100nm viral-like particles resulted in a distinct VLP layer formed at the outer surface of particles which blocked the access and binding of other VLPs (Wu et al., 2013). This result suggested the need for larger pore size to accommodate viral vector purification using particle-packed columns. Moreover, this study further highlights a major drawback of porous-particle based chromatography, which is a low dynamic binding capacity. The latter is an important parameter for any chromatographic physical structure as it usually refers to the total amount of protein bound to a chromatography matrix at certain conditions in terms of solvent and protein concentration. Therefore, the lower this protein capacity parameter, the less efficient a chromatographic medium is at target purification.

The development of monolith-based chromatography offered several advantages compared to porous-particles and their value has been recognized for several downstream processing of viral vectors. Monolithic adsorbent is a single continuous porous polymeric surface with connected channels that takes a columnar shape, allowing uninterrupted flow of the mobile phase through the stationary phase (Hahn et al., 2007; Podgornik et al., 2010). Unlike the inter-particle porosity of packed resins, monolith do not have a void volume within the column. Their active binding sites for target capture are located in the large flow-through channels that are fully accessible, which in turn leads to

a high resolution of purification. Additionally, the main advantage of monolith-based chromatography compared to packed porous beads is that mass transfer is based on convection rather than diffusion. Mass transport based on convection is governed by the average velocity of all molecules present in a bulk solution; whereas transport based on diffusion relies on the randomized velocity of individual molecule i.e. Brownian motion, which is inferior to the average velocity of the total molecules in a fluid. This convective characteristic of monolith enables the column to be unaffected by the flow rate, allowing 10-20X higher rates without loss of dynamic binding capacity. Therefore, using monolith columns for purification, shorter purification times can be achieved with a higher chromatographic productivity by at least an order of magnitude compared to porous particle chromatography (Strancar et al., 2002).

Lastly, the stationary phase can consist of membrane materials for chromatographic separation. There are three types of membrane adsorbers: flat sheets, hollow fibers and radial-flow devices (Ghosh, 2002; Charcosset, 2006). The main advantage of membrane adsorbers, similarly to monoliths, for viral vector separation is their convective mass transfer of materials in the mobile phase, with no limitations by diffusion (Ghosh, 2002; Charcosset, 2006; Hahn et al., 2007; Vicente et al., 2011). This is due to their well interconnected channels and large pore sizes with small constriction for material transport and high dynamic binding capacity (Jungbauer and Hahn, 2008; Wolff et al., 2010). Monolith based columns however have been demonstrated to attain higher dynamic binding capacity than membranes, as well as allowing more controllable flow distribution compared to hollow fiber and radial-flow membrane adsorbers (Gagnon, 2008). Moreover, the formation of eddy currents, which is the swirling and reverse current of a fluid, have been demonstrated for most chromatographic matrices except for monoliths (Wolf and Reichl, 2011). Given the labile structure of viral particles, this phenomenon in fluid dynamic should be considered for viral vector purification as eddy formation can cause viral particle damages resulting in lower infectious vector elution from chromatographic columns. Therefore, monolith-based chromatography offer several advantages over particle or membrane

adsorber-based columns. A new generation of commercially available columns, the analytical CIM (convective interaction media) disk monolith from BIA Separations have been designed and optimized for the purification of large biomolecules. These columns have been reported to outperform the capacity of many established particle based columns (Peterka et al., 2006). Accordingly, CIM monoliths have been demonstrated to be provide superior recoveries with high dynamic binding capacity compared to both particle- and membrane-based resin for lentiviral purification (Lesch et al., 2011; Peterka et al., 2011; Bandeira et al., 2012).

7.2.2.2 Surface chemistry of stationary phase: affinity chromatography

As discussed earlier, different modes of chromatographic surface chemistry are currently employed for the separation of LV particles. Anion exchange chromatography applications are widely used for VSV-g pseudotyped LV purification for both clinical and research applications (Slepushkin et al., 2003; Rodrigues et al., 2007; Schweizer and Merten, 2010; Lesch et al., 2011). However, since this process exploits charge-charge interactions between viral surface and matrix-immobilized anions, it suffers from low specificity resulting low viral target dynamic binding capacity due to background absorption of impurities that affect the quality of the purified product. This method of LVs purification also often results in co-elution of negatively charge contaminates such as nucleic acid as its elution is non-specific. This in turn requires additional techniques for vector polishing. Therefore, in the absence of a suitable specific affinity-based chromatographic purification method that offers vector specificity, AEX is the widely-applied method of choice for LV purification.

As mentioned in Section 1.3.4.5.1.2, seeing that there are no known specific ligands for LVs, less-specific ligands such as heparin (Segura et al., 2007) or harsh desorption columns such as IMAC (Yu and Schaffer, 2006; Cheeks et al., 2009) have been used for labile LV purification. Moreover, as discussed in Chapter 4, similarly to this work, the desthiobiotinylation of LVs allowed their affinity purification by monomeric avidin (R. Chen et al., 2010). However, due

to the type of modification, as well as the usage of the non-specific biotin receptor avidin, a streptavidin specific biotin mimic may offer superior resolution in terms of target purification and product purity. Therefore, the separation of viral vector engineered with an affinity-tag that provides high specificity, coupled with gentle elution, would provide an attractive alternative for the affinity-based chromatographic separation of LVs.

7.3 Aims

In the previous chapters, we have established the capture of Ctag modified LVs by streptavidin magnetic beads; and their subsequent competitive elution using biotin, resulting in recoveries ≥ 60%. As an affinity purification of infectious viruses, the interaction between Ctag and streptavidin provides high levels of specificity and resolution in terms of vector isolation in a one-step process from clarified cellular supernatant.

The potential of this developed method is dependent on its scalability in terms of vector volume processing. Therefore, the aims of this chapter are:

- Determining the feasibility of our developed purification to process large volumes of Ctag-LV.
- Demonstrating the application of our purification as an affinity chromatography using streptavidin analytical monolith columns with efficient adsorption and desorption of modified vectors.

7.4 Scaling LV purification using streptavidin coated particles

7.4.1 Large polystyrene particles

Our purification methodology was developed using spherical magnetic particles, Dynabeads, which are not economically feasible for the processing of large volume of viral vectors. Accordingly, we sought out to test our capture method using an alternative cost-effective matrix such as polystyrene beaded SPHERO™ streptavidin coated particles (SVP) that are 100X larger than Dynabeads. We had aimed to capture a larger amount of vector volume using the larger SVP particles. In order to accurately compare them to the latter, the amount of SVP used was normalized to the amount of Dynabeads used, from prior Dynabeads optimization (Section 4.8), based on their surface areas (Table 7.1). In preliminary capture experiments in Chapter 4, 50μL of Dynabeads was used to capture all infectious Ctag-LVs. To determine the amount of SVP beads required for a comparison, the equivalent of 100μL of Dynabeads surface area (9.92 x10^7 μm^2) for SVP particles was used. The number of beads was determined by calculating the SA of both Dynabeads and SVP, as well as the number of beads/μL. Accordingly, the equivalent surface area of 100μL of Dynabeads for SVP, which contained 23 beads/μL, was 137μL of SVP.

DynaBeads (1μm)					Spherotech (100μm)			
Surface Area (SA) μm^2/bead	Beads/μL	SA / μL of beads	SA of amount of beads used		Surface Area (SA) μm^2/bead	Beads/μL	Equivalent SA to Dynabeads	
			μL of beads	SA in μm^2			No. of beads	μL
3.14	3.16E+05	9.92E+05	100	9.92E+07	3.14E+04	23	3159	137
			50	4.96E+07			1579	69
			25	2.48E+07			790	34

Table 7.1: Equivalent number of Dynabeads and plastic polystyrene streptavidin beads based on surface area.

It should be noted that as plastic polystyrene particles, SVP beads could not be separated by magnetization. Since these particles could not be sediment by centrifugation, the washing and recovery of these particles in the different

steps of this experiment was conducted by utilizing 40μm cell strainers onto which the 100μm particles would be retained. Therefore, having a relatively awkward process handling of these particles, we proceeded to attempt capturing Ctag-LVs with SVPs. Accordingly, SVPs were washed with PBS and then were incubated with both NM-LV and Ctag-LV containing medium, with 137μL of particles per mL of virus, for 2 hours at 4°C. Subsequently, SVP were separated from flow-through by loading onto cell strainer and polystyrene particles were washed 5 times with cold PBS and then resuspended in plain DMEM. SVP were then recovered by inverting the strainers and washing off SVPs onto a 10cm dish. Neat, flow-through and SVP beads captured fractions were collected and their virus titres were determined by infectivity assay (Figure 7.1a). SVP particles did not seem to bind any Ctag-LVs, as indicated by the presence of the complete Ctag-LV titre in the flow-through fraction; resulting in no statistical difference compared to its neat fraction. To determine whether streptavidin conjugated on SVP particles are functional, both Dynabeads and SVP beads were stained with biotin conjugated to APC (Figure 7.1b). As expected streptavidin Dynabeads resulted in a biotin-positive population compared to its unstained control. Conversely, SVP particles did not seem to bind biotin resulting in a lack of APC signal compared to unstained control. However, based on their respective binding capacities in nanomoles per mg of beads for free biotin, provided by their manufacturer, SVP particles' binding capacity in moles per bead was calculated to be 100-fold higher than that of streptavidin Dynabeads. Therefore, the failure of SVP beads to capture Ctag-LV was likely due to the coating of defective streptavidin in the SVP batch obtained from manufacturer.

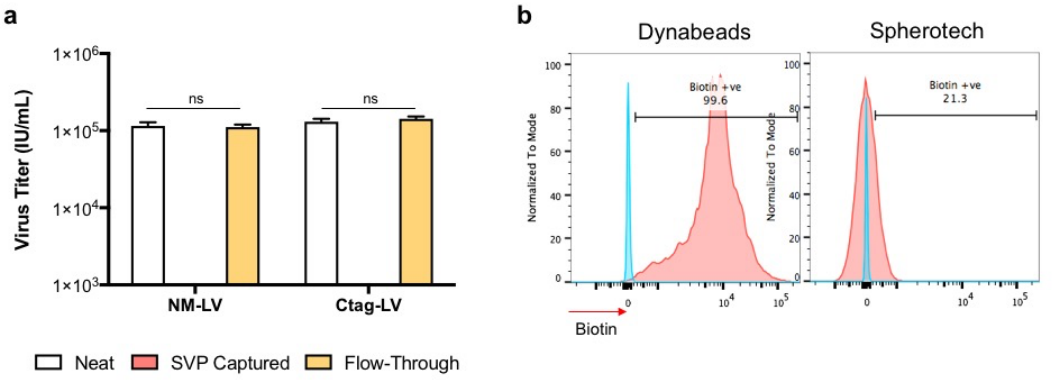

c

	Dyna (10mg/mL)	SVP (10mg/mL)
Binding Capacity (nmol/mg of bead)	1.1	0.01
Beads / mL	3.1E+8	2.3E+4
Binding Capacity (nmol/mL of bead, since both 10mg/mL)	11	0.1
Binding capacity in mol/Bead	**3.5E-17**	**4.3E-15**

Figure 7.1: Testing Ctag-LV capture by 100µm streptavidin plastic polystyrene particles. (a) NM- and Ctag-LVs from stock were incubated with Spherotech SVP streptavidin coated 100µm particles for 2 hours at 4°C with gentle rotation. Loading of mixture onto 40µm cell strainers isolated SVP particles from flow-through fractions. Viral titres for all collected fractions were determined by infectivity and values are presented ± standard deviation (SD) of triplicate determinations with ns $p \geq 0.05$. **(b)** Histograms of streptavidin magnetic Dynabeads and Spherotech SVP particles stained with biotin conjugated to APC. **(c)** Calculation of binding capacity for both resins in moles of biotin per bead for both Dynabeads (Dyna) and SVP particles: by converting manufacturer's information of binding capacity from nmol per mg to nmol per mL with a concentration of 10mg/mL of both beads. Then having quantified the number of beads per mL, the binding capacity in mol per beads was calculated and presented.

7.4.2 Super-paramagnetic Dynabeads

At this stage in the project, the highest volume of vector containing medium was 10mL that was tested for capture using streptavidin Dynabeads. This was due to the very high cost of the beads. Therefore, to obtain the proof of concept for the processing of large vector volume using our methodology, as well as establish the possibility of captured vector concentration by volume reduction, the Dynabeads were tested for the processing of 50mL of Ctag-LV (Figure 7.2). Thawed NM- and Ctag-LVs were incubated with pre-washed streptavidin Dynabeads at the optimized beads volume per mL of vector, for 2 hours at 4°C. Then, after flow-through collection, beads were washed 5 times with cold

PBS and a fraction was collected for viral assessment without any volume reduction (i.e. 1X volume resuspension). Subsequently, beads were resuspended in 100X volume reduction of starting material in plain DMEM and a fraction was also collected. Plain DMEM was then removed and beads were incubated with 100X volume reduction of X-vivo^{TM} supplemented with 1mM biotin and 1% BSA for 2hours at 4°C for the elution of bead-bound Ctag-LV particles. It should be noted that higher concentration of both biotin and BSA were used in this experiment, as the vector volume processed was 10X higher compared to previous experiments. Both eluate and beads eluate (at also 100X volume reduction) were then collected and along with previous steps' fractions, viral titres of all samples were determined by infectious assay (Figure 7.2a). As expected, Ctag-LV particles captured on Dynabeads resuspended in 1X volume resulted in an increase in viral titre (1.42 x10^5 IU/mL) compared to starting material (9.65 x10^4 IU/mL) of 1.48-fold. Moreover, only 68% of neat viral titre was captured by streptavidin Dynabeads as indicated by the presence of 32% of Ctag-LV in the flow-through fraction. This indicated that the optimized number of beads for 1mL could not be applied in a linear manner with 100-fold volume processing increase which is common for process scale-up. Nevertheless, the reduction in volume by 100X after Ctag-LV capture of bead fraction resulted in a 99-fold increase in viral titre (9.54 x10^6 IU/mL) compared to starting material. This result further highlights the increase in transduction efficiency of vector bound to magnetic beads even at 100X volume reduction, as only 68% of Ctag is bound to the beads. Additionally, biotin-mediated elution of 100X concentrated Ctag-LV resulted in an overall yield of 30% with an increased viral titre of 2.83 x10^6 IU/mL. Also, similarly to previous results, the remaining portion of captured Ctag-LV was not displaced by biotin and was still bound to the beads as indicated by the viral titre of beads eluate fraction of 6.35 x10^6 IU/mL, which represented 66% of starting material, even though this value may be overestimated given the bead-dependent increase in infectivity. Nonetheless, in this experiment we have demonstrated the applicability of Ctag-dependent LV purification on a larger scale by processing 50mL of viral supernatant resulting in the recovery of concentrated

LVs. Further optimization would be required with the use of these beads for the intended scale.

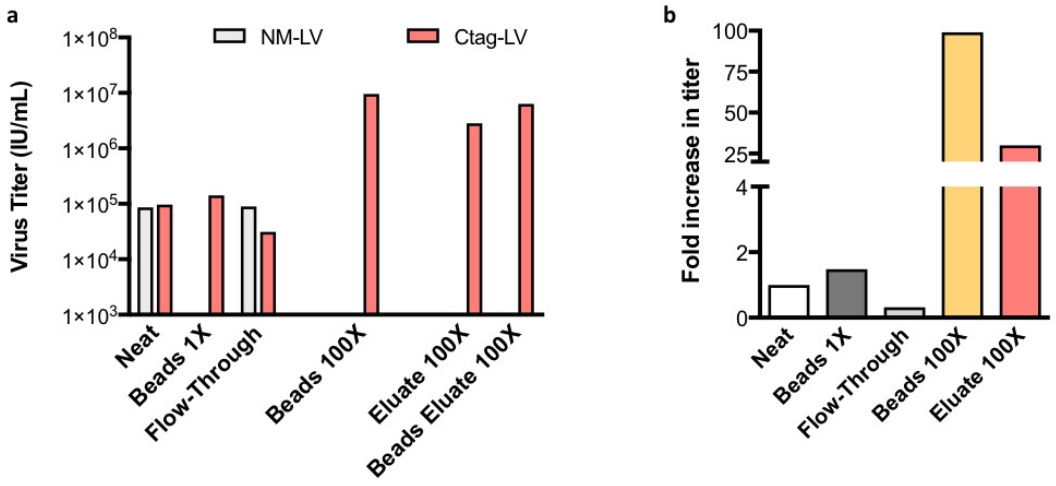

Figure 7.2: Scalable purification and concentration of Ctag-LV using streptavidin magnetic beads. (a) NM- and Ctag-LVs from stock were subjected to the developed purification process with magnetic Dynabeads. Post-capture of viral vectors, elution reaction occurred in 100X volume reduction for concentration of eluted vectors. Viral titres were determined for all collected fractions by infectivity assay and values represent n=1. **(b)** The fold increase in viral titre of each fraction collected relative to neat starting viral titre are presented.

7.5 Monolith based affinity chromatography for vector purification

The use of Dynabeads for large vector volume processing is not an economically feasible option. An alternative platform that can be easily scaled up with good economics is thus required for the wide-spread applicability of our method. Correspondingly, streptavidin-based affinity chromatographic purification of viruses is an attractive option. Monoliths-based columns offer several advantages compared bead-packed or membrane-based columns. In a collaboration with BIA separation, we aimed at testing their CIMac^{TM} streptavidin 0.1mL analytical columns for the purification and subsequent biotin-mediated elution of captured Ctag-LVs. CIMac^{TM} analytical columns are high-performance monolithic columns which have a bed volume of 100µL and can be scaled up to 8L column volume capacity. Seeing that this type of

column has never been tested for chromatographic purification of LVs, BIA separation generated five different columns with varying 1- column chemistry (the use of aldehyde or carbonyldiimidazole), 2- streptavidin immobilization conditions, 3- reactive group deactivation on the column and 4- ligand density (ranging from 2.7 to 4.8mg). However, in the scope of this project, only one column was tested which contained a streptavidin density of 4.3mg. Based on the manufacturer's recommendation, the column was placed in an upright position and connected to a peristaltic pump using connector tubes as indicated in Figure 7.3a. A protocol was also developed for this column specifically as illustrated in Figure 7.3b. After having sterilized and washed the tubing with 70% ethanol and PBS, respectively; the column was fitted with an upward flow and connected to the pump with the connector tubes. The column was then washed with 50 column volume (CV) of PBS with a flow rate of 1.5mL/min. Subsequently, the column was primed with 50 CV of plain DMEM, which represent the vector-containing media of viral supernatants. Then to determine the non-specific binding of the CIMac^{TM} streptavidin analytical column, 5mL of NM-LV was loaded with a flow rate of 2mL/min, and its flow-through was collected. After having washed the column with 50mL of PBS, corresponding to 500 CV, thawed Ctag-LV was loaded into the system at 1.5mL/min and five flow-through fractions of 10mL were collected. Column was then washed twice with 300 CV with PBS and wash flow-throughs were also collected to assess for non-specific displacement of potentially bound vector. Next, 15mL of X-vivo^{TM} based elution buffer, containing a saturating concentration of biotin of 15mM, supplemented with 0.5% BSA, was filtered through 0.22µm and loaded into the column, which represented a third of Ctag-LV total loaded volume for concentration of eluted vector. With a dead volume of 4mL in the tubing system and the fact that X-vivo^{TM} is coloured compared to PBS, two fractions of 1.5mL, termed E1 and E2, were collected as they represented the point of mixture between wash and elution solutions. Four elution fractions of 1.5mL were then collected (E3 – E6), followed by a final 7.5mL elution fraction (E7). All collected vector samples were then assayed for viral titre by infectivity assay (Figure 7.3c-e). The loading of control NM-LV resulted in a significant difference in the viral titres between input (4.17 ±0.36

x10^4 IU/mL) and flow-through (2.95 ±0.27 x10^4 IU/mL). This observed difference in titres could have been caused by either non-specific binding of the monolith column to LVs; or the dead volume of the pumping system (4mL) (Figure 7.3c).

The loading of 50mL Ctag-LV supernatant (4.58 ±0.28 x10^4 IU/mL) onto the column resulted in significant vector binding to immobilized streptavidin, as indicated by the presence of 9.11 x 10^4 total TU detected in all of the five 10mL collected flow-through fractions, which represented a total yield of 4% of transducing units (Figure 7.3d-e). The low starting viral titre was likely due to the use of non-optimized conditions of serum-free freeze-thawed viral supernatant. Moreover, the washing of the column did not displace any bound LVs indicating specific and high binding affinity of Ctag-LV to the column. Furthermore, captured vector was eluted and six fractions (E1 to E6) of 1.5mL total volume each were collected followed by a 7.5mL E7 fraction. Upon loading of the elution buffer, the first collected fraction E1 contained 1.01 ±0.09 x10^4 IU/mL of Ctag-LV, which represents 22 ±1.5% of input viral titre. The second elution fraction E2contained a clear eluted viral peak containing a concentrated titre of 8.21 ±0.3 x10^4 IU/mL, representing 180 ±11% of starting vector material. The elution of Ctag-LV continued in E3 with 4.40 ±0.91 x10^4 IU/mL and in E4 with 2.82 ±0.71 x10^4 IU/mL, which represented 96% and 61% of starting titre, respectively. Interestingly, in the last collected fractions of E5 to E7, Ctag-LV displacement continued in a stable manner, with similar titres in all three fractions of 1.77 x10^4 IU/mL, representing 38% of input titre. Taking into consideration the volume of each fractions, an overall yield of 20% was achieved in all elution fractions by biotin-displacement of Ctag-LV in this preliminary affinity chromatography run (Figure 7.3e). Therefore, this experiment provided the feasibility of our developed methodology application into an affinity chromatographic purification of viral vectors and further optimization are required for higher yields.

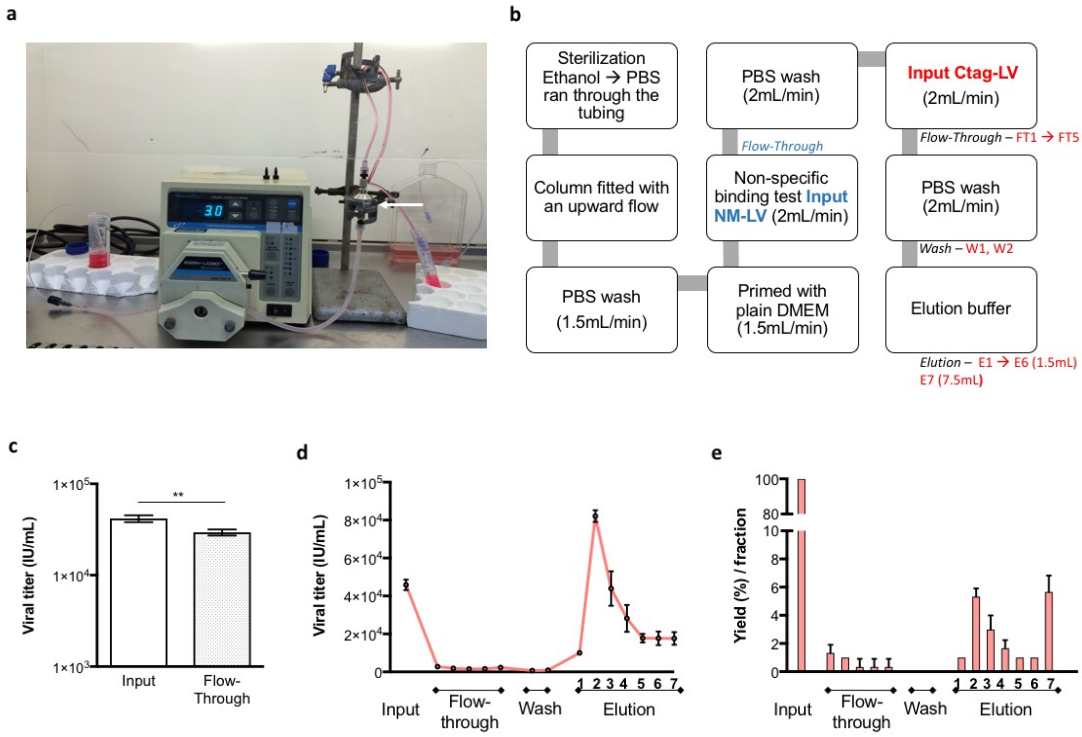

Figure 7.3: Affinity chromatography purification of Ctag-LV using CIMac™ streptavidin analytical column. (a) Image illustrating chromatographic run using peristaltic pump with a white arrow pointing to the CIMac™ column. **(b)** Diagram of the column purification step process with indicated fractions (in italic) that were collected and their viral titres determined by infectious assay. **(c)** Viral titres of NM-LVs input and flow-through fractions run through the column with ** as $p \leq 0.01$. **(d)** Viral titres of collected fractions of Ctag-LV loading onto the column and **(e)** yield of each fraction in terms of total transducing unit which are represented as a percentage from starting input transducing units. Values for (d) and (e) are presented with ± standard deviation (SD) of triplicate determinations.

7.6 Discussion

In this Chapter, we have demonstrated the feasibility of scaling up our developed one-step purification process which is based on the specific interaction between Ctag and streptavidin. This has been established by the affinity chromatographic purification of Ctag-LVs. Competitive elution of matrix-bound purified vectors by biotin resulted in an encouraging preliminary overall yield of 20%.

Affinity-based purification offers high resolution in viral isolation thus reducing the number of purification steps and in turn decreasing cost of vector processing (Cheeks et al., 2009). Different capturing matrix were investigated for the establishment of Ctag/streptavidin mediated purification for large scale processing of LVs. As a first attempt, we have tested streptavidin immobilized on large plastic particles from Spherotech, which are 10-fold bigger in size and smaller in cost compared to Dynabeads. However, these particles were deficient in the binding of streptavidin's natural ligand biotin, rendering them unusable. As the ultimate aim of this chapter was to determine the feasibility of our developed method for affinity based chromatographic isolation of LVs, monolith-based column purification was tested as a second attempt. Since the kinetics of binding between Ctag-LV and immobilized streptavidin on magnetic beads, as well as their respective densities, were not elucidated; the capture efficiency of modified particles in a column-based setting, with a set flow rate, was not known. The specificity of the column for Ctag was demonstrated by the lack of NM-LVs binding. Surprisingly, the analytical CIMac^{TM} monolith column captured a total of 2.26 x 10^6 transducing Ctag-LV units during the loading of 500CV viral supernatant at 2mL/min flow rate. These results highlight both the high dynamic binding capacity of monolith-based columns, as well as their adsorption efficacy. This is further emphasized by comparing the time required for total adsorption of Ctag-LVs between monolith disk and magnetic beads, which only attained partial capture with incubations ≤30 minutes (Section 4.8). Moreover, Ctag's interaction with streptavidin on the column seemed stable during column washing, highlighting their strong binding kinetics. Unlike the non-specific heparin affinity chromatography for LVs purification (Segura et al., 2007, 2008), streptavidin affinity chromatography selectively isolated Ctag expressing viral vectors, thus providing a high level of specificity. The quantification of total protein by silver stain would have been useful to determine the efficacy of protein clearance during the chromatographic run. Efficient removal of proteins and nucleic acid content from the starting viral supernatant has been validated in Chapter 6, with effective elimination of product- and process-related impurities using the Dynabeads. It could therefore be postulated that the same would be observed

during the chromatographic purification of Ctag-LV. Furthermore, the desorption of captured vectors from the matrix was achieved by the loading of the elution buffer formulated in X-vivo^{TM} containing 15mM biotin and 0.5% BSA; resulting in an overall yield of 20% with a 2-fold concentration at the second elution peak. Interestingly, matrix-bound LVs continued to desorb from the column even after the loading of 150CV elution buffer, indicating that the remainder of infectious vectors were still bound to the column and further optimization with elution buffer conditions should be tested.

The assessment of vector inactivation is an important factor to consider. The result from the column run indicated the presence, but lack of desorption, of functional infectious vectors bound to the column. The sensitivity and lability of LVs has been demonstrated by published reports that have purified vectors using affinity chromatography. The recovered LVs from heparin-based columns required the use of high salt concentration (0.35 M NaCl) and high ionic strength resulting in the recovery of 53% (Segura et al., 2007b). However, elution in high salt concentration significantly reduced the infectivity of LVs, up to 50% loss, likely due to high osmotic pressure causing viral surface damages (Segura et al., 2005; Zimmermann et al., 2011). Furthermore, the purification of hexahistidine (His_6)-tagged viral vectors using IMAC, either by random incorporation of host-cell derived His_6 protein (Cheeks et al., 2009) or using randomly inserted His_6 into engineered VSV-g variants (Yu and Schaffer, 2006); requires high concentration of imidazole for column desorption. Although reported elution efficiencies were high (69%), inactivation of LVs was demonstrated and was attributed to high imidazole concentrations (Ye et al., 2004; Cheeks et al., 2009; Segura et al., 2013). Therefore, affinity chromatographic processes relying on either heparin binding or incorporation of His_6 necessitate harsh desorption conditions, which are also often observed for AEX, impacting the infectivity of labile LVs. Our developed purification relying on the competitive elution of captured Ctag-LV by biotin, allowing the gentle column desorption of bound vectors. As discussed in Section 4.2.3, Chen et al., (2010) demonstrated the desthiobiotinylation of LVs and their subsequent purification using monomeric avidin-based column. Authors

reported the capture of 89% of LVs with an elution using 2mM biotin within 45 minutes (flow rate 0.4mL/min) resulting in 68% recovery of modified vectors. Comparatively, our streptavidin-based monolith chromatography resulted in complete capture of all infectious titre, all the while resulting in incomplete desorption from the column using 15mM biotin within approximately 7 minutes. Interestingly, the times of vector desorption from monomeric avidin was 5 times longer than that used in CIMac^{TM} column purification. This may suggest the need for longer incubation times of biotin in the monolith disk to efficiently outcompete bound Ctag molecules; resulting in higher portion of vector elution. Nonetheless, the preliminary recovery of 20% was encouraging since the recovery of approximately 30% is currently considered satisfactory for advanced therapy medicinal products and represents the upper limit of existing purification schemes' yield (Wolf and Reichl, 2011).

In conclusion, in this final result Chapter we have established the applicability and feasibility of our method as an affinity purification for scalable LVs purification. In collaboration with Dr. Glenda Dickson and Dr. David Darling from Prof. Farzin Farzaneh's laboratory at King's College London, the 4/5 remaining streptavidin analytical columns will be tested for the affinity chromatographic purification of Ctag-LV. Given the multi-process of most clinical-grade downstream processing of LVs, the use of our developed modified vector isolation effectively reduces the number of processes required for high purity vector product. This in turn would decrease the cost of vector processing and thus release the current bottleneck in LV manufacturing, allowing the maturity of LV for gene therapies application.

Chapter 8 Conclusion and future work

8.1 Concluding remarks

The current downstream processing technologies for LV purification represent a major bottleneck for their advancement in both pre-clinical and clinical applications. The inefficiency of each of these methods is emphasised by the requirement of purification schemes, which consist of at least 4 different technologies (Merten et al., 2016). These methods aim to either debulk the surrounding supernatant from viral vectors (e.g. UF/DF and SEC) or rely on overall charge of viral particles for purification (e.g. AEX). Although AEX suffers from low specificity and co-elution of negatively charge impurities, it is currently the most widely applied purification technology for both laboratory and clinical scale LV purification, with several commercial kits available such as Merck Millipore's Fast-Trap kit; ABM's PuRetro® LV kit; Cellbiolabs's ViraBind LV kit and finally Sartorius's Vivapure LentiSELECT kit. However, desorption from AEX matrices requires the use of harsh reagents and thus efficient elution comes at the cost of the most important objective of any downstream process which is to maintain vector infectivity. Thus, all of these limitations and the constraint in utilizing at least 4 technologies in the multi-step schemes, are in turn translated into the presently acceptable overall yield of 30% for clinical downstream processing of LVs, with published yields ranging between 20-40% (Merten et al., 2011).

It is well recognised that the development of a specific purification strategy based on affinity chromatography holds promising potential to both increase overall yield and in turn decrease total cost of goods in LV manufacturing, as fewer steps would be required. However, to date affinity purification of LVs has had limited success as vector specificity has not yet been coupled with gentle desorption from affinity ligands. These two features are key in any viral purification method for its efficacy in vector manufacturing, both technically and economically. Lectin-based affinity ligands suffer from non-specific vector capture but are nonetheless commercially available (e.g. GE Healthcare's

Capto Lenti Lectin). Alternatively, heparin or hexahistidine affinity tags can be used for LV isolation which have resulted in inefficient vector desorption from affinity columns leading to low infectious recovery (Segura et al., 2007; Cheeks et al., 2009). Thus, the development of a cost-effective affinity purification with gentle elution conditions is highly desirable for the widespread use of LVs in both clinical and research applications. Accordingly, the research presented in this thesis has addressed current limitations in LV downstream processes by the establishment of a novel one-step specific vector purification, which selectively isolated LVs, resulting in an overall yield of ≥ 60% with remarkably high levels of product purity.

A precedent to this project was the metabolic desthiobiotinylation of LVs with their subsequent purification using monomeric avidin followed by biotin-mediated desorption from column (Chen et al., 2010). However, this strategy had several limitations due to the relative complexity of viral engineering; involving co-expression of three exogenous proteins in packaging cells. Moreover, the synthesis of desthiobiotin in these cells requires the addition of 7-DAPA into the culture, which may contain traces of biotin rendering this strategy ineffective for complete viral capture. In our strategy, a cell surface expressing synthetic biotin mimicking peptide, Ctag was genetically engineered into packaging cells, thus effectively relieving the need of any exogenous protein expression other than the peptide itself. Strikingly, its passive incorporation onto the surface of viral particles upon virion budding was both necessary and sufficient for complete vector capture from viral supernatant in a one-step process. The simplicity and specificity of this affinity-based isolation was shown to be independent of viral envelope glycoproteins. The indirect nature of Ctag modification on viral particles effectively demonstrates that our developed purification may represent a universal viral vector isolation technique. As it is independent of vector genetic material, it could be applied to any strain of viral vectors; both enveloped viruses, without the requirement of envelope glycoprotein engineering, and non-enveloped viruses such as AAV, by engineering its capsid protein which is highly permissive to genetic alternations (Bartel et al., 2011). In addition, although

vectors in this project were produced transiently, our method can be translated and applied onto stable producer cell lines by their genetic engineering to express Ctag proteins. To the best of our knowledge, this report represents the first use of a synthetic biotin mimicking peptide for the purification of viral vectors. Moreover, the elegance and novelty in our desorption strategy is based on the competitive binding of biotin to streptavidin, thus displacing the bound mimic causing the release of LVs. This type of elution was carried out in mild and gentle conditions, thus retaining labile LV infectivity with routine overall yields of ≥ 60% from magnetic beads and 20% from the preliminary chromatographic monolith-based purification.

An important requirement for any vector purification is the removal of product and process related impurities. Extensive characterization and quality check of vector products are required for their use in human clinical trials. All vector purification technologies should provide high purity of concentrated vector materials, as well as allow for flexibility in terms of final vector formulation. To that end, our developed vector purification met all of these requirements, which can be attributed to its specific, efficient and gentle characteristics. In addition, the selectivity of our purification was demonstrated with the characterisation of eluted LVs in terms of both product- and process-related impurities. The selective capture of Ctag-expressing viral particles followed by their elution in a biotin-dependent manner resulted in a minimum of 3-logs and 2-logs reduction in DNA (<1ng/mL) and host cell-derived proteins (12 ng/mL) contaminants, respectively. To the best our knowledge, these reductions are comparable and competitive to reported values for both impurities in final LV product after its subjection to the multi-step purification schemes used, which in striking contrast, include benzonase treatments as well as at least one chromatographic purification step. Thus, our methodology seems to result in superior impurity removal in a one-step process compared to currently applied multi-step schemes.

The integration of such a vector-specific purification technique which combines high yield with high purity, would be highly advantageous for the clinical

manufacturing of LVs. The reduction of current schemes, after vector clarification, to potentially one affinity-based chromatographic purification step, (as depicted in Figure 8.1) would simultaneously decrease the cost of processing, all the while increasing volume bioprocessing; thus releasing the current bottleneck in LV manufacturing.

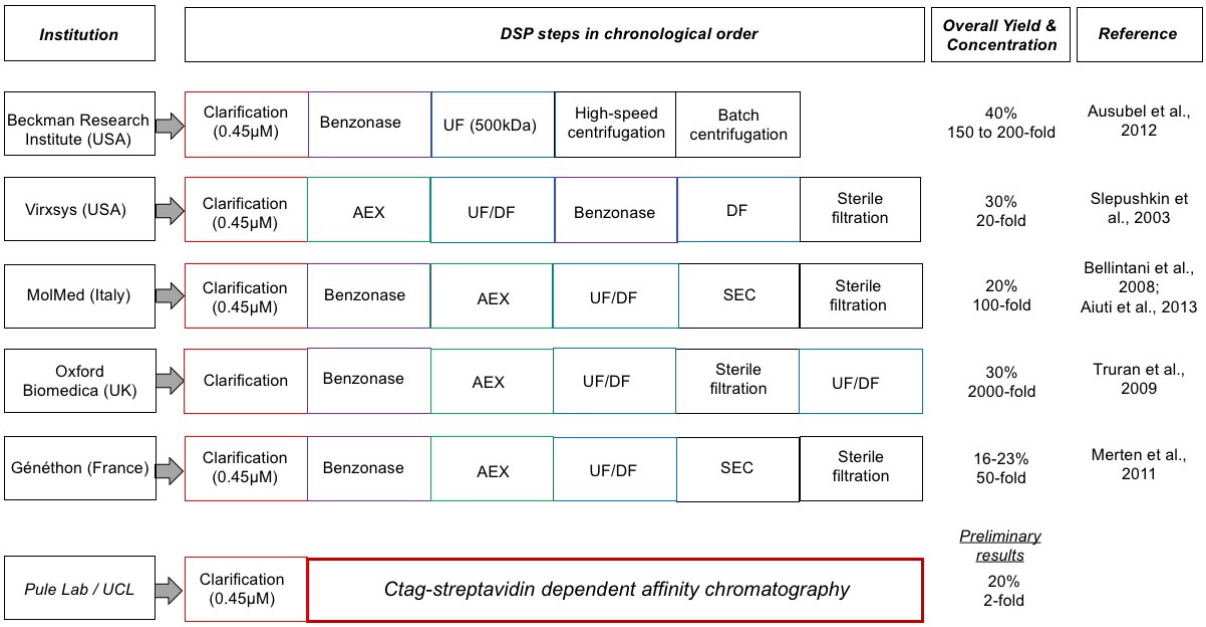

Figure 8.1: Perspective for developed purification.

8.2 Suggestions for future work

8.2.1 Ctag peptide binding characteristics

In this project, a cyclical streptavidin binding peptide Ctag, derived from a phage display screening by Giebel et al., (1995), was established as an affinity peptide allowing capture of targets with reversible binding by biotin out-competition. While the original study determined its binding affinity at 230nM, future efforts ought to define its kinetics by surface plasmon resonance (SPR) principle with an analytical instrument such as Biacore using secreted Ctag

proteins for binding onto a streptavidin immobilized chip. This method would however elucidate the binding affinity of Ctag to streptavidin at 1:1 ratio. Since several molecules of Ctag may be expressed per virion, more relevant to our purification method would be the testing of modified Ctag-LV for immobilized streptavidin binding. It should be mentioned however, that such an experiment would investigate the binding interactions between Ctag-LV and streptavidin on a two-dimension compared to the three-dimensional streptavidin magnetic bead capturing milieu. Furthermore, in Chapter 3, it was established that Ctag, an HPQ-containing mimic, was able to bind only streptavidin and not avidin, thus making it a streptavidin only binder, semi-mimicking biotin. This is in line with the few studies that have subjected their isolated HPQ-containing motif peptides to determine their universal mimicry, in which most have failed (Dudak et al., 2011). Further investigation into the molecular interactions of HPQ to streptavidin could elucidate its full interplay, which in turn would highlight key features that are responsible for streptavidin or avidin specific binding of mimics. Moreover, as Ctag demonstrated increased streptavidin binding compared to commercially used linear peptides of the Strep-Tag® system, investigating the binding kinetics of these two structurally different peptides would be interesting to further understand the superiority of cyclical peptides compared to linear ones. And finally, since Ctag with its flanked cysteine residues (**E**CHPQGPPC**IEGRK**) demonstrated increased streptavidin binding compared to un-flanked cysteine residues of sCtag (CHPQGPPC); the effect of these flanking residues on cyclical peptides should be determined as it would be interesting to assess whether they alter binding kinetics or rather stabilize the receptor binding complex. All of these investigations could elucidate information that would be in turn beneficial for peptide mimicry development.

8.2.2 Potential immunogenicity of LVs modified with Ctag

LVs are produced by budding from packaging cells, transiently or stably, which enables the decoration of viral particles with packaging cell-derived proteins along with viral envelope glycoprotein. This simple principle of protein incorporation was exploited for the purpose of this project and has already

been established in the scientific literature for endowing vectors with new functions such as purification (Chen et al., 2010) or immune response reduction by the passive incorporation of CD47 (Sosale et al., 2011) for example. As a streptavidin binding peptide, vectors modified with Ctag may hold promising prospective for several applications requiring or benefiting from a tagged-vector, such as most notably *in vivo* viral targeting. The potential for enhanced immune reactions against Ctag modified vectors should then be evaluated *in vivo*, which would not be required for *ex vivo* applications. Unlike AAV and AdV, LVs elicit very low immune responses which mainly targets the vector transgene rather than viral specific antigens (Bessis et al., 2004; Follenzi et al., 2007). Although, the intravenous administration of LVs into immunodeficient mice resulted in no apparent sign of toxicity with stable gene expression (Pfeifer et al., 2001; Follenzi et al., 2002; VandenDriessche et al., 2002); administration of vectors carrying CMV-driven transgenes into immunocompetent mice resulted in immune responses against transgenes leading to clearance of transduced cells (Follenzi et al., 2004; Annoni et al., 2007). Thus, the investigation of Ctag-mediated immune response could be evaluated by the systemic administration in immunocompetent C57BL/6 mice with both NM-LV and Ctag-LV, separately. The potential Ctag-mediated induction of humoral immune response can then be analysed a couple of weeks after injection by the detection of anti-Ctag antibodies. Additionally, the adoptive transfer of splenocytes can be used to assess Ctag-mediated immune reaction, in which spleens of treated mice could be harvested and co-culture *in vitro* with mice-derived cell lines, such as BW5, transduced to express Ctag. If Ctag-LV induced an immune response *in vivo*, then accordingly the co-culture of Ctag-LV injected mice's splenocytes with mice cell lines expressing Ctag would result in effector functions that can be detected such as IFNγ production for example. Given its relative size and possible low density per virion, it may be unlikely for Ctag-modified LV to induce an immune response greater than that observed for control non-modified vectors. Since Ctag exhibited superior streptavidin binding, as well as efficient displacement by biotin out-competition, it may be proposed that Ctag offers several advantageous compared to other streptavidin binding

proteins, that do not exhibit these features such as the Streptag® derivatives. And thus, once verified, Ctag's potential lack of immunogenicity would expand Ctag's prospective as an affinity tag for several peptide applications, not limited to viral vectors only, but also for target proteins or cells due to its high specificity.

8.2.3 Ctag quantification on modified vectors

The density alteration of Ctag peptides per viral particles was demonstrated to impact both capture and release from streptavidin matrix. The quantification of the number of peptide per particle would have greatly aided the investigation and troubleshooting of its elution in terms of overall vector avidity for streptavidin. SEM analysis of modified vectors was performed on negatively stained samples with streptavidin conjugated to colloidal-gold particles and resulted in unsuccessful peptide quantification due to significant non-specific background staining. Future efforts for Ctag quantification on viral particles could be achieved by staining immobilized modified vectors with streptavidin conjugated to a quantum dot (Qdot). The recently developed Qdot are fluorescent semiconductor nanocrystals composed of a cadmium selenide core which can overcome spectral limitations of organic fluorophores such as decrease in photochemical bleaching and narrow emission spectrum (Kampani et al., 2007). Relevantly, streptavidin conjugated to Qdot have been used to successfully stain and detect biotinylated envelopes on LV viral vectors (Joo et al., 2008; Rawsthorne et al., 2009; Chen et al., 2010; Huang et al., 2012). The quantification of proteins on the surface of viral vectors is technically challenging due to their size. Nonetheless, several efforts have been made to determine the number of trimeric envelope spikes on HIV-1 wild-type viruses by cryo-electron microscopy and was found to be around 7 to 14 per virion (Zhu et al., 2006; Schiller and Chackerian, 2014; Stano et al., 2017). This techniques in which samples are fixed by freezing, is ideal for examination of membranes and vesicles and thus could be used in conjunction to streptavidin gold-labeling for Ctag quantification per virion. Finally, an alternative strategy for Ctag quantification could be accomplished by super resolution microscopy analysis of Ctag-LV stained with immunofluorescently

labeled streptavidin. Although the density of wild-type gp120 HIV-1 envelope glycoprotein has been studied, the quantification of pseudotyping envelopes on HIV-1 based vector has not yet been investigated. The parallel staining of envelope glycoproteins along with Ctag on modified vectors would be beneficial to determine the ratio of pseudotyping glycoprotein to synthetic peptide. This ratio in turn could further elucidate the inclusion of non-viral host-derived proteins on budding virions through random/passive incorporation.

8.2.4 Purified vector product formulation

Vector product formulation is an important factor to consider for viral particle stabilization as demonstrated in the elution optimization chapter (Chapter 5). The orders of magnitude difference between Ctag and biotin binding affinities was sufficient for the recovery of ≥ 60% of streptavidin-captured Ctag-LV. Biotin-mediated elution of infectious particles was demonstrated simultaneously with a buffer exchange step into three commonly used viral cultivation medium (X-vivo^{TM}-15, OptiMEM and DMEM). However functional vector recovery required the addition of excipients such as BSA to biotin-containing solutions. The supplementation of protein additives for increased infectious vector recovery is in line with Carmo et al., (2008) which demonstrated the necessity of both human serum albumin and a protein solution derived from bovine serum for increased LV stability. Due to these vectors' inherent lability, product formulation to conserve functional infectivity during downstream processing is an essential area of research that has yet to receive the required attention from the field. This may be due to the relative infancy of LV bioprocessing and their use in both pre-clinical and clinical applications. With their clinical and potential commercial progression, future efforts into optimal LV formulation is highly desirable. The use of animal-derived excipients however is not appropriate from a regulatory point of view. Thus other excipients would have to be used for therapeutic application of LVs and should be tested such as amino acids like arginine and glutamate to increase proteins solubility; or sugars like glycerol as a stabilizing osmolyte (Bolen and Baskakov, 2001).

8.2.5 Large-scale application for GMP grade vector production

It is worth mentioning that the developed method can be used on both laboratory and clinical grade LV purification. The use of magnetic beads for the former may be cost-effective given the increased transduction efficiency observed with vector bound to large immobilizing-particles. However, since our purification holds very promising potential in terms of high overall yield and product purity, its translation for both pre-clinical and clinical applications require the use of alternative streptavidin conjugated platforms that allow the processing of large-scale LV volumes. This was validated in Chapter 7, whereby a monolith-based streptavidin chromatographic column was tested for the purification of Ctag-LVs and resulted in 20% overall yield with a 2-fold concentration in eluted viral peak. The column used in this project represents 1 out of 5 streptavidin analytical columns generated by BIA Separation for the collaborative work between our laboratory and that of Prof. Farzin Farzaneh (King's College London) for the translation of our method into affinity chromatographic purification of large-scale LV volumes. Future work will aim to compare and contrast the efficiency of adsorption of the different columns for Ctag-LV as their differential ligand density may impact efficacy of purification due to the multivalence nature of both adsorption and subsequent desorption (Wolf and Reichl, 2011). Furthermore, future efforts will focus on the optimization of desorption conditions to achieve higher overall yield, which is in conjunction with final vector formulation for optimal recovery and stability of purified vectors. Moreover, an additional collaboration with Spheritech is currently on-going as well for the translation of our method into large-scale vector downstream processing. With Spheritech's innovation in polymer design and manufacturing, chromatographic column molded with monomeric streptavidin immobilized on biodegradable polymers will be tested for Ctag-LV purification. Interestingly, the use of monomeric streptavidin may be advantageous compared to tetrameric streptavidin due to its monovalency which may lead to a lower overall avidity to Ctag-LV and in turn potentially result in overall yield > 20%.

Finally, a further leap for efficient LV downstream processing for commercial gene therapy applications can also be achieved by rendering our purification into a fully automated bioprocessing by the use of integrated continuous bioprocessing technologies. Continuous technology platforms are designed to intensify efficient processes with reduced time for both set-up and mechanical maintenance. This type of technology is a well-established tool for the efficient separation of binary mixtures for small pharmaceutical molecules (Kessler et al., 2007). Their potential and use have also been demonstrated for influenza virus purification which resulted in up to 4 times higher overall productivity compared to batch mode chromatography (Kröber et al., 2013). Relevantly, Pall Life Sciences have recently developed the first disposable simulated moving bed chromatography platform for continuous compound purification which is both compliant and scalable for GMP manufacturing allowing integration of continuous manufacturing for clinical bioprocessing (Frick et al., 2016). It could be envisaged that upon process optimisation and refinement for Ctag-dependent vector purification, Ctag-LVs produced either transiently or stably from packaging cells, may be processed in a fully-automated operation unit which allows for microfiltration followed by a continuous chromatographic streptavidin-based column for affinity purification. Such a specific and efficient downstream processing of LVs could effectively replace the current multi-step technologies employed for large-scale vector bioprocessing for both research and clinical applications. With their increasing demand in both pre-clinical and clinical studies, this in turn would aid the progression of LV gene therapies towards wider supply for routine clinical practices.

8.2.6 Potential application of passive incorporation beyond vector purification

The development of this project has far reaching applications beyond vector purifications, which can also be applied to different vectors based on envelopes viruses such as γ-RV. The passive process of “painting” viral particles with exogenously expressed surface proteins opens up the possibility of endowing vector particles with new functions. As our laboratory specialises

in the production of genetically engineered CAR-T cells for immunotherapy applications, a project was developed in which we aimed at engineering viruses to deliver lymphocyte stimulation as well as transduction in a one-step process.

Although, LV vectors can efficiently transfer genes into T lymphocytes some cells still remain refractory to lentiviral transduction despite several improvements (Follenzi et al., 2000; Salmon et al., 2000). In particular, this includes early progenitor hematopoietic stem cells in G0 (Sutton et al., 1999) and resting T lymphocytes (Dardalhon et al., 2001). However, it has been shown that inducing resting T cells to enter the G1b cell cycle phase by stimulation through the T-cell receptor (signal 1) and CD28 co-stimulation receptor (signal 2) using anti-CD3 and anti-CD28 antibodies, renders cells susceptible to HIV-1 infection (Korin and Zack, 1998). The common practice to transduce T cells *ex vivo* uses this accepted two-signal model of lymphocyte activation (June et al., 1994), with clinical grade monoclonal antibodies (mAbs) against both CD3 and CD28. Commercially available products for these antibodies are either in a soluble format (Miltenyi Biotec), covalently coupled to magnetic beads (Dynabeads® Human T-Activator CD3/CD28, Thermofisher Scientific) or conjugated to polymeric nanomatrix (TransAct CD3/CD28 kit, Miltenyi Biotec), all of which are very expensive. The preferred method of activation is achieved by using Dynabeads® Human T-Activator CD3/CD28 which has been shown to induce superior stimulation of cells compared to soluble mAbs (Levine and June, 2013). Since these beads are under restricted license and require an extra step for their removal in CAR T cell manufacturing, it is desirable to induce T cell stimulation followed by transduction in a simplified manner.

It was proposed that if single chain variable fragments (scFvs) of anti-CD3 and anti-CD28 mAbs are expressed on LV surfaces, then both activation and transduction of T cells would occur in a one-step process. There is however a precedent for the expression of aCD3 scFv on LVs, whereby the MLV envelope was engineered to express the protein on its amino terminus

(Maurice et al., 2002). Even though modified viral particles targeted T cells and induced their activation, infectivity was very poor due to deficient fusion activity. To overcome this limitation and rescue infectivity, chimeric envelopes were co-expressed with wild-type VSV-g. The process of viral particle painting relieves this problem as membrane bound scFv of aCD3 and aCD28 expressed on CD8α stalks would get passively incorporated onto viral particles, in a similar manner as Ctag. This method may offer several advantages over the current protocol used for *ex vivo* T cell expansion and activation for LV transduction by eliminating the need to purchase expensive reagents and reducing time in culture for adoptive T cell therapy protocols. Moreover, this process may also enable the modulation of lymphocyte signals as desired. Since the expression of scFvs on viral particles is achieved by retroviral transduction of LV producer cells, regulating the transduction efficiencies of these cells can therefore modify the type of molecules and their plasma membrane densities. Optimal T cell stimulations can then be reached by fine-tuning the viral painting process. For example, both signal 1 and 2 (aCD3 and aCD28) can be expressed along with various cytokines such as IL15 and IL7 that have been shown to induce differentiation of naïve cells into memory phenotype (Cieri et al., 2013), which has been shown to be associated with efficient CAR modified T cell efficacy and persistence *in vivo* (Sun et al., 2015). Therefore, if this method induces similar transduction and stimulation profile of LV modified CAR T cells compared to Dynabeads® Human T-Activator CD3/CD28, its application would shorten production process; as well as enable modulation of product stimulation and differentiation for optimal anti-tumour efficacy.

Finally, the merger of Ctag along with scFvs for T cell stimulation onto viral vectors may ultimately allow (i) their purification, either by affinity chromatography or magnetic bead capture by streptavidin, followed by (ii) the simultaneous activation and transduction of T lymphocytes. Such a process would further enhance the production of CAR T cell therapy and progressing their clinical applications.

Appendix

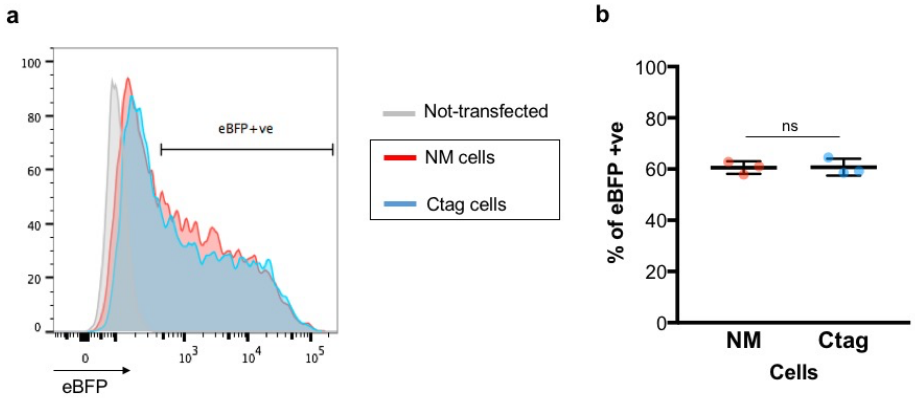

Appendix 1: Testing engineered Ctag-cells' transfectibility. NM- and Ctag- 293T cells were transiently transfected with MLV-based plasmid SFG.eBFP. Marker expression was determined 48 hours after transfection by flow cytometry. **(a)** Overlaid histogram of BFP expression of NT, NM and Ctag cells (which were gated for eGFP to ensure analysis of Ctag-positive cells). **(b)** Percentage of BFP positive cells for Nm and Ctag cells are presented with ± standard deviation (SD) of triplicate determinations, with non-significant (ns) $p > 0.05$.

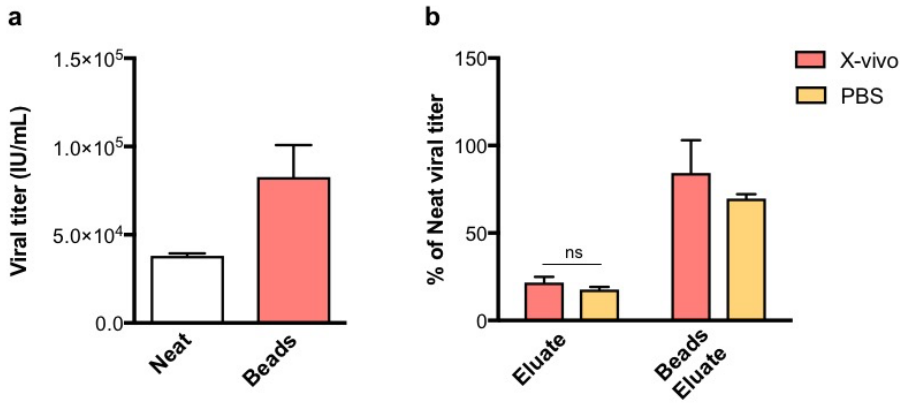

Appendix 2: Comparison of Ctag-LV recovery using X-vivo™ and PBS. (a) Ctag-LV from vector stock was thawed and subjected to developed purification using streptavidin magnetic Dynabeads. Viral titres of starting material (neat) and collected bead fractions were determined by infectivity assay. (b) Vector captured on beads were then incubated with either X-vivo™ or PBS supplemented with 500µM biotin and 0.5% BSA for 2 hours at 4°C. Eluate and beads eluate fractions were collected and their viral titres were determined and plotted as percentage of starting material. Values are presented with are presented with ± standard deviation (SD) of triplicate determinations, with non-significant (ns) $p > 0.05$.

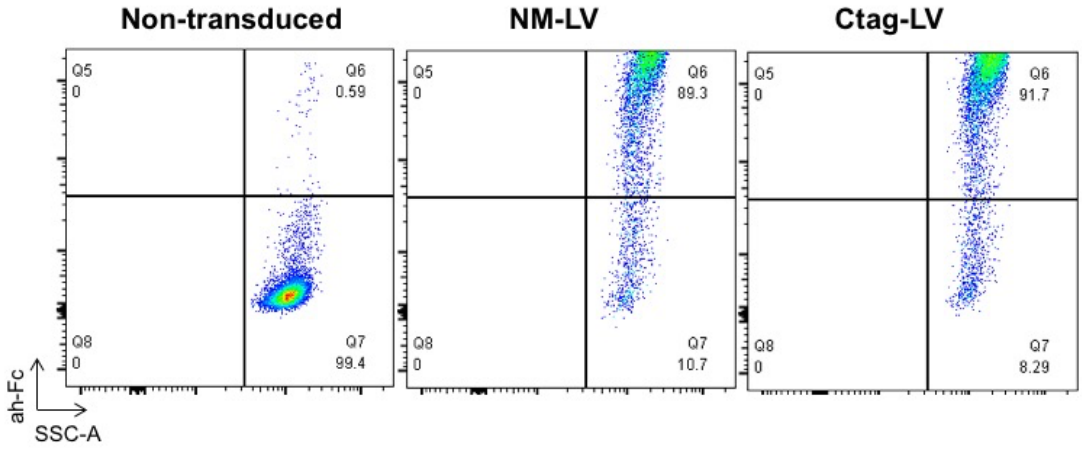

Appendix 3: Assessment of Ctag-LV efficiency for T-cell transduction. RDpro pseudotyped LV particles encoding a chimeric antigen receptor (CAR) with a human-Fc spacer were produced from both NM- and Ctag-293T cells. Both virus supernatants (NM-LV and Ctag-LV) were then used to transduce T-cell derived from a healthy donor using retronectin-coated plates. Post-retronectin recovery, non-transduced and transduced T cells were harvested and stained with an anti-human-Fc (ah-Fc-649) antibody to determine transduction efficiencies by Flow Cytometry (FACS). Dot plots of ah-Fc vs SSC-A are presented for each sample.

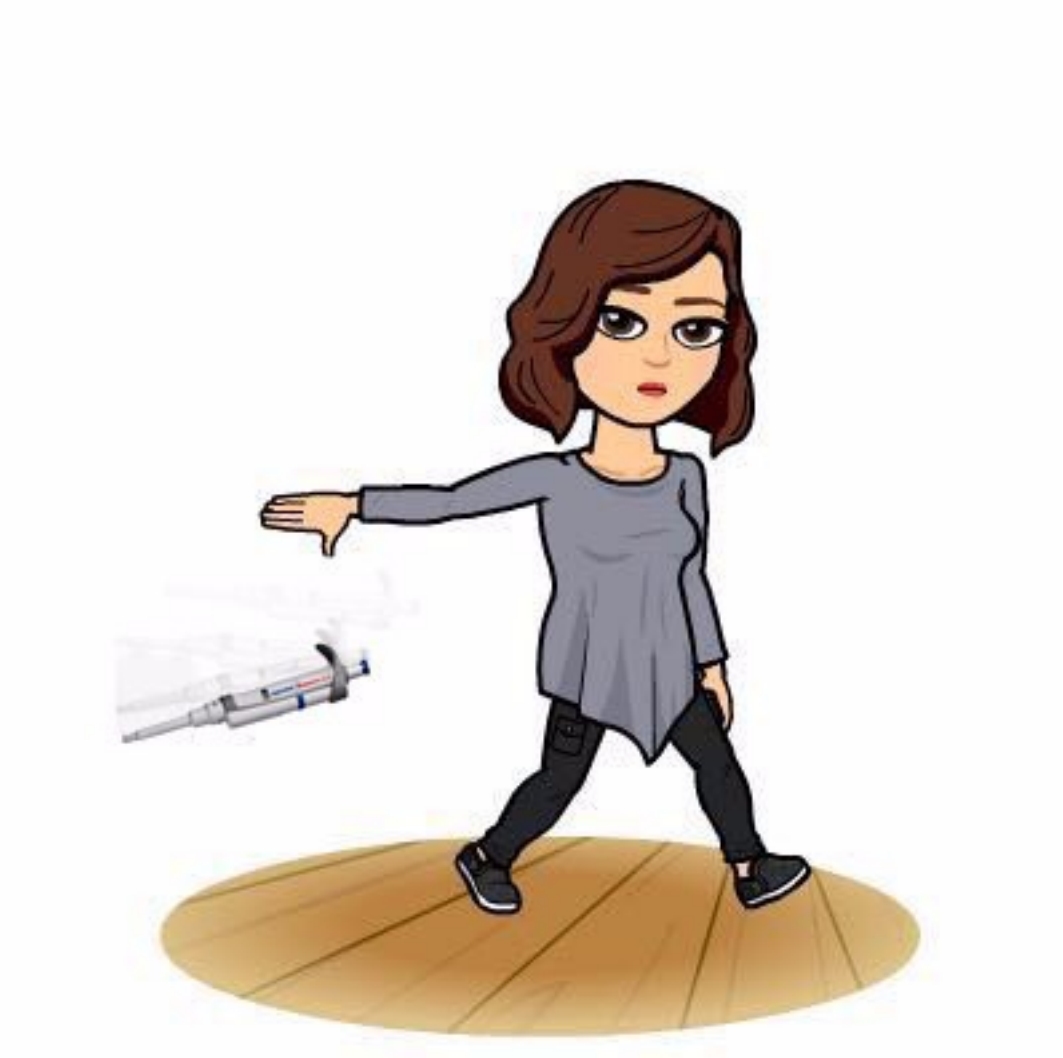

References

1. Abordo-Adesida, E., Follenzi, A., Barcia, C., Sciascia, S., Castro, M.G., Naldini, L., Lowenstein, P.R., 2005. Stability of lentiviral vector-mediated transgene expression in the brain in the presence of systemic antivector immune responses. Hum. Gene Ther. 16, 741–751. doi:10.1089/hum.2005.16.741
2. Ageichik, A., Buchholz, C.J., Collins, M.K., 2011. Lentiviral vectors targeted to MHC II are effective in immunization. Hum. Gene Ther. 22, 1249–1254. doi:10.1089/hum.2010.184
3. Ahani, R., Roohvand, F., Cohan, R.A., Etemadzadeh, M.H., Mohajel, N., Behdani, M., Shahosseini, Z., Madani, N., Azadmanesh, K., 2016. Sindbis Virus-Pseudotyped Lentiviral Vectors Carrying VEGFR2-Specific Nanobody for Potential Transductional Targeting of Tumor Vasculature. Mol. Biotechnol. 58, 738–747. doi:10.1007/s12033-016-9973-7
4. Aiuti, A., Biasco, L., Scaramuzza, S., Ferrua, F., Cicalese, M.P., Baricordi, C., Dionisio, F., Calabria, A., Giannelli, S., Castiello, M.C., Bosticardo, M., Evangelio, C., Assanelli, A., Casiraghi, M., Nunzio, S.D., Callegaro, L., Benati, C., Rizzardi, P., Pellin, D., Serio, C.D., Schmidt, M., Kalle, C.V., Gardner, J., Mehta, N., Neduva, V., Dow, D.J., Galy, A., Miniero, R., Finocchi, A., Metin, A., Banerjee, P.P., Orange, J.S., Galimberti, S., Valsecchi, M.G., Biffi, A., Montini, E., Villa, A., Ciceri, F., Roncarolo, M.G., Naldini, L., 2013. Lentiviral Hematopoietic Stem Cell Gene Therapy in Patients with Wiskott-Aldrich Syndrome. Science 341, 1233151. doi:10.1126/science.1233151
5. Anderson, W.F., Blaese, R.M., Culver, K., 1990. The ADA human gene therapy clinical protocol: Points to Consider response with clinical protocol, July 6, 1990. Hum. Gene Ther. 1, 331–362. doi:10.1089/hum.1990.1.3-331
6. Andreadis, S.T., Roth, C.M., Le Doux, J.M., Morgan, J.R., Yarmush, M.L., 1999. Large-Scale Processing of Recombinant Retroviruses for Gene Therapy. Biotechnol. Prog. 15, 1–11. doi:10.1021/bp980106m
7. Anliker, B., Abel, T., Kneissl, S., Hlavaty, J., Caputi, A., Brynza, J., Schneider, I.C., Münch, R.C., Petznek, H., Kontermann, R.E., Koehl, U., Johnston, I.C.D., Keinänen, K., Müller, U.C., Hohenadl, C., Monyer, H., Cichutek, K., Buchholz, C.J., 2010. Specific gene transfer to neurons, endothelial cells and hematopoietic progenitors with lentiviral vectors. Nat. Methods 7, 929–935. doi:10.1038/nmeth.1514
8. Annoni, A., Battaglia, M., Follenzi, A., Lombardo, A., Sergi-Sergi, L., Naldini, L., Roncarolo, M.-G., 2007. The immune response to lentiviral-delivered transgene is modulated in vivo by transgene-expressing antigen-presenting cells but not by CD4+CD25+ regulatory T cells. Blood 110, 1788–1796. doi:10.1182/blood-2006-11-059873
9. Ansorge, S., Henry, O., Kamen, A., 2010. Recent progress in lentiviral vector mass production. Biochem. Eng. J., Invited Review Issue 2010 48, 362–377. doi:10.1016/j.bej.2009.10.017
10. Ansorge, S., Lanthier, S., Transfiguracion, J., Durocher, Y., Henry, O., Kamen, A., 2009. Development of a scalable process for high-yield lentiviral

vector production by transient transfection of HEK293 suspension cultures. J. Gene Med. 11, 868–876. doi:10.1002/jgm.1370
11. Argaraña, C.E., Kuntz, I.D., Birken, S., Axel, R., Cantor, C.R., 1986. Molecular cloning and nucleotide sequence of the streptavidin gene. Nucleic Acids Res. 14, 1871–1882.
12. Arhel, N.J., Souquere-Besse, S., Munier, S., Souque, P., Guadagnini, S., Rutherford, S., Prévost, M.-C., Allen, T.D., Charneau, P., 2007. HIV-1 DNA Flap formation promotes uncoating of the pre-integration complex at the nuclear pore. EMBO J. 26, 3025–3037. doi:10.1038/sj.emboj.7601740
13. Ausubel, L.J., Hall, C., Sharma, A., Shakeley, R., Lopez, P., Quezada, V., Couture, S., Laderman, K., McMahon, R., Huang, P., Hsu, D., Couture, L., 2012. Production of CGMP-Grade Lentiviral Vectors. BioProcess Int. 10, 32–43.
14. Baek, H., Uchida, H., Jun, K., Kim, J.-H., Kuroki, M., Cohen, J.B., Glorioso, J.C., Kwon, H., 2011. Bispecific Adapter-Mediated Retargeting of a Receptor-Restricted HSV-1 Vector to CEA-Bearing Tumor Cells. Mol. Ther. 19, 507–514. doi:10.1038/mt.2010.207
15. Baekelandt, V., Eggermont, K., Michiels, M., Nuttin, B., Debyser, Z., 2003. Optimized lentiviral vector production and purification procedure prevents immune response after transduction of mouse brain. Gene Ther. 10, 1933–1940. doi:10.1038/sj.gt.3302094
16. Bandeira, V., Peixoto, C., Rodrigues, A.F., Cruz, P.E., Alves, P.M., Coroadinha, A.S., Carrondo, M.J.T., 2012a. Downstream processing of lentiviral vectors: releasing bottlenecks. Hum. Gene Ther. Methods 23, 255–263. doi:10.1089/hgtb.2012.059
17. Bandeira, V., Peixoto, C., Rodrigues, A.F., Cruz, P.E., Alves, P.M., Coroadinha, A.S., Carrondo, M.J.T., 2012b. Downstream processing of lentiviral vectors: releasing bottlenecks. Hum. Gene Ther. Methods 23, 255–263. doi:10.1089/hgtb.2012.059
18. Bandeira, V., Peixoto, C., Rodrigues, A.F., Cruz, P.E., Alves, P.M., Coroadinha, A.S., Carrondo, M.J.T., 2012c. Downstream Processing of Lentiviral Vectors: Releasing Bottlenecks. Hum. Gene Ther. Methods 23, 255–263. doi:10.1089/hgtb.2012.059
19. Barnett, A.L., Cunningham, J.M., 2001. Receptor Binding Transforms the Surface Subunit of the Mammalian C-Type Retrovirus Envelope Protein from an Inhibitor to an Activator of Fusion. J. Virol. 75, 9096–9105. doi:10.1128/JVI.75.19.9096-9105.2001
20. Barrette-Ng, I.H., Wu, S.-C., Tjia, W.-M., Wong, S.-L., Ng, K.K.S., 2013. The structure of the SBP-Tag–streptavidin complex reveals a novel helical scaffold bridging binding pockets on separate subunits. Acta Crystallogr. D Biol. Crystallogr. 69, 879–887. doi:10.1107/S0907444913002576
21. Barry, M.A., Campos, S.K., Ghosh, D., Adams, K.E., Mok, H., Mercier, G.T., Parrott, M.B., 2003. Biotinylated gene therapy vectors. Expert Opin. Biol. Ther. 3, 925–940. doi:10.1517/14712598.3.6.925
22. Bartel, M., Schaffer, D., Büning, H., 2011. Enhancing the Clinical Potential of AAV Vectors by Capsid Engineering to Evade Pre-Existing Immunity. Front. Microbiol. 2. doi:10.3389/fmicb.2011.00204
23. Bates, D.L., Barthel, K.K.B., Wu, Y., Kalhor, R., Stroud, J.C., Giffin, M.J., Chen, L., 2008. Crystal structure of NFAT bound to the HIV-1 LTR

tandem kappaB enhancer element. Struct. Lond. Engl. 1993 16, 684–694. doi:10.1016/j.str.2008.01.020
24. Baugh, L., Le Trong, I., Stayton, P.S., Stenkamp, R.E., Lybrand, T.P., 2016. A Streptavidin Binding Site Mutation Yields an Unexpected Result: An Ionized Asp128 Residue Is Not Essential for Strong Biotin Binding. Biochemistry (Mosc.) 55, 5201–5203. doi:10.1021/acs.biochem.6b00698
25. Baumann, F., Bauer, M.S., Milles, L.F., Alexandrovich, A., Gaub, H.E., Pippig, D.A., 2016. Monovalent Strep-Tactin for strong and site-specific tethering in nanospectroscopy. Nat. Nanotechnol. 11, 89–94. doi:10.1038/nnano.2015.231
26. Baumgärtel, V., Ivanchenko, S., Dupont, A., Sergeev, M., Wiseman, P.W., Kräusslich, H.-G., Bräuchle, C., Müller, B., Lamb, D.C., 2011. Live-cell visualization of dynamics of HIV budding site interactions with an ESCRT component. Nat. Cell Biol. 13, 469–474. doi:10.1038/ncb2215
27. Beckett, D., Kovaleva, E., Schatz, P.J., 1999. A minimal peptide substrate in biotin holoenzyme synthetase-catalyzed biotinylation. Protein Sci. 8, 921–929. doi:10.1110/ps.8.4.921
28. Beer, C., Meyer, A., Müller, K., Wirth, M., 2003. The temperature stability of mouse retroviruses depends on the cholesterol levels of viral lipid shell and cellular plasma membrane. Virology 308, 137–146.
29. Bell, A.J., Fegen, D., Ward, M., Bank, A., 2010. RD114 envelope proteins provide an effective and versatile approach to pseudotype lentiviral vectors. Exp. Biol. Med. 235, 1269–1276. doi:10.1258/ebm.2010.010053
30. Bellintani, 2009. 723. Large Scale Process for the Production and Purification of Lentiviral Vectors for Clinical Applications. Mol. Ther. 17, S276. doi:10.1016/S1525-0016(16)39081-5
31. Bender, E., 2016. Gene therapy: Industrial strength. Nature 537, S57–S59. doi:10.1038/537S57a
32. Bessis, N., GarciaCozar, F.J., Boissier, M.-C., 2004. Immune responses to gene therapy vectors: influence on vector function and effector mechanisms. Gene Ther. 11 Suppl 1, S10-17. doi:10.1038/sj.gt.3302364
33. Bestor, T.H., 2000. Gene silencing as a threat to the success of gene therapy. J. Clin. Invest. 105, 409–411.
34. Biffi, A., Bartolomae, C.C., Cesana, D., Cartier, N., Aubourg, P., Ranzani, M., Cesani, M., Benedicenti, F., Plati, T., Rubagotti, E., Merella, S., Capotondo, A., Sgualdino, J., Zanetti, G., von Kalle, C., Schmidt, M., Naldini, L., Montini, E., 2011. Lentiviral vector common integration sites in preclinical models and a clinical trial reflect a benign integration bias and not oncogenic selection. Blood 117, 5332–5339. doi:10.1182/blood-2010-09-306761
35. Binder, G.K., Dropulic, B., 2008. Lentivirus Vectors, in: Boroopulic, Carter, B.J. (Eds.), Concepts in Genetic Medicine. John Wiley & Sons, Inc., pp. 19–37. doi:10.1002/9780470184585.ch3
36. Bischof, D., Cornetta, K., 2010. Flexibility in cell targeting by pseudotyping lentiviral vectors. Methods Mol. Biol. Clifton NJ 614, 53–68. doi:10.1007/978-1-60761-533-0_3
37. Blaese, R.M., Culver, K.W., Miller, A.D., Carter, C.S., Fleisher, T., Clerici, M., Shearer, G., Chang, L., Chiang, Y., Tolstoshev, P., Greenblatt, J.J., Rosenberg, S.A., Klein, H., Berger, M., Mullen, C.A., Ramsey, W.J.,

Muul, L., Morgan, R.A., Anderson, W.F., 1995. T lymphocyte-directed gene therapy for ADA- SCID: initial trial results after 4 years. Science 270, 475–480.
38. Blumenthal, R., Durell, S., Viard, M., 2012. HIV Entry and Envelope Glycoprotein-mediated Fusion. J. Biol. Chem. 287, 40841–40849. doi:10.1074/jbc.R112.406272
39. Boer, E. de, Rodriguez, P., Bonte, E., Krijgsveld, J., Katsantoni, E., Heck, A., Grosveld, F., Strouboulis, J., 2003. Efficient biotinylation and single-step purification of tagged transcription factors in mammalian cells and transgenic mice. Proc. Natl. Acad. Sci. 100, 7480–7485. doi:10.1073/pnas.1332608100
40. Bolen, D.W., Baskakov, I.V., 2001. The osmophobic effect: natural selection of a thermodynamic force in protein folding1. J. Mol. Biol. 310, 955–963. doi:10.1006/jmbi.2001.4819
41. Bonini, C., Grez, M., Traversari, C., Ciceri, F., Marktel, S., Ferrari, G., Dinauer, M., Sadat, M., Aiuti, A., Deola, S., Radrizzani, M., Hagenbeek, A., Apperley, J., Ebeling, S., Martens, A., Kolb, H.J., Weber, M., Lotti, F., Grande, A., Weissinger, E., Bueren, J.A., Lamana, M., Falkenburg, J.H.F., Heemskerk, M.H.M., Austin, T., Kornblau, S., Marini, F., Benati, C., Magnani, Z., Cazzaniga, S., Toma, S., Gallo-Stampino, C., Introna, M., Slavin, S., Greenberg, P.D., Bregni, M., Mavilio, F., Bordignon, C., 2003. Safety of retroviral gene marking with a truncated NGF receptor. Nat. Med. 9, 367–369. doi:10.1038/nm0403-367
42. Bonner, M., Ma, Z., Zhou, S., Ren, A., Chandrasekaran, A., Gray, J.T., Sorrentino, B.P., Throm, R.E., 2015. 81. Development of a Second Generation Stable Lentiviral Packaging Cell Line in Support of Clinical Gene Transfer Protocols. Mol. Ther. 23, S35. doi:10.1016/S1525-0016(16)33686-3
43. Bourinbaiar, A.S., 1994. The ratio of defective HIV-1 particles to replication-competent infectious virions. Acta Virol. 38, 59–61.
44. Brandau, D.T., Jones, L.S., Wiethoff, C.M., Rexroad, J., Middaugh, C.R., 2003. Thermal stability of vaccines. J. Pharm. Sci. 92, 218–231. doi:10.1002/jps.10296
45. Breckpot, K., Escors, D., Arce, F., Lopes, L., Karwacz, K., Lint, S.V., Keyaerts, M., Collins, M., 2010. HIV-1 Lentiviral Vector Immunogenicity Is Mediated by Toll-Like Receptor 3 (TLR3) and TLR7. J. Virol. 84, 5627–5636. doi:10.1128/JVI.00014-10
46. Brenner, M.K., Heslop, H.E., 2003. Is retroviral gene marking too dangerous to use? Cytotherapy 5, 190–193. doi:10.1080/14653240310001307
47. Brentjens, R.J., Davila, M.L., Riviere, I., Park, J., Wang, X., Cowell, L.G., Bartido, S., Stefanski, J., Taylor, C., Olszewska, M., Borquez-Ojeda, O., Qu, J., Wasielewska, T., He, Q., Bernal, Y., Rijo, I.V., Hedvat, C., Kobos, R., Curran, K., Steinherz, P., Jurcic, J., Rosenblat, T., Maslak, P., Frattini, M., Sadelain, M., 2013. CD19-Targeted T Cells Rapidly Induce Molecular Remissions in Adults with Chemotherapy-Refractory Acute Lymphoblastic Leukemia. Sci. Transl. Med. 5, 177ra38-177ra38. doi:10.1126/scitranslmed.3005930

48. Briggs, J.A.G., Wilk, T., Fuller, S.D., 2003. Do lipid rafts mediate virus assembly and pseudotyping? J. Gen. Virol. 84, 757–768. doi:10.1099/vir.0.18779-0
49. Briggs, J.A.G., Wilk, T., Welker, R., Kräusslich, H.-G., Fuller, S.D., 2003. Structural organization of authentic, mature HIV-1 virions and cores. EMBO J. 22, 1707–1715. doi:10.1093/emboj/cdg143
50. Bruch, R.C., White, H.B., 1982. Compositional and structural heterogeneity of avidin glycopeptides. Biochemistry (Mosc.) 21, 5334–5341. doi:10.1021/bi00264a033
51. Bryant, L.M., Christopher, D.M., Giles, A.R., Hinderer, C., Rodriguez, J.L., Smith, J.B., Traxler, E.A., Tycko, J., Wojno, A.P., Wilson, J.M., 2013. Lessons learned from the clinical development and market authorization of Glybera. Hum. Gene Ther. Clin. Dev. 24, 55–64. doi:10.1089/humc.2013.087
52. Buchholz, C.J., Friedel, T., Büning, H., 2015. Surface-Engineered Viral Vectors for Selective and Cell Type-Specific Gene Delivery. Trends Biotechnol. 33, 777–790. doi:10.1016/j.tibtech.2015.09.008
53. Büeler, H., Mulligan, R.C., 1996. Induction of antigen-specific tumor immunity by genetic and cellular vaccines against MAGE: enhanced tumor protection by coexpression of granulocyte-macrophage colony-stimulating factor and B7-1. Mol. Med. Camb. Mass 2, 545–555.
54. Bukrinsky, M.I., Haggerty, S., Dempsey, M.P., Sharova, N., Adzhubel, A., Spitz, L., Lewis, P., Goldfarb, D., Emerman, M., Stevenson, M., 1993. A nuclear localization signal within HIV-1 matrix protein that governs infection of non-dividing cells. Nature 365, 666–669. doi:10.1038/365666a0
55. Bürckstümmer, T., Bennett, K.L., Preradovic, A., Schütze, G., Hantschel, O., Superti-Furga, G., Bauch, A., 2006. An efficient tandem affinity purification procedure for interaction proteomics in mammalian cells. Nat. Methods 3, 1013–1019. doi:10.1038/nmeth968
56. Burns, J.C., Friedmann, T., Driever, W., Burrascano, M., Yee, J.K., 1993. Vesicular stomatitis virus G glycoprotein pseudotyped retroviral vectors: concentration to very high titre and efficient gene transfer into mammalian and nonmammalian cells. Proc. Natl. Acad. Sci. U. S. A. 90, 8033–8037.
57. Campbell, E.M., Hope, T.J., 2015. HIV-1 capsid: the multifaceted key player in HIV-1 infection. Nat. Rev. Microbiol. 13, 471–483. doi:10.1038/nrmicro3503
58. Campos, S.K., Parrott, M.B., Barry, M.A., 2004. Avidin-Based Targeting and Purification of a Protein IX-Modified, Metabolically Biotinylated Adenoviral Vector. Mol. Ther. J. Am. Soc. Gene Ther. 9, 942–954. doi:10.1016/j.ymthe.2004.03.006
59. Carmo, M., Alves, A., Rodrigues, A.F., Coroadinha, A.S., Carrondo, M.J.T., Alves, P.M., Cruz, P.E., 2009. Stabilization of gammaretroviral and lentiviral vectors: from production to gene transfer. J. Gene Med. 11, 670–678. doi:10.1002/jgm.1353
60. Carmo, M., Panet, A., Carrondo, M.J.T., Alves, P.M., Cruz, P.E., 2008. From retroviral vector production to gene transfer: spontaneous inactivation is caused by loss of reverse transcription capacity. J. Gene Med. 10, 383–391. doi:10.1002/jgm.1163

61. Cartellieri, M., Bachmann, M., Feldmann, A., Bippes, C., Stamova, S., Wehner, R., Temme, A., Schmitz, M., Cartellieri, M., Bachmann, M., Feldmann, A., Bippes, C., Stamova, S., Wehner, R., Temme, A., Schmitz, M., 2010. Chimeric Antigen Receptor-Engineered T Cells for Immunotherapy of Cancer, Chimeric Antigen Receptor-Engineered T Cells for Immunotherapy of Cancer. BioMed Res. Int. BioMed Res. Int. 2010, 2010, e956304. doi:10.1155/2010/956304, 10.1155/2010/956304
62. Cass, B., Pham, P.L., Kamen, A., Durocher, Y., 2005. Purification of recombinant proteins from mammalian cell culture using a generic double-affinity chromatography scheme. Protein Expr. Purif. 40, 77–85. doi:10.1016/j.pep.2004.10.023
63. Chadwick, M.P., Morling, F.J., Cosset, F.L., Russell, S.J., 1999. Modification of retroviral tropism by display of IGF-I. J. Mol. Biol. 285, 485–494. doi:10.1006/jmbi.1998.2350
64. Chaiet, L., Wolf, F.J., 1964. THE PROPERTIES OF STREPTAVIDIN, A BIOTIN-BINDING PROTEIN PRODUCED BY STREPTOMYCETES. Arch. Biochem. Biophys. 106, 1–5.
65. Chan, D.C., Fass, D., Berger, J.M., Kim, P.S., 1997. Core Structure of gp41 from the HIV Envelope Glycoprotein. Cell 89, 263–273. doi:10.1016/S0092-8674(00)80205-6
66. Chan, L., Nesbeth, D., MacKey, T., Galea-Lauri, J., Gäken, J., Martin, F., Collins, M., Mufti, G., Farzaneh, F., Darling, D., 2005. Conjugation of Lentivirus to Paramagnetic Particles via Nonviral Proteins Allows Efficient Concentration and Infection of Primary Acute Myeloid Leukemia Cells. J. Virol. 79, 13190–13194. doi:10.1128/JVI.79.20.13190-13194.2005
67. Charcosset, C., 2006. Membrane processes in biotechnology: An overview. Biotechnol. Adv. 24, 482–492. doi:10.1016/j.biotechadv.2006.03.002
68. Charneau, P., Mirambeau, G., Roux, P., Paulous, S., Buc, H., Clavel, F., 1994. HIV-1 reverse transcription. A termination step at the center of the genome. J. Mol. Biol. 241, 651–662. doi:10.1006/jmbi.1994.1542
69. Check, E., 2005. Sanctions agreed over teenager's gene-therapy death. Nature 433, 674–674. doi:10.1038/433674b
70. Checkley, M.A., Luttge, B.G., Freed, E.O., 2011. HIV-1 Envelope Glycoprotein Biosynthesis, Trafficking, and Incorporation. J. Mol. Biol. 410, 582–608. doi:10.1016/j.jmb.2011.04.042
71. Cheeks, M.C., Kamal, N., Sorrell, A., Darling, D., Farzaneh, F., Slater, N.K.H., 2009. Immobilized metal affinity chromatography of histidine-tagged lentiviral vectors using monolithic adsorbents. J. Chromatogr. A 1216, 2705–2711. doi:10.1016/j.chroma.2008.08.029
72. Chen, H., 2011. Manufacturing of adeno-associated viruses, for example: AAV2. Methods Mol. Biol. Clifton NJ 737, 235–246. doi:10.1007/978-1-61779-095-9_10
73. Chen, R., Folarin, N., Ho, V.H.B., McNally, D., Darling, D., Farzaneh, F., Slater, N.K.H., 2010. Affinity recovery of lentivirus by diaminopelargonic acid mediated desthiobiotin labelling. J. Chromatogr. B 878, 1939–1945. doi:10.1016/j.jchromb.2010.05.019

74. Chen, Y.-H., Wang, C.-H., Chang, C.-W., Peng, C.-A., 2010. In situ formation of viruses tagged with quantum dots. Integr. Biol. 2, 258–264. doi:10.1039/B926852A
75. Chilkoti, A., Stayton, P.S., 1995. Molecular Origins of the Slow Streptavidin-Biotin Dissociation Kinetics. J. Am. Chem. Soc. 117, 10622–10628. doi:10.1021/ja00148a003
76. Chilkoti, A., Tan, P.H., Stayton, P.S., 1995. Site-directed mutagenesis studies of the high-affinity streptavidin-biotin complex: contributions of tryptophan residues 79, 108, and 120. Proc. Natl. Acad. Sci. U. S. A. 92, 1754–1758.
77. Chivers, C.E., Crozat, E., Chu, C., Moy, V.T., Sherratt, D.J., Howarth, M., 2010. A streptavidin variant with slower biotin dissociation and increased mechanostability. Nat. Methods 7, 391–393. doi:10.1038/nmeth.1450
78. Chivers, C.E., Koner, A.L., Lowe, E.D., Howarth, M., 2011. How the biotin–streptavidin interaction was made even stronger: investigation via crystallography and a chimaeric tetramer. Biochem. J. 435, 55–63. doi:10.1042/BJ20101593
79. Choe, H., Farzan, M., Sun, Y., Sullivan, N., Rollins, B., Ponath, P.D., Wu, L., Mackay, C.R., LaRosa, G., Newman, W., Gerard, N., Gerard, C., Sodroski, J., 1996. The beta-chemokine receptors CCR3 and CCR5 facilitate infection by primary HIV-1 isolates. Cell 85, 1135–1148.
80. Chu, T.H., Dornburg, R., 1995. Retroviral vector particles displaying the antigen-binding site of an antibody enable cell-type-specific gene transfer. J. Virol. 69, 2659–2663.
81. Chu, T.H., Martinez, I., Sheay, W.C., Dornburg, R., 1994. Cell targeting with retroviral vector particles containing antibody-envelope fusion proteins. Gene Ther. 1, 292–299.
82. Clements, J.E., Zink, M.C., 1996. Molecular biology and pathogenesis of animal lentivirus infections. Clin. Microbiol. Rev. 9, 100–117.
83. Cockrell, A.S., Kafri, T., 2007. Gene delivery by lentivirus vectors. Mol. Biotechnol. 36, 184–204.
84. Cockrell, A.S., Ma, H., Fu, K., McCown, T.J., Kafri, T., 2006. A Trans-Lentiviral Packaging Cell Line for High-Titre Conditional Self-Inactivating HIV-1 Vectors. Mol. Ther. 14, 276–284. doi:10.1016/j.ymthe.2005.12.015
85. Coffin, J.M., Hughes, S.H., Varmus, H.E., 1997. Retroviral “Lifestyles”: Simple versus Complex. Cold Spring Harbor Laboratory Press.
86. Cooper, A.R., Patel, S., Senadheera, S., Plath, K., Kohn, D.B., Hollis, R.P., 2011. Highly efficient large-scale lentiviral vector concentration by tandem tangential flow filtration. J. Virol. Methods 177, 1–9. doi:10.1016/j.jviromet.2011.06.019
87. Coroadinha, A. s., Silva, A. c., Pires, E., Coelho, A., Alves, P. m., Carrondo, M. j. t., 2006. Effect of osmotic pressure on the production of retroviral vectors: Enhancement in vector stability. Biotechnol. Bioeng. 94, 322–329. doi:10.1002/bit.20847
88. Cosset, F.L., Morling, F.J., Takeuchi, Y., Weiss, R.A., Collins, M.K., Russell, S.J., 1995. Retroviral retargeting by envelopes expressing an N-terminal binding domain. J. Virol. 69, 6314–6322.

89. Couzin, J., Kaiser, J., 2005. Gene therapy. As Gelsinger case ends, gene therapy suffers another blow. Science 307, 1028. doi:10.1126/science.307.5712.1028b
90. Craigie, R., 2001. HIV Integrase, a Brief Overview from Chemistry to Therapeutics. J. Biol. Chem. 276, 23213–23216. doi:10.1074/jbc.R100027200
91. Craigie, R., Bushman, F.D., 2012. HIV DNA Integration. Cold Spring Harb. Perspect. Med. 2. doi:10.1101/cshperspect.a006890
92. Cronan, J.E., 1990. Biotination of proteins in vivo. A post-translational modification to label, purify, and study proteins. J. Biol. Chem. 265, 10327–10333.
93. Cronin, J., Zhang, X.-Y., Reiser, J., 2005. Altering the Tropism of Lentiviral Vectors through Pseudotyping. Curr. Gene Ther. 5, 387–398.
94. Croyle, M.A., Callahan, S.M., Auricchio, A., Schumer, G., Linse, K.D., Wilson, J.M., Brunner, L.J., Kobinger, G.P., 2004. PEGylation of a vesicular stomatitis virus G pseudotyped lentivirus vector prevents inactivation in serum. J. Virol. 78, 912–921.
95. Croyle, M.A., Chirmule, N., Zhang, Y., Wilson, J.M., 2002. PEGylation of E1-deleted adenovirus vectors allows significant gene expression on readministration to liver. Hum. Gene Ther. 13, 1887–1900. doi:10.1089/104303402760372972
96. Croyle, M.A., Yu, Q.-C., Wilson, J.M., 2000. Development of a Rapid Method for the PEGylation of Adenoviruses with Enhanced Transduction and Improved Stability under Harsh Storage Conditions. Hum. Gene Ther. 11, 1713–1722. doi:10.1089/10430340050111368
97. Cruz, P.E., Carmo, M., Coroadinha, A.S., Bengala, A., Gonçalves, D., Teixeira, M., Merten, O.-W., Geny-Fiamma, C., Carrondo, M.J.T., 2005. Retroviral Vector Stability: Inactivation Kinetics and Membrane Properties, in: Animal Cell Technology Meets Genomics. Springer, Dordrecht, pp. 303–308. doi:10.1007/1-4020-3103-3_60
98. Cruz, P.E., Rodrigues, T., Carmo, M., Wirth, D., Amaral, A.I., Alves, P.M., Coroadinha, A.S., 2011. Manufacturing of retroviruses. Methods Mol. Biol. Clifton NJ 737, 157–182. doi:10.1007/978-1-61779-095-9_7
99. Dalgleish, A.G., Beverley, P.C., Clapham, P.R., Crawford, D.H., Greaves, M.F., Weiss, R.A., 1984. The CD4 (T4) antigen is an essential component of the receptor for the AIDS retrovirus. Nature 312, 763–767.
100. e las Mercedes Segura, M., Kamen, A., Garnier, A., 2008. Purification of Retrovirus Particles Using Heparin Affinity Chromatography, in: Le Doux, J., Doux, J.M.L. (Eds.), Gene Therapy Protocols, Methods in Molecular Biology™. Humana Press, pp. 1–11. doi:10.1007/978-1-60327-248-3_1
101. de las Mercedes Segura, M., Kamen, A., Lavoie, M.-C., Garnier, A., 2007. Exploiting heparin-binding properties of MoMLV-based retroviral vectors for affinity chromatography. J. Chromatogr. B 846, 124–131. doi:10.1016/j.jchromb.2006.08.032
102. DeLange, R.J., 1970. Egg white avidin. I. Amino acid composition; sequence of the amino- and carboxyl-terminal cyanogen bromide peptides. J. Biol. Chem. 245, 907–916.

103. Denèfle, P.P., 2011. Introduction to gene therapy: a clinical aftermath. Methods Mol. Biol. Clifton NJ 737, 27–44. doi:10.1007/978-1-61779-095-9_2
104. Deng, H., Liu, R., Ellmeier, W., Choe, S., Unutmaz, D., Burkhart, M., Di Marzio, P., Marmon, S., Sutton, R.E., Hill, C.M., Davis, C.B., Peiper, S.C., Schall, T.J., Littman, D.R., Landau, N.R., 1996. Identification of a major co-receptor for primary isolates of HIV-1. Nature 381, 661–666. doi:10.1038/381661a0
105. DePolo, N.J., Reed, J.D., Sheridan, P.L., Townsend, K., Sauter, S.L., Jolly, D.J., Dubensky, T.W., 2000. VSV-G pseudotyped lentiviral vector particles produced in human cells are inactivated by human serum. Mol. Ther. J. Am. Soc. Gene Ther. 2, 218–222. doi:10.1006/mthe.2000.0116
106. Di Nunzio, F., Piovani, B., Cosset, F.-L., Mavilio, F., Stornaiuolo, A., 2007. Transduction of human hematopoietic stem cells by lentiviral vectors pseudotyped with the RD114-TR chimeric envelope glycoprotein. Hum. Gene Ther. 18, 811–820. doi:10.1089/hum.2006.138
107. Ding, Z., Long, C.J., Hayashi, Y., Bulmus, E.V., Hoffman, A.S., Stayton, P.S., 1999. Temperature control of biotin binding and release with A streptavidin-poly(N-isopropylacrylamide) site-specific conjugate. Bioconjug. Chem. 10, 395–400. doi:10.1021/bc980108s
108. Dolgin, E., 2012. Gene therapies advance, but some see manufacturing challenges. Nat. Med. 18, 1718–1719. doi:10.1038/nm1212-1718
109. Dragic, T., Litwin, V., Allaway, G.P., Martin, S.R., Huang, Y., Nagashima, K.A., Cayanan, C., Maddon, P.J., Koup, R.A., Moore, J.P., Paxton, W.A., 1996. HIV-1 entry into CD4+ cells is mediated by the chemokine receptor CC-CKR-5. Nature 381, 667–673. doi:10.1038/381667a0
110. Dudak, F.C., Boyaci, I.H., Orner, B.P., 2011. The discovery of small-molecule mimicking peptides through phage display. Mol. Basel Switz. 16, 774–789. doi:10.3390/molecules16010774
111. Dull, T., Zufferey, R., Kelly, M., Mandel, R.J., Nguyen, M., Trono, D., Naldini, L., 1998. A third-generation lentivirus vector with a conditional packaging system. J. Virol. 72, 8463–8471.
112. Dundas, C.M., Demonte, D., Park, S., 2013a. Streptavidin-biotin technology: improvements and innovations in chemical and biological applications. Appl. Microbiol. Biotechnol. 97, 9343–9353. doi:10.1007/s00253-013-5232-z
113. Dundas, C.M., Demonte, D., Park, S., 2013b. Streptavidin–biotin technology: improvements and innovations in chemical and biological applications. Appl. Microbiol. Biotechnol. 97, 9343–9353. doi:10.1007/s00253-013-5232-z
114. Dunn, D.E., Yu, J., Nagarajan, S., Devetten, M., Weichold, F.F., Medof, M.E., Young, N.S., Liu, J.M., 1996. A knock-out model of paroxysmal nocturnal hemoglobinuria: Pig-a(-) hematopoiesis is reconstituted following intercellular transfer of GPI-anchored proteins. Proc. Natl. Acad. Sci. U. S. A. 93, 7938–7943.
115. Durand, S., Cimarelli, A., 2011. The Inside out of Lentiviral Vectors. Viruses 3, 132–159. doi:10.3390/v3020132

116. Earl, L.A., Lifson, J.D., Subramaniam, S., 2013. Catching HIV 'in the act' with 3D electron microscopy. Trends Microbiol. 21, 397–404. doi:10.1016/j.tim.2013.06.004
117. Edelstein, M.L., Abedi, M.R., Wixon, J., Edelstein, R.M., 2004a. Gene therapy clinical trials worldwide 1989-2004-an overview. J. Gene Med. 6, 597–602. doi:10.1002/jgm.619
118. Edelstein, M.L., Abedi, M.R., Wixon, J., Edelstein, R.M., 2004b. Gene therapy clinical trials worldwide 1989–2004—an overview. J. Gene Med. 6, 597–602. doi:10.1002/jgm.619
119. Engelman, A., Mizuuchi, K., Craigie, R., 1991. HIV-1 DNA integration: mechanism of viral DNA cleavage and DNA strand transfer. Cell 67, 1211–1221.
120. Escors, D., Breckpot, K., 2010. Lentiviral vectors in gene therapy: their current status and future potential. Arch. Immunol. Ther. Exp. (Warsz.) 58, 107–119. doi:10.1007/s00005-010-0063-4
121. Eshhar, Z., Waks, T., Gross, G., 2014. The emergence of T-bodies/CAR T cells. Cancer J. Sudbury Mass 20, 123–126. doi:10.1097/PPO.0000000000000027
122. Etemadzadeh, M.H., Arashkia, A., Roohvand, F., Ahani, R., Mohajel, N., Baniasadi, V., Norouzian, D., Azadmanesh, K., 2015. Expression of a biotin acceptor peptide-containing protein with potential incorporation on the lentiviral envelope as a viral surface engineering platform. Res. Pharm. Sci. 10, 268–274.
123. Fairhead, M., Howarth, M., 2015. Site-specific biotinylation of purified proteins using BirA. Methods Mol. Biol. Clifton NJ 1266, 171–184. doi:10.1007/978-1-4939-2272-7_12
124. Fan, J., Jiang, L., Zhou, Z., 2015. Recombinant lentiviral vector formulation. EP2829285 A4.
125. Farson, D., Witt, R., McGuinness, R., Dull, T., Kelly, M., Song, J., Radeke, R., Bukovsky, A., Consiglio, A., Naldini, L., 2001. A New-Generation Stable Inducible Packaging Cell Line for Lentiviral Vectors. Hum. Gene Ther. 12, 981–997. doi:10.1089/104303401750195935
126. FDA, C. for B.E. and, 1998. Cellular & Gene Therapy Guidances - Guidance for Industry: Guidance for Human Somatic Cell Therapy and Gene Therapy [WWW Document]. URL https://www.fda.gov/biologicsbloodvaccines/guidancecomplianceregulatoryinformation/guidances/cellularandgenetherapy/ucm072987.htm (accessed 7.8.17).
127. Feng, Y., Broder, C.C., Kennedy, P.E., Berger, E.A., 1996. HIV-1 entry cofactor: functional cDNA cloning of a seven-transmembrane, G protein-coupled receptor. Science 272, 872–877.
128. Fernandes, C.S.M., Barbosa, I., Castro, R., Pina, A.S., Coroadinha, A.S., Barbas, A., Roque, A.C.A., 2016. Retroviral particles are effectively purified on an affinity matrix containing peptides selected by phage-display. Biotechnol. J. 11, 1513–1524. doi:10.1002/biot.201600025
129. Fielding, A.K., Maurice, M., Morling, F.J., Cosset, F.-L., Russell, S.J., 1998. Inverse Targeting of Retroviral Vectors: Selective Gene Transfer in a Mixed Population of Hematopoietic and Nonhematopoietic Cells. Blood 91, 1802–1809.

130. Finkelshtein, D., Werman, A., Novick, D., Barak, S., Rubinstein, M., 2013. LDL receptor and its family members serve as the cellular receptors for vesicular stomatitis virus. Proc. Natl. Acad. Sci. U. S. A. 110, 7306–7311. doi:10.1073/pnas.1214441110
131. Fischer, A., Hacein-Bey-Abina, S., Cavazzana-Calvo, M., 2010. 20 years of gene therapy for SCID. Nat. Immunol. 11, 457–460. doi:10.1038/ni0610-457
132. Fitzpatrick, K., Skasko, M., Deerinck, T.J., Crum, J., Ellisman, M.H., Guatelli, J., 2010. Direct Restriction of Virus Release and Incorporation of the Interferon-Induced Protein BST-2 into HIV-1 Particles. PLOS Pathog. 6, e1000701. doi:10.1371/journal.ppat.1000701
133. Fletcher, T.M., Brichacek, B., Sharova, N., Newman, M.A., Stivahtis, G., Sharp, P.M., Emerman, M., Hahn, B.H., Stevenson, M., 1996. Nuclear import and cell cycle arrest functions of the HIV-1 Vpr protein are encoded by two separate genes in HIV-2/SIV(SM). EMBO J. 15, 6155–6165.
134. Fogen, D., Wu, S.-C., Ng, K.K.-S., Wong, S.-L., 2015. Engineering Streptavidin and a Streptavidin-Binding Peptide with Infinite Binding Affinity and Reversible Binding Capability: Purification of a Tagged Recombinant Protein to High Purity via Affinity-Driven Thiol Coupling. PLOS ONE 10, e0139137. doi:10.1371/journal.pone.0139137
135. Follenzi, A., Battaglia, M., Lombardo, A., Annoni, A., Roncarolo, M.G., Naldini, L., 2004. Targeting lentiviral vector expression to hepatocytes limits transgene-specific immune response and establishes long-term expression of human antihemophilic factor IX in mice. Blood 103, 3700–3709. doi:10.1182/blood-2003-09-3217
136. Follenzi, A., Sabatino, G., Lombardo, A., Boccaccio, C., Naldini, L., 2002. Efficient Gene Delivery and Targeted Expression to Hepatocytes In Vivo by Improved Lentiviral Vectors. Hum. Gene Ther. 13, 243–260. doi:10.1089/10430340252769770
137. Follenzi, A., Santambrogio, L., Annoni, A., 2007. Immune responses to lentiviral vectors. Curr. Gene Ther. 7, 306–315.
138. Frankel, A.D., Young, J.A.T., 1998. HIV-1: Fifteen Proteins and an RNA. Annu. Rev. Biochem. 67, 1–25. doi:10.1146/annurev.biochem.67.1.1
139. Frecha, C., Costa, C., Nègre, D., Amirache, F., Trono, D., Rio, P., Bueren, J., Cosset, F.-L., Verhoeyen, E., 2012. A novel lentiviral vector targets gene transfer into human hematopoietic stem cells in marrow from patients with bone marrow failure syndrome and in vivo in humanized mice. Blood 119, 1139–1150. doi:10.1182/blood-2011-04-346619
140. Frecha, C., Lévy, C., Costa, C., Nègre, D., Amirache, F., Buckland, R., Russell, S.J., Cosset, F.-L., Verhoeyen, E., 2011. Measles Virus Glycoprotein-Pseudotyped Lentiviral Vector-Mediated Gene Transfer into Quiescent Lymphocytes Requires Binding to both SLAM and CD46 Entry Receptors▽. J. Virol. 85, 5975–5985. doi:10.1128/JVI.00324-11
141. Freed, E.O., Englund, G., Martin, M.A., 1995. Role of the basic domain of human immunodeficiency virus type 1 matrix in macrophage infection. J. Virol. 69, 3949–3954.
142. Freitag, S., Le Trong, I., Klumb, L., Stayton, P.S., Stenkamp, R.E., 1997. Structural studies of the streptavidin binding loop. Protein Sci. Publ. Protein Soc. 6, 1157–1166. doi:10.1002/pro.5560060604

143. Freitag, S., Le Trong, I., Klumb, L.A., Chu, V., Chilkoti, A., Stayton, P.S., Stenkamp, R.E., 1999. X-ray crystallographic studies of streptavidin mutants binding to biotin. Biomol. Eng. 16, 13–19.
144. Frick, L., Levison, P.R., Bisschops, M., 2016. Continuous Chromatography Is Now Possible for Clinical Manufacturing. BioProcess Int.
145. Friedel, T., Hanisch, L.J., Muth, A., Honegger, A., Abken, H., Plückthun, A., Buchholz, C.J., Schneider, I.C., 2015. Receptor-targeted lentiviral vectors are exceptionally sensitive toward the biophysical properties of the displayed single-chain Fv. Protein Eng. Des. Sel. 28, 93–106. doi:10.1093/protein/gzv005
146. Friedmann, T., 1992. A brief history of gene therapy. Nat. Genet. 2, 93–98. doi:10.1038/ng1092-93
147. Froelich, S., Tai, A., Wang, P., 2010. Lentiviral vectors for immune cells targeting. Immunopharmacol. Immunotoxicol. 32, 208–218. doi:10.3109/08923970903420582
148. Fuentes, G.M., Rodríguez-Rodríguez, L., Palaniappan, C., Fay, P.J., Bambara, R.A., 1996. Strand displacement synthesis of the long terminal repeats by HIV reverse transcriptase. J. Biol. Chem. 271, 1966–1971.
149. Funke, S., Maisner, A., Mühlebach, M.D., Koehl, U., Grez, M., Cattaneo, R., Cichutek, K., Buchholz, C.J., 2008. Targeted Cell Entry of Lentiviral Vectors. Mol. Ther. 16, 1427–1436. doi:10.1038/mt.2008.128
150. Gallay, P., Hope, T., Chin, D., Trono, D., 1997. HIV-1 infection of nondividing cells through the recognition of integrase by the importin/karyopherin pathway. Proc. Natl. Acad. Sci. U. S. A. 94, 9825–9830.
151. Galy, A., Thrasher, A.J., 2011. Gene therapy for the Wiskott-Aldrich syndrome. Curr. Opin. Allergy Clin. Immunol. 11, 545–550. doi:10.1097/ACI.0b013e32834c230c
152. Gama-Norton, L., Botezatu, L., Herrmann, S., Schweizer, M., Alves, P.M., Hauser, H., Wirth, D., 2011. Lentivirus production is influenced by SV40 large T-antigen and chromosomal integration of the vector in HEK293 cells. Hum. Gene Ther. 22, 1269–1279. doi:10.1089/hum.2010.143
153. Gaszner, M., Felsenfeld, G., 2006. Insulators: exploiting transcriptional and epigenetic mechanisms. Nat. Rev. Genet. 7, 703–713. doi:10.1038/nrg1925
154. Gennari, F., Lopes, L., Verhoeyen, E., Marasco, W., Collins, M.K., 2009. Single-Chain Antibodies That Target Lentiviral Vectors to MHC Class II on Antigen-Presenting Cells. Hum. Gene Ther. 20, 554–562. doi:10.1089/hum.2008.189
155. Geraerts, M., Michiels, M., Baekelandt, V., Debyser, Z., Gijsbers, R., 2005. Upscaling of lentiviral vector production by tangential flow filtration. J. Gene Med. 7, 1299–1310. doi:10.1002/jgm.778
156. Geraerts, M., Willems, S., Baekelandt, V., Debyser, Z., Gijsbers, R., 2006. Comparison of lentiviral vector titration methods. BMC Biotechnol. 6, 34. doi:10.1186/1472-6750-6-34
157. Ghosh, R., 2002. Protein separation using membrane chromatography: opportunities and challenges. J. Chromatogr. A 952, 13–27. doi:10.1016/S0021-9673(02)00057-2

158. Giebel, L.B., Cass, R., Milligan, D.L., Young, D., Arze, R., Johnson, C., 1995. Screening of cyclic peptide phage libraries identifies ligands that bind streptavidin with high affinities. Biochemistry (Mosc.) 34, 15430–15435. doi:10.1021/bi00047a006
159. Ginn, S.L., Alexander, I.E., Edelstein, M.L., Abedi, M.R., Wixon, J., 2013. Gene therapy clinical trials worldwide to 2012 - an update. J. Gene Med. 15, 65–77. doi:10.1002/jgm.2698
160. Gitlin, G., Bayer, E.A., Wilchek, M., 1990. Studies on the biotin-binding sites of avidin and streptavidin. Tyrosine residues are involved in the binding site. Biochem. J. 269, 527–530.
161. Glatter, T., Wepf, A., Aebersold, R., Gstaiger, M., 2009. An integrated workflow for charting the human interaction proteome: insights into the PP2A system. Mol. Syst. Biol. 5, n/a-n/a. doi:10.1038/msb.2008.75
162. Goel, R., Beard, W.A., Kumar, A., Casas-Finet, J.R., Strub, M.P., Stahl, S.J., Lewis, M.S., Bebenek, K., Becerra, S.P., 1993. Structure/function studies of HIV-1 reverse transcriptase: Dimerization-defective mutant L289K. Biochemistry (Mosc.) 32, 13012–13018. doi:10.1021/bi00211a009
163. Goerner, M., Horn, P.A., Peterson, L., Kurre, P., Storb, R., Rasko, J.E., Kiem, H.P., 2001. Sustained multilineage gene persistence and expression in dogs transplanted with CD34(+) marrow cells transduced by RD114-pseudotype oncoretrovirus vectors. Blood 98, 2065–2070.
164. Goldsmith, C.S., Miller, S.E., 2009. Modern Uses of Electron Microscopy for Detection of Viruses. Clin. Microbiol. Rev. 22, 552–563. doi:10.1128/CMR.00027-09
165. Gollan, T.J., Green, M.R., 2002. Redirecting Retroviral Tropism by Insertion of Short, Nondisruptive Peptide Ligands into Envelope. J. Virol. 76, 3558–3563. doi:10.1128/JVI.76.7.3558-3563.2002
166. Granoff, A., Hirst, G.K., 1954. Experimental production of combination forms of virus. IV. Mixed influenza A-Newcastle disease virus infections. Proc. Soc. Exp. Biol. Med. Soc. Exp. Biol. Med. N. Y. N 86, 84–88.
167. Green, B.J., Lee, C.S., Rasko, J.E.J., 2004. Biodistribution of the RD114/mammalian type D retrovirus receptor, RDR. J. Gene Med. 6, 249–259. doi:10.1002/jgm.517
168. Green, N., Shinnick, T.M., Witte, O., Ponticelli, A., Sutcliffe, J.G., Lerner, R.A., 1981. Sequence-specific antibodies show that maturation of Moloney leukemia virus envelope polyprotein involves removal of a COOH-terminal peptide. Proc. Natl. Acad. Sci. U. S. A. 78, 6023–6027.
169. Green, N.M., 1990. Avidin and streptavidin. Methods Enzymol. 184, 51–67.
170. Green, N.M., 1975. Avidin. Adv. Protein Chem. 29, 85–133.
171. Greene, M.R., Lockey, T., Mehta, P.K., Kim, Y.-S., Eldridge, P.W., Gray, J.T., Sorrentino, B.P., 2012. Transduction of Human CD34+ Repopulating Cells with a Self-Inactivating Lentiviral Vector for SCID-X1 Produced at Clinical Scale by a Stable Cell Line. Hum. Gene Ther. Methods 23, 297–308. doi:10.1089/hgtb.2012.150
172. Gregory, D.A., Olinger, G.Y., Lucas, T.M., Johnson, M.C., 2014. Diverse viral glycoproteins as well as CD4 co-package into the same human immunodeficiency virus (HIV-1) particles. Retrovirology 11, 28. doi:10.1186/1742-4690-11-28

173. Grez, M., Reichenbach, J., Schwäble, J., Seger, R., Dinauer, M.C., Thrasher, A.J., 2011. Gene Therapy of Chronic Granulomatous Disease: The Engraftment Dilemma. Mol. Ther. 19, 28–35. doi:10.1038/mt.2010.232
174. Grupp, S.A., Kalos, M., Barrett, D., Aplenc, R., Porter, D.L., Rheingold, S.R., Teachey, D.T., Chew, A., Hauck, B., Wright, J.F., Milone, M.C., Levine, B.L., June, C.H., 2013. Chimeric antigen receptor-modified T cells for acute lymphoid leukemia. N. Engl. J. Med. 368, 1509–1518. doi:10.1056/NEJMoa1215134
175. Gutiérrez-Granados, S., Cervera, L., Gòdia, F., Carrillo, J., Segura, M.M., 2013. Development and validation of a quantitation assay for fluorescently tagged HIV-1 virus-like particles. J. Virol. Methods 193, 85–95. doi:10.1016/j.jviromet.2013.05.010
176. Haase, A.T., 1986. Pathogenesis of lentivirus infections. Nature 322, 130–136. doi:10.1038/322130a0
177. Hacein-Bey-Abina, S., Garrigue, A., Wang, G.P., Soulier, J., Lim, A., Morillon, E., Clappier, E., Caccavelli, L., Delabesse, E., Beldjord, K., Asnafi, V., MacIntyre, E., Dal Cortivo, L., Radford, I., Brousse, N., Sigaux, F., Moshous, D., Hauer, J., Borkhardt, A., Belohradsky, B.H., Wintergerst, U., Velez, M.C., Leiva, L., Sorensen, R., Wulffraat, N., Blanche, S., Bushman, F.D., Fischer, A., Cavazzana-Calvo, M., 2008. Insertional oncogenesis in 4 patients after retrovirus-mediated gene therapy of SCID-X1. J. Clin. Invest. 118, 3132–3142. doi:10.1172/JCI35700
178. Haeryfar, S.M.M., Hoskin, D.W., 2004. Thy-1: more than a mouse pan-T cell marker. J. Immunol. Baltim. Md 1950 173, 3581–3588.
179. Hahn, R., Tscheliessnig, A., Bauerhansl, P., Jungbauer, A., 2007. Dispersion effects in preparative polymethacrylate monoliths operated in radial-flow columns. J. Biochem. Biophys. Methods, Monolithic Materials (Continuous Beds) and their Applications 70, 87–94. doi:10.1016/j.jbbm.2006.09.005
180. Hammarstedt, M., Garoff, H., 2004. Passive and active inclusion of host proteins in human immunodeficiency virus type 1 gag particles during budding at the plasma membrane. J. Virol. 78, 5686–5697. doi:10.1128/JVI.78.11.5686-5697.2004
181. Hanawa, H., Kelly, P.F., Nathwani, A.C., Persons, D.A., Vandergriff, J.A., Hargrove, P., Vanin, E.F., Nienhuis, A.W., 2002. Comparison of various envelope proteins for their ability to pseudotype lentiviral vectors and transduce primitive hematopoietic cells from human blood. Mol. Ther. J. Am. Soc. Gene Ther. 5, 242–251. doi:10.1006/mthe.2002.0549
182. Hartung, T., 2013. Food for Thought Look Back in Anger – What Clinical Studies Tell Us About Preclinical Work. ALTEX 30, 275–291.
183. Heider, S., Kleinberger, S., Kochan, F., Dangerfield, J.A., Metzner, C., 2016. Immune Protection of Retroviral Vectors Upon Molecular Painting with the Complement Regulatory Protein CD59. Mol. Biotechnol. 58, 480–488. doi:10.1007/s12033-016-9944-z
184. Heider, S., Metzner, C., 2014. Quantitative real-time single particle analysis of virions. Virology 462–463, 199–206. doi:10.1016/j.virol.2014.06.005

185. Higashikawa, F., Chang, L., 2001. Kinetic analyses of stability of simple and complex retroviral vectors. Virology 280, 124–131. doi:10.1006/viro.2000.0743
186. Hinrichs, C.S., Rosenberg, S.A., 2014a. Exploiting the curative potential of adoptive T-cell therapy for cancer. Immunol. Rev. 257, 56–71. doi:10.1111/imr.12132
187. Hirsch, J.D., Eslamizar, L., Filanoski, B.J., Malekzadeh, N., Haugland, R.P., Beechem, J.M., Haugland, R.P., 2002. Easily reversible desthiobiotin binding to streptavidin, avidin, and other biotin-binding proteins: uses for protein labeling, detection, and isolation. Anal. Biochem. 308, 343–357. doi:10.1016/S0003-2697(02)00201-4
188. Hofmann, K., Wood, S.W., Brinton, C.C., Montibeller, J.A., Finn, F.M., 1980. Iminobiotin affinity columns and their application to retrieval of streptavidin. Proc. Natl. Acad. Sci. U. S. A. 77, 4666–4668.
189. Holic, N., Seye, A.K., Majdoul, S., Martin, S., Merten, O.W., Galy, A., Fenard, D., 2014. Influence of Mildly Acidic pH Conditions on the Production of Lentiviral and Retroviral Vectors. Hum. Gene Ther. Clin. Dev. 25, 178–185. doi:10.1089/humc.2014.027
190. Hollon, T., 2000. Researchers and regulators reflect on first gene therapy death. Nat. Med. 6, 6. doi:10.1038/71545
191. Holmberg, A., Blomstergren, A., Nord, O., Lukacs, M., Lundeberg, J., Uhlén, M., 2005a. The biotin-streptavidin interaction can be reversibly broken using water at elevated temperatures. Electrophoresis 26, 501–510. doi:10.1002/elps.200410070
192. Howarth, M., Chinnapen, D.J.-F., Gerrow, K., Dorrestein, P.C., Grandy, M.R., Kelleher, N.L., El-Husseini, A., Ting, A.Y., 2006. A monovalent streptavidin with a single femtomolar biotin binding site. Nat. Methods 3, 267–273. doi:10.1038/NMETHXXX
193. Hu, W.-S., Hughes, S.H., 2012. HIV-1 Reverse Transcription. Cold Spring Harb. Perspect. Med. 2, a006882. doi:10.1101/cshperspect.a006882
194. Huang, B.-H., Lin, Y., Zhang, Z.-L., Zhuan, F., Liu, A.-A., Xie, M., Tian, Z.-Q., Zhang, Z., Wang, H., Pang, D.-W., 2012. Surface Labeling of Enveloped Viruses Assisted by Host Cells. ACS Chem. Biol. 7, 683–688. doi:10.1021/cb2001878
195. Hughes, C., Galea-Lauri, J., Farzaneh, F., Darling, D., 2001. Streptavidin paramagnetic particles provide a choice of three affinity-based capture and magnetic concentration strategies for retroviral vectors. Mol. Ther. J. Am. Soc. Gene Ther. 3, 623–630. doi:10.1006/mthe.2001.0268
196. Hulme, A.E., Perez, O., Hope, T.J., 2011. Complementary assays reveal a relationship between HIV-1 uncoating and reverse transcription. Proc. Natl. Acad. Sci. 108, 9975–9980. doi:10.1073/pnas.1014522108
197. Humbert, O., Gisch, D.W., Wohlfahrt, M.E., Adams, A.B., Greenberg, P.D., Schmitt, T.M., Trobridge, G.D., Kiem, H.-P., 2016. Development of Third-generation Cocal Envelope Producer Cell Lines for Robust Lentiviral Gene Transfer into Hematopoietic Stem Cells and T-cells. Mol. Ther. doi:10.1038/mt.2016.70

198. Ikeda, Y., Takeuchi, Y., Martin, F., Cosset, F.-L., Mitrophanous, K., Collins, M., 2003. Continuous high-titre HIV-1 vector production. Nat. Biotechnol. 21, 569–572. doi:10.1038/nbt815
199. Ivanov, K.I., Bašić, M., Varjosalo, M., Mäkinen, K., 2014. One-step purification of twin-strep-tagged proteins and their complexes on strep-tactin resin cross-linked with bis(sulfosuccinimidyl) suberate (BS3). J. Vis. Exp. JoVE. doi:10.3791/51536
200. Jacques, D.A., McEwan, W.A., Hilditch, L., Price, A.J., Towers, G.J., James, L.C., 2016. HIV-1 uses dynamic capsid pores to import nucleotides and fuel encapsidated DNA synthesis. Nature 536, 349–353. doi:10.1038/nature19098
201. Jain, A., Cheng, K., 2017. The principles and applications of avidin-based nanoparticles in drug delivery and diagnosis. J. Controlled Release 245, 27–40. doi:10.1016/j.jconrel.2016.11.016
202. Jarvik, J.W., Telmer, C.A., 1998. Epitope tagging. Annu. Rev. Genet. 32, 601–618. doi:10.1146/annurev.genet.32.1.601
203. Jiang, A., Chu, T.-H.T., Nocken, F., Cichutek, K., Dornburg, R., 1998. Cell-Type-Specific Gene Transfer into Human Cells with Retroviral Vectors That Display Single-Chain Antibodies. J. Virol. 72, 10148–10156.
204. Joo, K.-I., Lei, Y., Lee, C.-L., Lo, J., Hamm-Alvarez, J.X.S.F., Wang, P., 2008. Site-Specific Labeling of Enveloped Viruses with Quantum Dots for Single Virus Tracking. ACS Nano 2, 1553–1562. doi:10.1021/nn8002136
205. Jorgenson, R.L., Vogt, V.M., Johnson, M.C., 2009. Foreign glycoproteins can be actively recruited to virus assembly sites during pseudotyping. J. Virol. 83, 4060–4067. doi:10.1128/JVI.02425-08
206. Jungbauer, A., Hahn, R., 2008. Polymethacrylate monoliths for preparative and industrial separation of biomolecular assemblies. J. Chromatogr. A, 50 Years Journal of Chromatography 1184, 62–79. doi:10.1016/j.chroma.2007.12.087
207. Junttila, M.R., Saarinen, S., Schmidt, T., Kast, J., Westermarck, J., 2005a. Single-step Strep-tag purification for the isolation and identification of protein complexes from mammalian cells. Proteomics 5, 1199–1203. doi:10.1002/pmic.200400991
208. Junttila, M.R., Saarinen, S., Schmidt, T., Kast, J., Westermarck, J., 2005b. Single-step Strep-tag® purification for the isolation and identification of protein complexes from mammalian cells. PROTEOMICS 5, 1199–1203. doi:10.1002/pmic.200400991
209. Kafri, T., van Praag, H., Ouyang, L., Gage, F.H., Verma, I.M., 1999. A Packaging Cell Line for Lentivirus Vectors. J. Virol. 73, 576–584.
210. Kaikkonen, M.U., Lesch, H.P., Pikkarainen, J., Räty, J.K., Vuorio, T., Huhtala, T., Taavitsainen, M., Laitinen, T., Tuunanen, P., Gröhn, O., Närvänen, A., Airenne, K.J., Ylä-Herttuala, S., 2009a. (Strept)avidin-displaying lentiviruses as versatile tools for targeting and dual imaging of gene delivery. Gene Ther. 16, 894–904. doi:10.1038/gt.2009.47
211. Kaikkonen, M.U., Lesch, H.P., Pikkarainen, J., Räty, J.K., Vuorio, T., Huhtala, T., Taavitsainen, M., Laitinen, T., Tuunanen, P., Gröhn, O., Närvänen, A., Airenne, K.J., Ylä-Herttuala, S., 2009b. (Strept)avidin-displaying lentiviruses as versatile tools for targeting and dual imaging of gene delivery. Gene Ther. 16, 894–904. doi:10.1038/gt.2009.47

212. Kalos, M., Levine, B.L., Porter, D.L., Katz, S., Grupp, S.A., Bagg, A., June, C.H., 2011. T cells with chimeric antigen receptors have potent antitumor effects and can establish memory in patients with advanced leukemia. Sci. Transl. Med. 3, 95ra73. doi:10.1126/scitranslmed.3002842
213. Kampani, K., Quann, K., Ahuja, J., Wigdahl, B., Khan, Z.K., Jain, P., 2007. A novel high throughput quantum dot-based fluorescence assay for quantitation of virus binding and attachment. J. Virol. Methods 141, 125–132. doi:10.1016/j.jviromet.2006.11.043
214. Kaplan, A.H., Swanstrom, R., 1991. Human immunodeficiency virus type 1 Gag proteins are processed in two cellular compartments. Proc. Natl. Acad. Sci. U. S. A. 88, 4528–4532.
215. Kastelein, J.J.P., Ross, C.J.D., Hayden, M.R., 2013. From mutation identification to therapy: discovery and origins of the first approved gene therapy in the Western world. Hum. Gene Ther. 24, 472–478. doi:10.1089/hum.2013.063
216. Katane, M., Takao, E., Kubo, Y., Fujita, R., Amanuma, H., 2002. Factors affecting the direct targeting of murine leukemia virus vectors containing peptide ligands in the envelope protein. EMBO Rep. 3, 899–904. doi:10.1093/embo-reports/kvf179
217. Katz, B.A., 1995. Binding to Protein Targets of Peptidic Leads Discovered by Phage Display: Crystal Structures of Streptavidin-Bound Linear and Cyclic Peptide Ligands Containing the HPQ Sequence. Biochemistry (Mosc.) 34, 15421–15429. doi:10.1021/bi00047a005
218. Kaul, M., Yu, H., Ron, Y., Dougherty, J.P., 1998. Regulated Lentiviral Packaging Cell Line Devoid of Most Viralcis-Acting Sequences. Virology 249, 167–174. doi:10.1006/viro.1998.9327
219. Kavanaugh, M.P., Miller, D.G., Zhang, W., Law, W., Kozak, S.L., Kabat, D., Miller, A.D., 1994. Cell-surface receptors for gibbon ape leukemia virus and amphotropic murine retrovirus are inducible sodium-dependent phosphate symporters. Proc. Natl. Acad. Sci. U. S. A. 91, 7071–7075.
220. Kay, B.K., Adey, N.B., He, Y.S., Manfredi, J.P., Mataragnon, A.H., Fowlkes, D.M., 1993. An M13 phage library displaying random 38-amino-acid peptides as a source of novel sequences with affinity to selected targets. Gene 128, 59–65.
221. Keefe, A.D., Wilson, D.S., Seelig, B., Szostak, J.W., 2001. One-step purification of recombinant proteins using a nanomolar-affinity streptavidin-binding peptide, the SBP-Tag. Protein Expr. Purif. 23, 440–446. doi:10.1006/prep.2001.1515
222. Keefe, A.D., Wilson, D.S., Seelig, B., Szostak, J.W., 2001. One-Step Purification of Recombinant Proteins Using a Nanomolar-Affinity Streptavidin-Binding Peptide, the SBP-Tag. Protein Expr. Purif. 23, 440–446. doi:10.1006/prep.2001.1515
223. Kelly, P.F., Vandergriff, J., Nathwani, A., Nienhuis, A.W., Vanin, E.F., 2000. Highly efficient gene transfer into cord blood nonobese diabetic/severe combined immunodeficiency repopulating cells by oncoretroviral vector particles pseudotyped with the feline endogenous retrovirus (RD114) envelope protein. Blood 96, 1206–1214.
224. Kershaw, M.H., Westwood, J.A., Parker, L.L., Wang, G., Eshhar, Z., Mavroukakis, S.A., White, D.E., Wunderlich, J.R., Canevari, S., Rogers-

Freezer, L., Chen, C.C., Yang, J.C., Rosenberg, S.A., Hwu, P., 2006. A phase I study on adoptive immunotherapy using gene-modified T cells for ovarian cancer. Clin. Cancer Res. Off. J. Am. Assoc. Cancer Res. 12, 6106–6115. doi:10.1158/1078-0432.CCR-06-1183

225. Kessler, L.C., Gueorguieva, L., Rinas, U., Seidel-Morgenstern, A., 2007. Step gradients in 3-zone simulated moving bed chromatography. Application to the purification of antibodies and bone morphogenetic protein-2. J. Chromatogr. A 1176, 69–78. doi:10.1016/j.chroma.2007.10.087
226. Kim, S., Lim, K., 2017. Stability of Retroviral Vectors Against Ultracentrifugation Is Determined by the Viral Internal Core and Envelope Proteins Used for Pseudotyping. Mol. Cells 40, 339–345. doi:10.14348/molcells.2017.0043
227. Kim, V.N., Mitrophanous, K., Kingsman, S.M., Kingsman, A.J., 1998. Minimal requirement for a lentivirus vector based on human immunodeficiency virus type 1. J. Virol. 72, 811–816.
228. Kim, Y.K., Bourgeois, C.F., Isel, C., Churcher, M.J., Karn, J., 2002. Phosphorylation of the RNA Polymerase II Carboxyl-Terminal Domain by CDK9 Is Directly Responsible for Human Immunodeficiency Virus Type 1 Tat-Activated Transcriptional Elongation. Mol. Cell. Biol. 22, 4622–4637. doi:10.1128/MCB.22.13.4622-4637.2002
229. Kimple, M.E., Brill, A.L., Pasker, R.L., 2013. Overview of Affinity Tags for Protein Purification. Curr. Protoc. Protein Sci. Editor. Board John E Coligan Al 73, Unit-9.9. doi:10.1002/0471140864.ps0909s73
230. Kingsman, S.M., Kingsman, A.J., 1996. The Regulation of Human Immunodeficiency Virus Type-1 Gene Expression. Eur. J. Biochem. 240, 491–507. doi:10.1111/j.1432-1033.1996.0491h.x
231. Klages, N., Zufferey, R., Trono, D., 2000. A stable system for the high-titre production of multiply attenuated lentiviral vectors. Mol. Ther. J. Am. Soc. Gene Ther. 2, 170–176. doi:10.1006/mthe.2000.0103
232. Klasse, P.J., 2015. Molecular Determinants of the Ratio of Inert to Infectious Virus Particles. Prog. Mol. Biol. Transl. Sci. 129, 285–326. doi:10.1016/bs.pmbts.2014.10.012
233. Klasse, P.J., McKeating, J.A., 1993. Soluble CD4 and CD4 immunoglobulin-selected HIV-1 variants: a phenotypic characterization. AIDS Res. Hum. Retroviruses 9, 595–604. doi:10.1089/aid.1993.9.595
234. Knabel, M., Franz, T.J., Schiemann, M., Wulf, A., Villmow, B., Schmidt, B., Bernhard, H., Wagner, H., Busch, D.H., 2002. Reversible MHC multimer staining for functional isolation of T-cell populations and effective adoptive transfer. Nat. Med. 8, 631–637. doi:10.1038/nm0602-631
235. Kochenderfer, J.N., Dudley, M.E., Feldman, S.A., Wilson, W.H., Spaner, D.E., Maric, I., Stetler-Stevenson, M., Phan, G.Q., Hughes, M.S., Sherry, R.M., Yang, J.C., Kammula, U.S., Devillier, L., Carpenter, R., Nathan, D.-A.N., Morgan, R.A., Laurencot, C., Rosenberg, S.A., 2012. B-cell depletion and remissions of malignancy along with cytokine-associated toxicity in a clinical trial of anti-CD19 chimeric-antigen-receptor-transduced T cells. Blood 119, 2709–2720. doi:10.1182/blood-2011-10-384388
236. Kochenderfer, J.N., Wilson, W.H., Janik, J.E., Dudley, M.E., Stetler-Stevenson, M., Feldman, S.A., Maric, I., Raffeld, M., Nathan, D.-A.N.,

Lanier, B.J., Morgan, R.A., Rosenberg, S.A., 2010. Eradication of B-lineage cells and regression of lymphoma in a patient treated with autologous T cells genetically engineered to recognize CD19. Blood 116, 4099–4102. doi:10.1182/blood-2010-04-281931
237. Kola, I., Landis, J., 2004. Can the pharmaceutical industry reduce attrition rates? Nat. Rev. Drug Discov. 3, 711–715. doi:10.1038/nrd1470
238. Kooyman, D.L., Byrne, G.W., McClellan, S., Nielsen, D., Tone, M., Waldmann, H., Coffman, T.M., McCurry, K.R., Platt, J.L., Logan, J.S., 1995. In vivo transfer of GPI-linked complement restriction factors from erythrocytes to the endothelium. Science 269, 89–92.
239. Korndörfer, I.P., Skerra, A., 2002. Improved affinity of engineered streptavidin for the Strep-tag II peptide is due to a fixed open conformation of the lid-like loop at the binding site. Protein Sci. Publ. Protein Soc. 11, 883–893.
240. Kotsopoulou, E., Kim, V.N., Kingsman, A.J., Kingsman, S.M., Mitrophanous, K.A., 2000. A Rev-independent human immunodeficiency virus type 1 (HIV-1)-based vector that exploits a codon-optimized HIV-1 gag-pol gene. J. Virol. 74, 4839–4852.
241. Kramberger, P., Urbas, L., Štrancar, A., 2015. Downstream processing and chromatography based analytical methods for production of vaccines, gene therapy vectors, and bacteriophages. Hum. Vaccines Immunother. 11, 1010–1021. doi:10.1080/21645515.2015.1009817
242. Kröber, T., Wolff, M.W., Hundt, B., Seidel-Morgenstern, A., Reichl, U., 2013. Continuous purification of influenza virus using simulated moving bed chromatography. J. Chromatogr. A 1307, 99–110. doi:10.1016/j.chroma.2013.07.081
243. Kuate, S., Wagner, R., Überla, K., 2002. Development and characterization of a minimal inducible packaging cell line for simian immunodeficiency virus-based lentiviral vectors. J. Gene Med. 4, 347–355. doi:10.1002/jgm.290
244. Kutner, R.H., Puthli, S., Marino, M.P., Reiser, J., 2009. Simplified production and concentration of HIV-1-based lentiviral vectors using HYPERFlask vessels and anion exchange membrane chromatography. BMC Biotechnol. 9, 10. doi:10.1186/1472-6750-9-10
245. Kuznetsova, I.M., Turoverov, K.K., Uversky, V.N., 2014. What Macromolecular Crowding Can Do to a Protein. Int. J. Mol. Sci. 15, 23090–23140. doi:10.3390/ijms151223090
246. Kwon, Y.J., Hung, G., Anderson, W.F., Peng, C.-A., Yu, H., 2003. Determination of Infectious Retrovirus Concentration from Colony-Forming Assay with Quantitative Analysis. J. Virol. 77, 5712–5720. doi:10.1128/JVI.77.10.5712-5720.2003
247. Laitinen, O.H., Hytönen, V.P., Nordlund, H.R., Kulomaa, M.S., 2006. Genetically engineered avidins and streptavidins. Cell. Mol. Life Sci. CMLS 63, 2992–3017. doi:10.1007/s00018-006-6288-z
248. Laitinen, O.H., Nordlund, H.R., Hytönen, V.P., Kulomaa, M.S., 2007. Brave new (strept)avidins in biotechnology. Trends Biotechnol. 25, 269–277. doi:10.1016/j.tibtech.2007.04.001
249. Lamers, C.H., Sleijfer, S., van Steenbergen, S., van Elzakker, P., van Krimpen, B., Groot, C., Vulto, A., den Bakker, M., Oosterwijk, E., Debets,

R., Gratama, J.W., 2013. Treatment of metastatic renal cell carcinoma with CAIX CAR-engineered T cells: clinical evaluation and management of on-target toxicity. Mol. Ther. J. Am. Soc. Gene Ther. 21, 904–912. doi:10.1038/mt.2013.17

250. Lamla, T., Erdmann, V.A., 2004. The Nano-tag, a streptavidin-binding peptide for the purification and detection of recombinant proteins. Protein Expr. Purif. 33, 39–47. doi:10.1016/j.pep.2003.08.014

251. Larochelle, A., Peng, K.W., Russell, S.J., 2002. Lentiviral vector targeting. Curr. Top. Microbiol. Immunol. 261, 143–163.

252. Lavillette, D., Boson, B., Russell, S.J., Cosset, F.-L., 2001a. Activation of Membrane Fusion by Murine Leukemia Viruses Is Controlled in cis or in trans by Interactions between the Receptor-Binding Domain and a Conserved Disulfide Loop of the Carboxy Terminus of the Surface Glycoprotein. J. Virol. 75, 3685–3695. doi:10.1128/JVI.75.8.3685-3695.2001

253. Lavillette, D., Russell, S.J., Cosset, F.-L., 2001b. Retargeting gene delivery using surface-engineered retroviral vector particles. Curr. Opin. Biotechnol. 12, 461–466. doi:10.1016/S0958-1669(00)00246-9

254. Layne, S.P., Merges, M.J., Dembo, M., Spouge, J.L., Conley, S.R., Moore, J.P., Raina, J.L., Renz, H., Gelderblom, H.R., Nara, P.L., 1992. Factors underlying spontaneous inactivation and susceptibility to neutralization of human immunodeficiency virus. Virology 189, 695–714.

255. Lee, C.-L., Chou, M., Dai, B., Xiao, L., Wang, P., 2012. Construction of stable producer cells to make high-titre lentiviral vectors for dendritic cell-based vaccination. Biotechnol. Bioeng. 109, 1551–1560. doi:10.1002/bit.24413

256. Legler, D.F., Doucey, M.-A., Schneider, P., Chapatte, L., Bender, F.C., Bron, C., 2005. Differential insertion of GPI-anchored GFPs into lipid rafts of live cells. FASEB J. Off. Publ. Fed. Am. Soc. Exp. Biol. 19, 73–75. doi:10.1096/fj.03-1338fje

257. Lei, Y., Joo, K.-I., Wang, P., 2009. Engineering fusogenic molecules to achieve targeted transduction of enveloped lentiviral vectors. J. Biol. Eng. 3. doi:10.1186/1754-1611-3-8

258. Lesch, H.P., Laitinen, A., Peixoto, C., Vicente, T., Makkonen, K.-E., Laitinen, L., Pikkarainen, J.T., Samaranayake, H., Alves, P.M., Carrondo, M.J.T., Ylä-Herttuala, S., Airenne, K.J., 2011. Production and purification of lentiviral vectors generated in 293T suspension cells with baculoviral vectors. Gene Ther. 18, 531–538. doi:10.1038/gt.2010.162

259. Lesch, H.P., Pikkarainen, J.T., Kaikkonen, M.U., Taavitsainen, M., Samaranayake, H., Lehtolainen-Dalkilic, P., Vuorio, T., Määttä, A.-M., Wirth, T., Airenne, K.J., Ylä-Herttuala, S., 2009. Avidin Fusion Protein-Expressing Lentiviral Vector for Targeted Drug Delivery. Hum. Gene Ther. 20, 871–882. doi:10.1089/hum.2009.007

260. Lever, A.M.L., Strappe, P.M., Zhao, J., 2004. Lentiviral vectors. J. Biomed. Sci. 11, 439–449. doi:10.1159/000077893

261. Leverett, B.D., Farrell, K.B., Eiden, M.V., Wilson, C.A., 1998. Entry of amphotropic murine leukemia virus is influenced by residues in the putative second extracellular domain of its receptor, Pit2. J. Virol. 72, 4956–4961.

262. Levine, B.L., Humeau, L.M., Boyer, J., MacGregor, R.-R., Rebello, T., Lu, X., Binder, G.K., Slepushkin, V., Lemiale, F., Mascola, J.R., Bushman, F.D., Dropulic, B., June, C.H., 2006. Gene transfer in humans using a conditionally replicating lentiviral vector. Proc. Natl. Acad. Sci. 103, 17372–17377. doi:10.1073/pnas.0608138103
263. Lévy, C., Verhoeyen, E., Cosset, F.-L., 2015. Surface engineering of lentiviral vectors for gene transfer into gene therapy target cells. Curr. Opin. Pharmacol., Anti-infectives • New technologies 24, 79–85. doi:10.1016/j.coph.2015.08.003
264. Lewis, P., Hensel, M., Emerman, M., 1992. Human immunodeficiency virus infection of cells arrested in the cell cycle. EMBO J. 11, 3053–3058.
265. Li, Y., Franklin, S., Zhang, M.J., Vondriska, T.M., 2011. Highly efficient purification of protein complexes from mammalian cells using a novel streptavidin-binding peptide and hexahistidine tandem tag system: application to Bruton's tyrosine kinase. Protein Sci. Publ. Protein Soc. 20, 140–149. doi:10.1002/pro.546
266. Liang, M., Morizono, K., Pariente, N., Kamata, M., Lee, B., Chen, I.S.Y., 2009. Targeted transduction via CD4 by a lentiviral vector uses a clathrin-mediated entry pathway. J. Virol. 83, 13026–13031. doi:10.1128/JVI.01530-09
267. Lim, K.H., Huang, H., Pralle, A., Park, S., 2013. Stable, high-affinity streptavidin monomer for protein labeling and monovalent biotin detection. Biotechnol. Bioeng. 110, 57–67. doi:10.1002/bit.24605
268. Lin, A.H., Kasahara, N., Wu, W., Stripecke, R., Empig, C.L., Anderson, W.F., Cannon, P.M., 2001. Receptor-Specific Targeting Mediated by the Coexpression of a Targeted Murine Leukemia Virus Envelope Protein and a Binding-Defective Influenza Hemagglutinin Protein. Hum. Gene Ther. 12, 323–332. doi:10.1089/10430340150503957
269. Liu, F., Zhang, J.Z.H., Mei, Y., 2016. The origin of the cooperativity in the streptavidin-biotin system: A computational investigation through molecular dynamics simulations. Sci. Rep. 6, 27190. doi:10.1038/srep27190
270. Livnah, O., Bayer, E.A., Wilchek, M., Sussman, J.L., 1993. Three-dimensional structures of avidin and the avidin-biotin complex. Proc. Natl. Acad. Sci. U. S. A. 90, 5076–5080.
271. Ljunglöf, A., Bergvall, P., Bhikhabhai, R., Hjorth, R., 1999. Direct visualisation of plasmid DNA in individual chromatography adsorbent particles by confocal scanning laser microscopy. J. Chromatogr. A 844, 129–135. doi:10.1016/S0021-9673(99)00386-6
272. Locatelli-Hoops, S.C., Yeliseev, A.A., 2014. Use of Tandem Affinity Chromatography for Purification of Cannabinoid Receptor CB2. Methods Mol. Biol. Clifton NJ 1177, 107–120. doi:10.1007/978-1-4939-1034-2_9
273. Mahler, H.-C., Friess, W., Grauschopf, U., Kiese, S., 2009. Protein aggregation: pathways, induction factors and analysis. J. Pharm. Sci. 98, 2909–2934. doi:10.1002/jps.21566
274. Maier, T., Drapal, N., Thanbichler, M., Böck, A., 1998. Strep-Tag II Affinity Purification: An Approach to Study Intermediates of Metalloenzyme Biosynthesis. Anal. Biochem. 259, 68–73. doi:10.1006/abio.1998.2649

275. Marceau, N., Gasmi, M., 2013. Scalable lentiviral vector production system compatible with industrial pharmaceutical applications. WO2013076309 A1.
276. Marin, V., Stornaiuolo, A., Piovan, C., Corna, S., Bossi, S., Pema, M., Giuliani, E., Scavullo, C., Zucchelli, E., Bordignon, C., Rizzardi, G.P., Bovolenta, C., 2016. RD-MolPack technology for the constitutive production of self-inactivating lentiviral vectors pseudotyped with the nontoxic RD114-TR envelope. Mol. Ther. Methods Clin. Dev. 3, 16033. doi:10.1038/mtm.2016.33
277. Marino, M.P., Panigaj, M., Ou, W., Manirarora, J., Wei, C.-H., Reiser, J., 2015. A scalable method to concentrate lentiviral vectors pseudotyped with measles virus glycoproteins. Gene Ther. 22, 64–69. doi:10.1038/gt.2014.125
278. Marquet, R., Isel, C., Ehresmann, C., Ehresmann, B., 1995. tRNAs as primer of reverse transcriptases. Biochimie 77, 113–124.
279. Martín, F., Chowdhury, S., Neil, S., Phillipps, N., Collins, M.K., 2002. Envelope-Targeted Retrovirus Vectors Transduce Melanoma Xenografts but Not Spleen or Liver. Mol. Ther. 5, 269–274. doi:10.1006/mthe.2002.0550
280. Matano, T., Odawara, T., Iwamoto, A., Yoshikura, H., 1995. Targeted infection of a retrovirus bearing a CD4-Env chimera into human cells expressing human immunodeficiency virus type 1. J. Gen. Virol. 76 (Pt 12), 3165–3169.
281. Matheson, N.J., Peden, A.A., Lehner, P.J., 2014. Antibody-Free Magnetic Cell Sorting of Genetically Modified Primary Human CD4+ T Cells by One-Step Streptavidin Affinity Purification. PLOS ONE 9, e111437. doi:10.1371/journal.pone.0111437
282. Mátrai, J., Chuah, M.K., VandenDriessche, T., 2010a. Recent Advances in Lentiviral Vector Development and Applications. Mol. Ther. 18, 477–490. doi:10.1038/mt.2009.319
283. Mátrai, J., Chuah, M.K., VandenDriessche, T., 2010b. Recent Advances in Lentiviral Vector Development and Applications. Mol. Ther. 18, 477–490. doi:10.1038/mt.2009.319
284. Maurice, M., Mazur, S., Bullough, F.J., Salvetti, A., Collins, M.K.L., Russell, S.J., Cosset, F.-L., 1999. Efficient Gene Delivery to Quiescent Interleukin-2 (IL-2)–Dependent Cells by Murine Leukemia Virus-Derived Vectors Harboring IL-2 Chimeric Envelopes Glycoproteins. Blood 94, 401–410.
285. Maurice, M., Verhoeyen, E., Salmon, P., Trono, D., Russell, S.J., Cosset, F.-L., 2002. Efficient gene transfer into human primary blood lymphocytes by surface-engineered lentiviral vectors that display a T cell–activating polypeptide. Blood 99, 2342–2350. doi:10.1182/blood.V99.7.2342
286. Maus, M.V., Grupp, S.A., Porter, D.L., June, C.H., 2014. Antibody-modified T cells: CARs take the front seat for hematologic malignancies. Blood 123, 2625–2635. doi:10.1182/blood-2013-11-492231
287. McCarthy, M., 2000. US tightens oversight of gene-therapy trials. The Lancet 355, 997. doi:10.1016/S0140-6736(05)74745-0

288. McClure, M.O., Sommerfelt, M.A., Marsh, M., Weiss, R.A., 1990. The pH independence of mammalian retrovirus infection. J. Gen. Virol. 71 (Pt 4), 767–773. doi:10.1099/0022-1317-71-4-767
289. McGarrity, G.J., Hoyah, G., Winemiller, A., Andre, K., Stein, D., Blick, G., Greenberg, R.N., Kinder, C., Zolopa, A., Binder-Scholl, G., Tebas, P., June, C.H., Humeau, L.M., Rebello, T., 2013. Patient monitoring and follow-up in lentiviral clinical trials. J. Gene Med. 15, 78–82. doi:10.1002/jgm.2691
290. McLafferty, M.A., Kent, R.B., Ladner, R.C., Markland, W., 1993. M13 bacteriophage displaying disulfide-constrained microproteins. Gene 128, 29–36.
291. McTaggart, S., Al-Rubeai, M., 2000. Effects of Culture Parameters on the Production of Retroviral Vectors by a Human Packaging Cell Line. Biotechnol. Prog. 16, 859–865. doi:10.1021/bp000078j
292. Medof, M.E., Kinoshita, T., Nussenzweig, V., 1984. Inhibition of complement activation on the surface of cells after incorporation of decay-accelerating factor (DAF) into their membranes. J. Exp. Med. 160, 1558–1578.
293. Merten, O.-W., 2004. State-of-the-art of the production of retroviral vectors. J. Gene Med. 6 Suppl 1, S105-124. doi:10.1002/jgm.499
294. Merten, O.-W., Charrier, S., Laroudie, N., Fauchille, S., Dugué, C., Jenny, C., Audit, M., Zanta-Boussif, M.-A., Chautard, H., Radrizzani, M., Vallanti, G., Naldini, L., Noguiez-Hellin, P., Galy, A., 2011a. Large-scale manufacture and characterization of a lentiviral vector produced for clinical ex vivo gene therapy application. Hum. Gene Ther. 22, 343–356. doi:10.1089/hum.2010.060
295. Merten, O.-W., Charrier, S., Laroudie, N., Fauchille, S., Dugué, C., Jenny, C., Audit, M., Zanta-Boussif, M.-A., Chautard, H., Radrizzani, M., Vallanti, G., Naldini, L., Noguiez-Hellin, P., Galy, A., 2011b. Large-scale manufacture and characterization of a lentiviral vector produced for clinical ex vivo gene therapy application. Hum. Gene Ther. 22, 343–356. doi:10.1089/hum.2010.060
296. Merten, O.-W., Charrier, S., Laroudie, N., Fauchille, S., Dugué, C., Jenny, C., Audit, M., Zanta-Boussif, M.-A., Chautard, H., Radrizzani, M., Vallanti, G., Naldini, L., Noguiez-Hellin, P., Galy, A., 2011c. Large-scale manufacture and characterization of a lentiviral vector produced for clinical ex vivo gene therapy application. Hum. Gene Ther. 22, 343–356. doi:10.1089/hum.2010.060
297. Merten, O.-W., Charrier, S., Laroudie, N., Fauchille, S., Dugué, C., Jenny, C., Audit, M., Zanta-Boussif, M.-A., Chautard, H., Radrizzani, M., Vallanti, G., Naldini, L., Noguiez-Hellin, P., Galy, A., 2011d. Large-scale manufacture and characterization of a lentiviral vector produced for clinical ex vivo gene therapy application. Hum. Gene Ther. 22, 343–356. doi:10.1089/hum.2010.060
298. Merten, O.-W., Hebben, M., Bovolenta, C., 2016a. Production of lentiviral vectors. Mol. Ther. Methods Clin. Dev. 3, 16017. doi:10.1038/mtm.2016.17
299. Merten, O.-W., Hebben, M., Bovolenta, C., 2016b. Production of lentiviral vectors. Mol. Ther. Methods Clin. Dev. 3, 16017. doi:10.1038/mtm.2016.17

300. Merten, O.-W., Schweizer, M., Chahal, P., Kamen, A., 2014. Manufacturing of viral vectors: part II. Downstream processing and safety aspects. Pharm. Bioprocess. 2, 237–251.
301. Metzner, C., Dangerfiel, J., 2011. Surface Modification of Retroviral Vectors for Gene Therapy, in: Xu, K. (Ed.), Viral Gene Therapy. InTech.
302. Metzner, C., Dangerfield, J., 2011. Surface Modification of Retroviral Vectors for Gene Therapy. doi:10.5772/20568
303. Metzner, C., Kochan, F., Dangerfield, J.A., 2013a. Postexit Surface Engineering of Retroviral/Lentiviral Vectors. BioMed Res. Int. 2013. doi:10.1155/2013/253521
304. Metzner, C., Kochan, F., Dangerfield, J.A., 2013b. Fluorescence Molecular Painting of Enveloped Viruses. Mol. Biotechnol. 53, 9–18. doi:10.1007/s12033-012-9616-6
305. Metzner, C., Mostegl, M.M., Günzburg, W.H., Salmons, B., Dangerfield, J.A., 2008a. Association of glycosylphosphatidylinositol-anchored protein with retroviral particles. FASEB J. Off. Publ. Fed. Am. Soc. Exp. Biol. 22, 2734–2739. doi:10.1096/fj.08-108217
306. Metzner, C., Salmons, B., Günzburg, W.H., Dangerfield, J.A., 2008b. Rafts, anchors and viruses — A role for glycosylphosphatidylinositol anchored proteins in the modification of enveloped viruses and viral vectors. Virology 382, 125–131. doi:10.1016/j.virol.2008.09.014
307. Miller, M.D., Farnet, C.M., Bushman, F.D., 1997. Human immunodeficiency virus type 1 preintegration complexes: studies of organization and composition. J. Virol. 71, 5382–5390.
308. Mironov, G.G., Chechik, A.V., Ozer, R., Bell, J.C., Berezovski, M.V., 2011. Viral quantitative capillary electrophoresis for counting intact viruses. Anal. Chem. 83, 5431–5435. doi:10.1021/ac201006u
309. Miyauchi, K., Kim, Y., Latinovic, O., Morozov, V., Melikyan, G.B., 2009. HIV enters cells via endocytosis and dynamin-dependent fusion with endosomes. Cell 137, 433–444. doi:10.1016/j.cell.2009.02.046
310. Modlich, U., Bohne, J., Schmidt, M., von Kalle, C., Knöss, S., Schambach, A., Baum, C., 2006. Cell-culture assays reveal the importance of retroviral vector design for insertional genotoxicity. Blood 108, 2545–2553. doi:10.1182/blood-2005-08-024976
311. Montini, E., Cesana, D., Schmidt, M., Sanvito, F., Bartholomae, C.C., Ranzani, M., Benedicenti, F., Sergi, L.S., Ambrosi, A., Ponzoni, M., Doglioni, C., Di Serio, C., von Kalle, C., Naldini, L., 2009. The genotoxic potential of retroviral vectors is strongly modulated by vector design and integration site selection in a mouse model of HSC gene therapy. J. Clin. Invest. 119, 964–975. doi:10.1172/JCI37630
312. Montini, E., Cesana, D., Schmidt, M., Sanvito, F., Ponzoni, M., Bartholomae, C., Sergi Sergi, L., Benedicenti, F., Ambrosi, A., Di Serio, C., Doglioni, C., von Kalle, C., Naldini, L., 2006. Hematopoietic stem cell gene transfer in a tumor-prone mouse model uncovers low genotoxicity of lentiviral vector integration. Nat. Biotechnol. 24, 687–696. doi:10.1038/nbt1216
313. Morenweiser, R., 2005. Downstream processing of viral vectors and vaccines. Gene Ther. 12 Suppl 1, S103-110. doi:10.1038/sj.gt.3302624

314. Morizono, K., Xie, Y., Helguera, G., Daniels, T.R., Lane, T.F., Penichet, M.L., Chen, I.S.Y., 2009. A versatile targeting system with lentiviral vectors bearing the biotin-adaptor peptide. J. Gene Med. 11, 655–663. doi:10.1002/jgm.1345
315. Naldini, L., Blömer, U., Gallay, P., Ory, D., Mulligan, R., Gage, F.H., Verma, I.M., Trono, D., 1996. In vivo gene delivery and stable transduction of nondividing cells by a lentiviral vector. Science 272, 263–267.
316. Nasri, M., Karimi, A., Farsani, M.A., 2014. Production, purification and titration of a lentivirus-based vector for gene delivery purposes. Cytotechnology 66, 1031–1038. doi:10.1007/s10616-013-9652-5
317. Neda, H., Wu, C.H., Wu, G.Y., 1991. Chemical modification of an ecotropic murine leukemia virus results in redirection of its target cell specificity. J. Biol. Chem. 266, 14143–14146.
318. Negré, 2008. 224. Long-Term Correction of Murine Beta-Thalassemia Following Busulfan Conditioning and Transplant of Bone Marrow Transduced with Clinical-Grade Lentiviral Vector (LentiGlobin^{TM}). Mol. Ther. 16, S85. doi:10.1016/S1525-0016(16)39627-7
319. Neri, F., Giolo, G., Potestà, M., Petrini, S., Doria, M., 2011. CD4 downregulation by the human immunodeficiency virus type 1 Nef protein is dispensable for optimal output and functionality of viral particles in primary T cells. J. Gen. Virol. 92, 141–150. doi:10.1099/vir.0.026005-0
320. Nesbeth, D., Williams, S.L., Chan, L., Brain, T., Slater, N.K.H., Farzaneh, F., Darling, D., 2006. Metabolic Biotinylation of Lentiviral Pseudotypes for Scalable Paramagnetic Microparticle-Dependent Manipulation. Mol. Ther. 13, 814–822. doi:10.1016/j.ymthe.2005.09.016
321. Nguyen, D.H., Hildreth, J.E., 2000. Evidence for budding of human immunodeficiency virus type 1 selectively from glycolipid-enriched membrane lipid rafts. J. Virol. 74, 3264–3272.
322. Ni, Y., Sun, S., Oparaocha, I., Humeau, L., Davis, B., Cohen, R., Binder, G., Chang, Y.-N., Slepushkin, V., Dropulic, B., 2005. Generation of a packaging cell line for prolonged large-scale production of high-titre HIV-1-based lentiviral vector. J. Gene Med. 7, 818–834. doi:10.1002/jgm.726
323. Nie, Z., Phenix, B.N., Lum, J.J., Alam, A., Lynch, D.H., Beckett, B., Krammer, P.H., Sekaly, R.P., Badley, A.D., 2002. HIV-1 protease processes procaspase 8 to cause mitochondrial release of cytochrome c, caspase cleavage and nuclear fragmentation. Cell Death Differ. 9, 1172–1184. doi:10.1038/sj.cdd.4401094
324. Olejnik, J., Sonar, S., Krzymañska-Olejnik, E., Rothschild, K.J., 1995. Photocleavable biotin derivatives: a versatile approach for the isolation of biomolecules. Proc. Natl. Acad. Sci. U. S. A. 92, 7590–7594.
325. Ortiz, R., Melguizo, C., Prados, J., Álvarez, P.J., Caba, O., Rodríguez-Serrano, F., Hita, F., Aránega, A., 2012. New gene therapy strategies for cancer treatment: a review of recent patents. Recent Patents Anticancer Drug Discov. 7, 297–312.
326. Ory, D.S., Neugeboren, B.A., Mulligan, R.C., 1996. A stable human-derived packaging cell line for production of high titre retrovirus/vesicular stomatitis virus G pseudotypes. Proc. Natl. Acad. Sci. U. S. A. 93, 11400–11406.

327. Pacchia, A.L., Adelson, M.E., Kaul, M., Ron, Y., Dougherty, J.P., 2001. An inducible packaging cell system for safe, efficient lentiviral vector production in the absence of HIV-1 accessory proteins. Virology 282, 77–86. doi:10.1006/viro.2000.0787
328. Pariente, N., Morizono, K., Virk, M.S., Petrigliano, F.A., Reiter, R.E., Lieberman, J.R., Chen, I.S.Y., 2007. A novel dual-targeted lentiviral vector leads to specific transduction of prostate cancer bone metastases in vivo after systemic administration. Mol. Ther. J. Am. Soc. Gene Ther. 15, 1973–1981. doi:10.1038/sj.mt.6300271
329. Parrott, M.B., Adams, K.E., Mercier, G.T., Mok, H., Campos, S.K., Barry, M.A., 2000. Metabolically Biotinylated Adenovirus for Cell Targeting, Ligand Screening, and Vector Purification. Mol. Ther. J. Am. Soc. Gene Ther. 1, 96–104. doi:10.1006/mthe.1999.0011
330. Parrott, M.B., Barry, M.A., 2001. Metabolic Biotinylation of Secreted and Cell Surface Proteins from Mammalian Cells. Biochem. Biophys. Res. Commun. 281, 993–1000. doi:10.1006/bbrc.2001.4437
331. Pearson, S., Jia, H., Kandachi, K., 2004. China approves first gene therapy. Nat. Biotechnol. 22, 3–4. doi:10.1038/nbt0104-3
332. Perbandt, M., Bruns, O., Vallazza, M., Lamla, T., Betzel, C., Erdmann, V.A., 2007a. High resolution structure of streptavidin in complex with a novel high affinity peptide tag mimicking the biotin binding motif. Proteins 67, 1147–1153. doi:10.1002/prot.21236
333. Perbandt, M., Bruns, O., Vallazza, M., Lamla, T., Betzel, C., Erdmann, V.A., 2007b. High resolution structure of streptavidin in complex with a novel high affinity peptide tag mimicking the biotin binding motif. Proteins 67, 1147–1153. doi:10.1002/prot.21236
334. Peterka, M., Jarc, M., Banjac, M., Frankovič, V., Benčina, K., Merhar, M., Gaberc-Porekar, V., Menart, V., Štrancar, A., Podgornik, A., 2006. Characterisation of metal–chelate methacrylate monoliths. J. Chromatogr. A, Advances in Monoliths 1109, 80–85. doi:10.1016/j.chroma.2005.08.057
335. Peterka, M., Strancar, A., Banjac, M., Kramberger, P., Maurer, E., Muster, T., 2011. Method for influenza virus purification. EP2361975 A1.
336. Pfeifer, A., Kessler, T., Yang, M., Baranov, E., Kootstra, N., Cheresh, D.A., Hoffman, R.M., Verma, I.M., 2001. Transduction of liver cells by lentiviral vectors: analysis in living animals by fluorescence imaging. Mol. Ther. J. Am. Soc. Gene Ther. 3, 319–322. doi:10.1006/mthe.2001.0276
337. Pham, L., Ye, H., Cosset, F.L., Russell, S.J., Peng, K.W., 2001. Concentration of viral vectors by co-precipitation with calcium phosphate. J. Gene Med. 3, 188–194. doi:10.1002/1521-2254(2000)9999:9999<::AID-JGM159>3.0.CO;2-9
338. Physiologic relevance of the membrane attack complex inhibitory protein CD59 in human seminal plasma: CD59 is present on extracellular organelles (prostasomes), binds cell membranes, and inhibits complement-mediated lysis, 1993. . J. Exp. Med. 177, 1409–1420.
339. Pichlmair, A., Diebold, S.S., Gschmeissner, S., Takeuchi, Y., Ikeda, Y., Collins, M.K., Sousa, C.R. e, 2007. Tubulovesicular Structures within Vesicular Stomatitis Virus G Protein-Pseudotyped Lentiviral Vector Preparations Carry DNA and Stimulate Antiviral Responses via Toll-Like Receptor 9. J. Virol. 81, 539–547. doi:10.1128/JVI.01818-06

340. Pickl, W.F., Pimentel-Muiños, F.X., Seed, B., 2001. Lipid Rafts and Pseudotyping. J. Virol. 75, 7175–7183. doi:10.1128/JVI.75.15.7175-7183.2001
341. Podgornik, A., Jančar, J., Mihelič, I., Barut, M., Strancar, A., 2010. Large volume monolithic stationary phases: preparation, properties, and applications. Acta Chim. Slov. 57, 1–8.
342. Pollard, V.W., Malim, M.H., 1998. The HIV-1 Rev protein. Annu. Rev. Microbiol. 52, 491–532. doi:10.1146/annurev.micro.52.1.491
343. Popik, W., Alce, T.M., Au, W.-C., 2002. Human Immunodeficiency Virus Type 1 Uses Lipid Raft-Colocalized CD4 and Chemokine Receptors for Productive Entry into CD4+ T Cells. J. Virol. 76, 4709–4722. doi:10.1128/JVI.76.10.4709-4722.2002
344. Porter, D.L., Levine, B.L., Kalos, M., Bagg, A., June, C.H., 2011. Chimeric Antigen Receptor–Modified T Cells in Chronic Lymphoid Leukemia. N. Engl. J. Med. 365, 725–733. doi:10.1056/NEJMoa1103849
345. Qian, W., Wang, Y., Li, R., Zhou, X., Liu, J., Peng, D., 2017. Prolonged Integration Site Selection of a Lentiviral Vector in the Genome of Human Keratinocytes. Med. Sci. Monit. Int. Med. J. Exp. Clin. Res. 23, 1116–1122. doi:10.12659/MSM.903094
346. Qureshi, M.H., Yeung, J.C., Wu, S.C., Wong, S.L., 2001. Development and characterization of a series of soluble tetrameric and monomeric streptavidin muteins with differential biotin binding affinities. J. Biol. Chem. 276, 46422–46428. doi:10.1074/jbc.M107398200
347. Raha, T., Cheng, S.W.G., Green, M.R., 2005. HIV-1 Tat Stimulates Transcription Complex Assembly through Recruitment of TBP in the Absence of TAFs. PLOS Biol. 3, e44. doi:10.1371/journal.pbio.0030044
348. Rasko, J.E., Battini, J.L., Gottschalk, R.J., Mazo, I., Miller, A.D., 1999. The RD114/simian type D retrovirus receptor is a neutral amino acid transporter. Proc. Natl. Acad. Sci. U. S. A. 96, 2129–2134.
349. Ratner, L., Haseltine, W., Patarca, R., Livak, K.J., Starcich, B., Josephs, S.F., Doran, E.R., Rafalski, J.A., Whitehorn, E.A., Baumeister, K., 1985. Complete nucleotide sequence of the AIDS virus, HTLV-III. Nature 313, 277–284.
350. Rawsthorne, H., Phister, T.G., Jaykus, L.-A., 2009. Development of a Fluorescent In Situ Method for Visualization of Enteric Viruses. Appl. Environ. Microbiol. 75, 7822–7827. doi:10.1128/AEM.01986-09
351. Reeves, L., Cornetta, K., 2000. Clinical retroviral vector production: step filtration using clinically approved filters improves titres. Publ. Online 01 Dec. 2000 Doi101038sjgt3301328 7. doi:10.1038/sj.gt.3301328
352. Rehman, H., Silk, A.W., Kane, M.P., Kaufman, H.L., 2016. Into the clinic: Talimogene laherparepvec (T-VEC), a first-in-class intratumoral oncolytic viral therapy. J. Immunother. Cancer 4. doi:10.1186/s40425-016-0158-5
353. Rigaut, G., Shevchenko, A., Rutz, B., Wilm, M., Mann, M., Séraphin, B., 1999. A generic protein purification method for protein complex characterization and proteome exploration. Nat. Biotechnol. 17, 1030–1032. doi:10.1038/13732
354. Rittner, K., Churcher, M.J., Gait, M.J., Karn, J., 1995. The human immunodeficiency virus long terminal repeat includes a specialised initiator

element which is required for Tat-responsive transcription. J. Mol. Biol. 248, 562–580. doi:10.1006/jmbi.1995.0243
355. Rodrigues, T., Carrondo, M.J.T., Alves, P.M., Cruz, P.E., 2007. Purification of retroviral vectors for clinical application: biological implications and technological challenges. J. Biotechnol. 127, 520–541. doi:10.1016/j.jbiotec.2006.07.028
356. Romano, G., Kasten, M., De Falco, G., Micheli, P., Khalili, K., Giordano, A., 1999. Regulatory functions of Cdk9 and of cyclin T1 in HIV Tat transactivation pathway gene expression. J. Cell. Biochem. 75, 357–368. doi:10.1002/(SICI)1097-4644(19991201)75:3<357::AID-JCB1>3.0.CO;2-K
357. Rooney, I.A., Heuser, J.E., Atkinson, J.P., 1996. GPI-anchored complement regulatory proteins in seminal plasma. An analysis of their physical condition and the mechanisms of their binding to exogenous cells. J. Clin. Invest. 97, 1675–1686.
358. Rosenberg, S.A., Aebersold, P., Cornetta, K., Kasid, A., Morgan, R.A., Moen, R., Karson, E.M., Lotze, M.T., Yang, J.C., Topalian, S.L., 1990. Gene transfer into humans--immunotherapy of patients with advanced melanoma, using tumor-infiltrating lymphocytes modified by retroviral gene transduction. N. Engl. J. Med. 323, 570–578. doi:10.1056/NEJM199008303230904
359. Rosenberg, S.A., Restifo, N.P., 2015. Adoptive cell transfer as personalized immunotherapy for human cancer. Science 348, 62–68. doi:10.1126/science.aaa4967
360. Rosenberg, S.A., Yang, J.C., Sherry, R.M., Kammula, U.S., Hughes, M.S., Phan, G.Q., Citrin, D.E., Restifo, N.P., Robbins, P.F., Wunderlich, J.R., Morton, K.E., Laurencot, C.M., Steinberg, S.M., White, D.E., Dudley, M.E., 2011. Durable complete responses in heavily pretreated patients with metastatic melanoma using T-cell transfer immunotherapy. Clin. Cancer Res. Off. J. Am. Assoc. Cancer Res. 17, 4550–4557. doi:10.1158/1078-0432.CCR-11-0116
361. Rosenberg, S.A., Yannelli, J.R., Yang, J.C., Topalian, S.L., Schwartzentruber, D.J., Weber, J.S., Parkinson, D.R., Seipp, C.A., Einhorn, J.H., White, D.E., 1994. Treatment of patients with metastatic melanoma with autologous tumor-infiltrating lymphocytes and interleukin 2. J. Natl. Cancer Inst. 86, 1159–1166.
362. Rossetti, M., Gregori, S., Hauben, E., Brown, B.D., Sergi, L.S., Naldini, L., Roncarolo, M.-G., 2011. HIV-1-derived lentiviral vectors directly activate plasmacytoid dendritic cells, which in turn induce the maturation of myeloid dendritic cells. Hum. Gene Ther. 22, 177–188. doi:10.1089/hum.2010.085
363. Rothenberg, S.M., Olsen, M.N., Laurent, L.C., Crowley, R.A., Brown, P.O., 2001. Comprehensive Mutational Analysis of the Moloney Murine Leukemia Virus Envelope Protein. J. Virol. 75, 11851–11862. doi:10.1128/JVI.75.23.11851-11862.2001
364. Roux, P., Jeanteur, P., Piechaczyk, M., 1989. A versatile and potentially general approach to the targeting of specific cell types by retroviruses: application to the infection of human cells by means of major histocompatibility complex class I and class II antigens by mouse ecotropic murine leukemia virus-derived viruses. Proc. Natl. Acad. Sci. U. S. A. 86, 9079–9083.

365. Rybak, J.-N., Scheurer, S.B., Neri, D., Elia, G., 2004. Purification of biotinylated proteins on streptavidin resin: A protocol for quantitative elution. PROTEOMICS 4, 2296–2299. doi:10.1002/pmic.200300780
366. Saad, J.S., Miller, J., Tai, J., Kim, A., Ghanam, R.H., Summers, M.F., 2006. Structural basis for targeting HIV-1 Gag proteins to the plasma membrane for virus assembly. Proc. Natl. Acad. Sci. 103, 11364–11369. doi:10.1073/pnas.0602818103
367. Sakuma, T., De Ravin, S.S., Tonne, J.M., Thatava, T., Ohmine, S., Takeuchi, Y., Malech, H.L., Ikeda, Y., 2010. Characterization of Retroviral and Lentiviral Vectors Pseudotyped with Xenotropic Murine Leukemia Virus-Related Virus Envelope Glycoprotein. Hum. Gene Ther. 21, 1665–1673. doi:10.1089/hum.2010.063
368. Sanber, K.S., Knight, S.B., Stephen, S.L., Bailey, R., Escors, D., Minshull, J., Santilli, G., Thrasher, A.J., Collins, M.K., Takeuchi, Y., 2015. Construction of stable packaging cell lines for clinical lentiviral vector production. Sci. Rep. 5. doi:10.1038/srep09021
369. Sandrin, V., 2002. Lentiviral vectors pseudotyped with a modified RD114 envelope glycoprotein show increased stability in sera and augmented transduction of primary lymphocytes and CD34+ cells derived from human and nonhuman primates. Blood 100, 823–832. doi:10.1182/blood-2001-11-0042
370. Sano, T., Cantor, C.R., 1995. Intersubunit contacts made by tryptophan 120 with biotin are essential for both strong biotin binding and biotin-induced tighter subunit association of streptavidin. Proc. Natl. Acad. Sci. U. S. A. 92, 3180–3184.
371. Sano, T., Vajda, S., Cantor, C.R., 1998. Genetic engineering of streptavidin, a versatile affinity tag. J. Chromatogr. B. Biomed. Sci. App. 715, 85–91.
372. Sastry, L., Xu, Y., Cooper, R., Pollok, K., Cornetta, K., 2004. Evaluation of plasmid DNA removal from lentiviral vectors by benzonase treatment. Hum. Gene Ther. 15, 221–226. doi:10.1089/104303404772680029
373. Savage, M.D., 1996. An Introduction to Avidin-Biotin Technology and Options for Biotinylation, in: Meier, D.T., Fahrenholz, D.F. (Eds.), A Laboratory Guide to Biotin-Labeling in Biomolecule Analysis, BioMethods. Birkhäuser Basel, pp. 1–29. doi:10.1007/978-3-0348-7349-9_1
374. Scarlata, S., Carter, C., 2003. Role of HIV-1 Gag domains in viral assembly. Biochim. Biophys. Acta BBA - Biomembr., Membrane Fusion 1614, 62–72. doi:10.1016/S0005-2736(03)00163-9
375. Schaffer, D.V., Koerber, J.T., Lim, K., 2008. Molecular Engineering of Viral Gene Delivery Vehicles. Annu. Rev. Biomed. Eng. 10, 169–194. doi:10.1146/annurev.bioeng.10.061807.160514
376. Scherer, F., Anton, M., Schillinger, U., Henke, J., Bergemann, C., Krüger, A., Gänsbacher, B., Plank, C., 2002. Magnetofection: enhancing and targeting gene delivery by magnetic force in vitro and in vivo. Gene Ther. 9, 102–109. doi:10.1038/sj.gt.3301624
377. Scherr, B., 2002. Efficient gene transfer into the CNS by lentiviral vectors purified by anion exchange chromatography. Publ. Online 29 Novemb. 2002 Doi101038sjgt3301848 9. doi:10.1038/sj.gt.3301848

378. Schiller, J., Chackerian, B., 2014. Why HIV Virions Have Low Numbers of Envelope Spikes: Implications for Vaccine Development. PLoS Pathog. 10. doi:10.1371/journal.ppat.1004254
379. Schimmer, J., Breazzano, S., 2016. Investor Outlook: Rising from the Ashes; GSK's European Approval of Strimvelis for ADA-SCID. Hum. Gene Ther. Clin. Dev. 27, 57–61. doi:10.1089/humc.2016.29010.ind
380. Schmidt, M., Schwarzwaelder, K., Bartholomae, C., Zaoui, K., Ball, C., Pilz, I., Braun, S., Glimm, H., von Kalle, C., 2007. High-resolution insertion-site analysis by linear amplification-mediated PCR (LAM-PCR). Nat. Methods 4, 1051–1057. doi:10.1038/nmeth1103
381. Schmidt, T.G., Koepke, J., Frank, R., Skerra, A., 1996. Molecular interaction between the Strep-tag affinity peptide and its cognate target, streptavidin. J. Mol. Biol. 255, 753–766. doi:10.1006/jmbi.1996.0061
382. Schmidt, T.G.M., Batz, L., Bonet, L., Carl, U., Holzapfel, G., Kiem, K., Matulewicz, K., Niermeier, D., Schuchardt, I., Stanar, K., 2013. Development of the Twin-Strep-tag® and its application for purification of recombinant proteins from cell culture supernatants. Protein Expr. Purif. 92, 54–61. doi:10.1016/j.pep.2013.08.021
383. Schulze-Gahmen, U., Lu, H., Zhou, Q., Alber, T., 2014. AFF4 binding to Tat-P-TEFb indirectly stimulates TAR recognition of super elongation complexes at the HIV promoter. eLife 3. doi:10.7554/eLife.02375
384. Schur, F.K.M., Hagen, W.J.H., Rumlová, M., Ruml, T., Müller, B., Kräusslich, H.-G., Briggs, J.A.G., 2015. Structure of the immature HIV-1 capsid in intact virus particles at 8.8 Å resolution. Nature 517, 505–508. doi:10.1038/nature13838
385. Schweizer, M., Merten, O.-W., 2010a. Large-scale production means for the manufacturing of lentiviral vectors. Curr. Gene Ther. 10, 474–486.
386. Schweizer, M., Merten, O.-W., 2010b. Large-scale production means for the manufacturing of lentiviral vectors. Curr. Gene Ther. 10, 474–486.
387. Segura, M. de las M., Kamen, A., Trudel, P., Garnier, A., 2005. A novel purification strategy for retrovirus gene therapy vectors using heparin affinity chromatography. Biotechnol. Bioeng. 90, 391–404. doi:10.1002/bit.20301
388. Segura, M. de L.M., Kamen, A., Garnier, A., 2006. Downstream processing of oncoretroviral and lentiviral gene therapy vectors. Biotechnol. Adv. 24, 321–337. doi:10.1016/j.biotechadv.2005.12.001
389. Segura, M.M., Garnier, A., Durocher, Y., Coelho, H., Kamen, A., 2007. Production of lentiviral vectors by large-scale transient transfection of suspension cultures and affinity chromatography purification. Biotechnol. Bioeng. 98, 789–799. doi:10.1002/bit.21467
390. Segura, M.M., Kamen, A.A., Garnier, A., 2011. Overview of Current Scalable Methods for Purification of Viral Vectors, in: Merten, O.-W., Al-Rubeai, M. (Eds.), Viral Vectors for Gene Therapy. Humana Press, Totowa, NJ, pp. 89–116.
391. Segura, M.M., Mangion, M., Gaillet, B., Garnier, A., 2013a. New developments in lentiviral vector design, production and purification. Expert Opin. Biol. Ther. 13, 987–1011. doi:10.1517/14712598.2013.779249
392. Segura, M.M., Mangion, M., Gaillet, B., Garnier, A., 2013b. New developments in lentiviral vector design, production and purification. Expert Opin. Biol. Ther. 13, 987–1011. doi:10.1517/14712598.2013.779249

393. Sena-Esteves, M., Tebbets, J.C., Steffens, S., Crombleholme, T., Flake, A.W., 2004. Optimized large-scale production of high titre lentivirus vector pseudotypes. J. Virol. Methods 122, 131–139. doi:10.1016/j.jviromet.2004.08.017
394. Seshagiri, P.B., Adiga, P.R., 1987. Identification and molecular characterisation of a biotin-binding protein distinct from avidin of chicken egg white and comparison with yolk biotin-binding protein. Biochim. Biophys. Acta 926, 321–330.
395. Shaw, M.L., Stone, K.L., Colangelo, C.M., Gulcicek, E.E., Palese, P., 2008. Cellular proteins in influenza virus particles. PLoS Pathog. 4, e1000085. doi:10.1371/journal.ppat.1000085
396. Shehu-Xhilaga, M., Crowe, S.M., Mak, J., 2001. Maintenance of the Gag/Gag-Pol Ratio Is Important for Human Immunodeficiency Virus Type 1 RNA Dimerization and Viral Infectivity. J. Virol. 75, 1834–1841. doi:10.1128/JVI.75.4.1834-1841.2001
397. Sheridan, C., 2011. Gene therapy finds its niche. Nat. Biotechnol. 29, 121–128. doi:10.1038/nbt.1769
398. Sheu, J., Beltzer, J., Fury, B., Wilczek, K., Tobin, S., Falconer, D., Nolta, J., Bauer, G., 2015. Large-scale production of lentiviral vector in a closed system hollow fiber bioreactor. Mol. Ther. Methods Clin. Dev. 2, 15020. doi:10.1038/mtm.2015.20
399. Shimoboji, T., Ding, Z.L., Stayton, P.S., Hoffman, A.S., 2002. Photoswitching of ligand association with a photoresponsive polymer-protein conjugate. Bioconjug. Chem. 13, 915–919.
400. Shirgaonkar, I.Z., Lanthier, S., Kamen, A., 2004. Acoustic cell filter: a proven cell retention technology for perfusion of animal cell cultures. Biotechnol. Adv. 22, 433–444. doi:10.1016/j.biotechadv.2004.03.003
401. Skerra, A., Schmidt, T.G.M., 1999. Applications of a peptide ligand for streptavidin: the Strep-tag. Biomol. Eng. 16, 79–86. doi:10.1016/S1050-3862(99)00033-9
402. Slepushkin, V., Chang, N., Cohen, R., 2003. Large-scale purification of a lentiviral vector by size exclusion chromatography or Mustang Q ion exchange capsule.
403. Snitkovsky, S., Niederman, T.M., Mulligan, R.C., Young, J.A., 2001. Targeting avian leukosis virus subgroup A vectors by using a TVA-VEGF bridge protein. J. Virol. 75, 1571–1575. doi:10.1128/JVI.75.3.1571-1575.2001
404. Snitkovsky, S., Niederman, T.M.J., Carter, B.S., Mulligan, R.C., Young, J.A.T., 2000. A TVA–Single-Chain Antibody Fusion Protein Mediates Specific Targeting of a Subgroup A Avian Leukosis Virus Vector to Cells Expressing a Tumor-Specific Form of Epidermal Growth Factor Receptor. J. Virol. 74, 9540–9545.
405. Snitkovsky, S., Young, J.A.T., 2002. Targeting Retroviral Vector Infection to Cells That Express Heregulin Receptors Using a TVA–Heregulin Bridge Protein. Virology 292, 150–155. doi:10.1006/viro.2001.1314
406. Song, J., Li, Y., Ji, C., Zhang, J.Z.H., 2015. Functional Loop Dynamics of the Streptavidin-Biotin Complex. Sci. Rep. 5, 7906. doi:10.1038/srep07906

407. Sosale, N., Tsai, R.K., Ivanovska, I., Zoltick, P.W., Discher, D.E., 2011. Reducing Immune Response against Lentiviral Vectors: Lentiviral Vector Presentation of CD47, The 'Marker of Self.' Biophys. J. 100, 403a. doi:10.1016/j.bpj.2010.12.2393
408. Sparacio, S., Pfeiffer, T., Schaal, H., Bosch, V., 2001. Generation of a Flexible Cell Line with Regulatable, High-Level Expression of HIV Gag/Pol Particles Capable of Packaging HIV-Derived Vectors. Mol. Ther. 3, 602–612. doi:10.1006/mthe.2001.0296
409. Stano, A., Leaman, D.P., Kim, A.S., Zhang, L., Autin, L., Ingale, J., Gift, S.K., Truong, J., Wyatt, R.T., Olson, A.J., Zwick, M.B., 2017. Dense Array of Spikes on HIV-1 Virion Particles. J. Virol. 91, e00415-17. doi:10.1128/JVI.00415-17
410. Stayton, P.S., Freitag, S., Klumb, L.A., Chilkoti, A., Chu, V., Penzotti, J.E., To, R., Hyre, D., Le Trong, I., Lybrand, T.P., Stenkamp, R.E., 1999. Streptavidin-biotin binding energetics. Biomol. Eng. 16, 39–44.
411. Stewart, H.J., Fong-Wong, L., Strickland, I., Chipchase, D., Kelleher, M., Stevenson, L., Thoree, V., McCarthy, J., Ralph, G.S., Mitrophanous, K.A., Radcliffe, P.A., 2011. A stable producer cell line for the manufacture of a lentiviral vector for gene therapy of Parkinson's disease. Hum. Gene Ther. 22, 357–369. doi:10.1089/hum.2010.142
412. Stewart, H.J., Fong-Wong, L., Strickland, I., Chipchase, D., Kelleher, M., Stevenson, L., Thoree, V., McCarthy, J., Ralph, G.S., Mitrophanous, K.A., Radcliffe, P.A., 2010. A Stable Producer Cell Line for the Manufacture of a Lentiviral Vector for Gene Therapy of Parkinson's Disease. Hum. Gene Ther. 22, 357–369. doi:10.1089/hum.2010.142
413. Stewart, H.J., Leroux-Carlucci, M.A., Sion, C.J.M., Mitrophanous, K.A., Radcliffe, P.A., 2009. Development of inducible EIAV-based lentiviral vector packaging and producer cell lines. Gene Ther. 16, 805–814. doi:10.1038/gt.2009.20
414. Stolz, J., Ludwig, A., Sauer, N., 1998. Bacteriophage lambda surface display of a bacterial biotin acceptor domain reveals the minimal peptide size required for biotinylation. FEBS Lett. 440, 213–217.
415. Stornaiuolo, A., Piovani, B.M., Bossi, S., Zucchelli, E., Corna, S., Salvatori, F., Mavilio, F., Bordignon, C., Rizzardi, G.P., Bovolenta, C., 2013. RD2-MolPack-Chim3, a Packaging Cell Line for Stable Production of Lentiviral Vectors for Anti-HIV Gene Therapy. Hum. Gene Ther. Methods 24, 228–240. doi:10.1089/hgtb.2012.190
416. Strancar, A., Podgornik, A., Barut, M., Necina, R., 2002. Short monolithic columns as stationary phases for biochromatography. Adv. Biochem. Eng. Biotechnol. 76, 49–85.
417. Stumptner-Cuvelette, P., Morchoisne, S., Dugast, M., Le Gall, S., Raposo, G., Schwartz, O., Benaroch, P., 2001. HIV-1 Nef impairs MHC class II antigen presentation and surface expression. Proc. Natl. Acad. Sci. U. S. A. 98, 12144–12149. doi:10.1073/pnas.221256498
418. Sueda, S., Yoneda, S., Hayashi, H., 2011. Site-specific labeling of proteins by using biotin protein ligase conjugated with fluorophores. Chembiochem Eur. J. Chem. Biol. 12, 1367–1375. doi:10.1002/cbic.201000738

419. Sutton, R.E., Reitsma, M.J., Uchida, N., Brown, P.O., 1999. Transduction of human progenitor hematopoietic stem cells by human immunodeficiency virus type 1-based vectors is cell cycle dependent. J. Virol. 73, 3649–3660.
420. Swanstrom, R., Wills, J.W., 1997. Synthesis, Assembly, and Processing of Viral Proteins, in: Coffin, J.M., Hughes, S.H., Varmus, H.E. (Eds.), Retroviruses. Cold Spring Harbor Laboratory Press, Cold Spring Harbor (NY).
421. Swiecki, M., Omattage, N.S., Brett, T.J., 2013. BST-2/tetherin: Structural biology, viral antagonism, and immunobiology of a potent host antiviral factor. Mol. Immunol. 54, 132–139. doi:10.1016/j.molimm.2012.11.008
422. Tabaka, M., Kalwarczyk, T., Szymanski, J., Hou, S., Holyst, R., 2014. The effect of macromolecular crowding on mobility of biomolecules, association kinetics, and gene expression in living cells. Front. Phys. 2. doi:10.3389/fphy.2014.00054
423. Tai, C.-K., Logg, C.R., Park, J.M., Anderson, W.F., Press, M.F., Kasahara, N., 2003. Antibody-mediated targeting of replication-competent retroviral vectors. Hum. Gene Ther. 14, 789–802. doi:10.1089/104303403765255174
424. Tailor, C.S., Nouri, A., Zhao, Y., Takeuchi, Y., Kabat, D., 1999. A Sodium-Dependent Neutral-Amino-Acid Transporter Mediates Infections of Feline and Baboon Endogenous Retroviruses and Simian Type D Retroviruses. J. Virol. 73, 4470–4474.
425. Tanaka, M., Ueno, T., Nakahara, T., Sasaki, K., Ishimoto, A., Sakai, H., 2003. Downregulation of CD4 is required for maintenance of viral infectivity of HIV-1. Virology 311, 316–325. doi:10.1016/S0042-6822(03)00126-0
426. Tareen, S.U., Nicolai, C.J., Campbell, D.J., Flynn, P.A., Slough, M.M., Vin, C.D., Kelley-Clarke, B., Odegard, J.M., Robbins, S.H., 2013. A Rev-Independent gag/pol Eliminates Detectable psi-gag Recombination in Lentiviral Vectors. BioResearch Open Access 2, 421–430. doi:10.1089/biores.2013.0037
427. Thomas, J.A., Ott, D.E., Gorelick, R.J., 2007. Efficiency of Human Immunodeficiency Virus Type 1 Postentry Infection Processes: Evidence against Disproportionate Numbers of Defective Virions. J. Virol. 81, 4367–4370. doi:10.1128/JVI.02357-06
428. Throm, R.E., Ouma, A.A., Zhou, S., Chandrasekaran, A., Lockey, T., Greene, M., De Ravin, S.S., Moayeri, M., Malech, H.L., Sorrentino, B.P., Gray, J.T., 2009. Efficient construction of producer cell lines for a SIN lentiviral vector for SCID-X1 gene therapy by concatemeric array transfection. Blood 113, 5104–5110. doi:10.1182/blood-2008-11-191049
429. Transfiguracion, J., Jaalouk, D.E., Ghani, K., Galipeau, J., Kamen, A., 2003. Size-exclusion chromatography purification of high-titre vesicular stomatitis virus G glycoprotein-pseudotyped retrovectors for cell and gene therapy applications. Hum. Gene Ther. 14, 1139–1153. doi:10.1089/104303403322167984
430. Treuheit, M.J., Kosky, A.A., Brems, D.N., 2002. Inverse relationship of protein concentration and aggregation. Pharm. Res. 19, 511–516.

431. Truran, R., Buckley, R., Radcliffe, P., Miskin, J., Mitrophanous, K., 2009. Virus purification. US20090325284 A1.
432. Väkevä, A., Jauhiainen, M., Ehnholm, C., Lehto, T., Meri, S., 1994. High-density lipoproteins can act as carriers of glycophosphoinositol lipid-anchored CD59 in human plasma. Immunology 82, 28–33.
433. Valsesia-Wittmann, S., Drynda, A., Deléage, G., Aumailley, M., Heard, J.M., Danos, O., Verdier, G., Cosset, F.L., 1994. Modifications in the binding domain of avian retrovirus envelope protein to redirect the host range of retroviral vectors. J. Virol. 68, 4609–4619.
434. VandenDriessche, T., Thorrez, L., Naldini, L., Follenzi, A., Moons, L., Berneman, Z., Collen, D., Chuah, M.K.L., 2002. Lentiviral vectors containing the human immunodeficiency virus type-1 central polypurine tract can efficiently transduce nondividing hepatocytes and antigen-presenting cells in vivo. Blood 100, 813–822.
435. Venkiteshwaran, A., Fogle, J., Patnaik, P., Kowle, R., Chen, D., 2015. Mechanistic evaluation of virus clearance by depth filtration. Biotechnol. Prog. 31, 431–437. doi:10.1002/btpr.2061
436. Verhoeyen, E., Cosset, F.-L., 2004. Surface-engineering of lentiviral vectors. J. Gene Med. 6, S83–S94. doi:10.1002/jgm.494
437. Verhoeyen, E., Dardalhon, V., Ducrey-Rundquist, O., Trono, D., Taylor, N., Cosset, F.-L., 2003. IL-7 surface-engineered lentiviral vectors promote survival and efficient gene transfer in resting primary T lymphocytes. Blood 101, 2167–2174. doi:10.1182/blood-2002-07-2224
438. Vicente, T., Fáber, R., Alves, P.M., Carrondo, M.J.T., Mota, J.P.B., 2011. Impact of ligand density on the optimization of ion-exchange membrane chromatography for viral vector purification. Biotechnol. Bioeng. 108, 1347–1359. doi:10.1002/bit.23058
439. Vogt, V.M., Simon, M.N., 1999. Mass determination of rous sarcoma virus virions by scanning transmission electron microscopy. J. Virol. 73, 7050–7055.
440. Votteler, J., Sundquist, W.I., 2013. Virus budding and the ESCRT pathway. Cell Host Microbe 14, 232–241. doi:10.1016/j.chom.2013.08.012
441. Waehler, R., Russell, S.J., Curiel, D.T., 2007. Engineering targeted viral vectors for gene therapy. Nat. Rev. Genet. 8, 573–587. doi:10.1038/nrg2141
442. Wagner, E.K., 2008. Basic virology. Blackwell Pub., Malden, MA; Oxford.
443. Ward, M., Sattler, R., Grossman, I.R., Bell, A.J., Skerrett, D., Baxi, L., Bank, A., 2003. A stable murine-based RD114 retroviral packaging line efficiently transduces human hematopoietic cells. Mol. Ther. J. Am. Soc. Gene Ther. 8, 804–812.
444. Warnock, J.N., Merten, O.-W., Al-Rubeai, M., 2006. Cell Culture Processes for the Production of Viral Vectors for Gene Therapy Purposes. Cytotechnology 50, 141–162. doi:10.1007/s10616-005-5507-z
445. Weber, P.C., Pantoliano, M.W., Salemme, F.R., 1995. Crystallographic and thermodynamic comparison of structurally diverse molecules binding to streptavidin. Acta Crystallogr. D Biol. Crystallogr. 51, 590–596. doi:10.1107/S0907444995001405

446. Weber, P.C., Pantoliano, M.W., Thompson, L.D., 1992. Crystal structure and ligand binding studies of a screened peptide complexed with streptavidin. Biochemistry (Mosc.) 31, 9350–9354. doi:10.1021/bi00154a004
447. Weissenhorn, W., Dessen, A., Harrison, S.C., Skehel, J.J., Wiley, D.C., 1997. Atomic structure of the ectodomain from HIV-1 gp41. Nature 387, 426–430. doi:10.1038/387426a0
448. Wielgosz, M.M., Kim, Y.-S., Carney, G.G., Zhan, J., Reddivari, M., Coop, T., Heath, R.J., Brown, S.A., Nienhuis, A.W., 2015a. Generation of a lentiviral vector producer cell clone for human Wiskott-Aldrich syndrome gene therapy. Mol. Ther. — Methods Clin. Dev. 2, 14063. doi:10.1038/mtm.2014.63
449. Wielgosz, M.M., Kim, Y.-S., Carney, G.G., Zhan, J., Reddivari, M., Coop, T., Heath, R.J., Brown, S.A., Nienhuis, A.W., 2015b. Generation of a lentiviral vector producer cell clone for human Wiskott-Aldrich syndrome gene therapy. Mol. Ther. Methods Clin. Dev. 2, 14063. doi:10.1038/mtm.2014.63
450. Wilchek, M., Bayer, E.A., 1990. Applications of avidin-biotin technology: literature survey. Methods Enzymol. 184, 14–45.
451. Wilchek, M., Bayer, E.A., Livnah, O., 2006. Essentials of biorecognition: the (strept)avidin-biotin system as a model for protein-protein and protein-ligand interaction. Immunol. Lett. 103, 27–32. doi:10.1016/j.imlet.2005.10.022
452. Williams, S.L., Nesbeth, D., Darling, D.C., Farzaneh, F., Slater, N.K.H., 2005. Affinity recovery of Moloney Murine Leukaemia Virus. J. Chromatogr. B 820, 111–119. doi:10.1016/j.jchromb.2005.03.016
453. Wilson, D.S., Keefe, A.D., Szostak, J.W., 2001. The use of mRNA display to select high-affinity protein-binding peptides. Proc. Natl. Acad. Sci. U. S. A. 98, 3750–3755. doi:10.1073/pnas.061028198
454. Witting, S.R., Li, L.-H., Jasti, A., Allen, C., Cornetta, K., Brady, J., Shivakumar, R., Peshwa, M.V., 2012. Efficient Large Volume Lentiviral Vector Production Using Flow Electroporation. Hum. Gene Ther. 23, 243–249. doi:10.1089/hum.2011.088
455. Wolf, M.W., Reichl, U., 2011a. Downstream processing of cell culture-derived virus particles. Expert Rev. Vaccines 10, 1451–1475. doi:10.1586/erv.11.111
456. Wolf, M.W., Reichl, U., 2011b. Downstream processing of cell culture-derived virus particles. Expert Rev. Vaccines 10, 1451–1475. doi:10.1586/erv.11.111
457. Wolff, M.W., Siewert, C., Hansen, S.P., Faber, R., Reichl, U., 2010. Purification of cell culture-derived modified vaccinia ankara virus by pseudo-affinity membrane adsorbers and hydrophobic interaction chromatography. Biotechnol. Bioeng. 107, 312–320. doi:10.1002/bit.22797
458. Wu, B.W., Cannon, P.M., Gordon, E.M., Hall, F.L., Anderson, W.F., 1998. Characterization of the Proline-Rich Region of Murine Leukemia Virus Envelope Protein. J. Virol. 72, 5383–5391.
459. Wu, P., Kudrolli, T.A., Chowdhury, W.H., Liu, M.M., Rodriguez, R., Lupold, S.E., 2010. Adenovirus Targeting to Prostate-specific Membrane

Antigen through Virus-displayed Semi-random Peptide Library Screening. Cancer Res. 70, 9549–9553. doi:10.1158/0008-5472.CAN-10-1760
460. Wu, S.-C., Wong, S.-L., 2013. Structure-Guided Design of an Engineered Streptavidin with Reusability to Purify Streptavidin-Binding Peptide Tagged Proteins or Biotinylated Proteins. PLOS ONE 8, e69530. doi:10.1371/journal.pone.0069530
461. Wu, Y., Simons, J., Hooson, S., Abraham, D., Carta, G., 2013. Protein and virus-like particle adsorption on perfusion chromatography media. J. Chromatogr. A 1297, 96–105. doi:10.1016/j.chroma.2013.04.062
462. Xu, K., Ma, H., McCown, T.J., Verma, I.M., Kafri, T., 2001. Generation of a stable cell line producing high-titre self-inactivating lentiviral vectors. Mol. Ther. J. Am. Soc. Gene Ther. 3, 97–104. doi:10.1006/mthe.2000.0238
463. Yamada, K., McCarty, D.M., Madden, V.J., Walsh, C.E., 2003. Lentivirus vector purification using anion exchange HPLC leads to improved gene transfer. BioTechniques 34, 1074–1078, 1080.
464. Yang, G., Zhong, Q., Huang, W., Reiser, J., Schwarzenberger, P., 2005. Retrovirus molecular conjugates: a versatile and efficient gene transfer vector system for primitive human hematopoietic progenitor cells. Cancer Gene Ther. 13, 460–468. doi:10.1038/sj.cgt.7700911
465. Yang, L., Bailey, L., Baltimore, D., Wang, P., 2006. Targeting lentiviral vectors to specific cell types in vivo. Proc. Natl. Acad. Sci. 103, 11479–11484. doi:10.1073/pnas.0604993103
466. Yang, S., Karne, N.K., Goff, S.L., Black, M.A., Xu, H., Bischof, D., Cornetta, K., Rosenberg, S.A., Morgan, R.A., Feldman, S.A., 2012. A Simple and Effective Method to Generate Lentiviral Vectors for Ex Vivo Gene Delivery to Mature Human Peripheral Blood Lymphocytes. Hum. Gene Ther. Methods 23, 73–83. doi:10.1089/hgtb.2011.199
467. Ye, K., Dhiman, H.K., Suhan, J., Schultz, J.S., 2003. Effect of pH on infectivity and morphology of ecotropic moloney murine leukemia virus. Biotechnol. Prog. 19, 538–543. doi:10.1021/bp0200705
468. Ye, K., Jin, S., Ataai, M.M., Schultz, J.S., Ibeh, J., 2004. Tagging Retrovirus Vectors with a Metal Binding Peptide and One-Step Purification by Immobilized Metal Affinity Chromatography. J. Virol. 78, 9820–9827. doi:10.1128/JVI.78.18.9820-9827.2004
469. Yee, J.K., Miyanohara, A., LaPorte, P., Bouic, K., Burns, J.C., Friedmann, T., 1994. A general method for the generation of high-titre, pantropic retroviral vectors: highly efficient infection of primary hepatocytes. Proc. Natl. Acad. Sci. U. S. A. 91, 9564–9568.
470. Yu, H., Rabson, A.B., Kaul, M., Ron, Y., Dougherty, J.P., 1996. Inducible human immunodeficiency virus type 1 packaging cell lines. J. Virol. 70, 4530–4537.
471. Yu, J.H., Schaffer, D.V., 2006. Selection of novel vesicular stomatitis virus glycoprotein variants from a peptide insertion library for enhanced purification of retroviral and lentiviral vectors. J. Virol. 80, 3285–3292. doi:10.1128/JVI.80.7.3285-3292.2006
472. Yumura, K., Ui, M., Doi, H., Hamakubo, T., Kodama, T., Tsumoto, K., Sugiyama, A., 2013. Mutations for decreasing the immunogenicity and maintaining the function of core streptavidin. Protein Sci. Publ. Protein Soc. 22, 213–221. doi:10.1002/pro.2203

473. Závada, J., 1982. The pseudotypic paradox. J. Gen. Virol. 63 (Pt 1), 15–24. doi:10.1099/0022-1317-63-1-15
474. Zempleni, J., Hassan, Y.I., Wijeratne, S.S., 2008. Biotin and biotinidase deficiency. Expert Rev. Endocrinol. Metab. 3, 715–724. doi:10.1586/17446651.3.6.715
475. Zennou, V., Petit, C., Guetard, D., Nerhbass, U., Montagnier, L., Charneau, P., 2000. HIV-1 genome nuclear import is mediated by a central DNA flap. Cell 101, 173–185. doi:10.1016/S0092-8674(00)80828-4
476. Zhang, B., Xia, H.Q., Cleghorn, G., Gobe, G., West, M., Wei, M.Q., 2001. A highly efficient and consistent method for harvesting large volumes of high-titre lentiviral vectors. Gene Ther. 8, 1745–1751. doi:10.1038/sj.gt.3301587
477. Zhang, H., Pomerantz, R.J., Dornadula, G., Sun, Y., 2000. Human Immunodeficiency Virus Type 1 Vif Protein Is an Integral Component of an mRNP Complex of Viral RNA and Could Be Involved in the Viral RNA Folding and Packaging Process. J. Virol. 74, 8252–8261. doi:10.1128/JVI.74.18.8252-8261.2000
478. Zhao, Y., Zhu, L., Lee, S., Li, L., Chang, E., Soong, N.-W., Douer, D., Anderson, W.F., 1999. Identification of the block in targeted retroviral-mediated gene transfer. Proc. Natl. Acad. Sci. U. S. A. 96, 4005–4010.
479. Zhu, P., Liu, J., Bess, J., Chertova, E., Lifson, J.D., Grisé, H., Ofek, G.A., Taylor, K.A., Roux, K.H., 2006. Distribution and three-dimensional structure of AIDS virus envelope spikes. Nature 441, 847–852. doi:10.1038/nature04817
480. Zimmermann, K., Scheibe, O., Kocourek, A., Muelich, J., Jurkiewicz, E., Pfeifer, A., 2011. Highly efficient concentration of lenti- and retroviral vector preparations by membrane adsorbers and ultrafiltration. BMC Biotechnol. 11, 55. doi:10.1186/1472-6750-11-55
481. Zufferey, R., Donello, J.E., Trono, D., Hope, T.J., 1999. Woodchuck hepatitis virus posttranscriptional regulatory element enhances expression of transgenes delivered by retroviral vectors. J. Virol. 73, 2886–2892.
482. Zufferey, R., Dull, T., Mandel, R.J., Bukovsky, A., Quiroz, D., Naldini, L., Trono, D., 1998. Self-inactivating lentivirus vector for safe and efficient in vivo gene delivery. J. Virol. 72, 9873–9880.
483. Zufferey, R., Nagy, D., Mandel, R.J., Naldini, L., Trono, D., 1997. Multiply attenuated lentiviral vector achieves efficient gene delivery in vivo. Nat. Biotechnol. 15, 871–875. doi:10.1038/nbt0997-871